

Durham E-Theses

*The role of ocean forcing in early deglaciation of the
British-Irish Ice Sheet during the Last Glacial
Maximum: A micropalaeontological and
sedimentological study of sediment cores from the
Malin Sea and Slyne Trough*

O'NEILL, BRENDAN

How to cite:

O'NEILL, BRENDAN (2020) *The role of ocean forcing in early deglaciation of the British-Irish Ice Sheet during the Last Glacial Maximum: A micropalaeontological and sedimentological study of sediment cores from the Malin Sea and Slyne Trough*, Durham theses, Durham University. Available at Durham E-Theses Online: <http://etheses.dur.ac.uk/14038/>

Use policy

The full-text may be used and/or reproduced, and given to third parties in any format or medium, without prior permission or charge, for personal research or study, educational, or not-for-profit purposes provided that:

- a full bibliographic reference is made to the original source
- a [link](#) is made to the metadata record in Durham E-Theses
- the full-text is not changed in any way

The full-text must not be sold in any format or medium without the formal permission of the copyright holders.

Please consult the [full Durham E-Theses policy](#) for further details.

Academic Support Office, The Palatine Centre, Durham University, Stockton Road, Durham, DH1 3LE
e-mail: e-theses.admin@durham.ac.uk Tel: +44 0191 334 6107
<http://etheses.dur.ac.uk>

ABSTRACT

The contribution of the polar ice sheets to global sea level rise has tripled within the last two decades, and remains the largest yet most uncertain source of future sea level rise. Critical to this problem are the sensitive marine-terminating margins of ice sheets, which can propagate marine-forced changes into the ice-sheet interior but whose responses remain insufficiently understood and challenging to simulate. Improving our understanding of ice sheet-ocean interactions is therefore an essential prerequisite to accurate projections of future sea level rise. Geological records of ice sheet-ocean interaction are valuable to this effort, as they can span centennial to millennial timescales, providing longer-term context to instrumental observations and important means of informing and testing numerical ice-sheet models used in predictions of sea-level rise. The last British-Irish Ice Sheet (BIIS) has important potential in this regard, due to its largely marine-based configuration and proximity to pathways of poleward heat transport in the northeast Atlantic. This study avails of this by investigating whether ocean forcing played a role in early deglaciation in two sectors along the Atlantic margin of the BIIS, the Malin shelf and Porcupine Bank-Slyne Trough region, using foraminiferal assemblages. The results suggest that warm Atlantic Water was present during early deglaciation (from ≥ 25.5 ka BP) in the Porcupine Bank-Slyne Trough region, and passively drove retreat offshore central western Ireland. In contrast, deglaciation on the Malin shelf occurred in a cold glaciomarine environment from ≥ 25.9 ka BP and was likely internally-driven through glacioisostatic adjustment-induced relative sea-level rise, consistent with recent results from two other sectors along the BIIS's Atlantic margin. The findings expose the role of bathymetry in locally conditioning the BIIS to ocean forcing, and imply a BIIS influence by Atlantic Water advection in the northeast Atlantic during the coldest stadials of the last glacial period.

The role of ocean forcing in early deglaciation of the British-Irish Ice Sheet during the Last Glacial Maximum:

A micropalaeontological and sedimentological study of sediment cores from the Malin Sea and Slyne Trough

Brendan O'Neill

Department of Geography
University of Durham

Thesis submitted for the degree of Master of Science by research
December 2020



Table of Contents

| | |
|---|------|
| Abstract | |
| Table of Contents | i |
| List of Figures | iv |
| List of Tables | vii |
| List of Appendices | vii |
| List of Abbreviations | viii |
| Declaration | ix |
| Acknowledgements | x |
| CHAPTER 1 | |
| <i>INTRODUCTION AND APPROACH</i> | |
| 1.1. Introduction and rationale | 1 |
| 1.2. Overall aim and research questions | 3 |
| 1.3. Objectives | 3 |
| CHAPTER 2 | |
| <i>LITERATURE REVIEW</i> | |
| 2.1. Use of benthic foraminiferal assemblages in palaeoceanographic reconstructions | 5 |
| 2.1.1. Water-mass influence on benthic foraminiferal distributions | 5 |
| 2.1.2. Determining environmental controls on foraminiferal distributions | 8 |
| 2.2. Deglacial reconstructions from the BIIS's Atlantic margin | 9 |
| 2.2.1. The Celtic shelf and Irish Sea | 11 |
| 2.2.2. The central western Irish shelf and Porcupine Bank | 15 |
| 2.2.3. Offshore Donegal Bay (the northwest Irish shelf) | 18 |
| 2.2.4. The Malin shelf (Barra Fan Ice Stream) | 22 |
| 2.2.5. The Minch and northern Hebridean shelf | 25 |
| 2.3. Northeast Atlantic palaeoceanography during the last glacial period | 29 |
| 2.3.1. Background to the North Atlantic | 29 |
| 2.3.2. Interstadial conditions | 30 |
| 2.3.3. Stadial conditions | 32 |
| 2.4. Summary | 38 |
| 2.4.1. Deglacial reconstructions | 38 |
| 2.4.2. Northeast Atlantic palaeoceanographic conditions during BIIS retreat | 39 |

CHAPTER 3*STUDY AREAS*

| | |
|--------------------------------------|----|
| 3.1. The Malin shelf | 41 |
| 3.2. Porcupine Bank and Slyne Trough | 45 |

CHAPTER 4*MATERIAL AND METHODS*

| | |
|--|----|
| 4.1. Material | 53 |
| 4.2. Methods | 53 |
| Laboratory work | 53 |
| 4.2.1. Core logging | 53 |
| 4.2.2. Grain-size analysis | 54 |
| 4.2.3. Foraminiferal analysis | 55 |
| Taxonomy | 57 |
| Data analysis | 57 |
| 4.2.4. Sedimentologic data | 57 |
| 4.2.5. Foraminiferal absolute abundance and diversity statistics | 58 |
| 4.2.6. Faunal assemblage zones | 59 |

CHAPTER 5*RESULTS*

| | |
|------------------------------------|----|
| 5.1. JC106-146VC | 61 |
| 5.1.1. Setting in deglacial record | 61 |
| 5.1.2. Lithofacies | 61 |
| 5.1.3. Foraminiferal assemblages | 69 |
| 5.2. JC106-198VC | 74 |
| 5.2.1. Setting in deglacial record | 74 |
| 5.2.2. Lithofacies | 76 |
| 5.2.3. Foraminiferal assemblages | 81 |
| Benthic foraminiferal assemblages | 82 |
| Planktic foraminiferal assemblages | 86 |

CHAPTER 6*INTERPRETATION*

| | |
|--|-----|
| 6.1. JC106-146VC | 89 |
| 6.1.1. Lithofacies and foraminiferal assemblages | 89 |
| 6.1.2. Summary and relation of interpretations to geomorphological context of core 146VC | 98 |
| 6.2. JC106-198VC | 100 |
| 6.2.1. Lithofacies and foraminiferal assemblages | 100 |
| 6.2.2. Summary and relation of interpretations to geomorphological context of core 198VC | 107 |

CHAPTER 7*DISCUSSION*

| | |
|---|-----|
| 7.1. Drivers and modulators of early deglaciation | 112 |
| 7.1.1. The Malin shelf | 113 |
| Drivers of deglaciation | 113 |
| Modulating factors | 114 |
| 7.1.2. Porcupine Bank and Slyne Trough | 114 |
| Drivers of deglaciation | 114 |
| Modulating factors | 118 |
| 7.2. The role of bathymetry in ocean forcing along the BIIS's Atlantic margin | 119 |
| Significance | 121 |

CHAPTER 8*CONCLUSIONS*

| | |
|--|-----|
| 8.1. Deglacial environments in the Malin shelf and Porcupine Bank-Slyne Trough sectors | 123 |
| 8.1.1. Research question 1 | 123 |
| The Malin shelf | 123 |
| Porcupine Bank and Slyne Trough | 124 |
| 8.1.2. Research question 2 | 124 |
| The Malin shelf | 125 |
| Porcupine Bank-Slyne Trough | 125 |
| 8.1.3. Research question 3 | 125 |
| The Malin shelf | 125 |
| Porcupine Bank-Slyne Trough | 126 |
| 8.1.4. Research question 4 | 127 |
| 8.2. Forcing and modulation of deglaciation along the BIIS's Atlantic margin | 127 |
| 8.2.1. The Malin shelf | 127 |
| 8.2.2. Porcupine Bank-Slyne Trough | 128 |
| 8.2.3. The role of bathymetry in controlling Atlantic Water access to the BIIS margin | 128 |

| | |
|-------------------|-----|
| REFERENCES | 130 |
|-------------------|-----|

| | |
|-------------------|-----|
| APPENDICES | 163 |
|-------------------|-----|

List of Figures
CHAPTER 1

- Fig. 1.1 Map showing the locations of studied cores in relation to Atlantic Water current pathways 2

CHAPTER 2

- Fig. 2.1 Schematic figure of a glaciated Arctic continental shelf influenced by Atlantic Water, showing key factors influencing benthic foraminiferal assemblages, after Domack & Ishman (1993) 7
- Fig. 2.2 Percent relative abundance of selected benthic foraminiferal species along Wijdefjorden, Svalbard, after Korsun & Hald (1997) 8
- Fig. 2.3 Map showing the locations of BIIS sectors discussed in the text, in relation to present pathways of Atlantic Water currents along the NW European margin 9
- Fig. 2.4 Seafloor geomorphology of the former bed of the ISIS west of Anglesey, from van Landeghem et al. (2009) 12
- Fig. 2.5 Benthic foraminiferal assemblages in deglacial sediments from the Celtic shelf, from Scourse et al. (2019) 13
- Fig. 2.6 Deglacial environments during BIIS retreat from the Porcupine Bank as proposed by Peters et al. (2015) 16
- Fig. 2.7 Isochrones of BIIS retreat offshore Galway Bay, from Ó Cofaigh et al. (submitted) 17
- Fig. 2.8 Glacial geomorphological features offshore Donegal Bay in relation to ridges on the southern Malin shelf, from Dunlop et al. (2011) 20
- Fig. 2.9 Benthic foraminiferal assemblages from the mid-shelf offshore Donegal Bay, from Ó Cofaigh et al. (2019) 21
- Fig. 2.10 Geomorphic features mapped on the southern Malin shelf by Dunlop et al. (2010) 23
- Fig. 2.11 Isochrones of BIIS retreat across the Malin shelf, from Callard et al. (2018) 25
- Fig. 2.12 Seafloor geomorphology near the southeast coast of the Isle of Lewis, from Bradwell & Stoker (2015) 27
- Fig. 2.13 Map of the Minch and Hebridean shelf showing glacial geomorphological features, seafloor sediments and chronological constraints, from Bradwell et al. (2019) 28
- Fig. 2.14 Map of the Northeast Atlantic and Nordic Seas showing major surface and deep currents, after Hoff et al. (2016) 30
- Fig. 2.15 Schematic map of the Northeast Atlantic during transitional cooling phases, after Hoff et al. (2016) 31
- Fig. 2.16 Conceptual diagram showing evolution of Northeast Atlantic surface water conditions over the Bond cycles of the last 45 ka, from Maslin et al. (1995) 32
- Fig. 2.17 Stadal-interstadial palaeoceanographic changes in Northeast Atlantic hydrography, as proposed by Rasmussen & Thomsen (2004) 34
- Fig. 2.18 % *N. pachyderma* records spanning GS-3 along the Irish-Scottish margin, after Hibbert (2010) 35
- Fig. 2.19 IRD and % *N. pachyderma* records spanning 35-15 ka BP along the Scottish-Norwegian margin, from Becker et al. (2018) 37

CHAPTER 3

- Fig. 3.1 Bathymetric map of the Malin shelf showing core 146VC site, from Callard et al. (2018) 42

| | |
|---|-----|
| Fig. 3.2 Vertical salinity profile across the mid-outer Malin shelf, after Gowen et al. (1998) | 43 |
| Fig. 3.3 Distributions of seafloor sediment types on the southern Malin shelf, from Evans et al. (2015) | 45 |
| Fig. 3.4 Bathymetric map of the Porcupine region showing core 198VC site and regional circulation patterns | 46 |
| Fig. 3.5 Vertical hydrographic sections from the Porcupine Bank region, after Kloppmann et al. (2001); White (2007) | 47 |
| Fig. 3.6 Images of the most common benthic foraminifers found by Smeulders et al. (2014) in the Porcupine Seabight | 50 |
| Fig. 3.7 Images of the most common planktic foraminifers retrieved by Harbers et al. (2010) in the Porcupine Seabight | 52 |
| CHAPTER 5 | |
| Fig. 5.1 Maps and sub-bottom profiler transect showing the location of core 146VC, after Callard et al. (2018) | 62 |
| Fig. 5.2 Sedimentologic data for core 146VC | 64 |
| Fig. 5.3 X-radiographs of lithofacies from core 146VC | 66 |
| Fig. 5.4 Benthic foraminiferal species relative abundances ($\geq 5\%$) for core 146VC | 71 |
| Fig. 5.5 Benthic and planktic foraminiferal concentrations and diversity measures for core 146VC | 73 |
| Fig. 5.6 Maps and sub-bottom profiler transect showing the location of core 198VC, after Ó Cofaigh et al. (submitted) | 75 |
| Fig. 5.7 X-radiographs of lithofacies from core 198VC | 77 |
| Fig. 5.8 Possible shear planes seen in x-radiographs of facies Fld _c | 78 |
| Fig. 5.9 Sedimentologic data for core 198VC | 80 |
| Fig. 5.10 Benthic foraminiferal species relative abundances ($\geq 5\%$) for core 198VC | 83 |
| Fig. 5.11 Benthic and planktic foraminiferal concentrations and diversity measures for core 198VC | 85 |
| Fig. 5.12 Planktic foraminiferal species relative abundances ($\geq 2\%$) for core 198VC | 87 |
| CHAPTER 6 | |
| Fig. 6.1 X-radiograph of core 146VC showing sequence from facies Dmm _c to Fldef | 90 |
| Fig. 6.2 Thickness and sequence of laminae and massive intervals in the facies Fl unit | 94 |
| Fig. 6.3 Schematic figure showing deglacial depositional environments interpreted from 146VC | 100 |
| Fig. 6.4 X-radiograph of core 198VC showing part of facies Fld _c | 102 |
| Fig. 6.5 Stratigraphic correlation of contourites on the western slope of Porcupine Bank, after Øvebrø et al. (2006) | 104 |
| Fig. 6.6 Schematic figure showing deglacial depositional environments interpreted from 198VC | 108 |
| CHAPTER 7 | |
| Fig. 7.1 Benthic foraminiferal assemblage record from the Porcupine Seabight, from Rüggeberg et al. (2007) | 115 |
| Fig. 7.2 Seismic reflection profile and interpretation across the outer central western Irish shelf, after McCarron et al. (2018) | 117 |

| | |
|---|-----|
| Fig. 7.3 Schematic figure showing the hypothesised role of bathymetry in controlling Atlantic Water access to Atlantic BIIS sectors | 120 |
| Fig. 7.4 Schematic water-column structure in the southeast Norwegian Sea during stadials and interstadials, from Dokken et al. (2013) | 121 |
| APPENDICES | |
| Fig. A1 Benthic foraminiferal species relative abundances ($\geq 2\%$) for core 146VC | 175 |
| Fig. A2 Benthic foraminiferal species relative abundances ($\geq 2\%$) for core 198VC | 176 |

List of Tables

CHAPTER 4

| | |
|--|----|
| Table 1 Location, water depth and recovery information for the cores studied in this project | 53 |
|--|----|

CHAPTER 5

| | |
|---|----|
| Table 2 Lithofacies codes for the cores presented in this project | 63 |
|---|----|

APPENDICES

| | |
|---|-----|
| Table A1 146VC benthic foraminiferal count data | 163 |
| Table A2 146VC planktic foraminiferal count data | 166 |
| Table A3 146VC foraminiferal sample statistics | 167 |
| Table A4 198VC benthic foraminiferal count data | 168 |
| Table A5 198VC planktic foraminiferal count data | 173 |
| Table A6 198VC foraminiferal sample statistics | 174 |
| Table A7 List of foraminiferal species identified in 146VC | 178 |
| Table A8 List of foraminiferal species identified in 198VC | 181 |
| Table A9 146VC benthic foraminiferal diversity statistics | 182 |
| Table A10 198VC benthic foraminiferal diversity statistics | 182 |
| Table A11 198VC planktic foraminiferal diversity statistics | 183 |
| Table A12 146VC grain-size and water content measurements | 184 |
| Table A13 198VC grain-size and water content measurements | 184 |
| Table A14 146VC >2mm clast counts from x-radiographs | 185 |
| Table A15 198VC >2mm clast counts from x-radiographs | 186 |

List of Appendices

| | |
|--|-----|
| Appendix 1: Foraminiferal count data | 163 |
| Appendix 2: Faunal data plots including species accounting for $\geq 2\%$ relative abundance | 175 |
| Appendix 3: Foraminiferal species lists | 177 |
| Appendix 4: Foraminiferal diversity statistics | 182 |
| Appendix 5: Grain-size and water content data | 184 |
| Appendix 6: >2 mm clast counts from x-radiographs | 185 |

List of Abbreviations

| | |
|--------|---|
| AMS | Accelerator mass spectrometry |
| bFAZ | benthic foraminiferal assemblage zone |
| BFIS | Barra Fan Ice Stream |
| BGS | British Geological Survey |
| BIIS | British-Irish Ice Sheet |
| BP | Before present |
| CONISS | Constrained Incremental Sum of Squares |
| CTD | Conductivity Temperature Depth |
| DBL | Donegal Bay Lobe |
| EGC | East Greenland Current |
| EIC | East Iceland Current |
| ENAW | Eastern North Atlantic Water |
| FAZ | Foraminiferal assemblage zone |
| FC | Faeroe Current |
| GI-2 | Greenland Interstadial 2 |
| GIA | Glacioisostatic adjustment |
| gLGM | global Last Glacial Maximum |
| GS-2 | Greenland Stadial 2 |
| GS-3 | Greenland Stadial 3 |
| GSR | Greenland-Scotland Ridge |
| GZW | Grounding-zone wedge |
| IRD | Ice-rafted debris |
| ISB | Irish Sea Basin |
| ISIS | Irish Sea Ice Stream |
| LFA | Lithofacies association |
| LGM | Last Glacial Maximum (26.5-19 ka BP; Clark et al. 2009) |
| ILGM | Local Last Glacial Maximum |
| MIS | Marine Isotope Stage |
| MnIS | Minch Ice Stream |
| MOW | Mediterranean Outflow Water |
| MSGZC | Mid-Shelf Grounding-Zone Complex |
| NAC | North Atlantic Current |
| NADW | North Atlantic Deep Water |
| NwAC | Norwegian Atlantic Current |
| OD | Ordnance datum |
| pFAZ | planktic foraminiferal assemblage zone |
| PSU | Practical salinity units |
| RSL | Relative sea level |
| SEC | Shelf-edge current |
| SPM | Suspended particulate matter |

Declaration

I confirm that no part of the work presented as my own in this thesis has previously been submitted by me or any other person for a degree in this or any other institution. All material appearing in this thesis from the work of others is acknowledged below and in the text.

This research was made possible by the BRITICE-CHRONO project (PI Professor Chris Clark, University of Sheffield), which provided the sediment cores, marine geophysical data and chronological analyses on which this study and key publications forming its foundation it are based. This study specifically utilises x-radiographs, magnetic susceptibility, gamma-ray density, electrical resistivity, sediment shear strength data and radiocarbon dates for cores JC106-146VC and JC106-198VC (Chapter 5), provided by Professor Colm Ó Cofaigh, Dr Jeremy Lloyd and Dr Louise Callard. These data were partly published in Callard et al. (2018, *Quat. Sci. Rev.* 201, 280-302) and Ó Cofaigh et al. (submitted 2020 to *J. Quat. Sci.*). The sediment cores and these data (excluding radiocarbon dates) were collected during cruise JC106 of the RRS *James Cook* in July-August 2014. The radiocarbon measurements were made at the Scottish Universities Environmental Research Centre AMS Laboratory, Glasgow University, and Keck C Cycle AMS Laboratory, University of California, Irvine.

Statement of Copyright

The copyright of this thesis rests with the author. No quotation from it should be published without the author's prior written consent and information derived from it should be acknowledged.

Brendan O'Neill

Department of Geography
University of Durham
December 2020

Acknowledgements

I first thank my supervisors, Professor Colm Ó Cofaigh, Dr Jerry Lloyd and Dr Louise Callard for their support, guidance and feedback throughout this project. I deeply appreciate the time they have dedicated to providing advice, feedback and discussions, despite the challenges of a global pandemic. I am very grateful to Professor Ó Cofaigh and Dr Lloyd for their close involvement, support and encouragement during my applications for further study.

I am also very grateful to the laboratory and support staff at the Department of Geography, Durham, particularly Dr Eleanor Ross and Mervyn Brown for their helpfulness and patience in facilitating much of the lab work, and to Neil Tunstall for producing x-radiographs.

My sincere thanks to Peter Coxon (now Fellow Emeritus of Trinity College Dublin), for encouragement throughout my undergraduate studies and greatly aiding my transition to Durham. I will always be grateful to Professor Coxon, Dr Robin Edwards and Dr Carlos Rocha for the role they played in sparking and encouraging my interest in Earth Sciences through exemplary teaching and guidance at Trinity.

Thanks are also due to the community at the Department of Geography, Durham, for providing such a welcoming, friendly and hospitable social network during my time there, in particular: Iqbal, María Paz, Asikunnaby, Emmanuel, Cristina, Georgia, Mel and Josh. Muyeol and Shobhit – you made great company on the many night shifts in the microscope room!

My deepest appreciation to my parents, Tim and Christine, for allowing and encouraging me to pursue my studies.

CHAPTER 1**INTRODUCTION AND APPROACH****1.1. Introduction and rationale**

The effect of warm ocean currents on ice sheet margins is now recognised as being fundamentally important to the stability and dynamics of many contemporary marine-based ice streams and ice sheet sectors in Greenland and Antarctica (e.g. Jacobs et al. 2011; Lloyd et al. 2011; Straneo et al. 2011; Pritchard et al. 2012). However, much of our understanding of ice sheet-ocean interactions is based on instrumental records that span only a few decades (e.g. Pritchard et al. 2009; Seale et al. 2011; Rignot et al. 2012). Sedimentary records of ice sheet-ocean interaction spanning centennial to millennial timescales are required to place these instrumental observations into a longer-term context (Stokes et al. 2015). Offshore coring campaigns and developments in marine geophysical mapping techniques have lately facilitated valuable reconstructions of ice sheet destabilisation and retreat, over millennial timescales, for several marine-based sectors of past ice sheets including the British-Irish Ice Sheet (BIIS) (e.g. Evans et al. 2005; Peters et al. 2016; Callard et al. 2018; Bradwell et al. 2019; Ó Cofaigh et al. 2019). Studies of palaeo-ice sheets also provide vital empirical constraints needed to inform and validate the numerical models providing quantitative predictions of ice sheet mass loss and sea level rise (Stokes & Tarasov 2010; Livingstone et al. 2012).

The BIIS's Atlantic margin had a marine-based configuration and was proximal to present pathways of poleward heat transport in the northeast Atlantic (McCartney & Talley 1982; Orvik & Niiler 2002; Van Rooij et al. 2003; see Chapter 3) (Fig. 1.1). This gives deglacial records from this margin clear potential to provide longer-term context to current observations of 'ocean-forced' ice sheet instability and other drivers of marine-based ice decay, such as relative sea-level rise and atmospheric warming (Overpeck et al. 2006; Cook et al. 2019). Recent studies from two sectors on the Atlantic margin (Ó Cofaigh et al. 2019; Scourse et al. 2019) have tested a role for ocean forcing in initial BIIS retreat, using benthic foraminiferal assemblages. These studies found no evidence of Atlantic Water presence and instead suggest that retreat was internally triggered in these areas by glacioisostatic adjustment (GIA) -induced relative sea-level (RSL) rise. Chronological constraints for deglaciation along the BIIS's Atlantic margin consistently place initial retreat within Greenland Stadial 3, and this has been inferred as reducing the potential for external forcing in driving early deglaciation (Callard et al. 2018; Ó Cofaigh et al. 2019). Furthermore, the temporal coherence in onset of initial retreat along the BIIS's Atlantic margin has been considered consistent with GIA-induced RSL rise as the primary trigger (Scourse et al. 2019). However, as there is considerable palaeoceanographic evidence for Atlantic Water

advection to the Nordic Seas and Arctic Ocean during Greenland Stadial 3 (GS-3) (e.g. Rasmussen & Thomsen 2008; Hibbert 2010; Austin et al. 2012; see Section 2.3.3.), and considering the extent and bathymetric variability of the BIIS's Atlantic margin, deglacial palaeoceanographic conditions in other areas of the western BIIS remain important questions in our understanding of the drivers of early BIIS retreat.

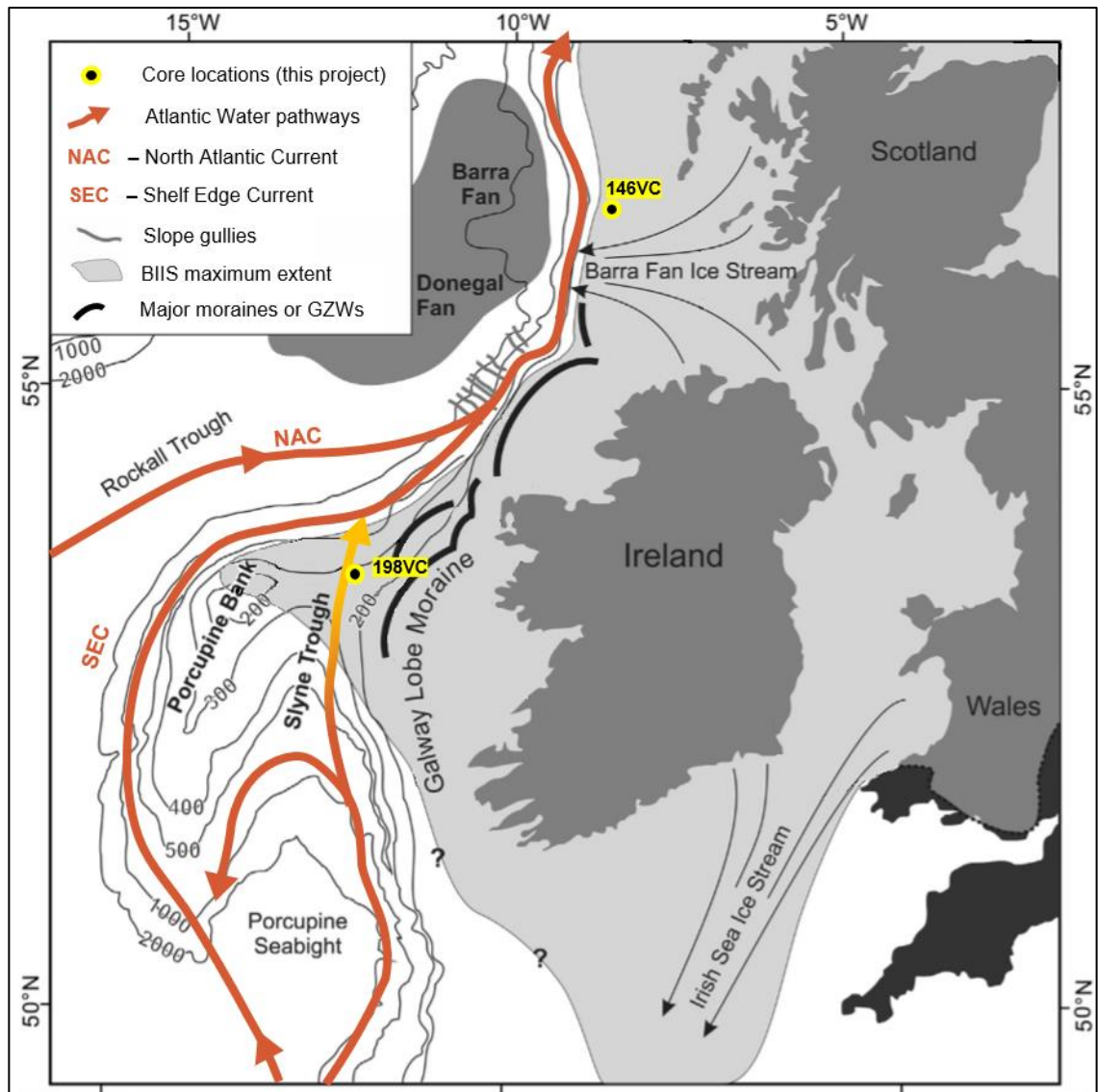


Fig. 1.1: Map showing the location of cores studied for this project in relation to schematic pathways of surface Atlantic waters (down to a maximum depth of ~700 m) along the Irish and Scottish continental shelf. The maximum extent of the BIIS is represented by the grey shaded area, with question marks denoting uncertain limits. See caption on Fig. 2.3 for further explanation. Modified after Peters et al. (2015).

Cross-shelf, chronologically-controlled reconstructions of BIIS retreat are available from the Malin Sea (Callard et al. 2018) and Porcupine Bank (Ó Cofaigh et al. submitted) regions, where a role of ocean warming in driving initial retreat is untested. This project therefore aims to address

this knowledge gap by investigating early deglacial foraminiferal assemblages in sediment cores from the outer continental shelf of the Malin Sea (JC106-146VC) and Porcupine Bank (JC106-198VC) (Fig. 1.1), following the approach outlined below and in Chapter 4.

1.2. Overall aim and research questions

The overall aim of this research project is to investigate the role of ocean forcing in driving initial retreat of the BIIS in the Malin Sea and Porcupine Bank regions. In order to achieve this, the project will address the following research questions:

1. Do benthic foraminiferal assemblages in early deglacial lithofacies from the Malin shelf and Porcupine Bank region imply the presence of Atlantic Water on the continental shelf during initial BIIS retreat?
2. Do planktic foraminiferal assemblages in early deglacial lithofacies from the Malin shelf and Porcupine Bank region provide information on surface water conditions in the adjacent open ocean during initial BIIS retreat?
3. What depositional environments were associated with early deglaciation on the Malin shelf and Porcupine Bank region, as recorded by sediment core lithofacies and foraminiferal assemblages?
4. How do the palaeoenvironmental conditions reconstructed from the foraminiferal assemblages relate to palaeoceanographic changes in the wider Northeast Atlantic during GS-3?

1.3. Objectives

These research questions will be addressed through the following four objectives:

1. Study the sedimentology of deglacial lithofacies in cores JC106-146VC (Malin shelf) and JC106-198VC (Porcupine Bank region) in detail to constrain the depositional environments associated with the foraminiferal assemblages.
2. Analyse benthic and planktic foraminiferal assemblages from deglacial lithofacies in cores JC106-146VC and JC106-198VC.

3. Combine this faunal and sedimentological information to reconstruct palaeoceanographic conditions on the outer Malin shelf and Porcupine Bank region during initial and early retreat (thereby testing any associated role for ocean forcing).

4. Use these reconstructions to investigate the influence of Northeast Atlantic palaeoceanographic evolution during GS-3 on initial retreat along the BIIS's Atlantic margin (and any implications for palaeoceanographic reconstructions from the produced records).

CHAPTER 2

LITERATURE REVIEW

This chapter is divided into three main sections, the first (Section 2.1.) discusses benthic foraminiferal assemblages as palaeoceanographic proxies; the second (Section 2.2.) addresses understanding of deglaciation along the Atlantic margin of the British-Irish Ice Sheet (BIIS), and the third (Section 2.3.) discusses palaeoceanographic conditions in the northeast Atlantic during BIIS retreat. Section 2.1.1. reviews the development of current understanding of water-mass influences on benthic foraminiferal distributions, and discusses how this supports use of assemblages in reconstructing glacially-influenced environments. Section 2.1.2. outlines the main empirical approaches used to investigate environmental controls on benthic foraminiferal distributions, and fundamental limitations of reconstructions. Section 2.2. aims to provide the first detailed review of current understanding of deglaciation in the five main sectors along the BIIS Atlantic margin reconstructed to date. It comprises five subsections, covering the Celtic shelf, the central western Irish shelf, offshore Donegal Bay, the Malin shelf and the northern Hebridean shelf. Section 2.3. introduces the glacial North Atlantic before discussing interstadial (Section 2.3.2.) and stadial (Section 2.3.3.) surface palaeoceanographic conditions, in order to assess the potential for ocean forcing in BIIS retreat. The chapter ends with a summary (Section 2.4.).

2.1. Use of benthic foraminiferal assemblages in palaeoceanographic reconstructions

The abundance, preservation potential and sensitivity to environmental conditions of benthic foraminifera supports use of their assemblages in palaeoceanographic reconstructions (Schmiedl et al. 1997; Van der Zwaan et al. 1999; Gooday & Jorissen 2012). Benthic foraminiferal assemblages have been used to reconstruct organic carbon flux to the seafloor, bottom- and porewater water temperature, salinity, oxygen concentrations and bottom current activity (Gooday 2003; Jorissen et al. 2007; Duros et al. 2014; e.g. den Dulk et al. 2000). In addition to using empirically-determined species-environment associations (see Section 2.1.2.), reconstructions have also been attempted through broad interpretations of test morphologies as functionally adapted to modes of life, assuming corresponding implications for the environmental conditions (e.g. Nigam et al. 1992; Verma et al. 2018, but see Jorissen et al. 1992; Moodley et al. 1997).

2.1.1. Water-mass influence on benthic foraminiferal distributions

It was originally held that bottom-water temperature and salinity were dominant influences on assemblage composition in most ocean settings, with specific assemblages considered

characteristic of major water masses such as North Atlantic Deep Water (e.g. Schnitker 1979; Belanger & Streeter 1980). This view changed with increased awareness of the spatial and temporal variability of water-mass physical properties (Gooday 2003; see e.g. van Aken 2000). Since influential results from upwelling zones and other dysoxic environments (e.g. Lutze & Coulbourn 1984; Mackensen & Douglas 1989; Loubere 1991; Bernhard 1992), organic matter flux and pore/bottom-water oxygen concentrations have been revealed as primary controls on benthic foraminiferal distributions, but predominantly in deeper and open-ocean settings (e.g. Jorissen et al. 1995; Wollenburg & Mackensen 1998; Fontanier et al. 2002; Husum et al. 2015).

In addition to surface productivity and levels of respiration in the sediment, organic matter availability and oxygen concentrations in the benthic environment will also partly depend on bottom-water mass sources/physical properties (Walsh et al. 1989; Gordon et al. 2002; Jorissen et al. 2007). This is evident in higher latitudes where warm, subtropically-sourced waters influence foraminiferal assemblages due to their often higher nutrient content relative to polar waters (Stefánsson & Ólafsson 1991; Lloyd 2006a; Rasmussen et al. 2012). Such interdependence of physical (abiotic) properties and nutrient-oxygen (biotic) characteristics can, however, complicate attribution of changes in modern/fossil assemblages without data/proxies for multiple variables (Gooday 2003; Altenbach et al. 2003; Blaauw et al. 2010).

Furthermore, the broad environmental tolerances of benthic foraminifers (e.g. Linke 1992; Sen Gupta & Machain-Castillo 1993; Moodley et al. 1997; Van der Zwaan et al. 1999) likely mean that a species' distribution will only be directly related to a given environmental parameter at times and in places where that parameter is limiting (Murray 1991; 2001; Altenbach et al. 2003). For example, as temperature influences the rate of bacterial respiration in sediments (Pomeroy et al. 1991; Moodley et al. 2005), temperature might control a species' distribution where it becomes too low for sufficient degraded organic matter to be available to feed the species (e.g. 2°C for *Cassidulina laevigata* in Mackensen & Hald 1988) (Mackensen 1997). This view would require that strong environmental gradients over the seafloor are necessary for benthic foraminiferal assemblages to change with physical parameters (Murray 2001; 2006; Gooday & Jorissen 2012). Spatial gradients in physical conditions are often steeper on continental shelves than in deep ocean settings, due to the presence of more contrasting water masses, stronger bottom currents and greater variability in substrate, bathymetry and sedimentation processes across shelf areas (Edwards 1982; Murray 1991; Culver & Buzas 2000; Gooday 2003; Jorissen et al. 2007).

These contrasts in conditions over the seafloor can be particularly pronounced in glacially-influenced fjord and continental shelf settings (Fig. 2.1). This reflects the often strong water-column stratification (e.g. where warm saline waters underly fresher polar waters and sea ice/meltwater-influenced surface water) and spatially-variable salinity and sedimentation

processes (e.g. due to glacier meltwater discharge) in these environments (Skei 1983; Jernas et al. 2018). Variable sea-ice cover, surface productivity, bathymetry and fjord circulation patterns also affect benthic environments here (Syvitski & Skei 1983; Schröder-Adams et al. 1990; Svendsen et al. 2002; Voronkov et al. 2013).

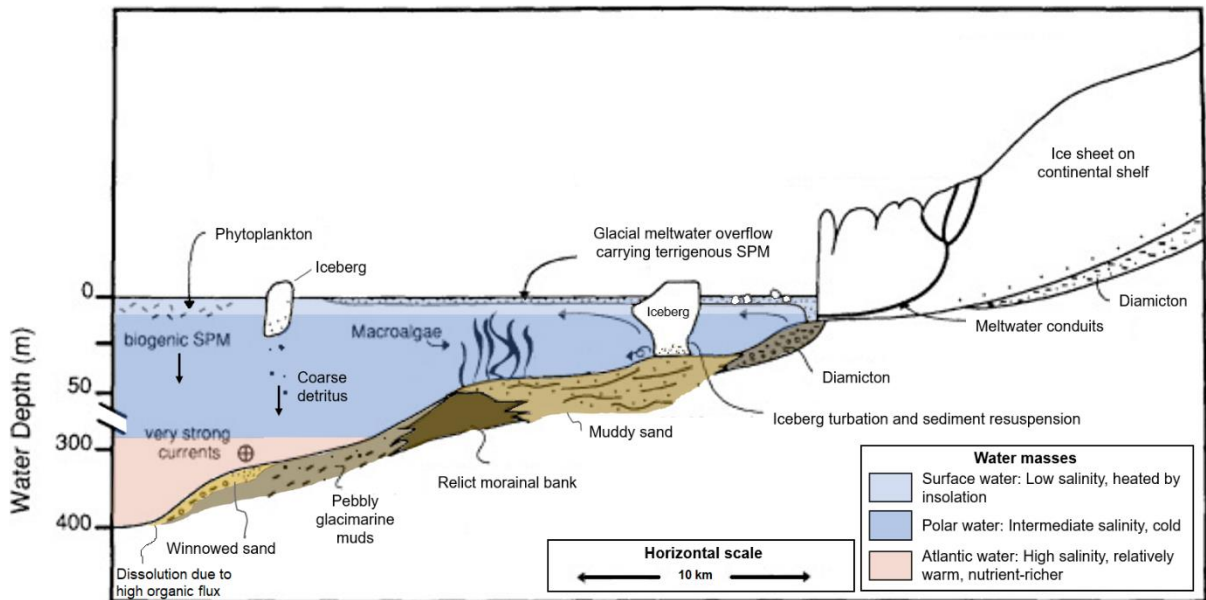


Fig. 2.1: Schematic figure of a glaciated Arctic continental shelf and slope influenced by Atlantic Water, showing key factors which can influence foraminiferal communities and their preservation (modified from Domack & Ishman 1993). Note the various substrates including algae and sediments resulting from glacial sedimentation processes and/or bottom-current winnowing. Seafloor environmental gradients shown include water-mass boundaries, changes in substrate, glacier proximity, organic matter flux and porewater oxygenation. Note offshore displacement of primary production by turbid meltwater overflow. ‘SPM’: suspended particulate matter.

Studies of assemblages in these settings, usually incorporating living and dead individuals, have demonstrated consistent associations between particular foraminifers and physical factors such as water-mass distributions and glacier proximity (e.g. Elverhøi et al. 1980; Schafer & Cole 1986; Jennings & Helgadottir 1994; Korsun et al. 1995; Hansen & Knudsen 1995; Jennings et al. 2004; Lloyd 2006a; Hald & Korsun 1997; Korsun & Hald 1998; see tables in Rasmussen & Thomsen 2008; Perner et al. 2012; Sheldon et al. 2016). These results strongly support the use of these observations in qualitative palaeoceanographic reconstructions of shelf deglacial environments, despite the challenges outlined above to assemblage-based reconstruction of physical parameters in deeper, more uniform benthic environments.

2.1.2. Determining environmental controls on foraminiferal distributions

Identifying the environmental factors controlling foraminiferal species distributions and the taphonomic processes locally affecting assemblages is necessary to make the most informed palaeoenvironmental interpretations of fossil assemblages in an area (Kidwell & Flessa 1995; Murray & Pudsey 2004; Murray 2006). This is usually undertaken through sampling total surface sediment assemblages (living and dead foraminifera; Fig. 2.2), measuring environmental parameters at the sampling sites (e.g. temperature and salinity using CTD) and using multivariate techniques to investigate the degree of faunal variation explained by the measured environmental parameters (e.g. De Deckker 2005; Lloyd 2006a; Szarek et al. 2009).

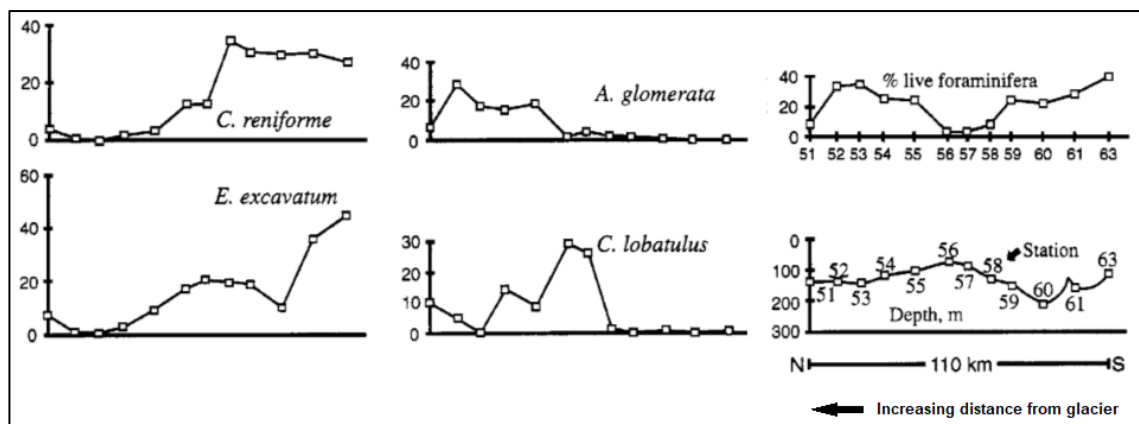


Fig. 2.2: Percent abundance of selected benthic foraminifers along a surface transect through Wijdefjorden, Svalbard (after Hald & Korsun 1997). *Elphidium excavatum* shows highest abundance nearest to the glacier margin, while *Adercotryma glomerata* increases in the outer fjord, implying preference for the Atlantic waters influencing the outer fjord (cf. Bergsten 1994; Lloyd 2006a). Data represents combined total (living + dead) assemblages.

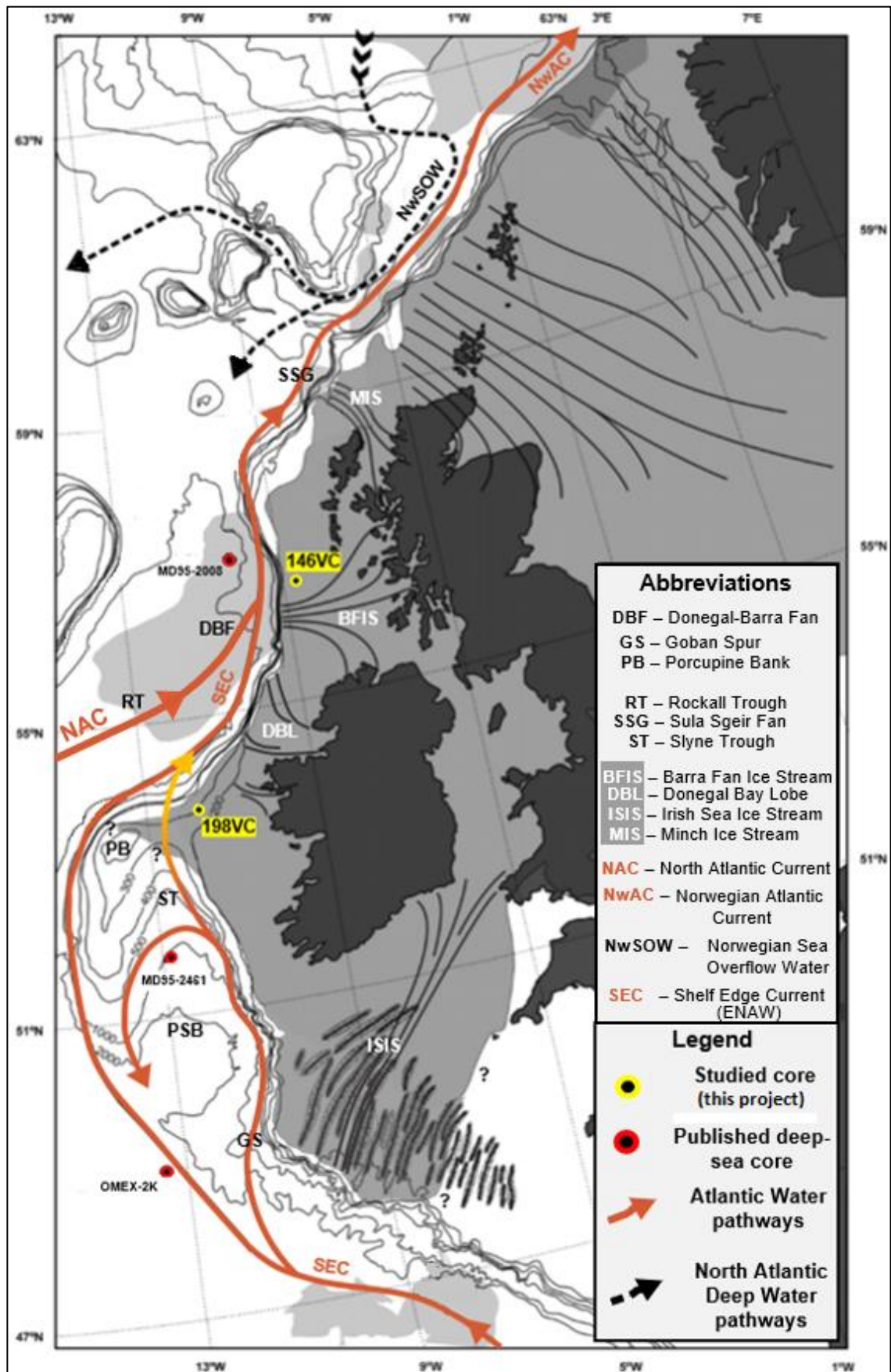
The environmental controls on species' distributions can be inferred directly (e.g. by canonical correspondence analysis, Ter Braak 1986; Palmer 1993) or indirectly (e.g. by mapping the distribution of assemblages generated by factor analysis, e.g. Mackensen et al. 1985; Schafer & Cole 1986; Husum et al. 2015). Analysis of the dead foraminiferal assemblages, whether separately or combined with the living assemblage ('total' assemblages) is essential for palaeoenvironmental utility of the results, as these are time-averaged representations of the fauna (beyond the time/season of sampling) and potentially modified by taphonomic processes, thereby more resembling fossil assemblages from the area (Scott & Medioli 1980; Murray 1982; Murray & Alve 1999; Diz & Francés 2009). Multivariate analyses have established qualitative to semiquantitative associations between benthic foraminifers and environmental variables, and have been extended to transfer function development for quantitative reconstruction of parameters (e.g. Loubere 1991; Sejrup et al. 2004; Wollenburg & Kuhnt 2000). However, palaeoceanographic reconstructions based on these empirical observations will depend on a

number of fundamental assumptions (discussed in Birks 1995; Belyea 2007; Birks et al. 2010), some of which are difficult or impossible to validate (e.g. negligible influence of unmeasured variables; Juggins & Birks 2012; Jackson et al. 2009). The latter problem highlights the importance of integrating analyses of fossil assemblages with sedimentology, chronology and additional proxies to constrain their palaeoenvironmental context as far as possible (e.g. Lloyd et al. 2005; Furze et al. 2018).

2.2. Deglacial reconstructions from the BIIS's Atlantic margin

The marine geological component of the BRITICE-CHRONO project (Ó Cofaigh et al. 2015) has recently produced cross-shelf deglaciation reconstructions from several marine-based sectors of the BIIS. These combine seafloor geomorphology and large-scale depositional architecture (from bathymetric data and seismic profiling) with sedimentology, micropalaeontology and radiocarbon dating on marine sediment cores. This integrated approach has allowed reconstruction of ice-sheet maximum extent, the timing and style of retreat, estimation of retreat rates and characterisation of depositional environments for entire marine-based sectors of the BIIS. Similar comprehensive reconstructions of shelf deglaciation have provided considerable insight into the behaviour of ice streams in Antarctica and Greenland (e.g. Lowe & Anderson 2002; Hogan et al. 2016), Norway (e.g. Vorren et al. 1984; Dahlgren & Vorren 2003) and Svalbard (e.g. Svendsen et al. 1992), but for the BIIS these succeeded more than a century of terrestrially-based research (Clark et al. 2012). This recent offshore work significantly increased the known extent of the ice sheet, revealing that the BIIS was approximately two thirds marine-based (Dove et al. 2015). This highlighted the potential of BIIS offshore deglacial reconstructions to provide insights aiding prediction of near-future mass loss from other largely marine-based ice sheets such as the West Antarctic Ice Sheet (Greenwood & Clark 2009; Clark et al. 2012; Patton et al. 2017). The deglaciation of five main sectors along the Atlantic margin of the BIIS has been reconstructed in detail to date: the Celtic shelf (Irish Sea Ice Stream), the central western Irish shelf, offshore Donegal Bay, the Malin shelf (Barra Fan Ice Stream) and the northern Hebridean shelf (Minch Ice Stream) (Fig. 2.3).

Fig. 2.3 (overleaf): Map showing the locations of BIIS sectors discussed in the text, in relation to schematic present pathways of Atlantic Water-advecting currents (to a maximum depth of ~700 m) along the NW European continental margin. The maximum extent of the BIIS is represented by the dark grey shaded area, with question marks denoting uncertain limits. Atlantic water pathways are based on Pingree & Le Cann (1989); Kloppmann et al. (2001); New & Smythe-Wright (2001); Orvik & Niiler (2002); Frank et al. (2004); Peck et al. (2007a) and White (2007). The northward SEC pathway through the Slynne Trough (yellow shaded arrow) is a shallower component not recirculated in the Porcupine Seabight and weakens through bathymetrically-forced shoaling and mixing with shelf water (Kloppmann et al. 2001). Modified after Scourse et al. (2009). 'ENAW' – Eastern North Atlantic Water.



2.2.1. *The Celtic shelf and Irish Sea*

Early research into the Quaternary history of the Irish Sea Basin (ISB) was largely concerned with defining glacial limits and regional stratigraphic correlation (e.g. Synge 1964; Bowen 1973; 1985) as opposed to the processes and depositional environments recorded by sedimentary sequences (McCarroll 2001). The stratigraphic framework resulting from this work (raised beach gravels→diamictos as representing the last interglacial→last glacial) was reinterpreted by Eyles & McCabe (1989) for the whole ISB as recording an event stratigraphy entirely of the last glaciation. However, limited chronological control was available to support this reinterpretation, which proposed a mostly glacimarine origin for the Pleistocene sedimentary record of the ISB, recording rapid calving retreat of the Irish Sea Ice Stream (ISIS; see Fig. 2.3) due to GIA-induced high RSL. This view was later strongly challenged [notably by McCarroll (2001)], and subsequent more detailed investigation of the onshore sedimentary record of the ISIS (e.g. Ó Cofaigh & Evans 2001a; Evans & Ó Cofaigh 2003; Hiemstra et al. 2006; Rijdsdijk et al. 2010). This work supported a predominantly terrestrial, ice-contact origin for the sedimentary sequences in the southern half of the ISB on account of their diagnostic deformation structures and evidence of high cumulative strain.

Radiocarbon, optically-stimulated luminescence and exposure age dating have been applied to reconstruct the extent of the ISIS in the ISB and southern Ireland (e.g. Ó Cofaigh and Evans 2007; Ballantyne 2010; Ó Cofaigh et al. 2012a; Small et al. 2018). Chiverell et al. (2013) used Bayesian modelling to produce the first regional reconstruction of deglaciation of the ISB. This indicated attainment of maximum extent 24-23.3 ka BP (mid-outer shelf, at southernmost core recovery of the Melville Till; Scourse et al. 1990), followed by very rapid (550 ma^{-1}) retreat to the southern Irish coast-Pembroke by 23.7-22.9 ka BP and slower but variable ($100\text{-}250 \text{ ma}^{-1}$) average rates thereafter. Chiverell et al. (2013) suggested the high rates to reflect initial eustatic rise and subsequent ocean warming associated with Heinrich Event 2, combined with much greater palaeotidal ranges and inherent instability of the ISIS both suggested by modelling. These authors also considered the variable retreat rates with respect to bed slope and conduit width, finding coincidence of higher retreat rates with reaches of reverse bed slope and wider basin also lacking topographic pinning points.

Until relatively recently, most information available regarding ISIS retreat timing and pattern was based on terrestrial data (Ballantyne & Ó Cofaigh 2017), with detailed offshore sediment studies recording a low-energy, cold-water glacimarine environment of retreat but lacking chronological control (e.g. Scourse et al. 1990). To date, few detailed offshore glacial geomorphological mapping investigations (e.g. van Landeghem et al. 2009; Fig. 2.4) have provided insight into glaciological conditions during ISIS retreat. The first chronological constraint on ISIS retreat

offshore was reported by Praeg et al. (2015), who investigated seismic profiles and cores and extended the ISIS limit of Scourse et al. (1990) by 150 km to the outer shelf of the Celtic Sea on the basis of glacitected glacimarine sediments radiocarbon-dated to 24.3 ka BP. These authors inferred retreat as a tidewater margin, in response to northward migration of the polar front following Heinrich Event 2 (cf. Scourse et al. 2009) from phasing between % *Neogloboquadrina pachyderma* changes and BIIS IRD flux peaks in northeast Atlantic deep-sea cores.

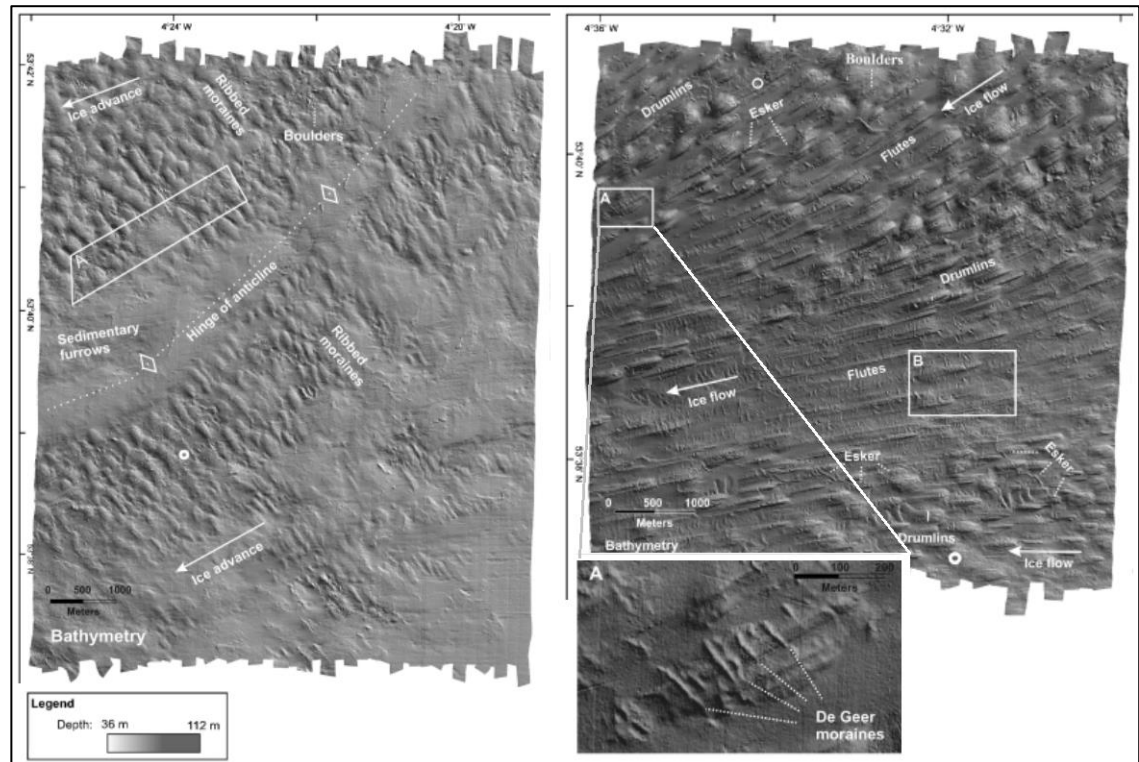


Fig. 2.4: Seafloor geomorphology of the former bed of the ISIS northwest of Anglesey (central ISB). Left panel shows ribbed moraine interpreted as recording fracturing of the frozen bed above an upstream-migrating thaw front (cf. Kleman & Hättestrand 1999). Right panel shows streamlined landforms (recording grounded, streaming ice) overprinted by sharp-crested De Geer moraines (inset) marking the position of a retreating tidewater margin. From van Landeghem et al. (2009).

A more detailed study by Scourse et al. (2019) has provided further insights into the timing and extent of the ISIS on the Celtic shelf. These workers examined seismic profiles and 51 cores from the inner shelf to the shelf edge, carrying out sedimentological, geochemical and micropalaeontological analysis and obtaining further radiocarbon ages. Eight lithofacies associations were recognised between the cores, comprising firm diamicton, overlain by massive, upward-fining shelly sands and variably deformed laminated and massive muds and sands with shell fragments, dropstones and commonly high shear strengths. The sequences were interpreted as recording advance of grounded ice and retreat involving readvance(s) before postglacial–Holocene transgression of the shelf. Acoustic facies equivalent to the deformed sands and muds

are distributed across the mid-outer shelf, suggesting pervasive readvance during retreat, but at present it is not possible to determine the extent or number of readvance(s) implied (Scourse et al. 2019). The retrieval of firm diamicton from a shelf break core extended the ISIS limit 20 km further south than implied by Praeg et al. (2015).

Foraminiferal analysis was carried out on the glacitectonised lithofacies in three cores, revealing a combination of temperate- and Arctic/glacimarine-associated species (Fig. 2.5) consistent with incorporation of pre-existing marine sediments into the subglacial deforming layer of the ISIS (e.g. Austin & McCarroll 1992; Shakesby et al. 2000).

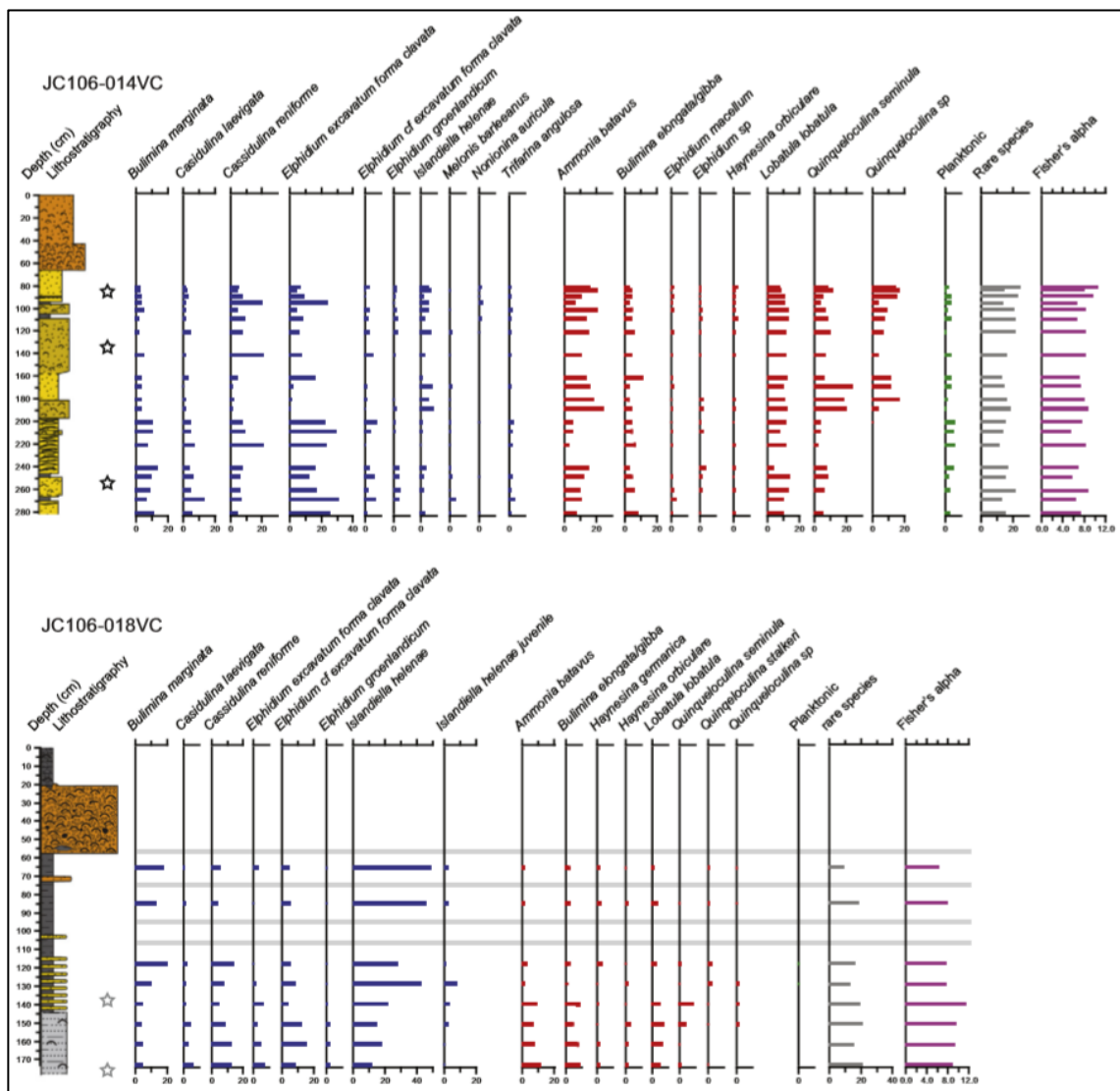


Fig. 2.5: Benthic foraminiferal assemblages in glacitectonised sands and muds from the outer Celtic shelf. Note the very low proportion of planktic foraminifera ($\leq 6\%$). Blue and red plotting represents interpreted species temperature preference (cold and warm, respectively). From Scourse et al. (2019).

Important Arctic-associated species are *Elphidium clavatum* and *Cassidulina reniforme* (along with *Islandiella helenae*, not reported in Ó Cofaigh et al. 2019 or Peters et al. 2015; 2020). In contrast to Peters et al. (2015; 2020), Scourse et al. (2019) consider *Cassidulina laevigata* a cold-water ‘indicator’ as opposed to Atlantic Water-associated. Various workers have associated *C. laevigata* with Atlantic Water (e.g. Mackensen & Hald 1988; Klitgaard Kristensen & Sejrup 1996), while others (e.g. van Weering & Qvale 1983) have reported it as cosmopolitan. Another contrast with other BIIS foraminiferal studies is the designation of *Lobatula lobatula* (= *C. lobatulus*) as a ‘thermophilous’ species. This widespread species is reported living in Mediterranean (e.g. Milker et al. 2009) to glacial marine environments (e.g. Jennings & Helgadottir 1994) and is usually considered to exploit stronger currents due to its filter-feeding habit (Schönfeld 1997; Gooday 2003). As Scourse et al. (2019) implied that all the ‘warm-water’ species were reworked, this contrasts with interpretations of *C. lobatulus* in Peters et al. (2015; 2020) and Ó Cofaigh et al. (2019) as recording strong bottom currents during deglaciation.

Far higher retreat rates ($\leq 600 \text{ ma}^{-1}$) than in other BIIS sectors are a notable characteristic of reconstructed ISIS behaviour (e.g. Chiverell et al. 2013; Small et al. 2018). This has been suggested to reflect an inherently brief existence of the ISIS due to its large throughput (Scourse et al. 2019), which could theoretically cause rapid drawdown of ice volume exceeding catchment accumulation (cf. ‘surge’ in Boulton & Hagdorn 2006). Bathymetric conditions on the Celtic shelf likely facilitated rapid retreat, with Small et al. (2018) noting the lack of a trough or topographic conduit south of St. George’s Channel (reached $\sim 25 \text{ ka BP}$) as resulting in a wide, thin ice margin vulnerable to destabilisation and conducive to rapid retreat through sea-level rise and high calving rates. Scourse et al. (2019) note that clear geomorphic indicators of ISIS lateral extent (e.g. shear margin moraines) are missing from the Celtic shelf, leaving this loosely constrained by core samples of the Melville Till and an ice limit on the Scilly Islands. An apparent lack of terminal moraines and GZWs on the Celtic shelf (see e.g. Praeg et al. 2015) is consistent with rapid ISIS retreat.

The earliest ages obtained by Scourse et al. (2019) of 27.2 and 26.6 ka BP likely constrain the initial ISIS advance to the outer shelf. The remaining ages of 24.9–24.4 ka BP constrain deglaciation and are consistent with the deglacial date of Praeg et al. (2015), and the %chalk IRD record (considered as ISIS-sourced IRD) from the Goban Spur (Haapaniemi et al. 2010; OMEX-2K in Fig. 2.3), which registers peaks centred on 25.5 ka BP and 24.5 ka BP. Scourse et al. (2019) proposed initial retreat driven by GIA-induced RSL rise, further suggesting that the temporal coherence of initial BIIS retreat revealed by recent work (see Sections 2.2.2.–2.2.4) reflected peaking of isostatic depression following attainment of maximum BIIS extent in these sectors.

2.2.2. *The central western Irish shelf and Porcupine Bank*

Evidence of grounded ice advance across the continental shelf west of Ireland was first reported by Haflidason et al. (1997) and King et al. (1998), who identified N-S-oriented, parallel to subparallel ridges on the outer- to mid-shelf using seismic profiles and interpreted these as terminal moraines of the last glacial period. The first detailed glacial geomorphological mapping of the western Irish shelf (Peters et al. 2015) was combined with radiocarbon dating, sedimentologic and foraminiferal analysis on four vibrocores retrieved from the Slyne Trough, a bathymetric saddle separating the continental shelf from the Porcupine Bank (Fig. 2.3), to provide the first insights into depositional environments and glacial chronology in the area. These authors identified sinuous, asymmetric and furrowed E-W-trending ridges in the Trough and on the northern Porcupine Bank, which they attributed to short-lived grounding of a floating calving margin. Three lithofacies associations traced between the cores comprised soft to firm sandy-muddy basal diamictons containing shell fragments, overlain by soft, massive, clast-supported diamicton or laminated silt/clay interbedding with laminated sand. These lithofacies are succeeded abruptly by shelly sands. This sequence was interpreted as recording subglacial and glacimarine deposition, succeeded by bottom current intensification and winnowing culminating in sand deposition during postglacial transgression. Three radiocarbon dates were obtained on bivalves and a coral fragment, which constrained the advance of grounded ice to after 24.7 ka BP, the development of glacimarine/sub-ice-shelf deposition to ≥ 20.2 ka BP and the intensive bottom current activity to ≥ 19.1 ka BP.

An important feature of Peters et al.'s (2015) proposed event sequence was the development of an ice-shelf over the Slyne Trough, proposed on the basis of diamicton characteristics in two cores (softness, presence of till pellets, upwards increase in foraminiferal density, the planktic:benthic ratio and bioturbation). These authors suggested ice-shelf development in response to influx of Atlantic Water into the Slyne Trough (Fig. 2.6). Within the sediments interpreted as sub-ice-shelf facies, their data shows species common in the Atlantic Water-influenced Slyne Trough at present (*Cassidulina laevigata* and *Uvigerina mediterranea*) (Margreth et al. 2009; Fentimen et al. 2020) increasing in abundance as Arctic/glacimarine-associated species decrease. However, differentiation of relict sub-ice-shelf deposits as distinct from tidewater glacimarine sediments can be complicated by suspension settling and rain-out of coarser grains/clasts occurring together in both settings (e.g. Evans & Pudsey 2002; Kilfeather et al. 2011). Descriptions of sub-ice-shelf deposits have noted a general stratigraphic sequence of coarse-grained, sometimes rubbly diamictons which may be clast-supported and contain pellets of mud as described by Peters et al. (2015), overlain by laminated muds and massive, clast-free muds succeeded by open-marine mud containing IRD (e.g. Powell et al. 1996; Domack & Harris 1998; Domack et al. 1999; Evans et al. 2005; Smith et al. 2019).

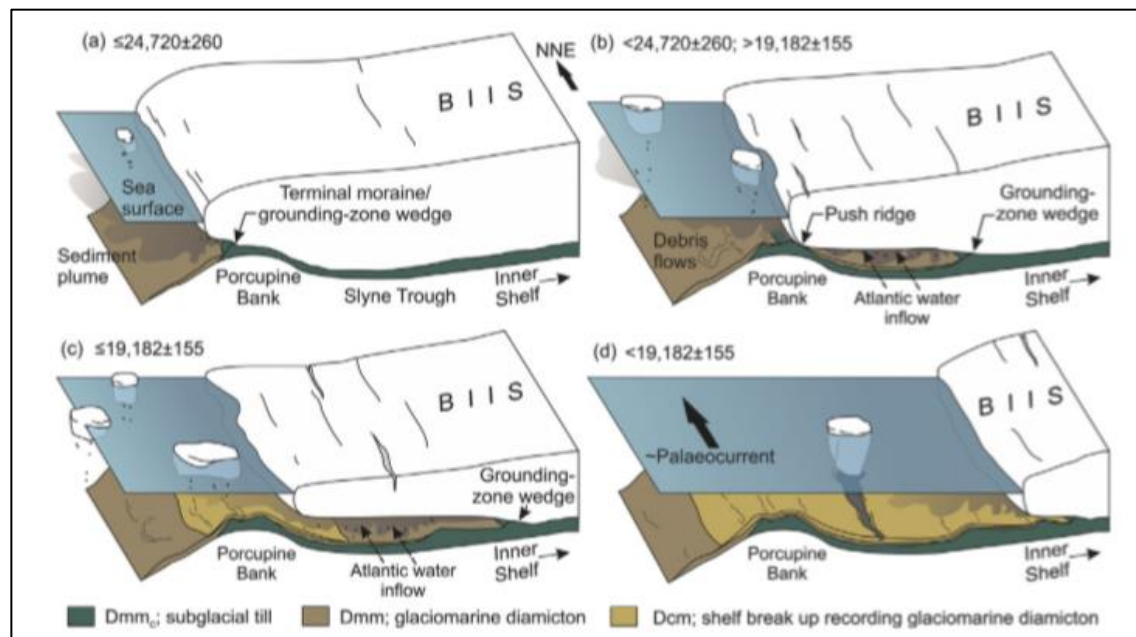


Fig. 2.6: Deglacial environments during BIIS retreat from the Porcupine Bank, including ice-shelf development in response to Atlantic water inflow, as proposed by Peters et al. (2015).

A subsequent study by Peters et al. (2016) extended the study area to the mid-shelf, and used a greater coverage of dated cores to constrain occupation of ice-marginal positions and estimate retreat rates onshore by interpolation to existing terrestrial exposure ages. Their earlier age for the onset of glaciomarine sedimentation in the Slyne Trough (21.8 ka BP) than at the ‘West Ireland Moraine’ (20.9 ka BP) was used to support the interpretation of ice-shelf formation and break-up outlined in Peters et al. (2015). A large, flat-topped ridge on the mid-shelf, the ‘Galway Lobe Grounding Zone Wedge’, was interpreted as a major stillstand position from 21.8–18.5 ka BP, formed beneath an ice-shelf fronting a lobe draining through Galway Bay. Subsequent investigation (McCarron et al. 2018) reported the stratigraphic structure associated with this feature as recording repeated occupation over ≥ 2 glacial periods, and Callard et al. (2020) suggested that the presence of this depocentre (the ‘Mid-Shelf Grounding Zone Complex’ [MSGZC]) preconditioned grounding-line stabilisation here during retreat of the last BIIS. Following retreat from the MSGZC, Peters et al. (2016) proposed that a readvance, correlative to the Clogher Head or Killard Point Stadial (McCabe et al. 2007a), occurred to a ridge nested inboard of the MSGZC. However, this was based on morphologic interpretation of this ridge as a readvance moraine. These authors also inferred post- global Last Glacial Maximum (gLGM) lobate readvances from Killary Harbour and Clew Bay, from the presence of smaller arcuate ridges on the mid-shelf. These ridges appear comparable to the Killala Bay ridges in Donegal Bay (Dunlop et al. 2010) in likely reflecting increased topographic influence on BIIS flow patterns (Fig. 2.7), and have since been interpreted as part of a shelf-wide 21 ka BP retreat isochrone by Roberts et al. (2020).

A recent study (Peters et al. 2020) of benthic foraminiferal assemblages in selected cores from Peters et al. (2016) found species associated with high productivity and temperate settings (*C. laevigata*, *Bulimina marginata* and *Bolivina sp.*; de Stigter et al. 1998; Gooday 2003) rapidly replacing the Arctic/glacimarine- associated species (*E. clavatum* and *C. reniforme*) during deglaciation. The importance of this ‘high-nutrient postglacial assemblage’ is greatest on the outer shelf, decreasing eastward towards the shallower inner shelf, and was interpreted to record either Atlantic Water or a meltwater-derived terrigenous nutrient supply (Peters et al. 2020).

The most recent retreat reconstruction for this sector (Ó Cofaigh et al. submitted; Fig. 2.7) presented 46 new radiocarbon dates and 13 new cores from ridges on Porcupine Bank and in the Slyne Trough, and also incorporated radiocarbon dates from Peters et al. (2015; 2016) and Callard et al. (2020) with terrestrial exposure ages from Roberts et al. (2020). Bayesian analysis (Bronk Ramsey 2008) was carried out on these compiled ages to provide a cross-shelf reconstruction of deglaciation from the outer shelf to onshore.

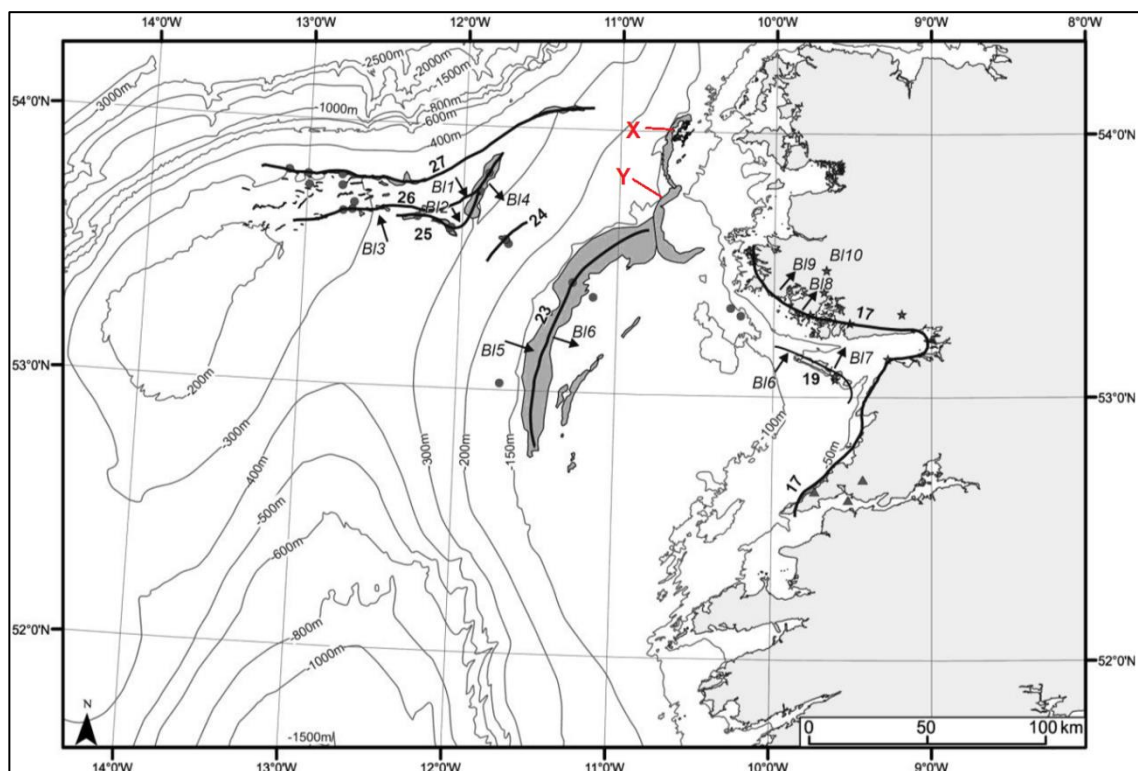


Fig. 2.7: Isochrones of BIIS retreat offshore Galway Bay, showing readvance positions, major moraines and grounding-zone wedges (GZWs), with approximate ages of occupation from Bayesian analysis in ka BP (from Ó Cofaigh et al. submitted). Note conformity of major GZW planforms with bathymetric contours. The two smaller arcuate moraines labelled X and Y on the mid-shelf were interpreted as recording later lobate readvances from Clew Bay and Killary Harbour by (Peters et al. 2016), and as belonging to a 21 ka BP retreat isochrone by Roberts et al. (2020).

The youngest maximum age reported for advance of grounded ice to the outer shelf by Ó Cofaigh et al. (submitted) was 25.1 ka BP, older than that of Peters et al. (2016) (24.1 ka BP), however constraining initial advance from these ages is complicated by the pervasive iceberg turbation suggested by some shell material in basal diamictons dating to as young as 17.6 ka BP (Ó Cofaigh et al. submitted). Importantly, the authors noted ages from glaciectonised glacimarine deposits as constraining a preceding retreat, and on this account reported minimum ages as early as 25.9 ka BP for initial retreat from the Bank. The timing of early-stage retreat during GS-3 is consistent with early gLGM recession of the BIIS elsewhere (Sections 2.2.1-2.2.6). These results are also consistent with the palaeoceanographic record of core MD01-2461 (Porcupine Seabight, Fig. 2.3) (Peck et al. 2006), which records a 400-year spike in the BIIS-sourced ice-rafted debris (IRD) flux beginning at 26.2 ka BP, and a negative salinity excursion implying increased meltwater contribution at 26 ka BP. Glaciectonised glacimarine sediments indicate retreat was characterised by periodic readvances, at least one reaching Porcupine Bank ~25 ka BP, and the Bayesian analysis of dates from these overridden deposits suggests the ice margin oscillated on the outer shelf until ~24.3 ka BP. This was followed by episodic, oscillatory retreat (~62 m a⁻¹) across the mid-inner shelf as evident from the successive grounding-zone wedges (GZWs) and moraines separated by overridden basin fills, with MSGZC occupation by 23.7 ka BP, and slow retreat (~8 m a⁻¹) from the Aran Islands, a probable pinning point, underway by 19.5 ka BP (Fig. 2.7) (Callard et al. 2020; Roberts et al. 2020). Ó Cofaigh et al. (submitted) excluded atmospheric warming as a driver of initial retreat on the basis of retreat beginning and extending to the mid-shelf within GS-3, and also argued against ocean forcing on account of concurrent % *N. pachyderma* values in northeast Atlantic cores including MD01-2461 (average 60% over 25.8-24.3 ka BP; Peck et al. 2007b) and OMEX-2K from the Goban Spur (average 95% over 25.8-24.3 ka BP; Haapaniemi et al. 2010). Instead, Ó Cofaigh et al. (submitted) suggested high RSL likely compounded by GIA as the initial driver, consistent with recent conclusions from three other Atlantic sectors of the BIIS (Sections 2.2.1.; 2.2.3.; 2.2.4.).

2.2.3. Offshore Donegal Bay (the northwest Irish shelf)

Prior to the availability of high-resolution geophysical data for the northwest Irish continental shelf, BIIS extension offshore in this region ('DBL' in Fig. 2.3) had been constrained by radiocarbon dates on reworked shells from diamicton underlying glacimarine muds at Glenulra Farm on the southern margin of Donegal Bay (McCabe et al. 2007b). These authors retrieved a maximum age for this implied advance of 28.2 ka BP and an earliest age for the subsequent glacimarine conditions of 28.3 ka BP, which they interpreted to represent a rapid (10² year-timescale) offshore advance preceding the LGM. McCabe et al. (2007b) noted the elevations (~80

m OD) of the Glenultra sequence as implying considerable glacioisostatic depression during its deposition, and proposed that its isostatically-depressed glacimarine depositional environment persisted from their youngest glacimarine age of 25.4 ka BP to dates of ~20 ka BP obtained by McCabe et al. (1986; 1993) from shelly muds elsewhere fringing Donegal Bay. This implied no significant offshore advance in the region during the LGM but persistence of an ice lobe centred in the Bay, which was locally inducing glacimarine conditions. This view of a more extensive pre-LGM BIIS was consistent with the conclusions of Bowen et al. (2002), who inferred multiple BIIS deglacial events from as early as 37 ka BP from ^{36}Cl dates mostly obtained from locations outside the traditional Midlandian limits in Ireland. These authors supported their findings on account of peaks in the Barra Fan IRD record extending to 45 ka BP (Knutz 2000), interpreting these as implying significant earlier BIIS expansions.

However, subsequent cosmogenic dating work contradicted this view of a less extensive LGM in northwest Ireland; Ballantyne et al. (2007) reported ^{10}Be ages for coastal deglaciation in County Donegal of 18.6-15.9 ka BP, and reconstructed the ice surface profile implied by the dated regional trimlines to indicate ice advance at least 20 km offshore. The earliest study reporting glacial features on the northwest Irish shelf was that of King et al. (1998), who described N-S-oriented, parallel to subparallel ridges on the outer shelf from shallow seismic profiles and interpreted these as terminal moraines. The first detailed geomorphological mapping of this shelf area (Benetti et al. 2010) identified features including a moraine along the shelf break (providing direct evidence for shelf-edge glaciation in the region), drumlin swarms on the inner shelf and extensive iceberg scouring on the outer shelf and slope. The 125 km-long, discontinuous outermost moraine is succeeded landward by numerous nested, narrower and more arcuate ridges with NE-SW orientation, backstepping for ~90 km to the entrance of Donegal Bay and interpreted as recessional moraines (Benetti et al. 2010; Fig. 2.8). These features were discussed in greater detail by Dunlop et al. (2011) and Ó Cofaigh et al. (2012b), who suggested their formation by episodic retreat of a NW-flowing ice lobe up to 120 km wide, sourced from the Donegal dome and Omagh Basin. However, as direct dating control for these ice-marginal positions was unavailable to construct a retreat chronology, preliminary constraints suggested by Ó Cofaigh et al. (2012b) (outer shelf occupation 29-27 ka BP, retreat beginning after 24 ka BP), were based on NE Atlantic IRD records.

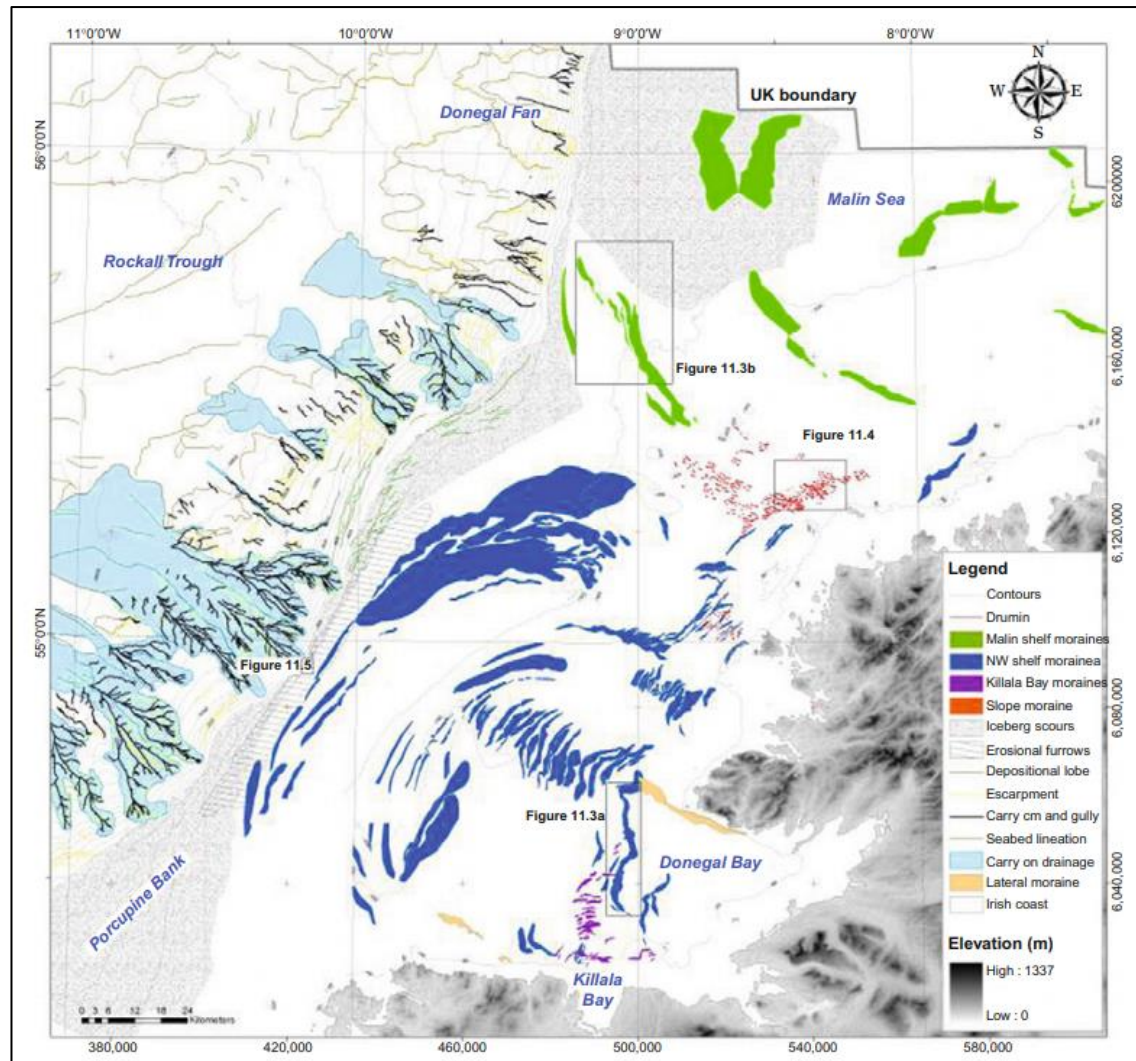


Fig. 2.8: Glacial geomorphological features offshore Donegal Bay in relation to ridges on the southern Malin shelf (from Dunlop et al. 2011).

A detailed deglacial reconstruction was carried out by Ó Cofaigh et al. (2019), who characterised and dated depositional environments by lithofacies analysis and radiocarbon dating on 27 vibrocores spanning the shelf break-inner shelf. Benthic foraminiferal analysis was also carried out on six cores to provide further constraints on depositional environments, particularly oceanographic conditions during deglaciation, to test the role of ocean forcing in initial retreat. Eight identified lithofacies comprised matrix-supported, occasionally shelly diamictons forming the shelf moraines, overlain by laminated, locally deformed soft muds with rare pebbles, usually transitioning abruptly into massive, locally bioturbated and diamictic muds. Seismic profiles along the core transects show these muds to infill basins between diamicton ridges, as seen offshore Galway Bay (Callard et al. 2020) and on the Malin shelf (Callard et al. 2018). The muds often interbed with laminated and upward-fining sands and then are succeeded abruptly by sands and shell-rich gravels. This sequence was interpreted as recording grounded ice advance to the

shelf break, followed by slow, episodic retreat as a grounded tidewater margin during which the numerous nested moraines were formed and muds were deposited into the inter-moraine depressions by suspension settling (Ó Cofaigh et al. 2019). The interbedded laminated and upward-fining sands were deposited by turbidity currents and the massive capping sands and gravels were laid down by bottom currents during postglacial transgression. Foraminiferal assemblages through the suspension-settled mud units (Fig. 2.9) are consistently dominated by two species; *Elphidium clavatum* and *Cassidulina reniforme*, generally considered ice-proximal and more distal species in glacial marine environments, respectively (e.g. Korsun & Hald 1998). Persistence of cold water temperatures throughout and following deglaciation is indicated by *E. clavatum*/*C. reniforme*-dominated assemblages remaining until <12.6 ka BP (see Ó Cofaigh et al. 2019; Wilson et al. 2019).

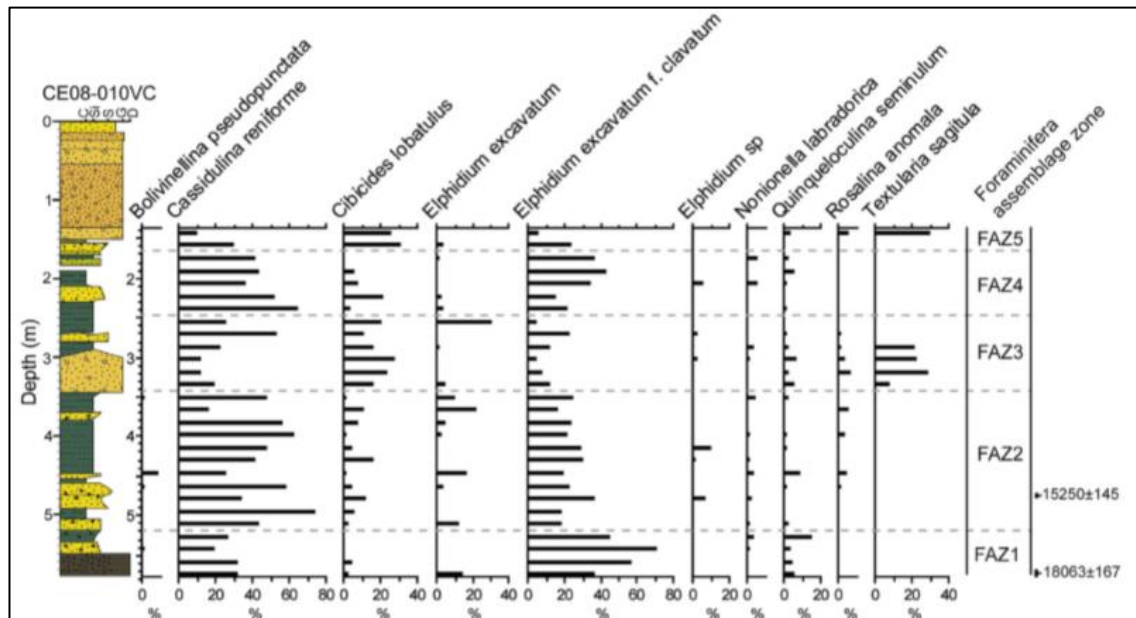


Fig. 2.9: Benthic foraminiferal assemblages from the mid-shelf offshore Donegal Bay (from Ó Cofaigh et al. 2019). The cold-water species *Cassidulina reniforme* and *Elphidium clavatum* clearly dominate the glacial marine muds and are reduced where concentration of *C. lobatulus* and *Textularia sagittula* occurs in the sand units. The latter two species are generally associated with strong currents and/or coarser substrates (e.g. Edwards 1982).

Twenty-two radiocarbon dates obtained from reworked and autochthonous marine carbonate were used to constrain the timing of advance and retreat of grounded ice across the shelf. The dates indicate that ice advanced to the shelf edge after 26.3 ka BP, had retreated to the mid shelf in a glacial marine environment by at least 24.8 ka BP, and had receded to ~10 km from the mouth of Donegal Bay by 17.4 ka BP (Ó Cofaigh et al. 2019). These constraints place initial deglaciation here to within the eustatic lowstand associated with the gLGM (Lambeck et al. 2014), which combined with the cold-water glacial marine environment of retreat indicated by the lithofacies and

foraminifera, suggests retreat was not driven by ocean forcing or atmospheric warming but was likely internally-initiated through GIA-induced RSL rise (Ó Cofaigh et al. 2019).

2.2.4. *The Malin shelf (Barra Fan Ice Stream)*

The first investigation of Quaternary sediments on the continental shelf of the Malin Sea (north of Ireland and west of Scotland) was carried out by Binns et al. (1974), who described core sequences and shallow seismic profiles from the inner shelf. These workers interpreted their general ‘till’→mud→sand sequence as recording the Devensian advance and retreat, followed by the Windermere Interstadial, Loch Lomond Stadial and Holocene. This was based on micropalaeontological investigations which revealed a ‘warm→cold→warm’ evolution of foraminiferal assemblages through the mud units, with the upper ‘warm’ assemblage returning a Holocene age. These workers identified advance of grounded Devensian ice to the outer shelf, however their interpretation of the ice streams (recognised from the cross-shelf troughs) as associated only with ice sheet build-up and retreat phases reflected the early stage of understanding of ice sheet drainage (Dove et al. 2015). Davies et al. (1984) further subdivided and extended Binns et al.’s (1974) regional stratigraphic framework, inferring several pre-Devensian shelf glaciations and proposing initial southwestward ice flow through the south Minch, deflected by the Outer Hebrides Ice Cap, before relatively insignificant volumes of ‘mainland’ ice flowed west to calve at the shelf break during the Devensian glacial maximum. While the distribution of large glacial ridges and debris fans in the region was known from geophysical, drilling and submersible investigations, predominantly by the British Geological Survey (BGS) for hydrocarbon exploration since the mid-1960s (Wilson 1977; Fannin 1989; Stoker et al. 1993), their affinities within regional glacial history lacked attention (with the exception of Selby 1989).

Multibeam echosounder and backscatter data from the Irish National Seabed Survey/Integrated Mapping for the Sustainable Development of Ireland’s Marine Resource project enabled the first detailed glacial geomorphological study of the Malin shelf (Dunlop et al. 2010), focusing on the area south of the Stanton Banks. This work revealed discontinuous NW-SE-trending ridges up to 50 km long, backstepping from the shelf break in an increasingly north-easterly direction, and a swarm of NW-SE-oriented streamlined mounds on the outer shelf (Fig. 2.10). These were interpreted as ice-marginal moraines and drumlinoid features, respectively, recording northwestward-flowing grounded ice from Donegal converging with Scottish ice (latter identified from ridge orientations) towards the shelf edge. Extensive furrowing on the outer shelf was interpreted to record initial retreat via calving triggered by RSL rise (Dunlop et al. 2010). Subsequent investigation by Howe et al. (2012) provided complementary evidence from the Sea

of Hebrides, revealing rock drumlins, megaflutes and grooves, interpreted as part of the onset zone of the same ice stream. Dove et al. (2015) presented further evidence of this onset zone in the Inner Hebrides, interpreting de Geer moraines in the overdeepened troughs as recording rapid retreat as a tidewater margin which slowed on reaching pinning points on the islands.

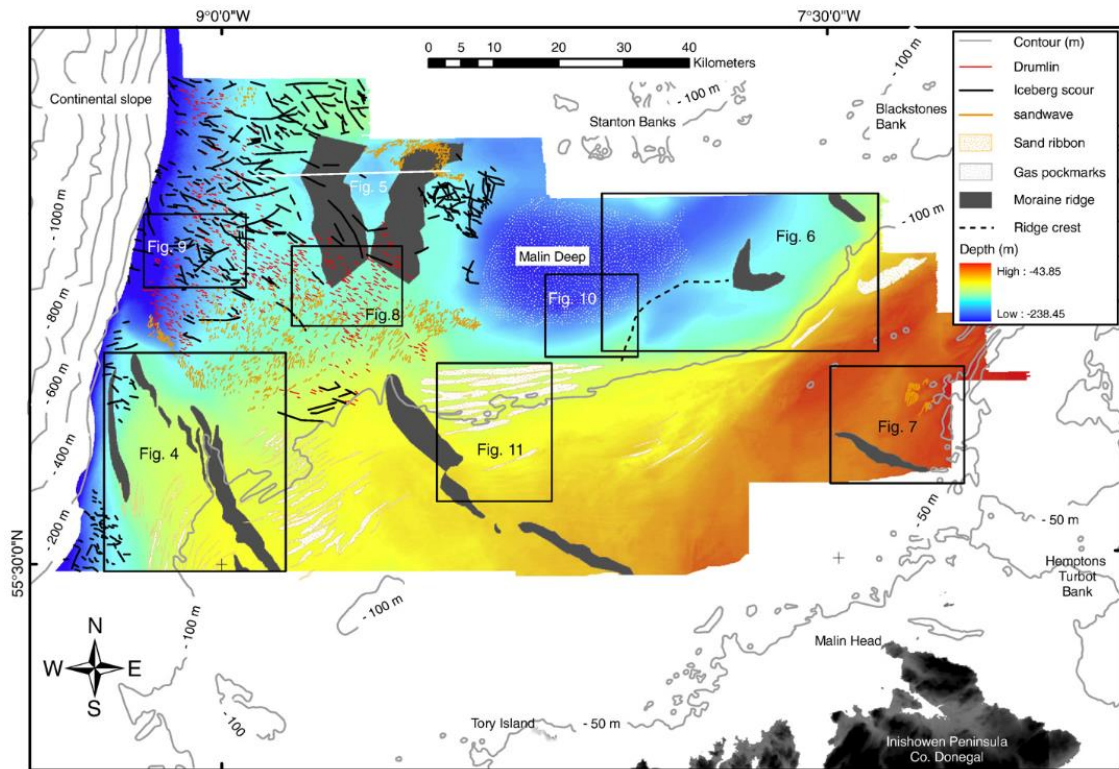


Fig. 2.10: Geomorphic features mapped on the southern Malin shelf by Dunlop et al. (2010). Note the signature of southwestward-flowing Scottish ice dominating the orientation of ridges backstepping across the southern area of the map. Compare with Fig. 2.11 for relation to retreat chronology.

Together, these geomorphological studies exposed the onset (Howe et al. 2012; Dove et al. 2015) and trunk zones (Dunlop et al. 2010) of the Barra Fan Ice Stream (BFIS; see Fig. 2.3) supplying the Barra-Donnegal Fan. While several studies of the IRD record from this fan (e.g. Knutz et al. 2001; 2002; Wilson et al. 2002; Scourse et al. 2009; see core MD95-2008 in Fig. 2.3) provide chronological control for marine-terminating ice presence on the Malin shelf during the last glacial period, uncertainty as to the glaciological implications of IRD records (e.g. whether ‘spikes’ reflect positive and/or negative mass balance (Scourse et al. 2009) and whether or not IRD concentration reliably tracks iceberg discharge (Clark et al. 2000)) prevented precise relation of geomorphological observations of the BFIS to climatic events and the evolution of the wider BIIS. However, a 2-3 kyr periodicity in alternating glacial and contouritic deposition on the

Barra-Donegal Fan since ~45 ka likely suggests responsiveness of the BIIS to Dansgaard-Oeschger variability-related circulation changes (Knutz et al. 2001).

By detailing the extent and flow history of the last BFIS, these investigations provided a basis for the retreat reconstruction of Callard et al. (2018), which examined 36 vibrocores along four sub-bottom profiler transects across the slope and outer to mid-shelf. These workers identified GZWs and small moraines on the outer shelf, and GZWs east of the Stanton Banks, interpreted as two broad areas of grounding-zone stabilisation. The width and low amplitude of the GZWs is consistent with restricted accommodation space beneath an ice-shelf, while the sharp-crested moraines imply formation at tidewater glacier margins (Batchelor & Dowdeswell 2015), implying changes in ice-margin configuration during retreat. Six lithofacies associations traceable between the shelf cores comprised extensive, firm shelly diamictos forming the moraines and GZWs, overlain by softer diamictic muds interbedded locally with occasionally deformed laminated muds forming drapes and basin infills. These were generally succeeded by soft, bioturbated, laminated then massive muds unconformably overlain by shelly sands and gravels. This sequence, similar to sedimentary successions previously reported from the Porcupine Bank (Peters et al. 2015; 2016) and Hebridean shelf (Austin & Kroon 1996), was interpreted as recording initial advance of grounded ice to the shelf break, followed by episodic retreat forming the moraines and GZWs, during which glacial marine conditions likely involving seasonal changes in the relative importance of ice-rafting and suspension settling deposited interbedded diamictic and laminated muds.

Increasingly ice-distal sedimentation recorded by massive and laminated mud was succeeded by winnowing and lag formation related to strengthening of bottom currents and postglacial sea level rise. Forty-four radiocarbon dates on reworked and autochthonous carbonate material indicated that grounded ice reached the shelf break after 26.7 ka BP, and began retreating in a glacial marine environment from the outer shelf by 25.9 ka BP and from the inner shelf by 23.2 ka BP (Fig. 2.11). A date of 20.2 ka BP on diamictic muds from the Inner Hebrides Trough provided a minimum age for full evacuation of grounded ice from the Malin Shelf. These dates revised existing interpretations of the Donegal-Barra Fan IRD record; including attainment of maximum BFIS extent by 27 ka BP (Wilson & Austin 2002), persistence of a shelf-edge BFIS through H2 (24 ka BP) (Scourse et al. 2009), a readvance to the outer shelf around 16-17 ka BP (Knutz et al. 2001) and major shelf deglaciation from 15 ka BP (Wilson et al. 2002). This highlights the difficulties associated with inferring glaciological events from IRD records in marine cores. The results of Callard et al. (2018) also revised the suggestion of Scourse et al. (2009) that the BFIS would have retreated relatively late on account of its proximity to the growth centre of the BIIS. Callard et al. (2018) discounted a role of atmospheric and ocean warming in the initial retreat of the BFIS, on the basis of the ≥ 2.6 kyr lead of their minimum age for initial retreat on the onset of

Greenland Interstadial 2 (23.3 ka BP on GICC05; Andersen et al. 2006), and on account of sea surface temperatures implied by surface Mg/Ca-palaeothermometry and % *N. pachyderma* from northeast Atlantic cores (6-9°C in Porcupine Seabight and 20-80% in Rockall Trough 26.7-25.9 ka BP; Peck et al. 2006; Hibbert et al. 2010 respectively). They instead proposed that deglaciation was driven by glacioisostatically-induced high RSL and aided by the reverse bed slope across the outer shelf.

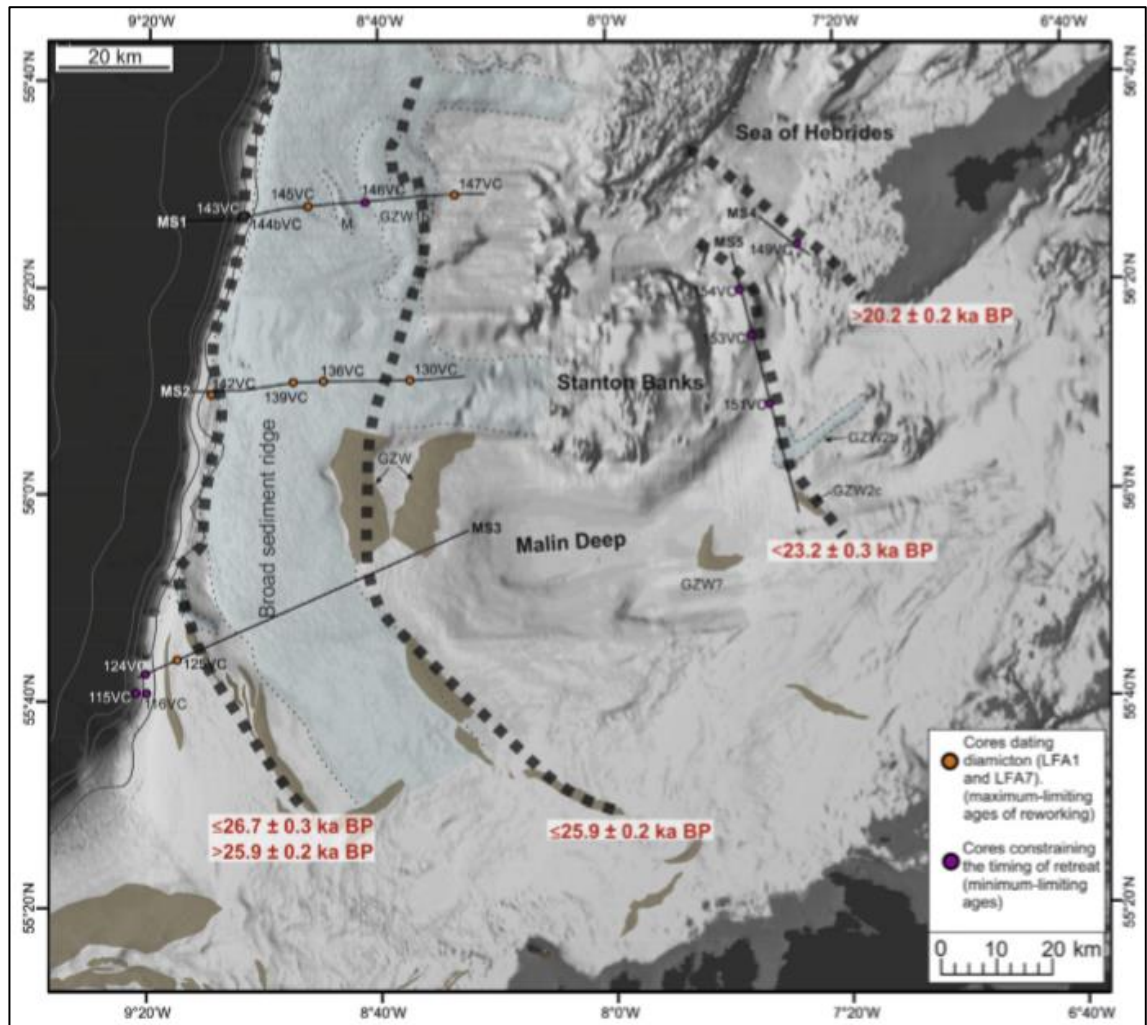


Fig. 2.11: Isochrones of BIIS retreat across the Malin shelf, showing grounding-zone wedges (brown) (from Callard et al. 2018).

2.2.5. The Minch and northern Hebridean shelf

The former drainage of ice into the North Minch (NW Scotland) was first inferred from terrestrial striae and erratic dispersal on the Isle of Lewis (von Weymarn 1979) and in the Northwest Highlands (Read et al. 1926; Johnstone & Mykura 1989; Stoker & Bradwell 2005; Bradwell et

al. 2007). Identification of elongated glacial erosion features such as megagrooves and drumlinoid ridges onshore and in seabed troughs subsequently allowed identification of the onset zone (including tributaries, e.g. Bradwell et al. 2008a; Bradwell 2013) of a Minch palaeo-ice stream (MnIS; see Fig. 2.3) (Stoker & Bradwell 2005; Bradwell et al. 2007). This ice stream drained ~15,000 km² of the BIIS and flowed northwest across the Hebridean shelf to terminate at the Sula Sgeir Trough-Mouth Fan (3750 km²) (Bradwell et al. 2008b). Subsequent investigations of seismic profiles within the Minch revealed multiple buried reflectors with a corrugated appearance interpreted as mega-scale glacial lineations, which combined with the size of the Sula Sgeir Fan suggests pre-Devensian activity of the MnIS (Stoker & Bradwell 2005). A seismostratigraphy for the Minch and Hebridean shelf was developed from BGS drilling and seismic surveying in the 1970s and 1980s (Fyfe et al. 1993; Stoker et al. 1993), and as in the case of the Malin Sea shelf, includes sequences from multiple glacial periods extending to at least the mid-Pleistocene. To date, however, direct dating and biostratigraphic investigation of deglacial sediments on the Hebridean shelf has been limited. Stoker (1988) described ridges and glacial sediments from the Hebridean shelf edge and upper slope (comprising a succession of debris flows overlain by diamictic muds), but considered these deposits to pre-date the LGM, reflecting contemporary views of an LGM BIIS limit in the Outer Hebrides (e.g. Sutherland & Walker 1984). The first detailed micropalaeontological analysis and radiocarbon constraints on deglacial sediments were reported by Graham et al. (1990), who described glacimarine environments from before 15 ka BP using foraminiferal and ostracod assemblages from a borehole in the North Minch.

The first detailed descriptions of seabed sediment ridges and interpretations of retreat style on the northwest Hebridean shelf were made by Bradwell & Stoker (2015; 2016), using seismic profiles and multibeam echosounder data. These authors identified subdued ridges up to 4.5 km wide and 50 km long on the outer shelf, and two broad arcuate ridges on the mid-shelf, interpreted as GZWs or moraines. On account of well-preserved streamlined landforms and an apparent absence of transverse ridges in the north Minch, Bradwell & Stoker (2015) tentatively inferred rapid retreat through the strait via calving across the regionally reverse bed slope (Fig. 2.12), before re-grounding as lobate outlets to form the arcuate moraines nearer the present coastline. Recent work (Bradwell et al. 2019) has advanced understanding of the retreat behaviour of the MnIS across the mid shelf to the present coastline, using single- and multibeam bathymetric data, seismic profiling, sediment cores and compiled terrestrial exposure and radiocarbon dates. This work revealed seventeen GZWs backstepping from the outer shelf to a point in the inner trough coinciding with an abrupt change in substrate and trough geometry (Fig. 2.13). Bayesian analysis of the compiled dates by Bradwell et al. (2019) found retreat rates increased to ~70 ma⁻¹ across the change in substrate and geometry. Geomorphic and sedimentary evidence of a sudden, high-

volume calving event associated with this transition up-ice from soft sediment to bedrock (intense furrowing and gravel-rich glacimarine drapes, respectively), was interpreted to record collapse of a buttressing ice-shelf related to thinning due to decreased grounding-line ice fluxes as the grounding-line retreated onto the rougher bedrock substrate.

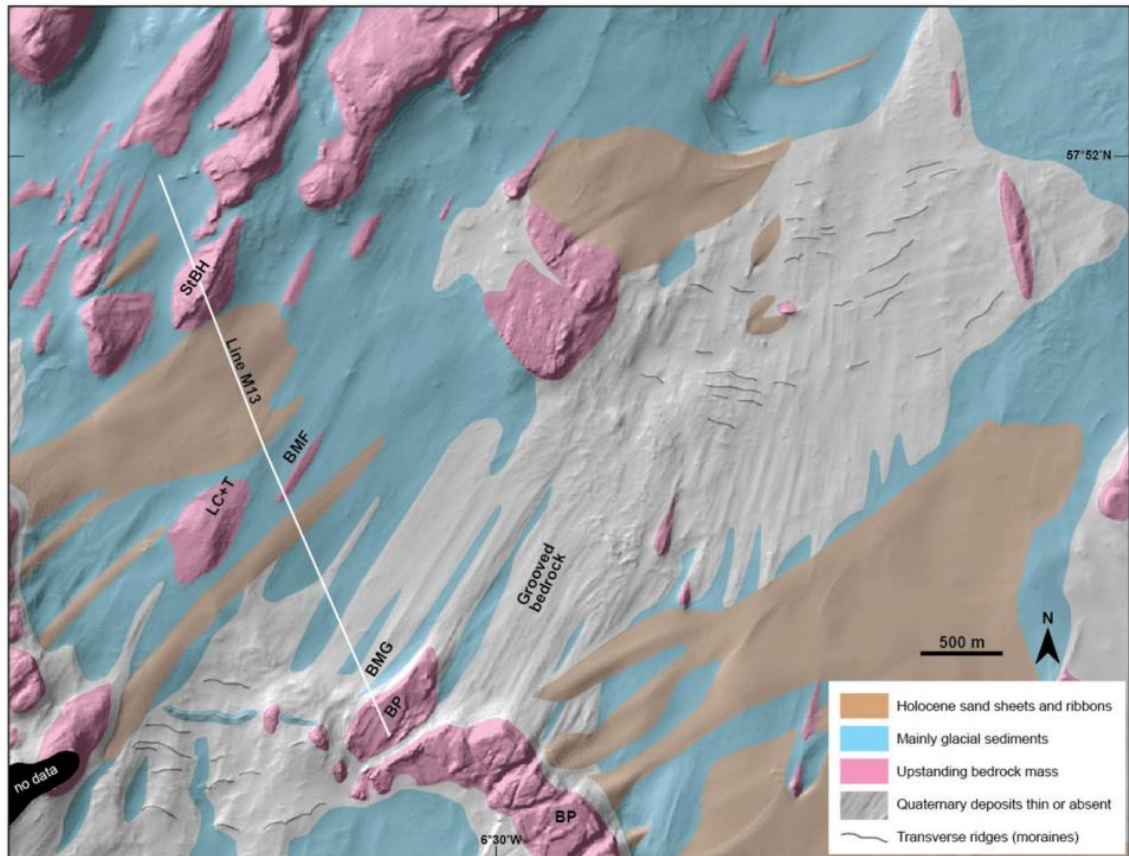


Fig. 2.12: Seafloor geomorphology near the southeast coast of the Isle of Lewis as mapped by Bradwell & Stoker (2015). This area of rocky seabed with thin, discontinuous sediment cover shows streamlined, converging elongated bedforms (crag-and-tails and megagrooves) formed through ice streaming in the onset zone, overprinted on shallower ground by transverse ridges interpreted as recessional moraines.

This was compounded by coincident widening of the trough, which would have reduced the importance of lateral drag in resisting the driving stress (Bradwell et al. 2019). From comparison with palaeoclimatic records, the authors inferred that this event (occurring between 18.5 and 16 ka BP) occurred in apparent absence of external forcing, implying the primacy of local factors in influencing this stage of retreat. Cosmogenic dates (Everest et al. 2013) indicate ice overrode North Rona (~40 km inboard of the Hebridean shelf edge) before ~25 ka, and are the only published chronological constraints on early stages of MIS retreat on the outer Hebridean shelf. These were recalculated by Bradwell et al. (2019) to ~27.5 ka BP, who suggest the MnIS grounding-line had retreated to the mid-shelf by this time. Interpolation between dated cores on the outer Hebridean shelf has yielded similarly slow early retreat rates for the MnIS (10-20 ma^{-1})

to those offshore Donegal Bay ($\geq 35.7 \text{ ma}^{-1}$; Ó Cofaigh et al. 2019) and Galway Bay ($\geq 19\text{-}30 \text{ ma}^{-1}$; Ó Cofaigh et al. submitted) (Bradwell et al. 2019).

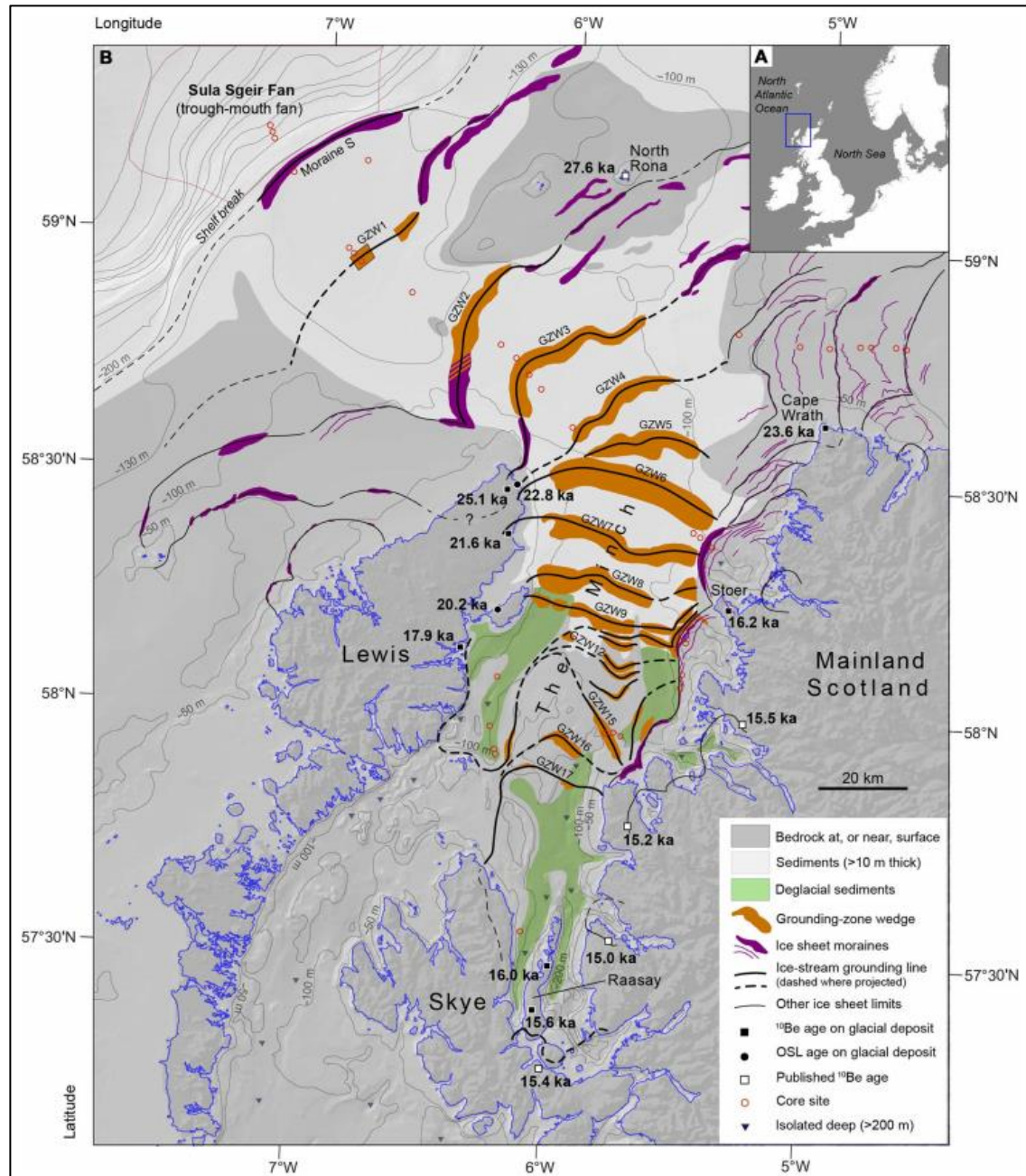


Fig. 2.13: Map of the Minch and Hebridean shelf from Bradwell et al. (2019) showing backstepping moraines and GZWs, seafloor substrate and terrestrial exposure ages. Note the changes in GZW size and planform across the transition to bedrock substrate. Bradwell et al. (2019) interpreted the smaller GZWs to have been deposited as the MnIS retreated by catastrophic calving events during its terminus transition from an ice-shelf to tidewater cliff.

2.3. Northeast Atlantic palaeoceanography during the last glacial period: potential for ocean forcing along the BIIS Atlantic margin?

2.3.1. Background to the North Atlantic

Since the recognition of millennial-scale climate variability (Dansgaard-Oeschger [D-O] events; Johnsen et al. 1992; Dansgaard et al. 1993) in North Atlantic marine records (Broecker et al. 1992; Bond et al. 1993; Bond & Lotti 1995; Fronval et al. 1995; Dokken & Hald 1996), a major research objective has been to understand the palaeoceanographic changes associated with these suborbital-scale climatic variations. This is because the millennial periodicity (~1.5 kyr) of D-O variability suggests a role for the ocean in transmitting this forcing, via threshold processes, into the marked climatic oscillations observed (Alley et al. 1999; McManus et al. 1999), though the ultimate driver of D-O variability remains uncertain (cf. Schulz 2002; Rahmstorf 2003; Wunsch 2006). In particular, the North Atlantic region, where D-O variability is most pronounced (Rasmussen et al. 2016), has been implicated as the key oceanic area as major iceberg-rafting events (Heinrich events) characterising peak stadial conditions there (Grousset et al. 1993; Andrews 1998; Hemming 2004) are considered to have supplied sufficient freshwater to disrupt its deep-water formation, a critical component of the global thermohaline circulation (e.g. Paillard & Labeyrie 1994; Cortijo et al. 1997; Ganopolski & Rahmstorf 2001).

Deep-water formation in the northern North Atlantic and Nordic Seas presently occurs through cooling and sinking (open-ocean convection) of warm, subtropically-sourced surface Atlantic Water (Hopkins 1991; Orvik & Niiler 2002). As this Atlantic Water (Fig. 2.14) is a major source of heat and moisture to higher latitudes, particularly to northwest Europe (Rasmussen et al. 1996a; Chapman & Shackleton 1998), variations in its influx to the Nordic Seas are expected to have accompanied D-O variability and to have had significant implications for the mass balance of circum-Atlantic ice sheets and sea-ice concentrations (Rasmussen et al. 1996b; Dokken & Jansen 1999; Rasmussen & Thomsen 2004; Boers et al. 2018; Sadatzki et al. 2019). However, some authors have challenged the importance of overturning circulation changes in D-O cyclicity, questioning the disruptive potential of Heinrich event freshwater fluxes and the importance of the North Atlantic as an ‘entry point’ to forcing changes in global thermohaline circulation patterns (e.g. Wunsch 2006; Huybers & Wunsch 2009; Wunsch 2010).

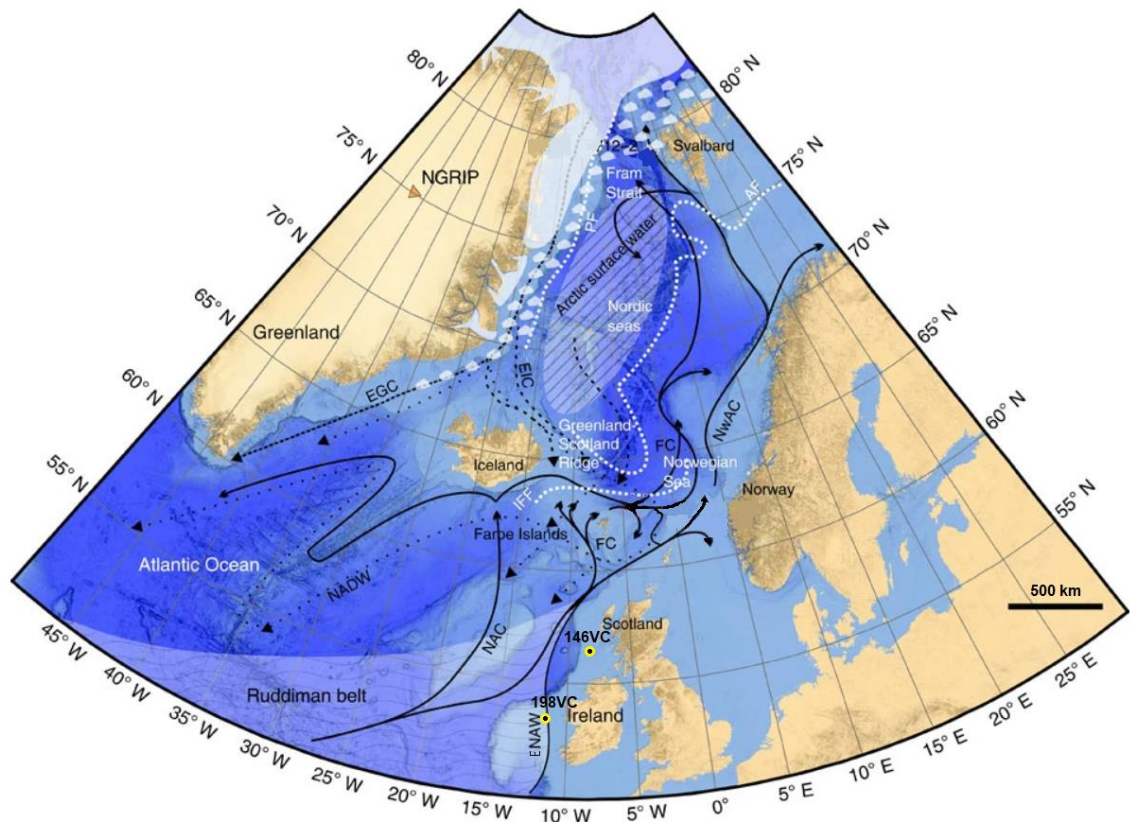


Fig. 2.14: Map of the Northeast Atlantic and Nordic Seas, including the major surface currents ('Atlantic Water'; solid lines) and deep outflow (dotted lines) pathways and present summer sea ice extent (white area). Locations of the cores studied in this project are indicated. EGC, East Greenland Current; EIC, East Icelandic Current; FC, Faroe Current; NAC, North Atlantic Current; NADW, North Atlantic Deep Water; ENAW, Eastern North Atlantic Water; NwAC, Norwegian Atlantic Current. The pathway labelled 'ENAW' represents the modern Shelf Edge Current. After Hoff et al. (2016).

2.3.2. Interstadial conditions

Early reconstructions of the northern North Atlantic during the last glacial period maintained perennial sea-ice cover over the Nordic Seas (e.g. CLIMAP Project Members 1976; 1981; Kellogg 1980). Well-ventilated deep/intermediate water in the glacial Nordic Seas was attributed to subsurface advection from south of the Polar Front, on account of the low reconstructed surface water salinities in the northern North Atlantic and suspected restriction of the North Atlantic Drift during glacial periods (e.g. Labeyrie & Duplessy 1985; Labeyrie et al. 1992; Boyle & Keigwin 1987; Duplessy et al. 1991; Oppo & Lehman 1993). Subsequent studies revealed at least seasonally open-water conditions throughout the Nordic Seas during the last glacial period, based on reconstructed sea-surface temperatures, $\delta^{13}\text{C}$ values and sedimentation rates found to be higher than under the present ice-covered central Arctic Ocean (e.g. Duplessy et al. 1992; Veum et al. 1992; Sarnthein et al. 1994; 1995; de Vernal et al. 2000; Fig. 2.15). With growing awareness of

D-O variability, succeeding studies increased temporal resolution and increasingly reported surface Atlantic Water inflow during the LGM and peaking during interstadials, from the southeast Nordic Seas into Fram Strait and the Arctic Ocean (e.g. Hebbeln et al. 1994; Maslin et al. 1995; Robinson et al. 1995; Dokken & Hald 1996; Hebbeln et al. 1998; Vogt et al. 2001; Nørgaard-Pedersen et al. 2003; Chauhan et al. 2014; Rasmussen et al. 2014; Müller & Stein 2014). This Atlantic Water and associated open-water conditions were proposed to explain the moisture source needed to sustain the growth to LGM extents of the adjacent Barents-Kara, Fennoscandian and British-Irish Ice Sheets (Hebbeln et al. 1994; Knies et al. 1999; Bauch et al. 2001; Hald et al. 2001; Knutz et al. 2001).

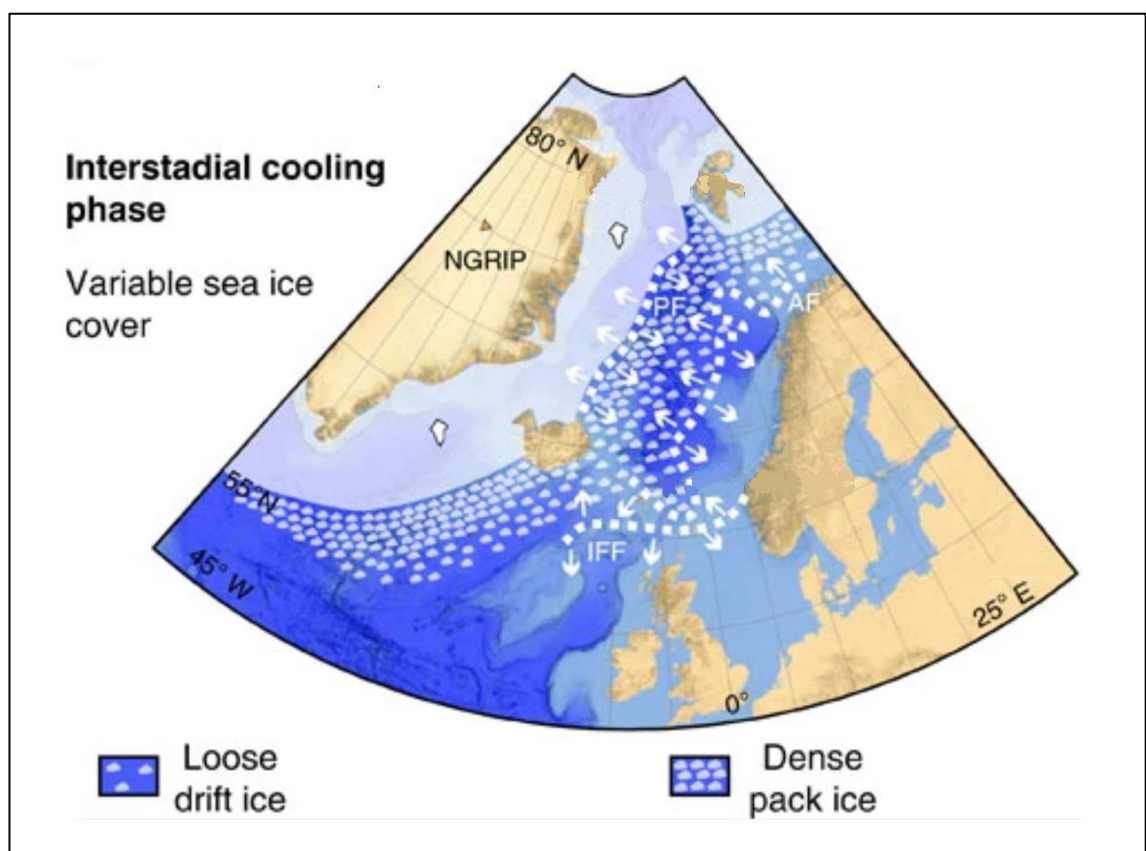


Fig. 2.15: Schematic map of the Northeast Atlantic and Nordic Seas during the transitional cooling phases between interstadials and stadials, showing migration of the Polar Front (PF) and Iceland-Faeroe Front (IFF) and the ice-free Atlantic Water corridor along the NW European margin. After Hoff et al. (2016).

Following the brief peaks of interstadial warmth, the Polar and Arctic Fronts and perennial sea-ice edge migrated southeastwards towards the Faeroe Islands during the transitional cooling intervals leading into the stadials (Lassen et al. 1999; Rasmussen & Thomsen 2004; Hoff et al. 2016) (Fig. 2.15). This frontal migration is apparent from the contrast in interstadial planktic and benthic foraminiferal and dinocyst assemblages across the Greenland-Scotland ridge (GSR,

separating the Nordic Seas and North Atlantic basins) (Rasmussen & Thomsen 2004; Wary et al. 2017a; cf. van Kreveld et al. 2000; Dokken et al. 2013; Wary et al. 2017b). Combined with generally heavy planktic and benthic $\delta^{18}\text{O}$ values and low/no sea ice biomarker concentrations, these assemblages imply at least seasonal open-water convection in the Nordic Seas, similar to the present configuration during much of the interstadials' durations (e.g. Rasmussen et al. 1996b; Dokken & Jansen 1999; Hagen & Hald 2002; Dokken et al. 2013; Hoff et al. 2016; Fig. 2.16). Present deep-water export across the GSR dominantly derives from and is compensated by the inflow of Atlantic Water (Hansen & Østerhus 2000; Blindheim & Østerhus 2005).

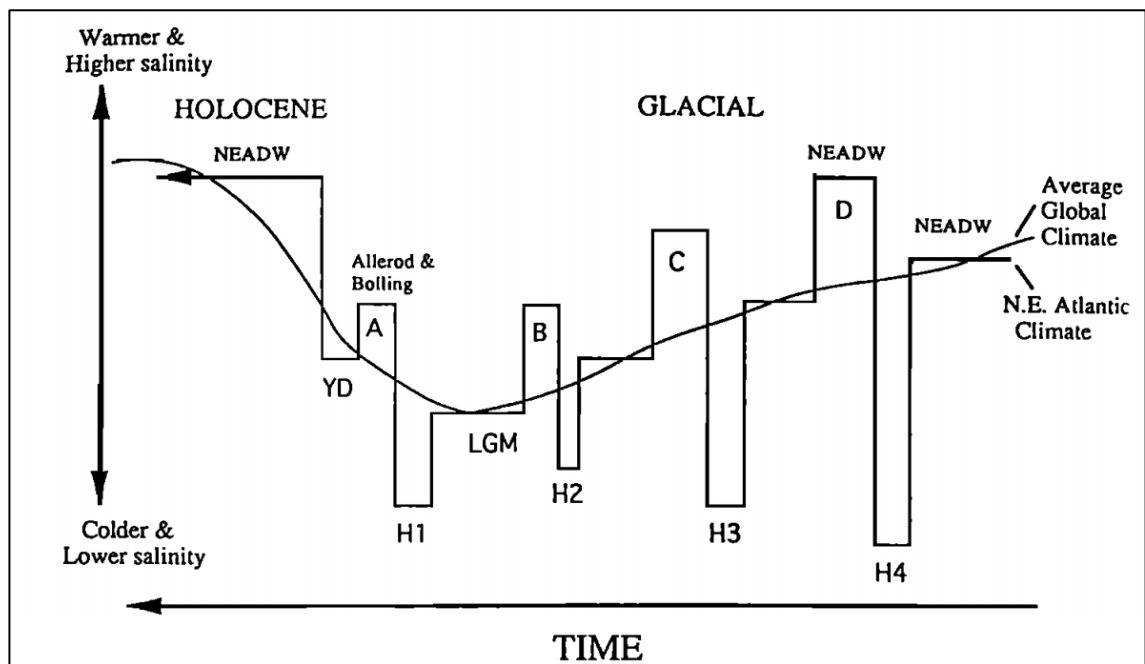


Fig. 2.16: Conceptual diagram showing evolution of Northeast Atlantic surface water conditions over the Bond cycles of the last ~45 ka. ‘NEADW’ labels denote periods where NADW formation is inferred in the Northeast Atlantic (from Maslin et al. 1995).

2.3.3. Stadial conditions

In contrast, stadials in both the North Atlantic and Nordic Seas were characterised by sea ice-, iceberg- and meltwater-influenced surface conditions, as implied by high % *N. pachyderma* (60-95%), light planktic $\delta^{18}\text{O}$ values and elevated IRD contribution relative to the interstadials (Rasmussen et al. 2002; Rasmussen & Thomsen 2004). Sea-ice biomarker and planktic foraminiferal records indicate that the perennial sea ice edge was usually located close to the Faeroe Islands, but extended further south during the coldest stadials (H6, H4 and H1; Lassen et al. 1999; Hoff et al. 2016). A stadial climatic gradient across the GSR is also evident in benthic foraminiferal assemblages, dominated by the chilled Atlantic Water-associated *C. neoteretis* in the southeast Norwegian Sea, but in the North Atlantic considerably more diverse and

characterised by temperate-associated species adapted to oligotrophic and dysoxic conditions (cf. Rasmussen et al. 1996a; 1996b; 1999; 2002).

Surprisingly, benthic $\delta^{18}\text{O}$ values are characteristically light during stadials on both sides of the GSR (Dokken & Jansen 1999; Meland et al. 2008). Interpretations of this observation have had varying implications for potential ice sheet-ocean interaction during stadials. Some workers have attributed these light $\delta^{18}\text{O}$ values to sinking of the low-salinity surface waters through brine rejection (e.g. Veum et al. 1992; Vidal et al. 1998; van Kreveld et al. 2000; Dokken et al. 2013), while others have linked them with the benthic assemblage interpretations as resulting from warming by subsurface Atlantic Water inflow (e.g. Bauch et al. 2001; Rasmussen et al. 2003; Rasmussen & Thomsen 2004; Fig. 2.17). The latter interpretation has since been supported by Mg/Ca analyses indicating warming at subsurface-intermediate depths during stadials in the Labrador Sea (Marcott et al. 2011), Arctic Ocean (Cronin et al. 2012), central north Atlantic (Jonkers et al. 2010) and southern Norwegian Sea (Ezat et al. 2014; Thornalley et al. 2015) apparently sufficient to explain the magnitudes of $\delta^{18}\text{O}$ depletion observed. This idea has also been proposed and modelled to explain the rapidity of interstadial warming by Atlantic Water resurfacing following halocline destabilisation (Kaspi et al. 2004; Shaffer et al. 2004; Rasmussen & Thomsen 2004; Mignot et al. 2007; Dokken et al. 2013). Rasmussen & Thomsen (2004) propose that subsurface penetration of Atlantic Water into the Nordic Seas was enabled by cessation of deep convection there due to migration of the Polar Front south of the GSR (e.g. Lassen et al. 1999; Hoff et al. 2016), acknowledging that this would require replacement of denser, intermediate-depth waters (see Meland et al. 2008).

Recently, Wary et al. (2016; 2017a; 2017b) have instead proposed surface Atlantic Water inflow above polar waters during stadials. However, this is largely based on a view (contrasting with ecological and biometrical studies; Bauch 1992; 1994; Carstens & Wefer 1992; Carstens et al. 1997; Kandiano & Bauch 2002) that residue fractions $>100\ \mu\text{m}$ overstate the importance of subpolar planktic foraminifera, leading to overestimated surface temperatures. This assumption resulted in a large contrast between reconstructed surface temperatures (warm, implied by dinocyst assemblages) and subsurface temperatures (cold, implied by % *N. pachyderma* abundances from the $>150\ \mu\text{m}$ fraction) during stadials, which Wary et al. (2016; 2017a; 2017b) interpreted as reflecting a strong pycnocline separating a thin Atlantic layer from underlying Polar waters. There are currently few additional studies supporting this view (e.g. Eynaud et al. 2002), and it is difficult to reconcile with the Mg/Ca and benthic faunal evidence noted in this section.

Upstream along the inferred stadial Atlantic Water influx, on the Irish and Scottish margins, fewer detailed faunal assemblage analyses are available but several % *N. pachyderma* records provide insight into surface/subsurface water conditions. A number of these records clearly document a

warming event during GS-3 which is not evident in the Greenland ice core records. This event was first reported by Rasmussen & Thomsen (2008, as *F-IS3b*) in core LINK17 from the North Sea slope, and termed *NEA-GS-3b* by Austin et al. (2012) as part of the local GS-3 event stratigraphy (Fig. 2.18).

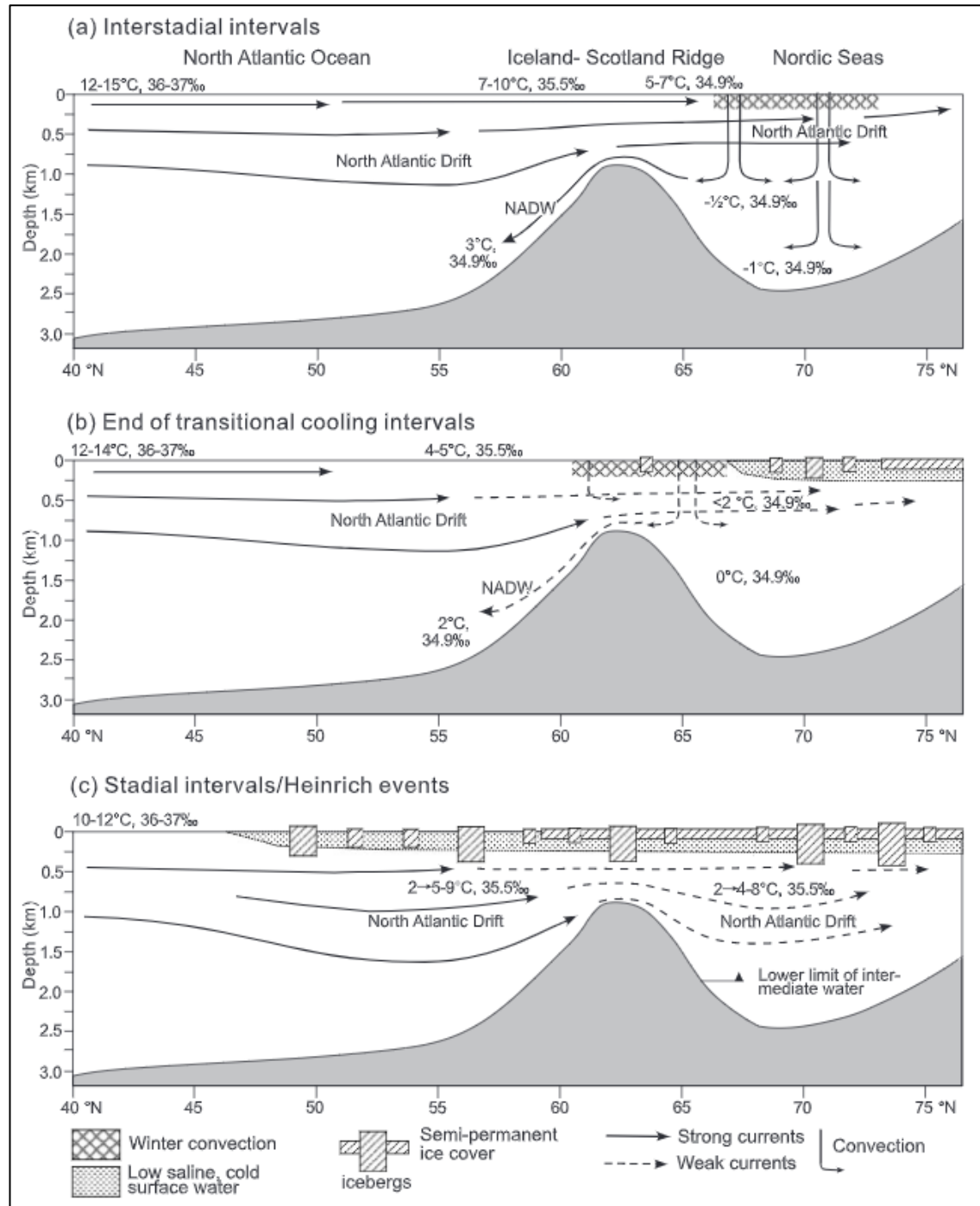


Fig. 2.17: Palaeoceanographic changes between interstadials and stadials in the Northeast Atlantic and Nordic Seas (from Rasmussen & Thomsen 2004). Stadial panel implies subsurface Atlantic Water inflow across the GSR under ~250 m of cold, low-salinity and iceberg-influenced open waters in a latitudinal range covering much of the BIIS's Atlantic margin. From Rasmussen & Thomsen (2004).

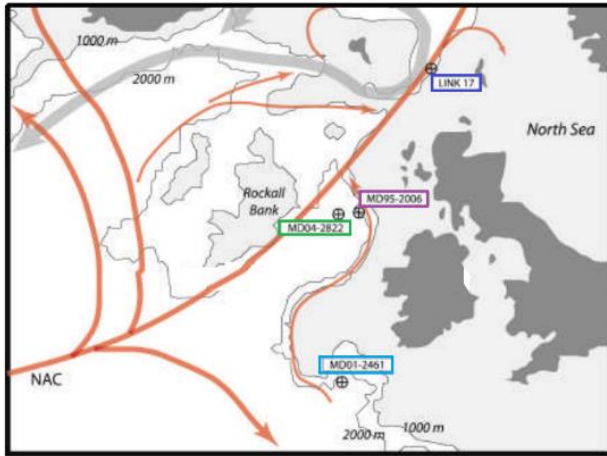
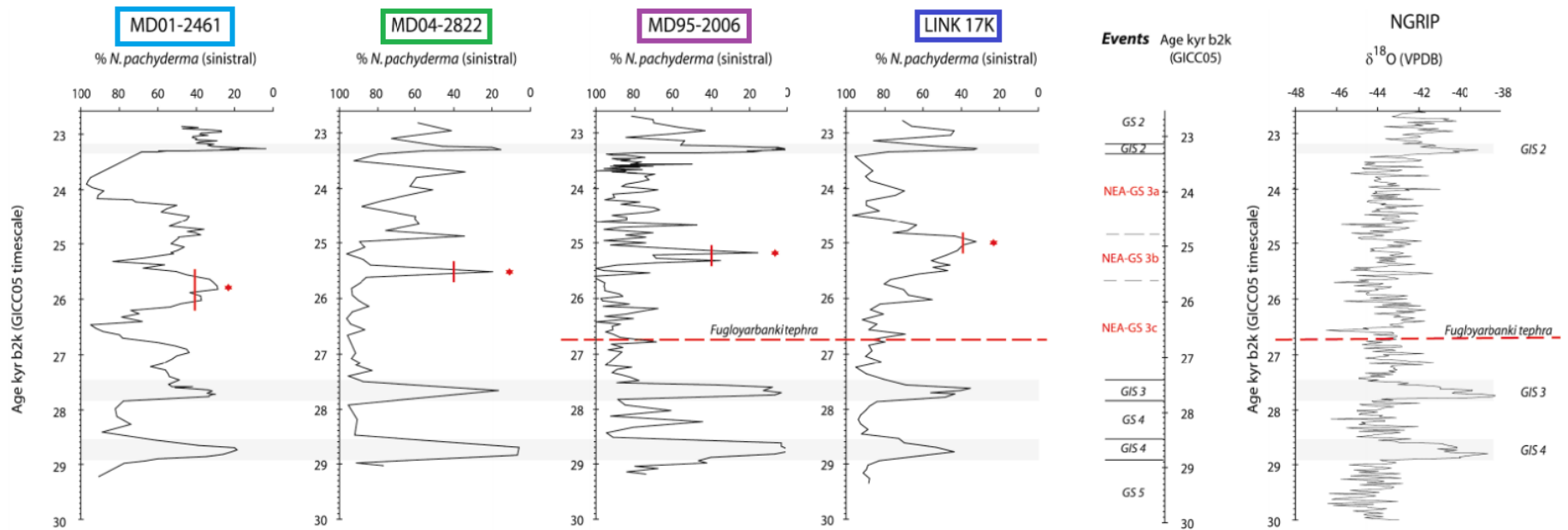


Fig. 2.18: % *N. pachyderma* records spanning GS-3 in cores along the Irish-Scottish margin from the Porcupine Seabight to the North Sea, showing the *NEA-GS-3b* warming event (red points). See Hibbert (2010) for details on the correlation methods, event stratigraphy generation and tuning of each record to the GICC05 timescale. Vertical red bars mark the 40% value of *N. pachyderma* relative abundance. *N. pachyderma* was counted from the >100 μm fraction in LINK17 and from the >150 μm fraction in the remaining cores. Modified from Hibbert (2010).



NEA-GS-3b registers as marked decreases in % *N. pachyderma* (to 20-40%; >100-150 μm fractions) from ~25.6-24.8 ka BP in the Porcupine Seabight (MD01-2461), Rockall Trough (MD04-2822), Barra Fan (MD95-2006) and North Sea slope (LINK17) (Hibbert 2010; Austin et al. 2012; Peters et al. 2008; Rasmussen & Thomsen 2008; Fig. 2.18). Mg/Ca-derived subsurface palaeotemperatures on *N. pachyderma* are available from one of these records (MD01-2461; Peck et al. 2008) and support the % *N. pachyderma*-inferred *NEA-GS-3b* warming, with estimated temperatures at ~150 m depth rising from ~7.5 to 9 °C in the event. Peck et al. (2008) suggested such ‘surprisingly high’ temperatures throughout the last ~55 ka BP to at least partially explain the high BIIS IRD flux from 26.5-17.5 ka BP, by providing moisture for accumulation while also ablating marine-based BIIS margins. These palaeotemperatures are consistent with those of Kandiano et al. (2004) and Maslin et al. (1995), but considerably higher than the GLAMAP 2000 reconstructions (Sarthein et al. 1995; 2000; Pflaumann et al. 2003), which inferred blockage and/or westward re-routing of the warmest Atlantic Water inflow along the Irish-Scottish margin by meltwater plumes during the gLGM.

As Hibbert (2010) and Austin et al. (2012) emphasise the difficulty determining the precise timing of *NEA-GS-3b* due to varying sedimentation rates and bioturbation between the above cores, a pronounced decrease in % *N. pachyderma* further south on the Celtic-Armorican margin at this time (see Zaragosi et al. 2001; Auffret et al. 2002; Mojtahid et al. 2005) may correspond to the event. Peters et al. (2008) suggest that *NEA-GS-3b* is evident in GSR overflow-intensity records from the Reykjanes Ridge (Moros et al. 2002; their ‘interstadial 3’). A weak warming from ~26-25 ka BP terminating at ~63°N, evident in Chapman & Shackleton (1998) and Weinelt et al. (2003), may also correspond to *NEA-GS-3b* but along the trunk axis of the North Atlantic Current. The magnitude of interstadial surface water warming rapidly decreases northward, along the North Sea and mid-Norwegian (Vøring) margins downstream on the inferred Atlantic Water pathway, where decreases in % *N. pachyderma* become lower in amplitude and *NEA-GS-3b* is not registered (Becker et al. 2018; Fig. 2.19). Austin et al. (2012) note that the absence of a corresponding warming signal in Greenland ice core records raises questions about the sensitivity of Greenland records to localised North Atlantic palaeoceanographic changes during the coldest stadials. This discrepancy would underline the importance of considering local event stratigraphies in investigating ice-ocean interactions during the last glacial period in the North Atlantic. A subsurface position (≥ 300 m depth; Dokken et al. 2013; Fig. 7.4) of inflowing Atlantic Water during stadials (e.g. Moros et al. 2002; Rasmussen & Thomsen 2004; Jonkers et al. 2010; Ezat et al. 2014) may explain the absence of a concurrent warming signal in the Greenland ice core records.

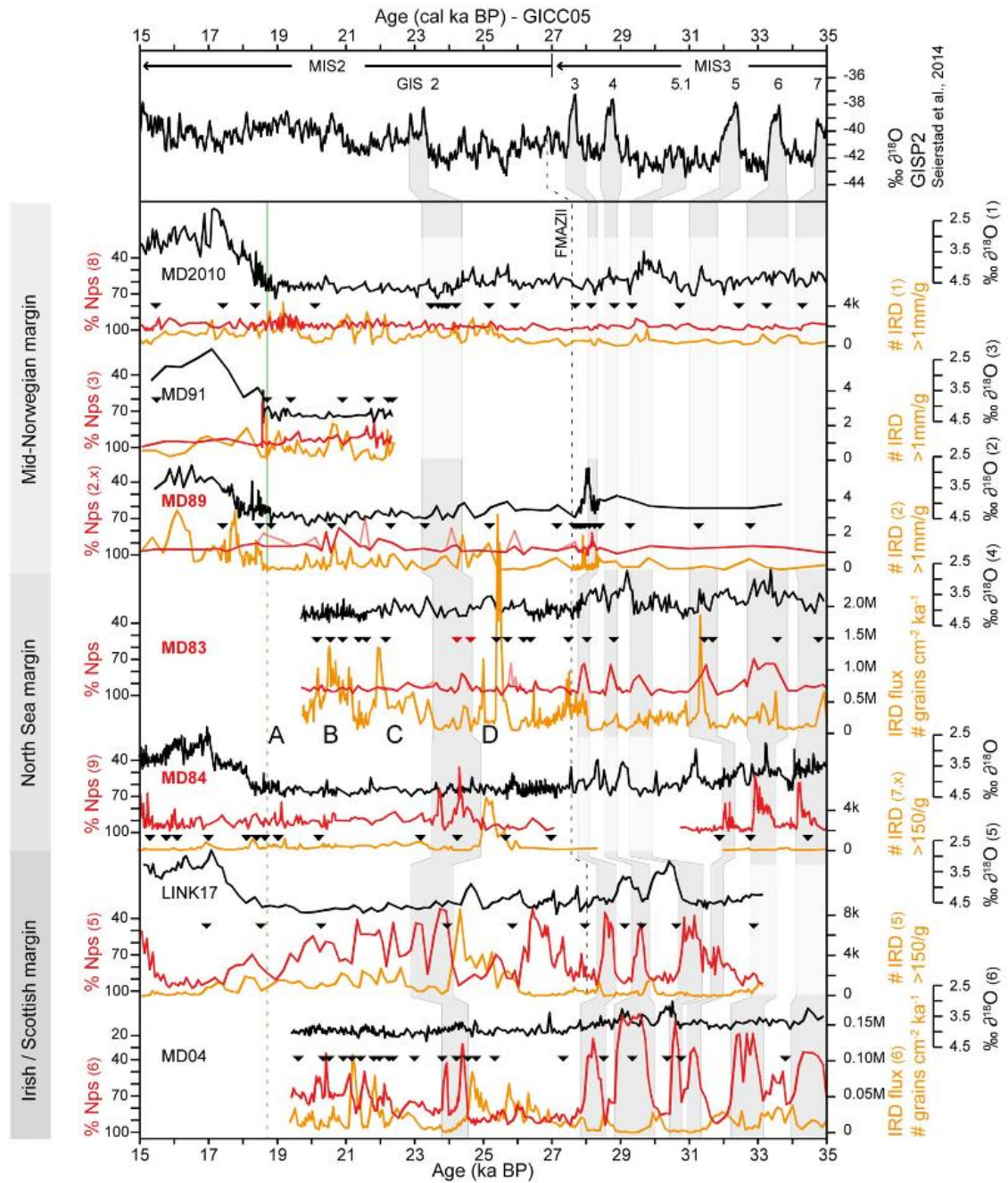


Fig. 2.19: IRD and % *N. pachyderma* records spanning 15-35 ka BP in cores along the Scottish and Norwegian margins from 59°N to 67°N. Note the arrangement in S-N order from left axis. Northward decline in the interstadial minima in % *N. pachyderma* and disappearance of the *NEA-GS-3b* event north of core MD84 are evident. % *N. pachyderma* represents the >150 μm fraction in all cores except LINK17 (>100 μm). From Becker et al. (2018).

2.4. Summary

2.4.1. Deglacial reconstructions

Section 2.2. above has detailed the current understanding of deglaciation for the five Atlantic BIIS sectors reconstructed to date. It has shown that all sectors exhibited temporal coherence in the onset of retreat, reached shelf-edge positions during the local LGM (ILGM) and began retreating under glacial conditions. Each sector then showed contrasting individual retreat behaviour reflecting the strong influence of local bathymetric conditions and glaciological factors:

- On the Celtic shelf, the ISIS commenced retreat after ~26.0 ka BP, initially characterised by extensive oscillation(s) but followed by very rapid retreat ($\leq 600 \text{ m a}^{-1}$) to St George's Channel by ~25 ka BP, with no evidence of intervening stabilisations. These very high retreat rates likely reflect the inherent glaciological instability of the ISIS related to high throughput, and its margin was probably wide, thin and susceptible to rapid retreat through RSL rise. Deglacial foraminiferal assemblages from the Celtic shelf are interpreted to record cold glacial conditions, although these show similar proportions of Arctic/glacial-associated and temperate, eutrophic- or shallow water-associated species. Ecological interpretations and assessments of reworking for these assemblages differ from those in other BIIS studies.
- Offshore central western Ireland, retreat was underway by 25.9 ka BP and characterised by oscillatory behaviour on the outer shelf, likely involving reoccupation of Porcupine Bank ~25.0 ka BP. It is likely that grounded ice on Porcupine Bank coincided with at least partially floating ice in the Slyne Trough during this time. Final retreat from the outer shelf occurred by 24.3 ka BP, and subsequent retreat was slow ($\sim 8\text{-}62 \text{ m a}^{-1}$) across the mid-inner shelf. This likely reflected the stabilising influences of normal bed slope, pre-existing ice-marginal structures and topographic pinning points. Deglacial foraminiferal assemblages from ~24.7 ka BP onwards (see Peters et al. 2015) are dominated by species associated with strong currents or temperate, nutrient-rich slope settings, with Arctic/glacial-associated species becoming more important on the mid-shelf. Atlantic Water presence has recently been inferred offshore central western Ireland from 21.5 ka BP onwards (Peters et al. 2020), but study is needed of earlier deglacial sediments to investigate whether this played a role in triggering and driving initial retreat in this sector.
- Offshore Donegal Bay, retreat began between 26.3 and 24.8 ka BP and occurred slowly ($5.5\text{-}\geq 35.7 \text{ m a}^{-1}$) and incrementally across the shelf as a grounded, lobate tidewater margin. Foraminiferal assemblages are clearly dominated by species associated with modern glacial and Arctic settings and indicate that Atlantic Water was not present

on the shelf during initial retreat. Slow retreat rates offshore Donegal Bay likely reflect influence of normal bed slope across the shelf in this region. In contrast to the ISIS and central western Irish sector, the Donegal Bay Lobe does not appear to have undergone substantial readvances during retreat.

- On the Malin shelf, retreat of the BFIS was underway by 25.9 ka BP and interrupted on the outer shelf by grounding-line stabilisations, during which extensive GZWs spanning the shelf were developed. These suggest an ice-shelf margin configuration during early retreat. Subsequent retreat across the mid-shelf between 25.9 ka BP and 23.2 ka BP was rapid and at least partly driven by reverse bed slopes and water depths in overdeepened troughs. Similarly to the Donegal Bay Lobe, there is no evidence of substantial marginal oscillation during BFIS retreat. A role for Atlantic Water in deglaciation has not been tested for the Malin shelf.
- On the northern Hebridean shelf, the MnIS probably reached the shelf break during the ILGM, but chronological control on retreat across the outer- to mid-shelf is presently limited. Recalculated exposure ages suggest ice-free conditions on the outer shelf as early as 27.6 ka BP. Retreat was slow and incremental across the normal bed slope of the outer-mid shelf, where the MnIS was probably terminating as an ice-shelf as implied by backstepping GZWs. Bathymetric and substrate controls were dominant influences on MnIS retreat behaviour across the mid-inner shelf. Involvement of Atlantic Water in MnIS retreat has not been investigated to date.

2.4.2. Northeast Atlantic palaeoceanographic conditions during BIIS retreat

Section 2.3. outlined current understanding of stadial and interstadial palaeoceanographic conditions in the adjacent and wider northeast Atlantic, to provide the palaeoceanographic context to deglaciation along the BIIS Atlantic margin as discussed in Section 2.2. and assess the potential for influence of warm water advection on BIIS retreat. It can be concluded that Atlantic Water advection is likely to have occurred along the western Irish-Scottish margin, at least episodically and probably beneath the surface, during the period of marine-based ice retreat in Atlantic BIIS sectors (which spans most of GS-3, GI-2 and much of GS-2):

- There is now substantial evidence for northward advection across the GSR of warm, likely subtropically-sourced Atlantic Water continuing during stadials. This Atlantic Water most likely occupied a subsurface position beneath cold, fresh surface waters strongly influenced by meltwater, sea ice and icebergs. The minimum depth of this Atlantic water mass is unclear, with estimates of ≥ 300 m in the southeast Norwegian Sea

but warming of 7.5 to 9 °C reconstructed for depths of ~150 m upstream in the Porcupine Seabight and further north along the Irish-Scottish slope.

- A pulse of Atlantic Water advection from ~25.6-24.8 ka BP, during GS-3, has been recognised in a number of cores along the continental slope from western Ireland to the North Sea. This event, termed *NEA-GS-3b*, occurs during the early period of retreat across the outer shelf in the four main Atlantic BIIS sectors with sufficient chronological control at present (the Celtic, central western Irish, Donegal and Malin shelves). This implies that Atlantic Water was present along the margin and therefore is a viable influence on early retreat of the BIIS provided it could access the ice margin on the shelf.
- It is now generally accepted that interstadial palaeoceanographic conditions involved surface Atlantic Water inflow into the Nordic Seas. The western Irish-Scottish margin and Faeroe-Shetland Channel adjacent to the northwestern BIIS were likely to have been an important pathway for this inflow, similarly to present conditions. The BIIS margin was retreating up the Irish Sea and across the mid-shelf in the remaining Atlantic-terminating sectors during GI-2. Recent studies offshore central western Ireland have suggested that Atlantic Water accompanied retreat across the mid-inner shelf during GS-3 and GI-2 in this area.

CHAPTER 3

STUDY AREAS

This chapter provides an overview of the modern environmental setting of the Malin shelf and the Porcupine Bank-Slyne Trough region, outlining key aspects of the hydrographic conditions, circulation, bathymetry and modern benthic foraminiferal communities. The glacial sediments, landforms and chronology have been detailed in Sections 2.2.2. and 2.2.4. for the study areas. Coring locations are given in Table 1 and smaller-scale maps showing the coring sites in their local geomorphic and bathymetric setting are included in Sections 5.1.1. and 5.2.1.

3.1. The Malin shelf

The Malin Sea is one of the northwest European shelf seas opening into the northeast Atlantic Ocean, and is located west of Scotland and north of Ireland approximately between 55-57°N and 7-10°W. The hydrography of the Malin Sea region is influenced by surface waters in the adjacent Rockall Trough, with Eastern North Atlantic Water (ENAW) dominating along the slope and on the outer shelf (Ellet 1979; Gowen et al. 1998; Stashchuk et al. 2017). ENAW originates in the Bay of Biscay, receiving contributions from underlying Mediterranean Outflow Water and Subpolar Intermediate Water, and has temperatures seasonally ranging from ~9-14 °C and salinities from ~35.4-35.5 PSU in the Rockall Trough (Ellet et al. 1986; Pollard et al. 1996; Holliday 2003). It is advected northward by the Shelf Edge Current (SEC), with a core typically above 500 m depth and seasonally and locally variable speeds of ~3-30 cm s⁻¹ (Pingree & Le Cann 1989; Burrows & Thorpe 1999; Stashchuk et al. 2017). The SEC represents the warmest, most saline Atlantic Water inflow pathway across the GSR to the Nordic Seas (Hansen & Østerhus 2002) and continues along the northwest European margin as the Norwegian Current before ultimately reaching the Arctic Ocean via the Barents Sea and Fram Strait (Hopkins 1991; Orvik & Niiler 2002). The Malin shelf edge is at a depth of ~150 m, and the continental slope descends steeply into the Rockall Trough (by ~50 m km⁻¹) (Fig. 3.1). This steepness of the continental slope encourages acceleration and 'leakage' of the SEC (ENAW) onto the outer Malin shelf, particularly in autumn and winter, with the extent onto the shelf modulated by tidal current strength (Ellet 1979; Hill 1995; Huthnance et al. 2009; Xing & Davies 2001) (Fig. 3.2). The ENAW is separated from the cooler, denser Malin shelf waters by a relatively sharp front on the outer shelf (Gowen et al. 1998). Mean bottom water temperatures on the outer shelf are ~10 °C in summer and ~8 °C in winter, and decrease slightly towards the inner shelf (~7.5 °C in winter), while mean bottom-water salinity is ~35.3 PSU on the outer shelf, decreasing to 34.5 PSU on the inner shelf (Elliott et al. 1991; Gowen et al. 1998; Murray 2003a; Hydes et al. 2004).

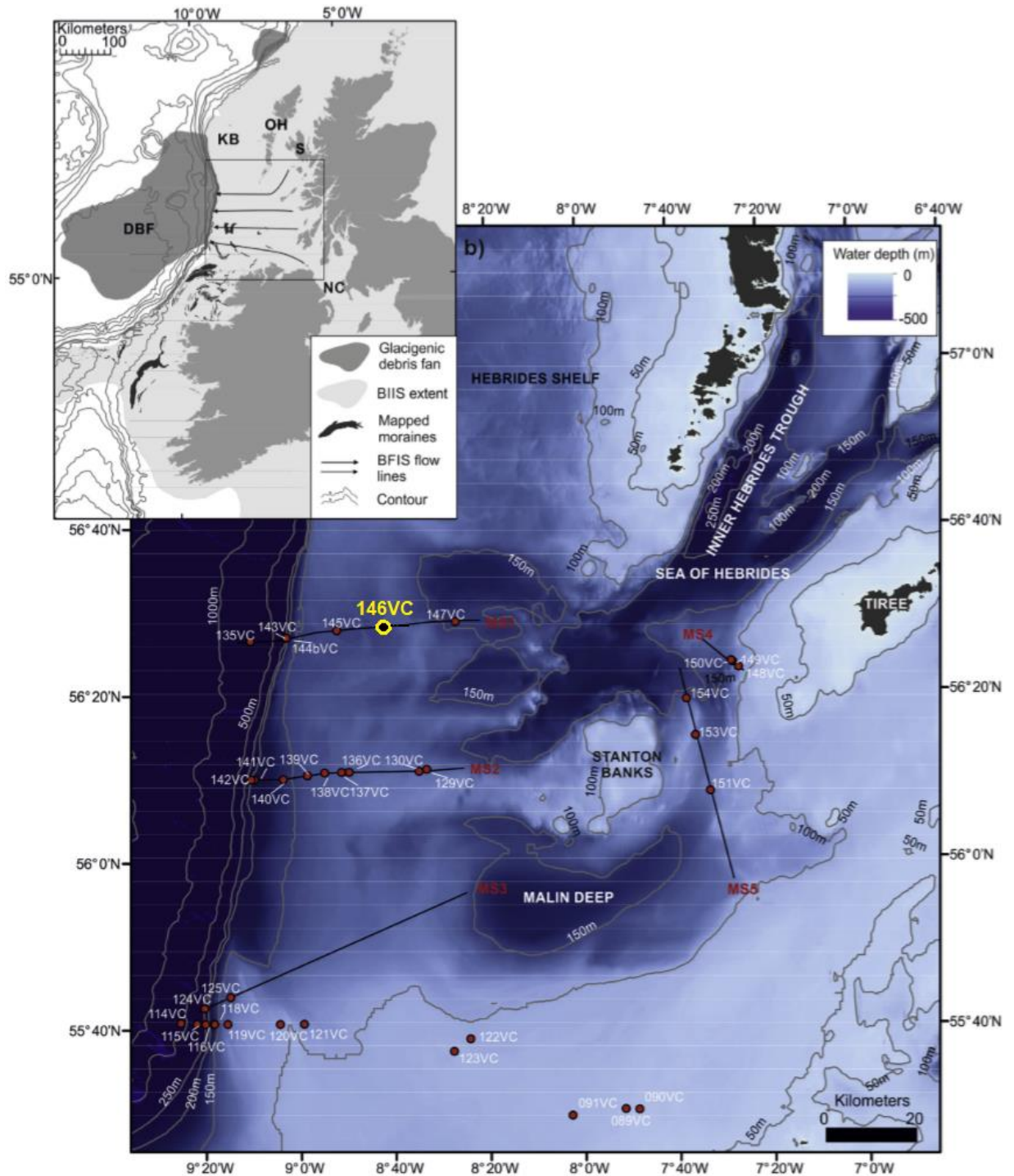


Fig. 3.1: Bathymetric map of the Malin shelf showing acoustic profile lines and coring sites, including 146VC, from the JC106 cruise. From Callard et al. (2018).

Water depths over the Malin shelf are generally less than 150 m, except for the central area of the shelf where there is a network of overdeepened basins centred around the Malin and Stanton Deeps (maximum depths of 190 m and 167 m, respectively), and a granitic high, the Stanton Banks (minimum depths of ~45 m) (Murray 2003a; McGonigle et al. 2009; Preston 2009; Garcia

et al. 2014) (Fig 3.1). The area is subject to relatively intensive wave action and tidal currents, with a 50-year significant wave height of 12-13 m, and maximum surface tidal current speeds of 51-102 cm s⁻¹ measured during spring tides (Lee & Ramster 1981; Stanton 1984). As a result, the shallower areas of the shelf, excluding the Deeps, are relatively high-energy environments subject to benthic disturbance during storms and by tidal currents (Murray 2003a).

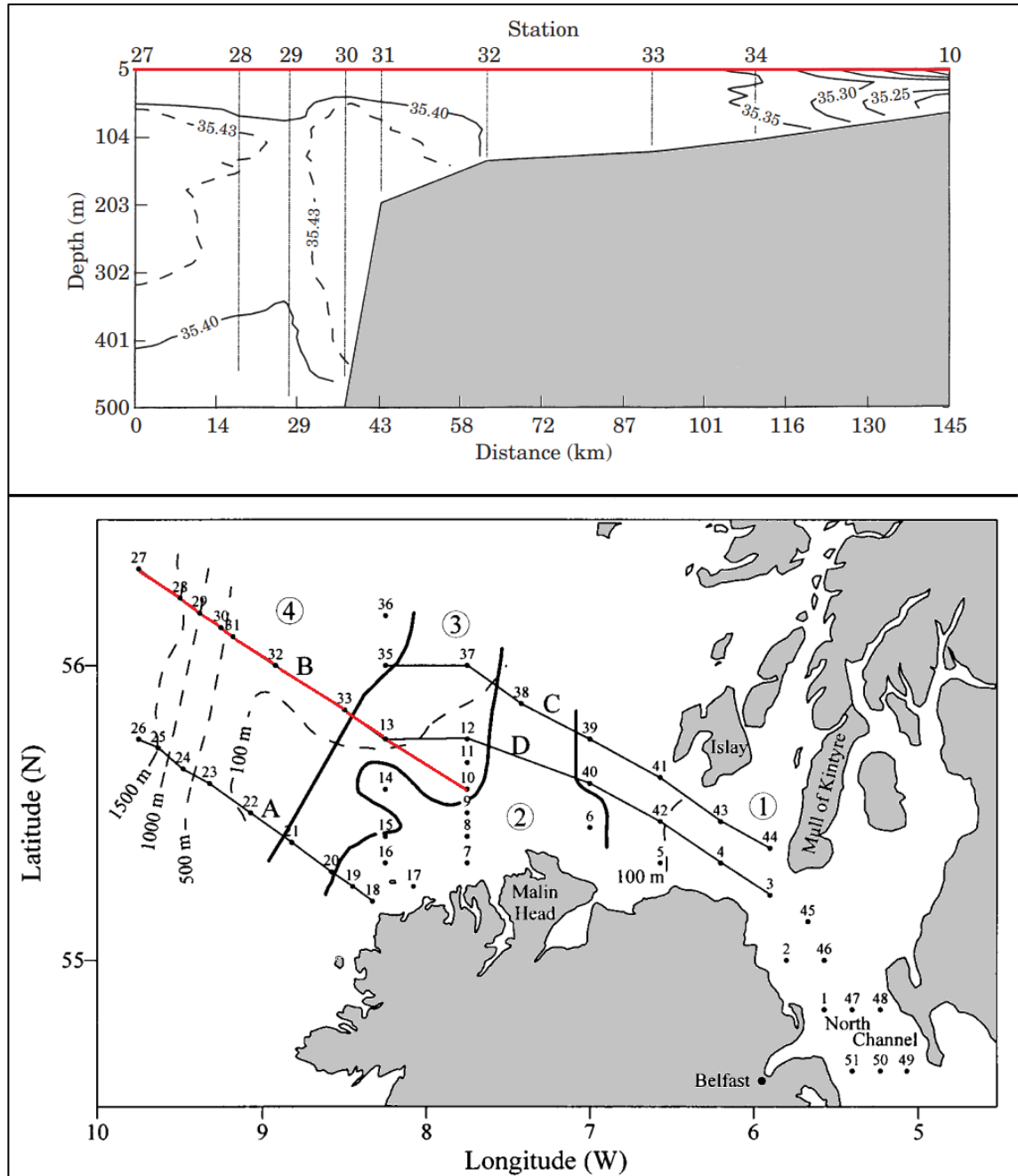


Fig. 3.2: Vertical salinity profile across the mid-outer Malin shelf, showing intrusion of Atlantic Water (≥ 35.40 PSU) onto the outer shelf from a saline core on the shelf break/upper slope. Data from August 1996. After Gowen et al. (1998).

The associated mixing by tidal currents, wind and waves leads to the water column on the shallower inner shelf remaining mixed year-round, while the water depths on the outer shelf prevent such breakdown of thermal stratification during summer (Simpson & Pingree 1978; Huthnance et al. 2009). The resultant front between mixed and stratified waters across the shelf during summer is particularly favourable for phytoplankton productivity (Pingree et al. 1978; Gowen et al. 1998), as are the energetic wind and wave conditions by mixing nutrients into the surface layer (McMahon et al. 1995). Annual mean primary production has been modelled to increase from an export flux of ~ 75 to $150 \text{ g C}_{\text{org}} \text{ m}^2 \text{ yr}^{-1}$ landward across the width of the Malin shelf (see Delhez 1998). The outer shelf is fully mixed during winter, as the strong wind and wave regime along the northwest European margin allows winter mixing depths of >600 m west of Ireland and Scotland (Meincke 1986; Hydes et al. 2004). The dominant nutrient supply on the Malin shelf is from exchange with the Atlantic Ocean, as terrigenous/fluvial fluxes are very low in the region (Huthnance et al. 2009). Shelf-ocean exchange across the Malin shelf break includes episodic cascading of nutrient-rich, cold, dense shelf water into the Rockall Trough in winter (e.g. Hill et al. 1998).

Sediment transport into the Malin Sea area is presently limited, and much of the seafloor sediments are considered to derive from winnowing of underlying Pleistocene deposits (Fyfe et al. 1993). This is reflected in the dominant substrates of rippled sands and gravelly lags on the shallower, higher-energy areas of the shelf (Pendlebury & Dobson 1976; Stoker et al. 1993). The southern Malin shelf experiences the strongest tidal currents and the seafloor sediments here are predominantly carbonate-rich gravelly sands (Fyfe et al. 1993; Evans et al. 2015, Fig. 3.3). Combined with the associated availability of hard substrates (mainly rocks and hydroids; Dobson & Haynes 1973), the current regime strongly influences the living benthic foraminiferal assemblages, which are of low diversity (Fisher's α values of 1-2) and dominated by attached epifaunal species such as *Cibicides lobatulus* (84-88%) and *Rosalina anomala* (4-8%) on the open shelf (Murray 1985). The dead assemblages are more diverse (average $\alpha = 7$), additionally containing abundant *Cassidulina carinata* (2-19%), *Eponides repandus* ($\leq 2\%$), *Quinqueloculina seminula*, *Textularia sagittula* (23-32%) and *Trifarina angulosa* (3-18%), with benthic:planktic ratios of 1.2-9 (Dobson & Haynes 1973; Murray 1985).

In contrast, the Deeps are lower-energy depositional environments with finer substrates, and living assemblages in these are instead characterised by infaunal species including *Nonionella turgida* (0-85%), *Bulimina marginata* (0-34%) and *Epistominella vitrea* (0-23%) (Murray 2003a). Dead assemblages are dominated by *T. sagittula* (1-32%), *C. lobatulus* (9-21%), *B. marginata* (1-22%), *Hyalinea baltica* (0-11%), *Gavelinopsis praegeri* (2-10%) and *Brizalina difformis* (0-9%) (Murray 2003a). Assemblages in the mid-shelf Deeps have been shown to receive large contributions ($\leq 50\%$) of dead tests (usually of attached epifaunal species) transported from the

shallower shelf (Murray 2003b). On the inner shelf, a diverse dead assemblage reported from a maerl bed by Austin & Cage (2010) also comprised a mixture of autochthonous and reworked tests, and was dominated by species including *Asteriginata mamilla* (16%), *Miliolinella subrotunda* forma *hauerinoides* (11%) and *Spiroplectamina wrightii* (10%) (latter grouped under *T. sagittula* in Murray (1985; 2003a).

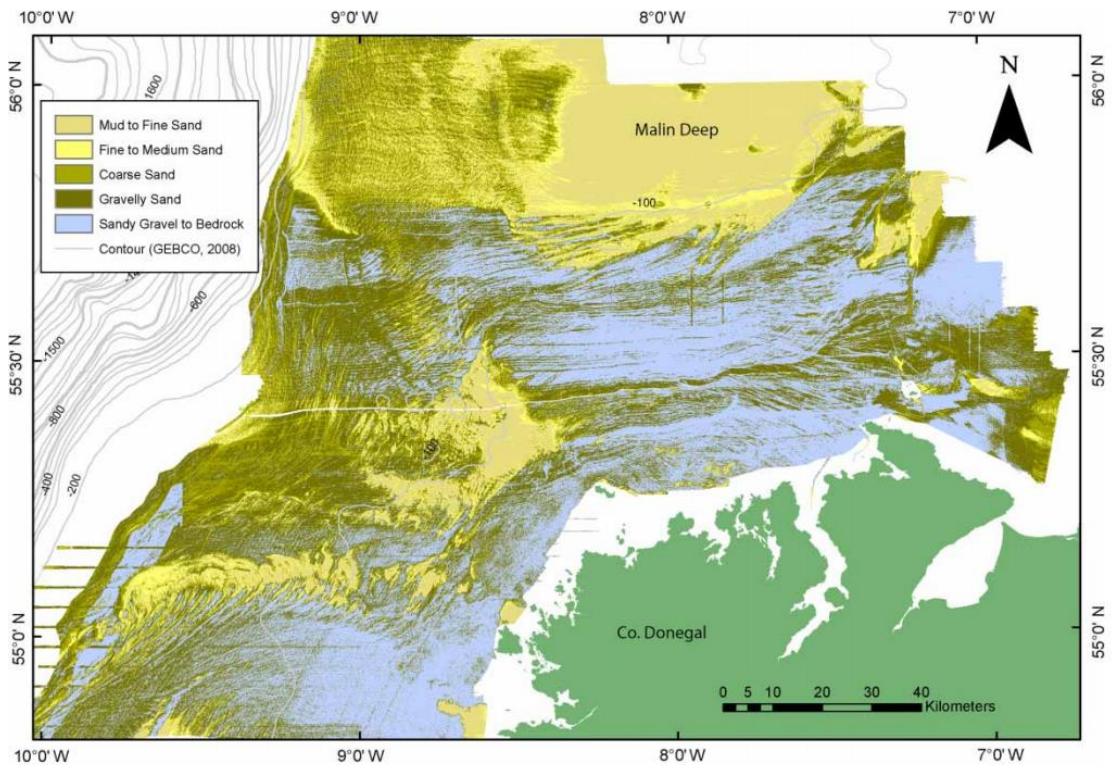


Fig. 3.3: Distribution of seafloor sediment types on the southern Malin shelf. Note substrate contrast between the Malin Deep and adjacent shallower shelf. From Evans et al. (2015).

3.2. Porcupine Bank and Slyne Trough

Porcupine Bank is an elongated, north-south oriented westward projection of the continental shelf off central western Ireland, approximately spanning 51-54°N and 13-15°W. The Bank is a horst block separated from the main Irish shelf by the Porcupine Seabight to the southeast and by the Slyne Trough to the east, both part of a failed rift system originating in the Carboniferous (Masson et al. 1989; Tate & Dobson 1998; Tate 1992) (Fig. 3.4). Water depths across the area of northern Porcupine Bank showing glacial ridges and iceberg scours are typically 200-400 m, but reach 145 m at the shallowest point (Thébaudeau et al. 2016). The Slyne Trough has minimum water depths of ~290 m, increasing progressively southwards into the Porcupine Seabight (maximum

depth 3000 m). The shelf break of the Irish mainland shelf is located at a depth of ~200 m (Fig. 3.5).

The surface/subsurface hydrography of the Porcupine Bank-Slyne Trough region is also dominated by ENAW, advected by the SEC in two branches, one curving around the western slope of Porcupine Bank and the other flowing along the eastern margin of the Seabight, through the Slyne Trough and probably re-joining the former along the northwest Irish shelf edge (McMahon et al. 1995; White & Bowyer 1997; Kloppmann et al. 2001) (Figs. 1.1, 2.3). In the region the SEC is focused between 200 and 400 m depth, and has spring/summer temperatures of 9.8-10.6 °C and salinities of 35.45-35.50 PSU (White et al. 1998; White 2007) (Fig. 3.5). The SEC has been shown to seasonally reverse direction in the area (Huthnance et al. 2001). Below ~600 m depth, higher-salinity Mediterranean Outflow Water also advected by the SEC fills the Seabight to a depth of ~1000 m (White 2007) (Fig. 3.5).

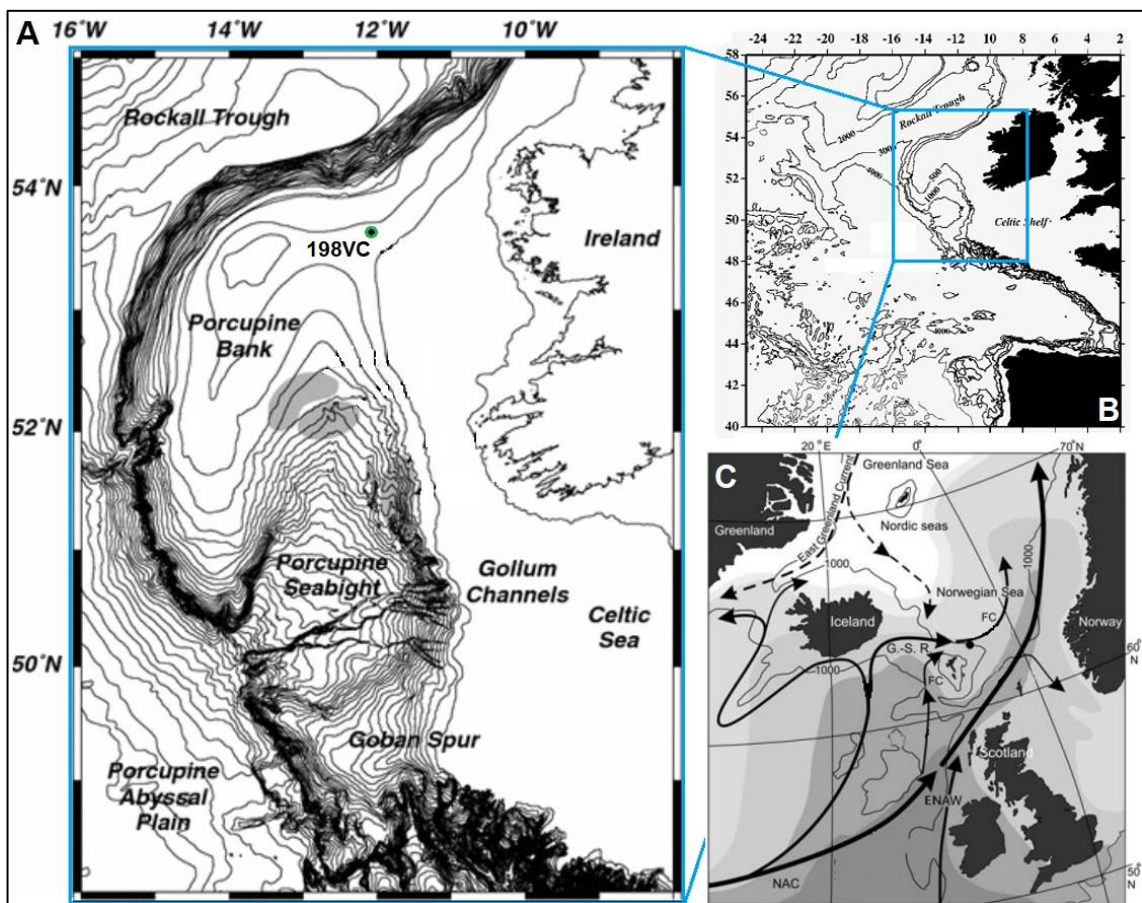
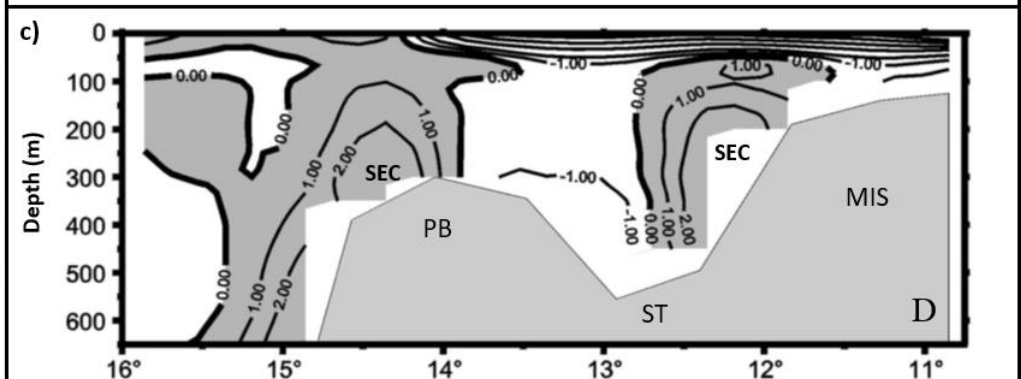
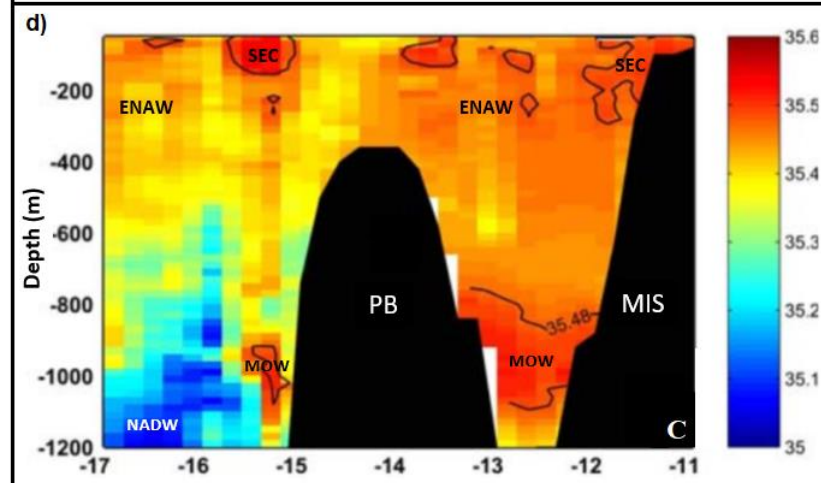
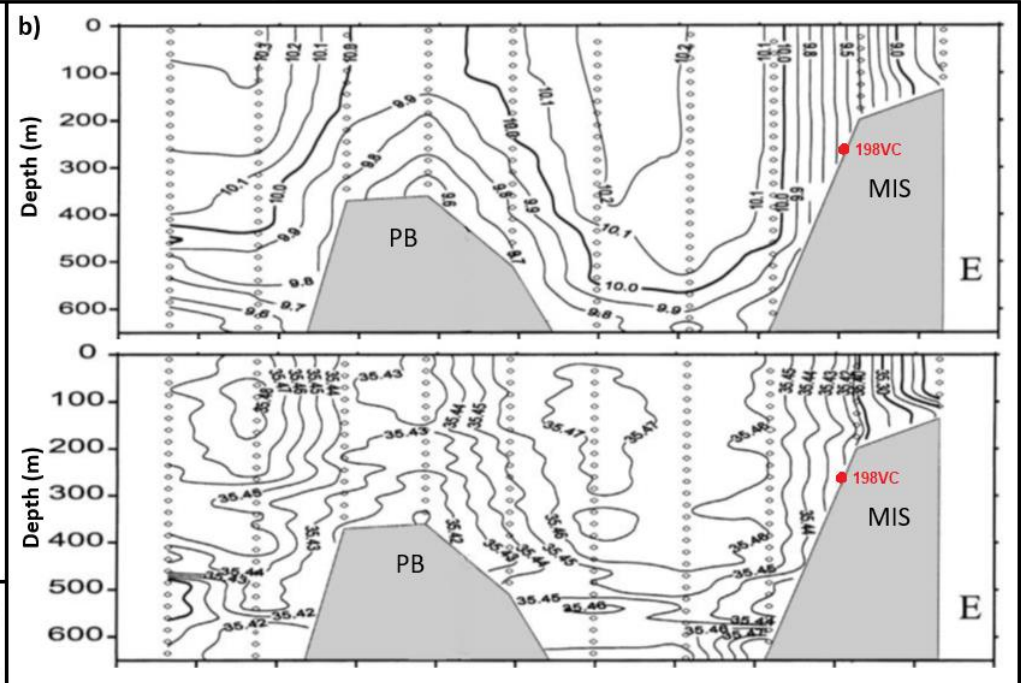
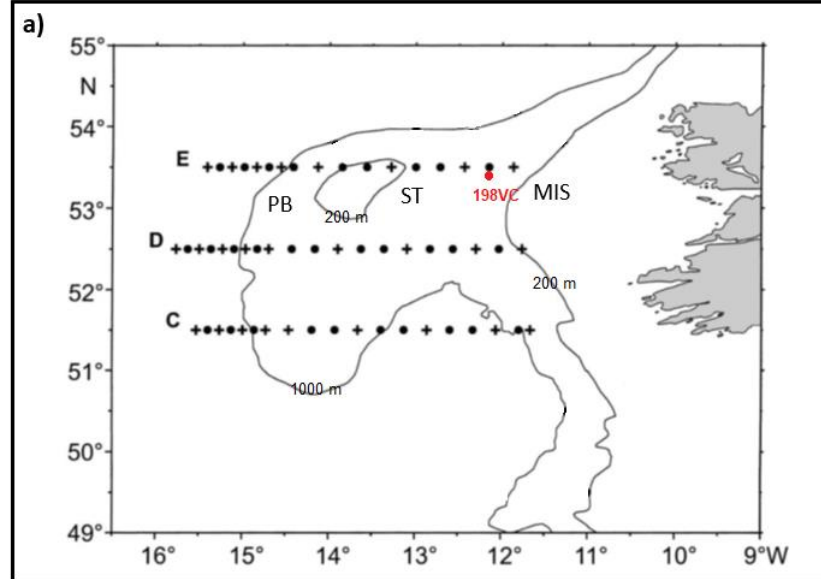


Fig. 3.4: A: Bathymetric map of the Porcupine Bank region, showing location of the core 198VC site. Shallowest contour is 100m and contour spacing is 100 m. Grey shaded areas are cold-water coral mound provinces, which are located around the water-mass boundary depth between ENAW and MOW (Schönfeld et al. 2011). B: Location of area in A relative to southern Rockall Trough and the Armorican margin. C: Key surface currents in the northeast Atlantic, showing ENAW pathway through the Slyne Trough and west of Porcupine Bank via the SEC. ‘FC’ – Faeroe Current; ‘NAC’ – North Atlantic Current. C modified from Rasmussen & Thomsen (2008).

A notable feature of the hydrography of the region is the persistent presence of a dome of colder, lower-salinity water over the Porcupine Bank (e.g. White et al. 1998; Hillgruber & Kloppmann 1999; Kloppmann et al. 2001) (Fig. 3.5). This dome structure is suggested to result from winter mixing and Taylor column circulation over the Bank, and therefore is rich in nutrients which are transported downslope in the benthic boundary layer, forming a food source to the northern Seabight (White et al. 1998; 2005; Mohn et al. 2002). East of the dome, in the Slyne Trough, warmer and more saline ENAW is present and influences the outer main Irish shelf eastwards to a sharp front with the cooler, fresher shelf water on the outer shelf (e.g. Huang et al. 1991) (Fig. 3.5). Open-ocean organic carbon export fluxes on the slope off central western Ireland are $\sim 100 \text{ g C}_{\text{org}} \text{ m}^2 \text{ yr}^{-1}$ (Joint et al. 1986; Delhez 1998). Porcupine Bank is characterised by particularly high productivity due to the Taylor column focusing of nutrients over the Bank (Mohn & White 2007). The open ocean is the major source of nutrients to the region, and shelf-ocean exchange partly occurs here as a subsurface compensation for Ekman-driven flow of warm surface water onto the shelf (White & Bowyer 1997; Huthnance et al. 2009). As in the Malin Sea region in autumn and winter, wind-related mixing is deep, and single storms can reinstate maximal primary production by doubling the mixed layer depth (Huthnance et al. 2001).

Modern benthic current speeds in the Slyne Trough are usually $2\text{-}20 \text{ cm s}^{-1}$, but locally reach 70 cm s^{-1} ; Ellet et al. 1986; Roberts et al. 2005; White 2007). In the Porcupine Seabight, maximum northward current velocities of 54 cm s^{-1} were measured by Pingree & Le Cann (1989) at the 1000 m contour. This energetic bottom-current regime is reflected in the surface sediments and bedforms of the region, which are dominated by carbonate-rich current-rippled sands, silty sands or gravelly muds, and variably by sand waves, ribbons and obstacle marks (Scoffin & Bowes 1988; Kenyon et al. 1998; Wheeler et al. 2000; Foubert et al. 2005; 2011). Some of the bedforms indicate that benthic currents could locally exceed 100 cm s^{-1} , near narrow channels or steeper slopes (Van Rooij et al. 2007a). Such current speeds are more than sufficient to entrain and transport foraminiferal tests from unconsolidated surface sediments (Alve 1999; Yordanova & Hohenegger 2007), and current transport of reworked tests is an important contributor to surface foraminiferal assemblage generation in the region (Smeulders et al. 2014).

Fig. 3.5 (overleaf): Vertical hydrographic sections from the Porcupine Bank region. A: Location map for labelled transects and 198VC site. B: Upper panel – potential temperature ($^{\circ}\text{C}$); lower panel - salinity (PSU); both from March/April 1994. Note the two cores of ENAW either side of the cooler, lower-salinity dome over Porcupine Bank (PB), and relatively sharp front with the lower-salinity shelf water across the upper slope to the east. C: Geostrophic velocity (cm s^{-1}), with northward currents shaded, from March/April 1994. Two arms of the Shelf Edge Current (SEC, advecting the ENAW northward) are clearly visible. D: Salinity (PSU) section including deeper hydrography (note depth scale), from June 2002. Two cores of very saline, northward-moving Mediterranean Outflow Water (MOW) are centred at 1000 m and two main branches of the SEC advecting ENAW are also visible. Panels A-C from Kloppmann et al. (2001); Panel D from White (2007). ‘MIS’ – Main Irish Shelf. ‘ST’ – Slyne Trough.



This importance of current transport of tests is implied by the very low contribution (1%) of living foraminifera to the overall foraminiferal abundance in surface sediment samples (top 1 cm), despite the high current strengths in the region (see Fentimen et al. 2020). No investigations are known of modern assemblages on the central western Irish shelf, and most studies of the benthic foraminiferal assemblages in the Porcupine region have focused on linkages between the assemblage compositions and the various benthic habitats occurring across cold-water coral mound complexes in the Porcupine Seabight (Margreth et al. 2009; Schönfeld et al. 2011; Smeulders et al. 2014; Fentimen et al. 2018; 2020). These studies have reported consistent differences in living and dead assemblage compositions between ‘off-mound’ areas (distal to the living coral structures, representing the wider slope environment) and ‘on-mound’ sites (the coral hardgrounds and surrounding rubble). Assemblages in sandy off-mound settings are characterised by low diversity (α values of 1-5; Schönfeld et al. 2011) with domination of attached epifaunal species, particularly *C. refulgens* and *C. lobatulus*, with infaunal *T. angulosa*, *Cibicidoides pachyderma* and *Gyroidinoides* (= *Hansenisca*) *soldanii* (Margreth et al. 2009; Schönfeld et al. 2011; Smeulders et al. 2014). The low diversity here is attributed to the limited benthic food flux and frequent physical disturbance due to the strong currents (Smeulders et al. 2014; Fentimen et al. 2020).

In general, diversity is higher in the on-mound areas (α 10-16; Schönfeld et al. 2011), where epifaunal and infaunal species both occur due to the availability of hard, elevated coral substrates and softer sediment pockets accumulated through baffling by the coral framework. Important living epifaunal species on-mound include *Discanomalina coronata* ($\leq 37\%$), *Planulina ariminensis*, *C. refulgens* and *Hanzawaia boueana*, while the infaunal species are dominated by *Globocassidulina subglobosa*, *C. laevigata*, *B. marginata*, *G. soldanii*, *Alabaminella weddellensis* and *Cassidulina obtusa* (e.g. Margreth et al. 2009; Smeulders et al. 2014; Fentimen et al. 2018) (Fig. 3.6). This prevalence of shallow-infaunal species on the mound structures is attributed to the effect of strong currents and epifaunal species in reducing the food availability within the sediment (Fentimen et al. 2018). The variability in substrate, food fluxes and food type across the mound provinces is generally considered to provide various niches, explaining the frequently elevated foraminiferal diversity on-mound and the associations of certain species with specific ‘facies’ within the provinces (e.g. Margreth et al. 2009; Smeulders et al. 2014; Fentimen et al. 2017). This view was challenged by Schönfeld et al. (2011), who found that only three species showed distributions exclusive enough to on-mound (*D. coronata*) or off-mound settings (*C. refulgens* [sand] and *Uvigerina mediterranea* [mud]) to attribute to facies control of their distributions, and that diversities on-mound were comparable to many off-mound sites across the Armorican-Celtic margin.



Fig. 3.6: Scanning electron microscope (SEM) images of the most common benthic foraminiferal species found by Smeulders et al. (2014) on- and off-mound in the Porcupine Seabight. 1: *Bulimina marginata*; 2: *Cassidulina laevigata*; 3: *Cassidulina obtusa*; 4: *Cibicides refulgens*; 5 and 6: *Discanomalina coronata*; 7: *Eggerella* sp.; 8: *Globocassidulina subglobosa*; 9: *Planulina ariminensis*; 10: *Trifarina angulosa*; 11: *Uvigerina mediterranea*. Scale bars are 200 μm . From Smeulders et al. (2014).

Smeulders et al. (2014) suggested the expansive sandy (off-mound) areas of the Porcupine region to be food-limited based on the current regime and their dominance by filter-feeding benthic

foraminiferal species. However, it is evident in the dead assemblage transect of Margreth et al. (2009) that these areas become increasingly dominated by high-productivity-associated infaunal species towards Porcupine Bank (*Cassidulina carinata* [max 50%, at 256 m], *Uvigerina peregrina* [max 41%, at 554 m], *B. marginata* and *Melonis barleeanum*). In the northern Porcupine Seabight down to 500 m depth, living assemblages are dominated by *C. carinata*, *T. angulosa*, *C. obtusa*, *C. lobatulus* and *Brizalina spathulata*, and show relatively high diversity (α 7-18) (Weston 1985). This implied increase in food availability at upper slope depths approaching Porcupine Bank could reflect a balance between the nutrient-rich conditions over the Bank (see above) and shallowing water depths with higher current velocities close to the Bank itself (e.g. Mohn & Beckmann 2002).

Dead assemblages in the region are generally more diverse than the living assemblages, despite several studies demonstrating their widespread loss of fragile agglutinated species such as *Adercotryma wrightii*, *Reophax scopiurus*, *Paratrochammina spp.* and *Trochammina spp.* (Schönfeld et al. 2011; Fentimen et al. 2020). A contribution of reworked glacial-associated species (*Elphidium excavatum*, *Cassidulina neoteretis* and *Sigmoilopsis schlumbergeri*) is usually present at varying proportions in the dead assemblages ($\leq 11\%$ in Schönfeld et al. 2011; average 32% in Fentimen et al. 2020), and as little as 38% of all identified species can be common to the dead and living assemblages in the Porcupine Seabight (e.g. Fentimen et al. 2020). The glacial contribution is attributed to bottom-current winnowing of glacial deposits, a process which is evident in the gravelly erosional moats developed around coral mound bases due to their local acceleration of currents (e.g. de Mol et al. 2002; Hebbeln et al. 2016).

Planktic foraminiferal populations in the Porcupine region presently comprise *Globigerina bulloides*, *Globigerinita glutinata*, *Globorotalia hirsuta*, *Globorotalia inflata*, *Globorotalia scitula*, *Turborotalita quinqueloba*, *Globigerinella siphonifera*, *Neogloboquadrina incompta*, *Neogloboquadrina pachyderma* and *Orbulina universa* (Harbers et al. 2010) (Fig. 3.7). Over 70% of the planktic foraminifera collected in a Porcupine Seabight sediment trap (63->500 μm) between April and August 2004 by these authors were unidentifiable individuals of 63-125 μm size. The most important species were *N. incompta* (~10%), *G. glutinata* (~5%), *G. hirsuta* (~3%), *G. bulloides* (~3%) and *T. quinqueloba* (~3%).

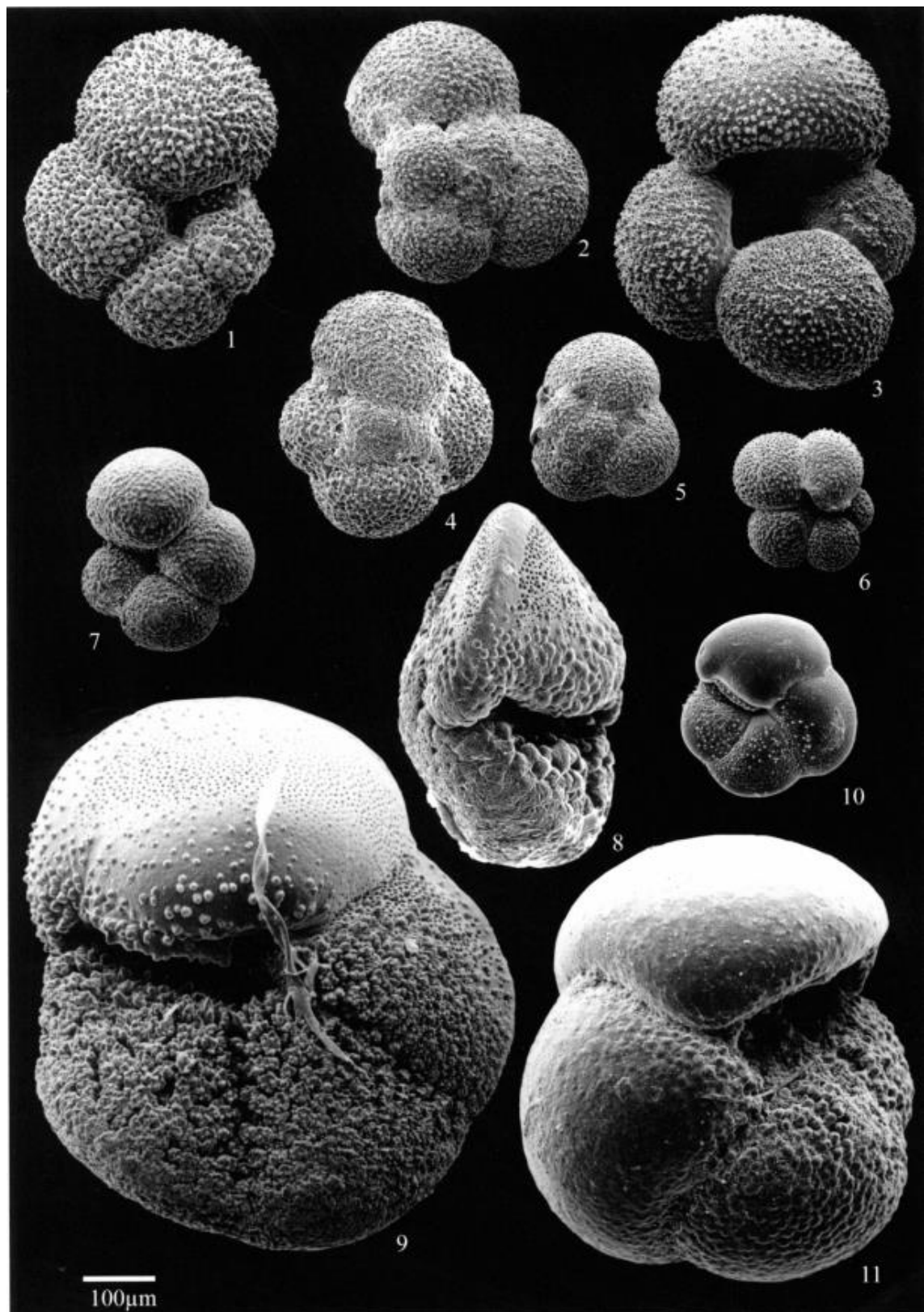


Fig. 3.7: SEM images of the most common planktic foraminiferal species retrieved by Harbers et al. (2010) in the Porcupine Seabight. 1: *Globigerinella siphonifera*; 2 and 3: *Globigerina bulloides*; 4 and 5: *Globigerinita glutinata*; 6: *Turborotalita quinqueloba*; 7: *Neogloboquadrina incompta*; 8 and 9: *Globorotalia hirsuta*; 10: *Globorotalia scitula*; 11: *Globorotalia inflata*. From Harbers et al. (2010).

CHAPTER 4

MATERIAL AND METHODS

4.1. Material

One vibrocore each from outer shelf positions on the Malin shelf and central western Irish shelf (JC106-146VC and JC106-198VC, respectively) was selected for sedimentologic and foraminiferal analysis (Figs. 5.1, 5.6, Table 1). The cores were retrieved in 2014 during cruise JC106 of the *RRS James Cook*, using the BGS vibrocorer (core diameter 8.3 cm and maximum core length 6 m) as part of the BRITICE-CHRONO project. Sedimentological data for both cores has been presented in recent studies (JC106-146VC in Callard et al. 2018 and JC106-198VC in Ó Cofaigh et al. submitted). This prior work comprehensively characterised the core lithofacies, provided radiocarbon age constraints and established lithofacies spatial and temporal position in the shelf deglacial record, but did not include foraminiferal analysis (see Sections 5.1.1. and 5.2.1.). These studies identified both cores as containing early deglacial sediments (either directly returning the oldest minimum deglacial ages in the core suite (146VC) or assigned to the earliest-dated glacial marine lithofacies (198VC). As such, the two cores are considered to be well-placed to test a role for ocean forcing in initial BIIS retreat from the shelf edge in these regions, by examining the foraminiferal assemblages preserved in the deglacial lithofacies.

Table 1: Location, water depth and recovery information for the cores studied in this project.

| Core name | Sampling location | Water depth (m) | Recovery (m) |
|--------------------|--------------------------|-----------------|--------------|
| JC106-146VC | 56°47.30' N, 8°70.70' W | 150 | 4.19 |
| JC106-198VC | 53°49.39' N, 11°50.43' W | 290 | 3.85 |

4.2. Methods

Laboratory work

4.2.1. Core logging

While data from both cores was presented in Callard et al. (2018) and Ó Cofaigh et al. (submitted), visual description was repeated and new x-radiographs were produced to revise the core sedimentological characterisations for this project, along with grain-size analyses and IRD counts not carried out in the previous studies.

Both cores were logged in detail, with information recorded on lithofacies structure (bedding/lamination, grading, sorting, nature of contacts, clast/matrix-support), clast characteristics (size, lithology, angularity, orientation), content of bioclasts, sedimentary structures and Munsell colour. X-radiographs (16-Bit, resolution 100 μ m/pixel) of all core sections (split) were produced using a *GEOTEK MSCL-XCT* core imaging system with x-ray voltage at ~95 kV and x-ray current at ~150 mA. The processed x-radiographs (Section 4.2.4) were examined to validate and add to laboratory observations of lamination/bedding, clast content, clast fabric and sedimentary structures (cf. Peters et al. 2016). *GEOTEK MSCL* measurements of gamma-ray density, magnetic susceptibility and electrical resistivity measured during cruise JC106 and *Torvane* measurements of sediment shear strength, partly reported in Callard et al. (2018) and Ó Cofaigh et al. (submitted), were re-used in this project. This comprehensive sedimentological re-characterisation of the core lithofacies was intended to provide a detailed sedimentologic context aiding interpretation of the faunal data.

4.2.2. Grain-size analysis

Grain-size variations in glacial marine sediments can reflect changes in ice margin proximity (and/or meltwater discharge) and the dominant sedimentation processes such as suspension settling and iceberg-rafting (Syvitski et al. 1996; Ó Cofaigh & Dowdeswell 2001). High-resolution sampling and laser granulometry to resolve grain-size variations within laminated lithofacies was unfortunately not possible (due to time-constraints) and only a broad characterisation of clay-silt, sand and granules-gravel was carried out on both cores. However, electrical resistivity data (measured at 2 cm intervals during cruise JC106) reflects porosity and hence provides some indication of relative grain-size variations in the laminated lithofacies in 146VC (these appear unaffected by glacial tectonic compaction).

The cores were sampled at 17 cm intervals (146VC) and 16 cm intervals (198VC) for determination of grain-size distributions and analysis of foraminiferal assemblages. Where these sampling intervals would have resulted in the omission of individual lithofacies, the sampling resolution was increased as necessary such that all intervals of all lithofacies were sampled at least once. This resulted in twenty-five samples from 146VC and twenty-four samples from 198VC. Approximately 4 cm³ of sediment was extracted for each sample from 146VC, and 2 cm³ for each from 198VC, as previous sampling for radiocarbon dating had indicated considerably lower foraminiferal concentrations in 146VC. Samples were weighed before drying at 40°C for at least 48 hours (146VC) or 24 hours (198VC) (due to the difference in sample volumes) and then re-weighed. The percentage difference between the wet and dry weights was then recorded as an indication of the moisture content of the sample. The dried samples were wet-sieved through

a sieve stack of 63 μm and 500 μm , and, once dry, the mass retained on each sieve was then weighed to find the percentage contribution of the 63-500 μm (very fine sand to coarse sand) and ≥ 500 μm fractions. The percentage contribution of the < 63 μm fraction (coarse silt and finer) was estimated by the difference between the total dry weight and the summed weights of the 63-500 μm and ≥ 500 μm fractions. It is acknowledged that this broad characterisation of grain-size does not differentiate lithic from biogenic grains.

4.2.3. Foraminiferal analysis

Benthic foraminifera can be abundant with high preservation potential in marine sediments, and show community changes in response to a wide range of environmental parameters (Gooday 2003; Jorissen et al. 2007; see Section 2.1). This supports use of their assemblages in palaeoceanographic reconstructions, where they have been used to inform on variables including organic carbon flux to the seafloor, bottom-water temperature, salinity, oxygenation and bottom current activity (Van der Zwaan et al. 1999; Jorissen et al. 2007; Gooday & Jorissen 2012). Studies of surface-sediment assemblages in high-latitude and glacially-influenced fjord and continental shelf settings have consistently associated certain benthic foraminifers with particular water mass physical properties and relative glacier proximity (see discussion and references in Section 2.1). The consistency of these observations strongly supports their use in reconstructing palaeoceanographic conditions on formerly glaciated margins, particularly the presence/absence of Atlantic waters, ice-margin proximity and meltwater discharge (e.g. Vorren et al. 1984; Lloyd et al. 1996; Lloyd 2006b; Jennings et al. 2014; Sheldon et al. 2016).

Planktic foraminifera are by definition more exclusively influenced by conditions in the water column than benthic foraminifera, particularly sea-surface temperature and phytoplankton biomass (Bé & Tolderlund 1971; Schiebel & Hemleben 2000; Husum & Hald 2012; Schiebel et al. 2017). Partly for this reason, water depth is another important factor influencing their distribution (Hemleben et al. 1989), as are turbidity (likely near glacier margins; Görlich et al. 1987; Korsun & Hald 1998) and sea ice conditions (Carstens et al. 1997). While planktic foraminiferal production is generally reduced over continental shelves (Gibson 1989; Hemleben et al. 1989; Murray 2004), planktic tests are readily advected into shelf areas (e.g. Murray et al. 1982; Schmuker 2000). As such, fossil planktic assemblages have potential to inform on surface characteristics of the open-ocean settings adjacent to shelf deglacial environments, and therefore were also analysed for this project.

Benthic and planktic foraminifera were dry-picked from the 63-500 μm fraction under a conventional binocular light microscope (*Leica MZ75*). Tests were picked from a brass picking tray (with an 8 \times 6.5 cm grid of 42 squares) using a fine paintbrush and placed onto

micropalaeontological slides for closer identification and counting. A target of at least 300 benthic individuals and 200 planktic individuals was set for each sample. Picking proceeded uninterrupted by removing all benthic and planktic tests from one square at a time until either a full tray had been counted (the slide was then counted pending further picking) or the picked quantity of tests had obviously exceeded the set targets. The set targets were therefore exceeded in all samples where the sample residue contained sufficient tests (this was the case for 6 samples in 146VC and all samples from 198VC). Foraminiferal concentrations were only large enough in one sample from 146VC (7 cm) and three samples from 198VC (41, 25 and 9 cm) that picking stopped before completion of a whole number of trays. In these cases, the number of squares picked on the uncompleted tray was recorded as a fraction of the 42 total to allow estimation of foraminiferal concentrations per unit weight of sediment (see Section 4.2.5). The expected foraminiferal abundance variations between 146VC and 198VC resulted in 0-319 benthic and 0-120 planktic individuals counted per sample in 146VC, and 316-670 and 222-467, respectively, in 198VC. Foraminiferal fragments, taken as a piece less than two thirds of the size of the original test, were also picked. This fragment size limit followed from the chosen minimum requirement of two-thirds of original size for counted tests, which was chosen to allow easier identification of damaged tests than the >50% intact condition needed to prevent double-counting.

The binomial distribution, frequently used to estimate the probability of finding an individual of a species with a given abundance level in a sample of a given size (e.g. Dennison & Hay 1967), returns a >99% probability of registering species accounting for $\geq 5\%$ in a sample of 100 individuals. This would essentially guarantee the statistical significance of relative abundance data for these most important species in 16 of the 25 samples from 146VC (Fatela & Taborda 2002). These considerations assume that all species are identified correctly and counted from a random sample. While the foraminiferal counts describe random samples from given 1 cm-depth intervals, their representation of the true fauna is likely affected by the numerous taphonomic processes pervasive on continental shelves (e.g. addition or removal of species by bottom currents and mass movement processes, displacement of individuals through bioturbation; Mackensen et al. 1993; Duros et al. 2014). Reworking of pre-existing marine deposits and destruction of delicate species by glacitectonism and iceberg turbation can contribute to this problem on glaciated margins (Vorren et al. 1984; Jennings & Weiner 1996; Shakesby et al. 2000; Rasmussen & Thomsen 2015). Furthermore, the 1 cm-thick samples necessarily represent mixtures of individuals accumulated over a time interval, which cannot be estimated as age-depth models are not available for the studied cores. Each individual was identified to species level where possible, however, species in the genus *Nonion* were lumped as *Nonion spp.*, and species of *Ammonia* were lumped as *Ammonia beccarii*.

The 63-500 μm fraction analysed extended foraminiferal analysis to considerably lower sizes than the >125 or >150 μm fractions used in previous studies from the BIIS margin (Peters et al. 2015; 2016; 2020; Scourse et al. 2019) and northeast Atlantic palaeoceanographic reconstructions (e.g. Peck et al. 2006; 2007; Haapaniemi et al. 2010; Hibbert et al. 2010). The 63-500 μm fraction (also used by Ó Cofaigh et al. 2019) was selected as several high-latitude studies have shown that considerable faunal information can be lost (including planktic species associated with warmer water e.g. *Turborotalita quinqueloba* and *Neogloboquadrina incompta*; Kandiano & Bauch 2002; Hald et al. 2007; Husum & Hald 2012) with the use of >125 μm fractions as polar and subpolar foraminifera (benthic and planktic) are commonly small (Schröder et al. 1987; Jennings & Helgadottir 1994; Carstens et al. 1997; Wollenburg & Mackensen 1998). The selected size fraction also maximised the potential faunal count in low-abundance glacial marine lithofacies (cf. Lloyd 2006a), allowed better representation of the foraminiferal fragment content measured for insight into detrital input and preservation quality, and allowed more representative estimation of diversity statistics (Lo Giudice Capelli & Austin 2019). Although every care was taken when sieving and handling residues, it is likely that the sample processing procedure outlined in Section 4.2.2. would have destroyed any fragile agglutinated species present through repeated wetting and drying (Ireland 1967).

Taxonomy

The main taxonomic references used were Barker (1960); Feyling-Hansen (1972); Murray (1979; 2003a); Seidenkrantz (1995); Milker & Schmiedl (2012); Ovsepyan & Taldenkova (2019); Tikhonova et al. (2019) and the online database *foraminifera.eu* (Hesemann 2015). *Uvigerina peregrina* and *Uvigerina mediterranea* were distinguished following Van der Zwaan et al. (1986). Reference was also made to type slides courtesy of J.M. Lloyd, Durham, from Donegal shelf cores used in Ó Cofaigh et al. (2019) and of calcareous benthic species from the Greenland shelf.

Data analysis

4.2.4. Sedimentologic data

X-radiographs were processed using the *GEOTEK QuickView* software, by enhancing contrast and applying a depth compensation for the increased x-ray attenuation in the core centre. The X-radiographs were also used to qualitatively assess the IRD content of the sediment by counting the grains >2 mm at 2 cm intervals (each interval therefore representing a sediment volume of ~ 54 cm^3). While this provides simple and rapid characterisation (Grobe 1987), typical core diameters represent restricted grain-size sampling areas in diamictic sediments and this is

particularly problematic where single large clasts may cause unrepresentatively low IRD counts across their depth intervals (Principato 2004). Interpretation of IRD data remains complicated by uncertainty as to whether IRD concentrations reliably track iceberg discharge (Clark et al. 2000; Andrews & Principato 2002). It was not always possible to distinguish shell fragments from lithic clasts on the x-radiographs and this should be considered when interpreting the IRD counts for (shell-rich) 198VC. Sedimentary logs were produced to summarise the lithofacies characteristics for display alongside graphs produced in *C2* v1.7.7. (Juggins 2016) of the following vs. core depth: weight% of the >500 μm , 63-500 μm and <63 μm fractions, X-ray-counted IRD >2 mm, water content, electrical resistivity, sediment shear strength, gamma-ray density and magnetic susceptibility.

4.2.5. Foraminiferal absolute abundance and diversity statistics

Whole-assemblage statistics can also be used for palaeoenvironmental interpretation, for example, absolute abundance (concentration) of foraminifera generally reflects food availability (e.g. Phleger 1964), and the ratio of planktic to benthic individuals increases with water depth (van der Zwaan et al. 1990). Benthic foraminiferal diversity and dominance increase predominantly with oxygen concentrations and organic carbon flux rates, respectively (Gooday 2003). Palaeoenvironmental reconstructions from foraminiferal assemblage characteristics are based on empirically-observed relationships between assemblage characteristics in surface sediment samples and environmental variables measured at the sampling sites (see Sections 2.1.2. and 2.1.3).

The count data was used to estimate foraminiferal test and fragment concentrations as individuals per gram dry sediment, and for 146VC, also the percentage of planktic individuals. Due to their high foraminiferal abundance, all 198VC residues were subsampled for picking, however, it was not possible to weigh the subsamples. The subsample weight was therefore estimated crudely by dividing the known (measured) weight of the full residue sample by the number of trays it could fill. Foraminiferal test and fragment concentrations in 198VC were then calculated based on a combination of this estimate and the fractional number of trays counted (using the squares, see Austin 1991 for an example). Due to the different counting targets set for benthic and planktic tests (Section 4.2.3), to estimate the benthic:planktic ratio the weight of residue processed for each sample was estimated on completing planktic counting and again on completing benthic counting, to allow normalisation of their separate totals to weight of processed residue.

Count data was converted to percentage relative abundance values and analysed for diversity (Fisher's α) and dominance (1-Simpson's Index) parameters using the program *Past* v4.01 (Hammer 2020). Fisher's α is a term used to predict the number of species represented by a given

number of individuals in a sample, assuming species abundance to follow a logarithmic probability density function where most species are represented by few or one individual(s) (Fisher et al. 1943), so the parameter increases in magnitude with diversity. This statistic was chosen to represent diversity instead of simply counting the species present (species richness), as absolute abundance varied considerably between some samples, the metric also takes into account the species' abundance, and because it allows comparison with foraminiferal diversity data from BIIS deglacial environments to date (Peters et al. 2015; Scourse et al. 2019). The use of Simpson's (1949) index D as its complement $1-D$ represents the probability that two individuals chosen at random from a sample represent different species (McCune & Grace 2002). The magnitude of $1-D$ thereby decreases with dominance (the unevenness of species' abundances in a population). Diversity measures were computed separately for the benthic and planktic datasets in 198VC. For 146VC, diversity measures were only calculated for the benthic fauna due to the low numbers of planktic individuals (0-33) in all but two samples. Two samples in 146VC (242 and 259 cm) were not included in this diversity analysis due to low/no foraminiferal content (0 and 2 individuals, respectively).

4.2.6. Faunal assemblage zones

Micropalaeontologic records may be subdivided into assemblage zones delimiting key changes in faunal composition through time, to aid reconstruction of palaeoenvironmental evolution (e.g. Jennings et al. 2014; Perner et al. 2015). A common zonation approach involves constrained cluster analysis (e.g. Lloyd 2006b), which measures the degree of similarity in faunal composition between samples but only forms clusters from stratigraphically-adjacent samples, with results displayed as a dendrogram from which zones are delineated by 'cutting' at a chosen degree of dissimilarity (Grimm 1987). However, clustering must be informed by additional aspects of the record, particularly lithostratigraphy, absolute abundance and preservation quality, to ensure delineation of reasonable zones accounting for unconformable contacts, microfossil provenance and statistical significance of species proportions. This is particularly important in records from glaciated margins, where a variety of reworking (glacitectonism, iceberg turbation, bioturbation) and erosive (winnowing, scouring) processes (e.g. Dahlgren et al. 2002; Callard et al. 2018) can complicate assemblage preservation and core age-depth relationships. Zonation in this project was only intended to identify key changes in the individual faunal records for use in palaeoceanographic reconstruction from the sediment core lithofacies.

Initially, stratigraphically-constrained cluster analysis (incremental sum of squares method) was applied separately to the 198VC benthic and planktic count data for species accounting for $\geq 2\%$ relative abundance, using *Tilia* v.2.6.1 (*CONISS*) (Grimm n.d.). The cluster analysis for 198VC

was run separately on samples from depths of 377-249 and 169-57 cm, to avoid clustering associated with a debris flow unit (244-173 cm) and unconformably capping sand unit (55-0 cm). For 146VC, clustering was run only on the benthic count data for species accounting for $\geq 5\%$, due to very low planktic abundance and frequently low benthic abundance causing most benthic species representing 2-5% of the benthic assemblages to have very infrequent appearances of only 1-3 individuals per sample. However, the clusters created by this analysis were not clearly guided by major faunal changes in either core. As a result, no zones were delineated for 146VC as the deglacial sedimentary sequence in this core showed no clear assemblage changes and is inferred to be conformable (see Section 6.1.1). In 198VC, the unconformities and mass-flow unit mentioned above were used, together with visual assessment of abundance trends, to delineate all zones for the benthic and planktic data. All faunal data was graphed using *C2* v1.7.7.

CHAPTER 5

RESULTS

This chapter describes the context of the two studied cores in their regional shelf deglacial record and presents the results of the sedimentologic and foraminiferal analyses.

5.1. JC106-146VC

Sedimentology

5.1.1. Setting in deglacial record

Core JC106-146VC (see Table 1) was retrieved on the outer Malin shelf (~140 km from the Scottish coast) from a basin at the distal foot of a broad sediment ridge identified as ‘grounding-zone wedge 1b’ (GZW1b) by Callard et al. (2018) (Fig. 5.1). It recovered an almost 4 m-long glacimarine basin infill sequence with a basal consolidated diamicton and capped by a shell-rich gravel unit (Callard et al. 2018). The onset of deposition is constrained by three AMS ^{14}C ages to before $25,897 \pm 178$ ka BP (all dates mentioned in the text are in calibrated years, $\pm 2\sigma$ and $\Delta R = 0$), the oldest minimum age for deglaciation obtained on the Malin shelf to date (Callard et al. 2018). Analysis of acoustic (sub-bottom profiler) data and lithofacies characteristics indicates the glacimarine infill was deposited during ice retreat and not subsequently overridden, and can be associated with similar deposits across the Malin shelf which infill depressions between ridges of consolidated diamictic sediments interpreted as subglacial till (Callard et al. 2018; Fig. 5.1C). While the ^{14}C ages from 146VC are not all in stratigraphic order, implying downslope remobilisation (Callard et al. 2018) which may be expected in a basin setting, lithofacies characteristics show no evidence of erosion/hiatuses. The glacimarine sequence in 146VC is therefore expected to represent a relatively undisturbed record of oceanographic conditions and depositional processes on the outer shelf from an early stage of retreat, including in an ice-proximal setting where it records ice-margin stabilisation at a major grounding-zone position (‘GZW1b’; Callard et al. 2018) 3-4 km from the site.

5.1.2. Lithofacies

Lithofacies codes used in this project follow the scheme of Evans & Benn (2004), with minor modifications (see Table 2). Grain-size terminology follows the Udden-Wentworth scale as subdivided by Blair & McPherson (1999). 146VC was divided into 8 lithofacies (Figs. 5.2; 5.3), described in detail below.

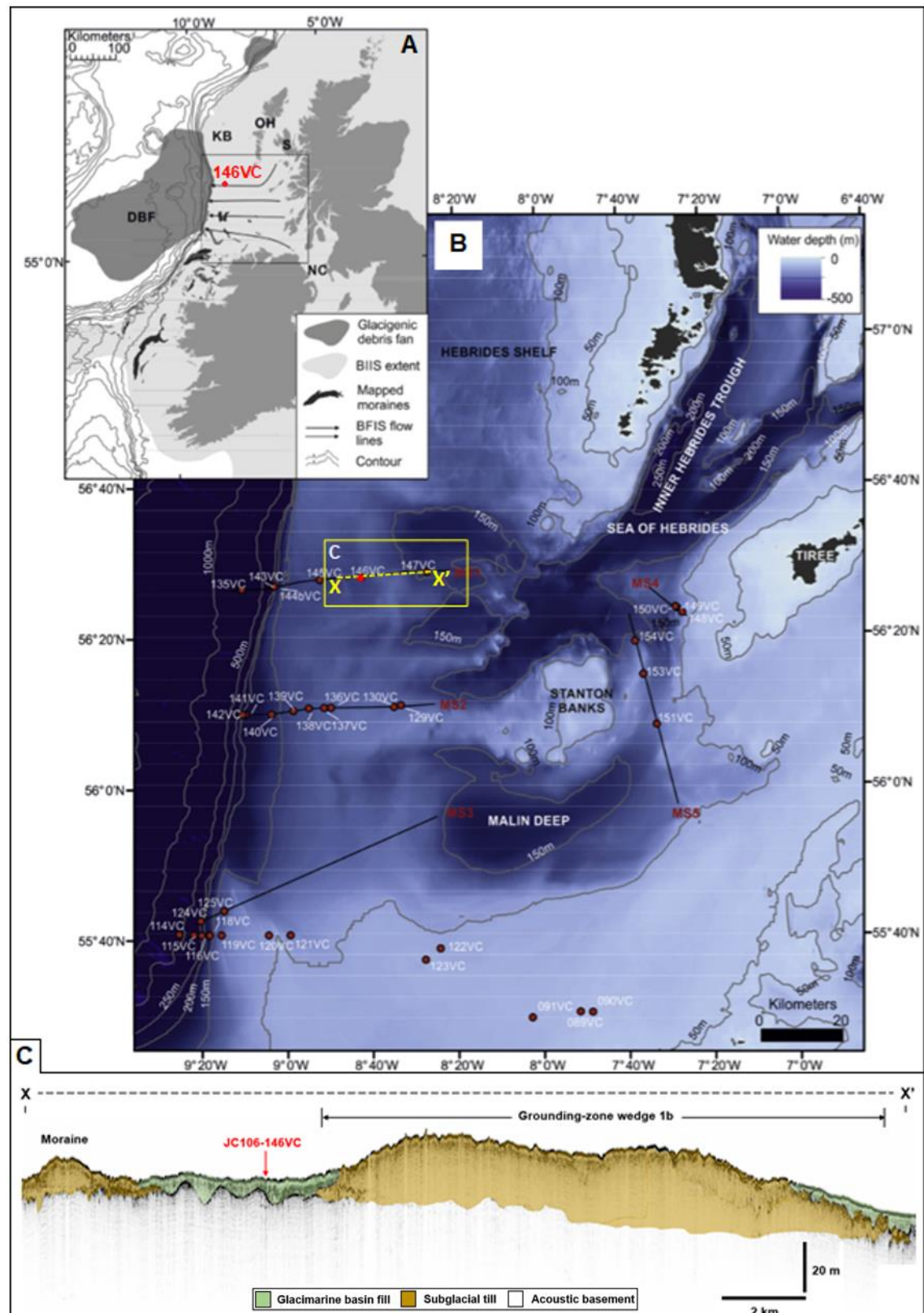


Fig. 5.1: A, B: Maps showing the location of 146VC on the Malin shelf (modified from Callard et al. 2018). C: Sub-bottom profiler transect from cruise JC106 showing the position of 146VC relative to ice-marginal structures and onlapping glacimarine sediments.

Table 2: Lithofacies codes for the cores presented in this project, modified after Evans & Benn (2004). Subscript ‘c’ denotes overconsolidation (shear strength >72 kPa). ‘Mud’ is used throughout the text to describe sediments dominated by silt and/or clay.

| Code | Description |
|---------------------------|--|
| Dmm, Dmm _c | Diamicton, matrix-supported, massive |
| Dms | Diamicton, matrix-supported and stratified via grain-size variations |
| Fl | Mud, laminated |
| Fld, Fld _c | Mud, laminated, with clasts of granule size or larger |
| Fldef, Fldef _c | Mud, with deformed (e.g. convolute) laminae |
| Fm | Mud, massive |
| Fmd, Fmd _c | Mud, massive, with clasts of granule size or larger |
| Gm | Gravel, clast-supported, massive |
| Sm | Sand, massive |

Dmm_c (419-405.2 cm)

The basal lithofacies of 146VC is a firm (shear strength 119 kPa), grey-brown diamicton with a matrix of clayey silt containing 26% fine-medium sand (Fig. 5.2). Water content is lowest (13%) and gamma-ray (wet bulk) density is highest (2.25 g/cm³) in this lithofacies. Shell fragments of fine sand-granule size are dispersed throughout the matrix. The diamicton has high magnetic susceptibility (462×10^{-5} SI), indicating a high content of terrigenous mineral grains (e.g. Diekmann et al. 2000). Its electrical resistivity (0.72-0.90 Ω-m) is high relative to most overlying lithofacies, indicating lower porosity and water content. Clasts are subangular-subrounded and reach medium pebble size (≤ 1.6 cm), with variable lithologies including chert, grey mudstone, red sandstone and crystalline metamorphic. X-radiographs show the clasts are well-dispersed and lack a long-axis fabric (Fig. 5.3). The contact with the overlying facies Fl is sharp.

Fl (405.2-393.5, 365.5-361 and 328.3-325.7 cm)

This clast-poor laminated mud facies directly overlies Dmm_c and initially occurs in the sequence as thin (~3 to 11 cm-thick) intervals alternating with the diamictons (~28-33 cm thick) of facies Dmm (Figs. 5.2; 5.3). This lithofacies consistently shows lower magnetic susceptibility, gamma-ray density and higher water content than Dmm. However, it shows significant variability in structure, lithologic composition and clast content between occurrences.

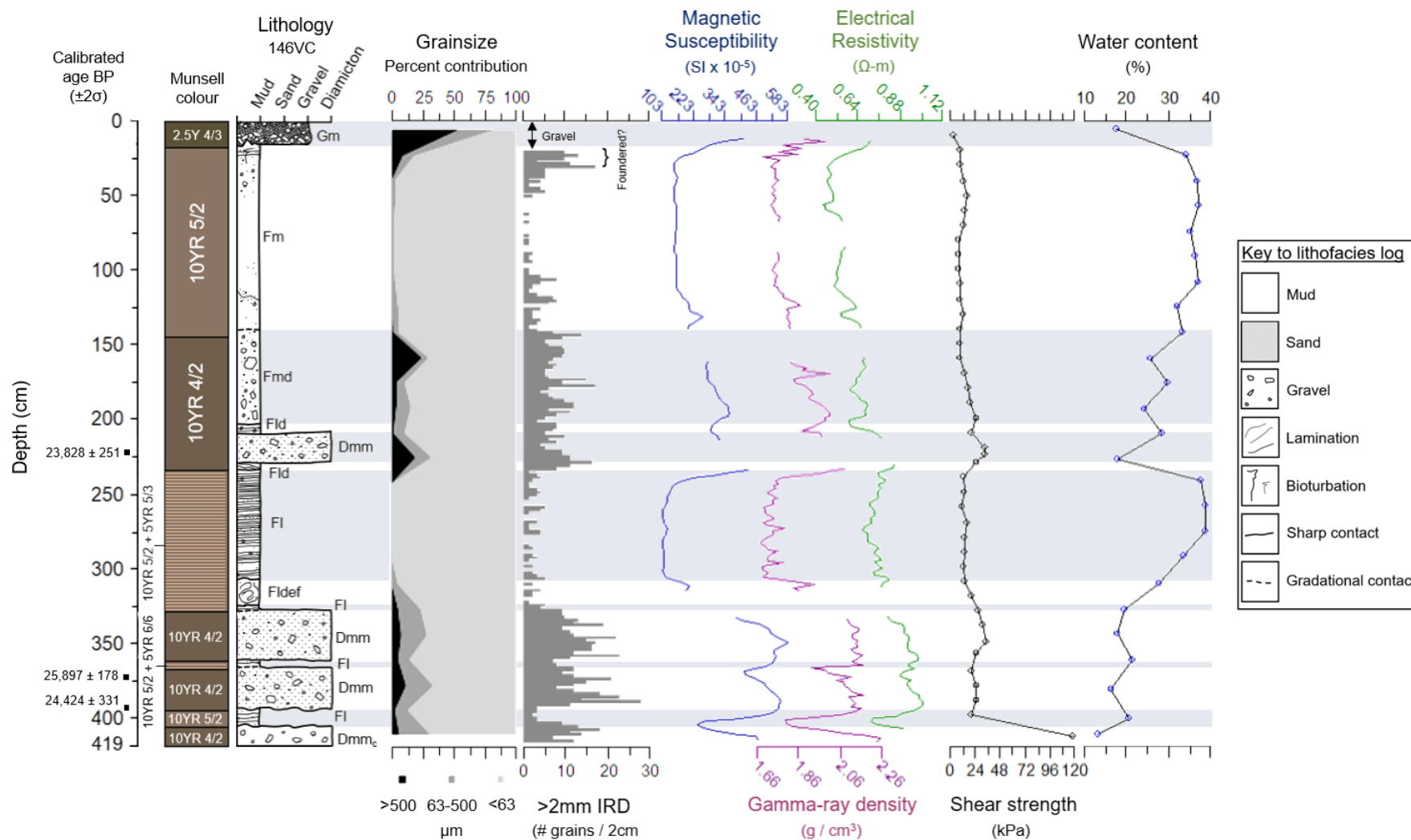


Fig. 5.2: Sedimentologic data for core 146VC. Radiocarbon ages, shear strength, magnetic susceptibility and gamma-ray density data were reported in Callard et al. (2018). The depth intervals of lithofacies indicated on the log are extended across the diagram as grey shading. Each value on the '>2 mm IRD' graph represents 54 cm³ of sediment. Lithofacies codes are explained in Table 2.

In the lowermost interval, laminae are ~ 2-3 mm thick with sharp contacts. Initially they occur as couplets of coarser and finer modal grain sizes (not measured as laser granulometry was not carried out). The coarser laminae (high in fine sand-granules) contain shell fragments and dark heavy mineral grains, and are associated with loading and water escape structures. This pattern is succeeded by consistently mud-grade lamination marked by alternating sediment colour, between light brown and pink. The x-radiographs show that these colour changes correspond to subtle grain-size variations (Fig. 5.3). The >2 mm IRD content is 2-3 grains/2 cm window. The second interval is laminated at 1-2 mm intervals, and the lamination pattern comprises coarser laminae usually separated by two fine laminae marked by the colour variation described above. Shell material is not observed in the second FI interval. Sharp and gradational laminae contacts occur. >2 mm IRD content (7-11 grains/2 cm window) is higher than in the first interval and lithologies include psammite, schist, vesicular basalt and pellets of consolidated sediment. The third occurrence of FI has similar characteristics to the second interval, however the laminae are 2-4 mm thick and the >2 mm IRD content is 1-2 grains/2 cm window.

Dmm (393.5-365.5 and 361-328.3 cm)

Two units of massive diamicton (Figs. 5.2; 5.3) separate the FI intervals described above, with sharp, undulating lower contacts and gradational upper contacts. The matrix is a soft (shear strength 20-34 kPa) grey-brown silty clay containing ~22% fine-medium sand. Material of coarse sand size and larger accounts for 8-12% (compare with 3-6% in FI). Clasts reach 2 cm (medium pebble size), are evenly distributed throughout the units and show no consistent long-axis alignment on the x-radiographs. They are generally angular but range to subrounded, with variable lithologies including greenschist, garnet-mica schist, green sandstone, psammite and pyroxenite. Shell fragments are more abundant, generally larger and better preserved than in Dmm_c. Two AMS ¹⁴C ages of 25,897±178 and 24,424±331 ka BP, not in stratigraphic order, were obtained on mixed benthic foraminifera from the lower Dmm unit by Callard et al. (2018).

Fldef (325.7-307.5 cm)

The third interval of FI is overlain along a sharp contact by ~18 cm of deformed laminated mud (Figs. 5.2; 5.3). The laminae resemble the coarse-fine lamination in the underlying FI intervals and are convoluted, retaining sharp contacts. Water content rises considerably to 28% and material coarser than medium sand accounts for only 0.9%. Clasts reach medium pebble size, but only occur in rare clusters. Shell material of fine-coarse sand size is dispersed throughout. Shear strength is low at 20 kPa and magnetic susceptibility ($131-204 \times 10^{-5}$ SI), gamma-ray density (1.71-1.94 g/cm³) and electrical resistivity (0.78-0.82 Ω-m) are at intermediate values for the core.

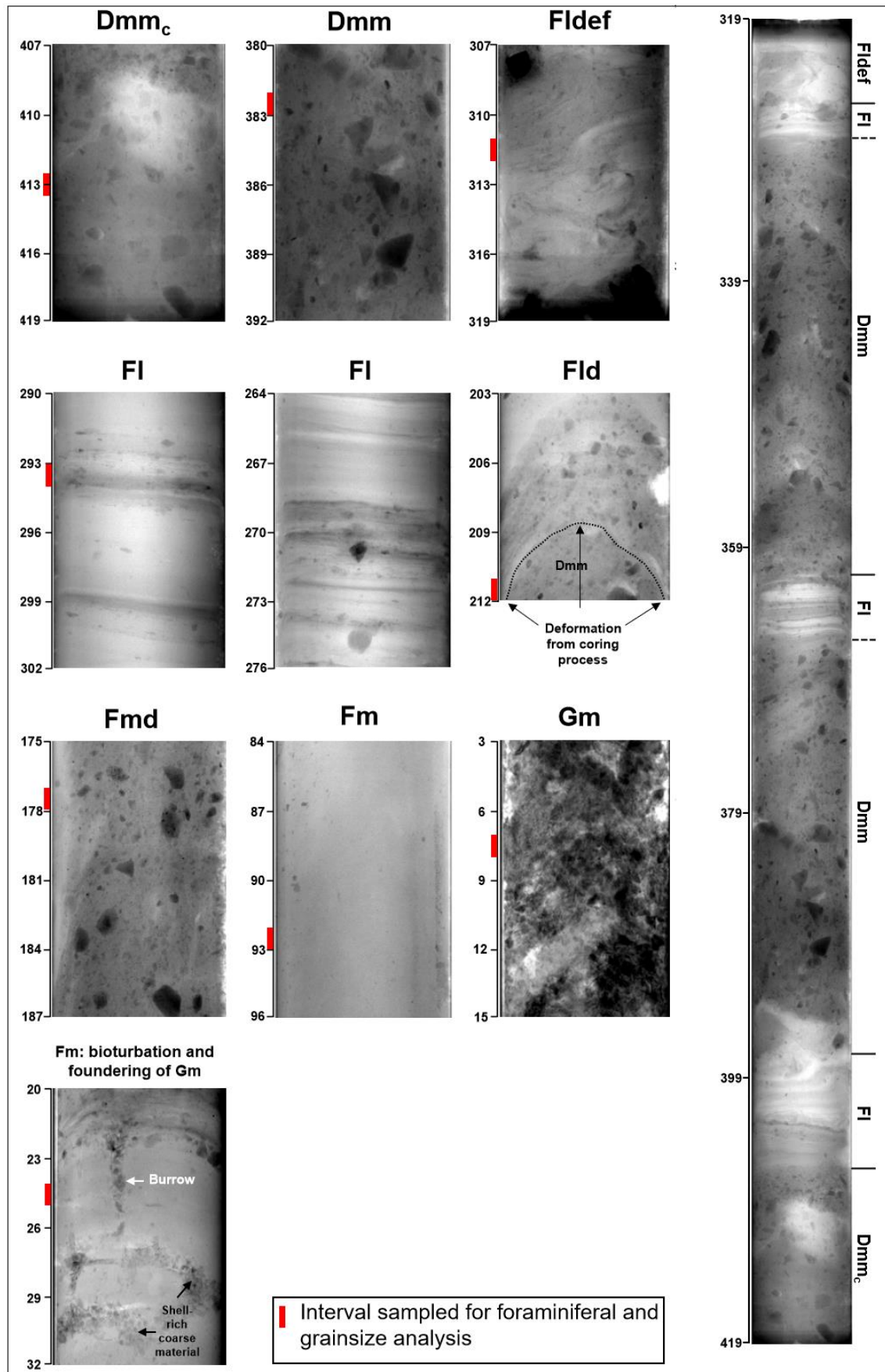


Fig. 5.3: X-radiographs of lithofacies from core 146VC.

Fl (307.5-233.5 cm)

Fldef is succeeded across a sharp, undulating contact by a 74 cm-thick Fl unit. This Fl unit is characterised by the lowest contents of sediment coarser than silt in the core (0.2-1.2%), and sustained low magnetic susceptibility ($104-220 \times 10^{-5}$ SI) and gamma-ray density (1.68-2.08 g/cm³). Water content increases to reach a core maximum of 39% and shear strength is low at 13-15 kPa. Electrical resistivity is generally lower (0.68-0.85 Ω -m) than in Dmm (0.82-1.02 Ω -m), reflecting the higher porosity and water content of Fl. Lamination is dominantly at clay/silt grade (but grain size not measured as laser granulometry was not carried out) and shows the brown-pink colour changes associated with subtle grain-size changes (likely clay-silt, see x-radiograph in Fig. 5.3) seen in earlier occurrences of Fl. Laminae are 2-5 mm thick and lamina thickness is zoned throughout the unit, with massive intervals 3-5 cm thick associated with minimal sand content and intervals of thinner, usually coarser laminae where sand and granules (including shell fragments) are concentrated. X-radiographs (Fig. 5.3) show the granules and small pebbles in facies Fl to have dominantly horizontal long axes, although some vertical orientations occur. >2 mm IRD remains low throughout (0-8 grains/2 cm window) and is regularly absent in this interval of the core, although isolated clasts of up to small pebble size are present.

Fld (233.5-230 and 209-202.5 cm)

This facies occurs only as thin intervals bracketing a Dmm unit. The lower interval overlies facies Fl along a sharp contact, whilst the upper interval is succeeded across a sharp contact by facies Fmd. The characteristics of Fld are transitional between those of Fl and Dmm, with coarse-fine lamination and >2 mm IRD counts of 8-11 grains/2 cm window. In this facies the coarser laminae texturally resemble the intervening Dmm and are thicker (≤ 5 mm) than the mud-grade laminae (~1 mm).

Dmm (230-209 cm)

The final Dmm unit in the sequence is similar to those from further down in the core that are described above. However, in its lower half the percentage of sediment that is coarser than medium sand is considerably higher, at 20%. Clasts are mostly subrounded, lack a long-axis fabric and have variable lithologies including gneiss, diorite, lherzolite and marble. Its upper and lower contacts (to the bracketing Fld intervals) are sharp. Shear strength (20-33 kPa) is slightly higher than in the underlying Fl interval and overlying facies Fmd. Measurements of magnetic susceptibility ($296-319 \times 10^{-5}$ SI), gamma-ray density (1.97-1.98 g/cm³) and electrical resistivity (0.73-0.79 Ω -m) are only available for the top of this unit but these values are lower than in the previous Dmm units.

Fmd (202.5-140 cm)

Facies Fmd succeeds the upper Fld interval and comprises light brown silty clay with up to 12% fine-medium sand, containing clasts of granule to coarse pebble size (≤ 4 cm) dispersed throughout. >2 mm IRD counts are high but fluctuating throughout (3-17 grains per 2 cm window). While these clasts occur throughout the unit, the sand fractions are unevenly distributed. The lower half of the unit is dominated by fine-medium sand, with the >500 μm comprising only 4-5%, the >500 μm fraction content then peaks in the upper half at 25% (see Fig. 5.2). Visual inspection of the core surface exposes concentrations of sand and granules forming convoluted bands and bifurcated, branching ribbons in the mud matrix. However, this is not obvious in the x-radiographs (Fig. 5.3). Shear strength is low in Fmd (9-25 kPa) and water content is high (24-33%). Granules and pebbles are angular to subrounded and show dominantly vertical alignments. Shell material is present but only observed in the sandy ribbons. Magnetic susceptibility and gamma-ray density values are $198\text{-}352 \times 10^{-5}$ SI and $1.82\text{-}2.01$ g/cm^3 , respectively, intermediate between those of Fl and Dmm.

Fm (140-15.5 cm)

Facies Fm comprises 124.5 cm of brown mud with a low content (2-5%) of fine-medium sand dispersed throughout and only rare grains larger than coarse sand. It succeeds the underlying facies Fmd across a gradational contact. Fm is soft (shear strength 8-15 kPa), with high water content (32-37%). Magnetic susceptibility, gamma-ray density and electrical resistivity are consistently lower than in Fmd, reflecting lower terrigenous mineral content, higher porosity and higher water content (Fig. 5.2). Granules-small pebbles are most abundant in the lower 34 cm, becoming rare above a diffuse band of coarse sediment at 122 cm. The average >2 mm IRD count in Fm is 3.4 grains/2 cm window below 120 cm and 1.5 grains/2 cm window above. Fm remains homogenous and clast-poor until 46 cm, where granules to small pebbles increase in abundance upwards to the contact with the overlying facies Gm. This increase in coarse material probably reflects the occurrence here of pods of medium sand-granules containing abundant, well-preserved shell fragments as seen in Gm. The x-radiographs clearly show Gm material infilling burrows penetrating the upper part of Fm (Fig. 5.3).

Gm (15.5-0 cm)

Core 146VC is capped by an upward-coarsening, shell-rich clast-supported gravel. The lower 7 cm of the unit comprises angular-subangular small to medium pebbles, grading to very large, rounded pebbles at the core top. The clast framework is filled with fine sand-small pebble-sized rock and shell material. Shell material is largest and best-preserved between 13 and 8 cm and is

high in fragments of the bivalve genera *Macoma* and *Pecten*. Lithologies are considerably less variable than in the underlying lithofacies and mostly comprise quartzite, black shale and sandstones.

Faunal data

5.1.3. Foraminiferal assemblages

69 calcareous and three agglutinated benthic species were identified in 146VC, along with six planktic species (see Appendix 1). Preservation is variable throughout the core, with all samples, including consolidated diamicton, containing both well-preserved, fragile species and chipped, abraded tests. No preservation quality is consistently associated with any species. 42 of the total species account for <2% relative abundance throughout, and 28 occur in less than three samples. Foraminiferal abundance varies considerably in 146VC, beginning with 38 individuals/g in Dmm_c, and reaching highest abundances in the diamictic lithofacies Dmm and Fmd (≤ 60 individuals/g). Lowest abundances occur in facies Fl and Fm (0-8 individuals/g from 302-235 cm and 117.5-49.5 cm, respectively) (see Fig. 5.4). In the uppermost unit, Gm, the concentration of foraminifera (5068 individuals/g) exceeds the average concentration in the glacial sequence by a factor >200.

Planktic foraminiferal abundance is extremely low (average benthic:planktic ratio = 35.9; 0-33 planktic individuals per sample) throughout the glacial sequence, rising to a benthic:planktic ratio = 4 in facies Gm. In 146VC, intervals of particularly low abundance (0-34 individuals per sample) occur from 302-235 and 117.5-49.5 cm, and have been highlighted in the data presentation as these likely represent harsh conditions for foraminifera and poor statistical significance of assemblage composition. Faunal zones have not been delineated for the 146VC assemblages (see Section 4.2.6. for explanation). Assemblages and ecological characteristics are therefore described below by lithofacies. All weights reported in the text refer to dry bulk sediment. All species relative abundance data presented and quoted represents percentages of the total (agglutinated + calcareous) assemblage (percentage abundances have been calculated separately for the benthic and planktic assemblages). Test and fragment concentrations reported refer to total benthic and planktic.

Basal diamicton (Dmm_c) (1 sample)

The assemblage in the basal consolidated diamicton is dominated by *Elphidium clavatum* (25%) and *Cassidulina reniforme* (19%), with *Elphidium excavatum* also important (13%). Minor

species are *Cibicides refulgens* (8%), *Cibicides lobatulus* (7%) and *Elphidium albiumbilicatum* (5%). Foraminiferal concentration (38 individuals/g) is lower than in overlying Dmm units but considerably higher than in facies Fl and Fm. Content of test fragments is high with respect to those in overlying glacial marine samples (18 fragments/g). Diversity measures are intermediate relative to the overlying lithofacies, with 19 taxa present and Fisher's $\alpha = 5.2$. Four planktic individuals were found, giving a planktic percentage of the total foraminifera of 2%.

Sequence of alternating Fl and Dmm units (405.2-328.3 cm, 5 samples)

Assemblages throughout the interbedded Fl and Dmm sequence (Fig. 5.4) closely resemble that in Dmm_c, consistently dominated by *E. clavatum* (17-27%), *C. reniforme* (18-25%) and *E. excavatum* (15-30%). Common species are *C. lobatulus* (6-8%), *E. albiumbilicatum* (2-8%) and *Lenticulina* spp. (1-6%). Present in $\geq 4/5$ samples and reaching $\geq 2\%$ are *Astrononion* sp., *Buccella* spp., *C. refulgens*, *Nonionellina labradorica*, *Nonion* spp. and *Quinqueloculina* spp. No consistent faunal or absolute abundance variations are seen between Fl and Dmm. The planktic foraminiferal proportion ranges from 1.6-3.3%. Diversity increases significantly from the first Fl interval (17 taxa, $\alpha = 5$) into the first Dmm unit (28 taxa, $\alpha = 7.7$), then gradually decreases through the succeeding Dmm and Fl alternations. Concentration of foraminifera appears to be significantly higher in Dmm (60 individuals/g) relative to Fl (30-37 individuals/g), although this increase is not seen in fragment concentrations. However, test and fragment concentration data is unavailable for the upper Dmm and uppermost Fl.

Fldef (325.7-307.5 cm, 1 sample)

The assemblage in the contorted mud package remains dominated by *E. clavatum* (17%), *C. reniforme* (22%) and *E. excavatum* (22%), with secondary proportions of *C. lobatulus* (4%) and *E. albiumbilicatum* (5%). *Astrononion gallowayi* and *Nonion* spp. account for 3%. No planktic specimens were found. Concentration of tests (25 individuals/g) and fragments (6 fragments/g) is lower than in the first two Fl intervals.

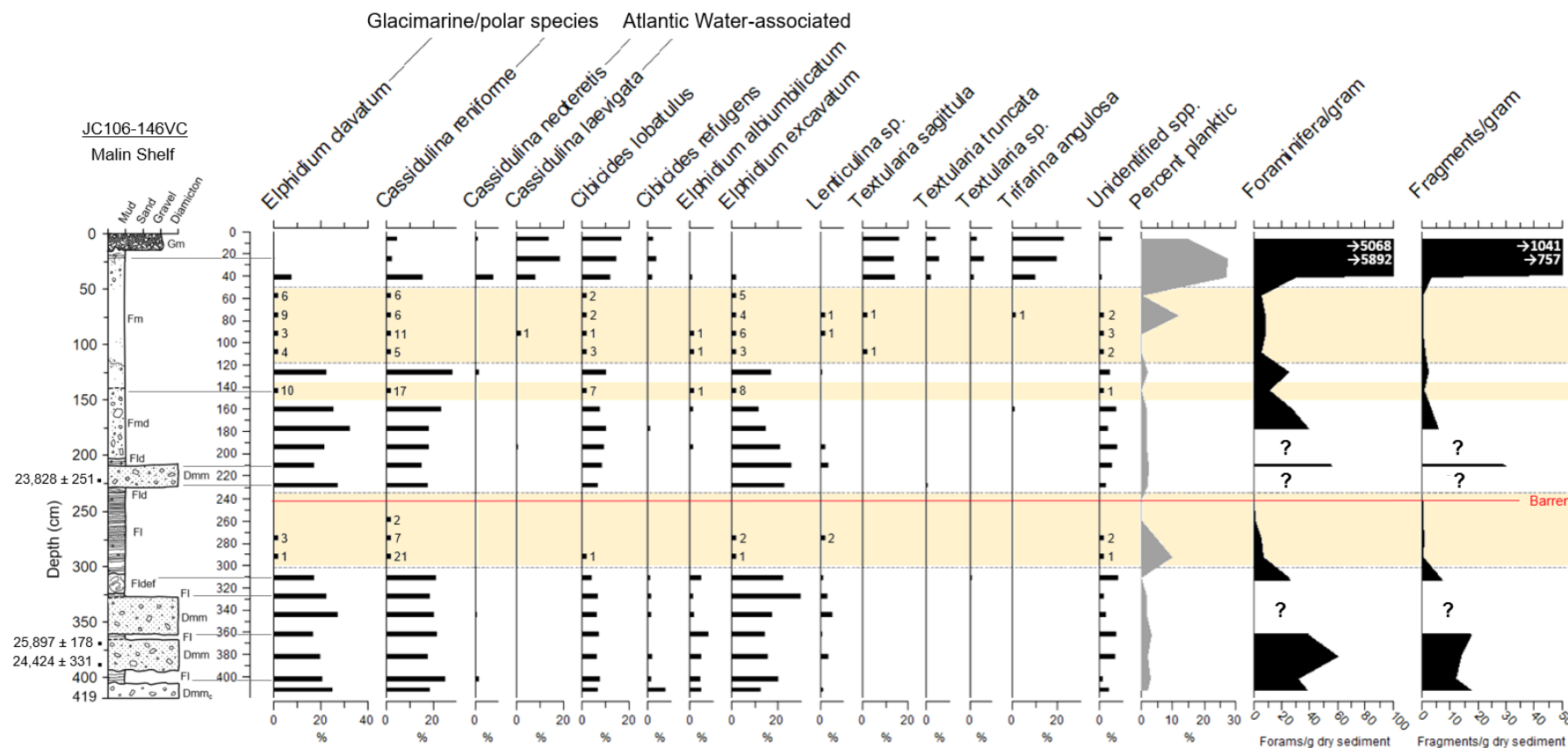


Fig. 5.4: Benthic foraminiferal species abundance for species comprising $\geq 5\%$ of the total (calcareous + agglutinated) benthic assemblage in 146VC. Abundance is presented as absolute counts for samples with low abundance (2-51 individuals/sample). Low-abundance intervals (low statistical significance) are highlighted in yellow. The red line marks a barren sample at 242 cm. Numbers in white give the quantity of tests and test fragments per gram for the uppermost two samples (note 10^2 -fold increase in these values). Question marks represent samples lacking this data (345, 328, 228 and 194 cm). Solid grey lines extending to the log clarify the sampled facies.

Fl (307.5-233.5 cm, 4 samples)

The 74 cm-thick Fl unit is characterised by significantly reduced foraminiferal abundance, decreasing through the interval from 7 individuals/g at 293 cm to zero at 242 cm. While samples in this unit contain only ≤ 31 individuals, preventing confidence in species proportions, *C. reniforme* was the most abundant species (35-100%) and appears to remain dominant over *E. clavatum* (0-15%) as in Fldef and the uppermost Fl interval. *E. excavatum* represents 0-10% of the individuals retrieved. *C. lobatulus*, *C. refulgens* and *E. albiumbilicatum*, minor species in almost all underlying lithofacies, disappear in this Fl unit. The lower two samples (with greatest abundance) were sampled from series of coarser laminae, while the barren samples from the upper half of the unit represent more homogenous, likely clay-silt alternations which separate thinner intervals of the coarser laminae throughout the unit. Planktic species (0-3 individuals) account for $\leq 10\%$ of the sampled foraminifera. The effect of low abundance is clearly reflected in the diversity statistics, with α falling from 7.3 to 3 into the unit from Fldef. Initial species richness (6-7 taxa) and α values in this Fl unit are considerably below those of the first occurrence of Fl overlying Dmm_c (17 taxa, $\alpha = 5$).

Dmm (230-209 cm, 2 samples)

Foraminiferal abundance increases significantly from the 74 cm-thick Fl unit into the final occurrence of facies Dmm, to ~ 55 individuals/g. The content of fragments also increases considerably, from < 1 to 30 fragments/g. The samples are dominated by *E. clavatum* (17-28%), *E. excavatum* (23-26%) and *C. reniforme* (15-18%), and display a shift to slight dominance of *E. clavatum* over *C. reniforme*. *C. lobatulus* (7-8%) and *Quinqueloculina spp.* (3-5%) are common. Abundances of *Brizalina spp.* and *Lenticulina spp.* reach 4% and planktic species account for 2%. Diversity also increases substantially into this uppermost Dmm from Fl, to 34 taxa and $\alpha = 10$, while dominance (0.84) returns to characteristic values for the sequence.

Fmd (202.5-140 cm, 4 samples)

Absolute abundance decreases throughout facies Fmd, from 40 to 12 individuals/g, and the content of test fragments is considerably reduced relative to the underlying Dmm (reaching only ≤ 6 fragments/gram). Fmd is still marginally dominated by *E. clavatum* (20-33%) over *C. reniforme* (18-33%) until the uppermost sample, and *E. excavatum* shows a sustained decline from 22-12%. *C. lobatulus* remains common throughout (8-14%), and minor species are *Buccella sp.* (0-4%) and *Quinqueloculina spp.* (0-3%). Planktic foraminiferal abundance remains similarly low in this lithofacies (0-1.7%) as through the earlier alternating sequence of Dmm and Fl.

Diversity decreases stepwise through Fmd, from 29-12 taxa present and $\alpha = 8.2$ to 5, while dominance remains at ~ 0.82 .

Fm (140-15.5 cm, 7 samples)

Foraminiferal abundance rises into lower Fm (to 24 individuals/g at 126 cm), then is considerably lower from 109-58 cm (≤ 8 individuals/g) before a significant increase to 5892 individuals/g at 24 cm. The richer sample at 126 cm is from a single diffuse band of coarser sediment which interrupts the lower part of the unit. Low abundance prevents confidence in assemblage composition from 109-58 cm, however, a slight dominance of *C. reniforme* (3-33%) over *E. clavatum* (0-30%) appears to generally persist from the uppermost facies Fmd throughout Fm. *E. excavatum* is important at $\leq 24\%$ until disappearing in the upper two samples, while *C. lobatulus* is common throughout (3-15%). The most persistent minor species (present in 4/7 samples) is *N. labradorica* (2-5%).

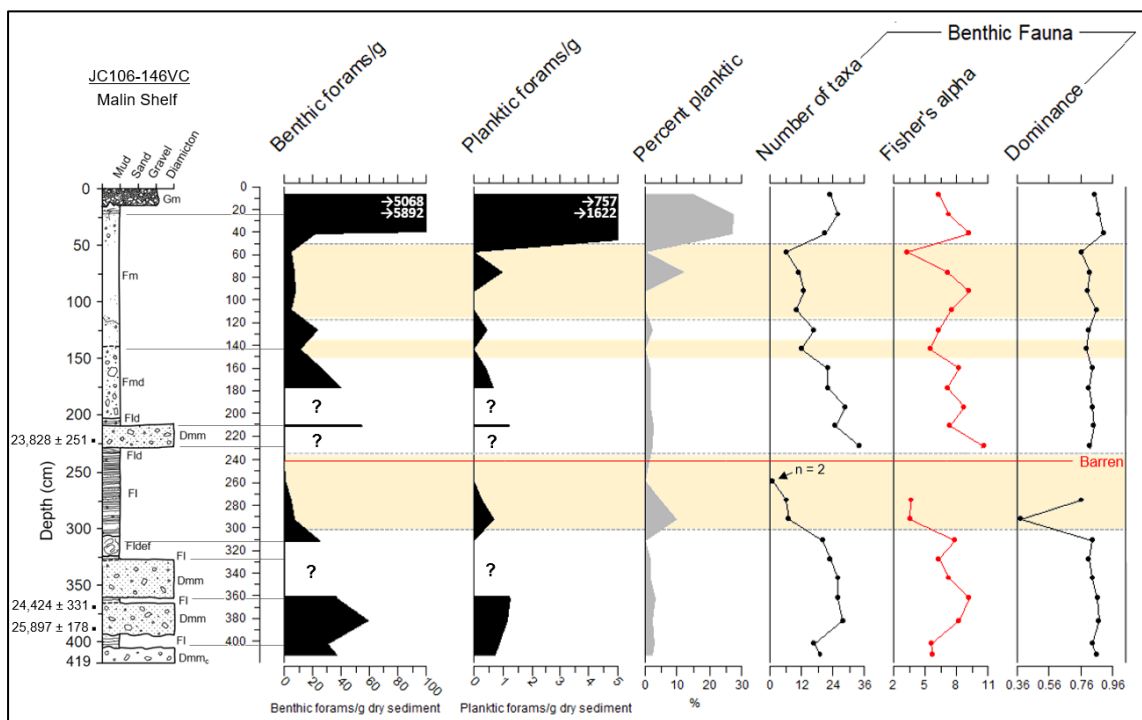


Fig. 5.5: Foraminiferal concentration, percentage of planktic individuals and diversity measures for 146VC. The annotation on the 'Number of taxa' graph refers to the sample size at 259 cm. See caption for Fig. 5.4 for explanation of other diagram features. Diversity parameter meanings are explained in Section 4.2.5.

A major faunal change occurs at 41 cm, with the first major appearances of *Cassidulina neoteretis* (8%), *Cassidulina laevigata* (8%), *Trifarina angulosa* (10%) and species of *Textularia* (19%), which increase further at 24 cm as *C. reniforme* and *E. clavatum* essentially disappear. These two

samples also display considerably increased planktic foraminiferal abundance (37%) and coincide with the appearance of bioturbation and pods of coarser, shell-rich material strongly resembling the overlying facies Gm (see x-radiograph in Fig. 5.3). Species richness changes follow those in absolute abundance particularly closely through facies Fm, beginning at 17 taxa before decreasing to 6 and rising to 26 at 24 cm. Changes in α are particularly exaggerated relative to changes in species richness from 109-58 cm, reflecting the disproportionate effect of the species occurring once in these low abundance samples.

Gm (15.5-0 cm, 1 sample)

Absolute abundance is high in the sample from facies Gm (5068 individuals/g), and test fragment content reaches a core maximum of 1041 fragments/g. The assemblage closely resembles that of the uppermost sample in Fm, mostly comprising *T. angulosa* (23%), *C. lobatulus* (17%), *Textularia sagittula* (16%) and *C. laevigata* (14%). *C. reniforme* represents a secondary component (5%) and *C. refulgens* accounts for 3%. Planktic foraminiferal abundance is high relative to underlying lithofacies at 15% (56 individuals).

5.2. JC106-198VC

Sedimentology

5.2.1. Setting in deglacial record

Core JC106-198VC (see Table 1) was recovered from a sediment ridge on the outer western Irish shelf (~110 km from the Connemara coastline) (Fig. 5.6). The ridge is located on the eastern margin of the Slyne Trough and is oriented NNE-SSW (parallel to the Trough axis and depth contours). Its cross-section is asymmetric, with a steeper offshore-facing slope (Ó Cofaigh et al. submitted). Acoustic data and sediment cores retrieved from the ridge show that internally, it comprises consolidated, likely massive diamictic sediment, overlain by 3-5 m of locally stratified deposits (Ó Cofaigh et al. submitted; Fig. 5.6C). The feature was termed the ‘West Ireland Moraine’ by Peters et al. (2016), who suggested its asymmetry was consistent with a ‘push moraine’. Core 198VC recovered a ~3.3 m glacial sequence comprising firm laminated muds separated from overlying soft, massive mud by a stratified diamicton, and unconformably capped by ~0.5 m of shell-rich sand (Ó Cofaigh et al. submitted). The firm muds in this sequence represent a lithofacies association retrieved from elsewhere on the ridge and outer shelf east of the Slyne Trough, and have been interpreted as glaciectonised glacial marine sediments recording

readvance of the oscillating ice margin during deglaciation (Callard et al. 2020; Ó Cofaigh et al. submitted).

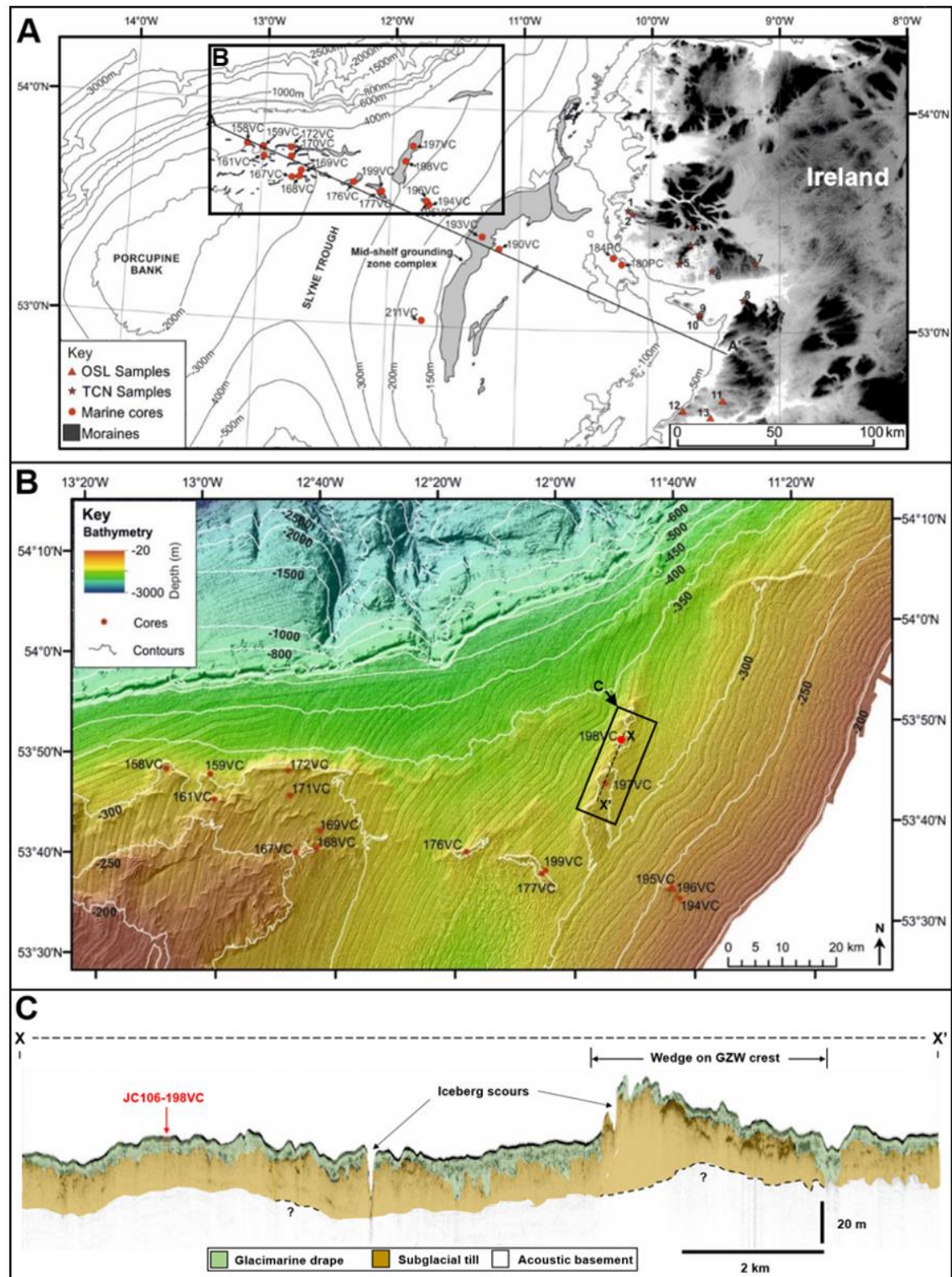


Fig. 5.6: A, B: Maps showing the location of 198VC on the western Irish shelf (modified from Ó Cofaigh et al. submitted). C: Sub-bottom profiler transect from cruise JC106 showing the position of 198VC relative to draping glacial sediments and a wedge overprinting the larger GZW.

This readvance(s) is also indicated by overprinting of the ridge by E-W trending smaller wedges aligned with narrow ridges further west (Peters et al. 2015; Ó Cofaigh et al. submitted). Bayesian analysis of radiocarbon ages from the glacitectonites constrains these readvance(s) on the outer shelf to between 25.9 ± 1.8 and 24.3 ± 0.2 ka BP (Ó Cofaigh et al. submitted). A radiocarbon age of 25.556 ± 0.237 ka BP from the base of the stratified diamicton in 198VC is a key date in the regional deglacial record, providing a minimum date for the final evacuation of grounded ice from the outer shelf (Ó Cofaigh et al. submitted). While the glacitectonites in 198VC have shear strengths ≤ 130 kPa, evidence of deformation is minimal (see below), suggesting weak homogenisation (Ó Cofaigh et al. submitted). Therefore, the firm muds in 198VC are expected to reliably record oceanographic conditions and sedimentary processes of the glacial marine environment of early retreat (from after 26.8 ka BP), until readvance over the core site sometime before 25.556 ± 0.237 ka BP. The overlying lithofacies record increasingly distal glacial marine depositional processes from approximately 25.556 ± 0.237 ka BP until sometime after 21.807 ± 0.210 ka BP.

5.2.2. Lithofacies

Five lithofacies were recognised in 198VC and are described below. Facies codes are explained in Table 2.

Fldef_c (385-375.5 cm)

The basal 9.5 cm of 198VC comprises very firm (shear strength 200 kPa) grey-brown sandy clay containing angular clasts of up to medium pebble size. Fine-medium sand accounts for 30% by weight and water content is at a core minimum of 13%. Angular, coarse sand-sized shell and coral fragments are abundant and dispersed throughout, at much greater density than in any glacial marine lithofacies in 146VC. While the working surface of this lithofacies appeared massive during logging, x-radiographs (Fig. 5.7) show the internal structure contains strongly curved, planar grain-size variations (deformed laminae). Clasts show no long-axis fabric on the radiographs. Gamma-ray density is relatively high compared to overlying lithofacies, at 2.13 g/cm^3 . Magnetic susceptibility values are intermediate relative to overlying lithofacies, averaging 106.7×10^{-5} SI (Fig. 5.9). The contact with the overlying *Fld_c* is sharp and interleaved.

Fld_c (375.5-244 cm)

Facies *Fld_c* is a ~1.3 m-thick unit of firm (shear strength 73-130 kPa) laminated pebbly mud. Laminae alternate between clayey silt and sandy silt, usually have sharp contacts and vary in

thickness between 2-30 mm (Fig. 5.7). Angular-subangular granules and pebbles are dispersed throughout but concentrated in the sandy silt laminae, which also contain higher proportions of the fine sand-granule-sized shell material also present throughout. The content of fine sand and coarser material is 15-30%. Two features (over 357-347 cm and 296-291 cm) were tentatively identified as shear planes in x-radiographs of facies Fld_c , the upper appearing to offset a lamina (Fig. 5.8A) and the lower appearing to form the base of a set of inclined laminae (Fig. 5.8B).

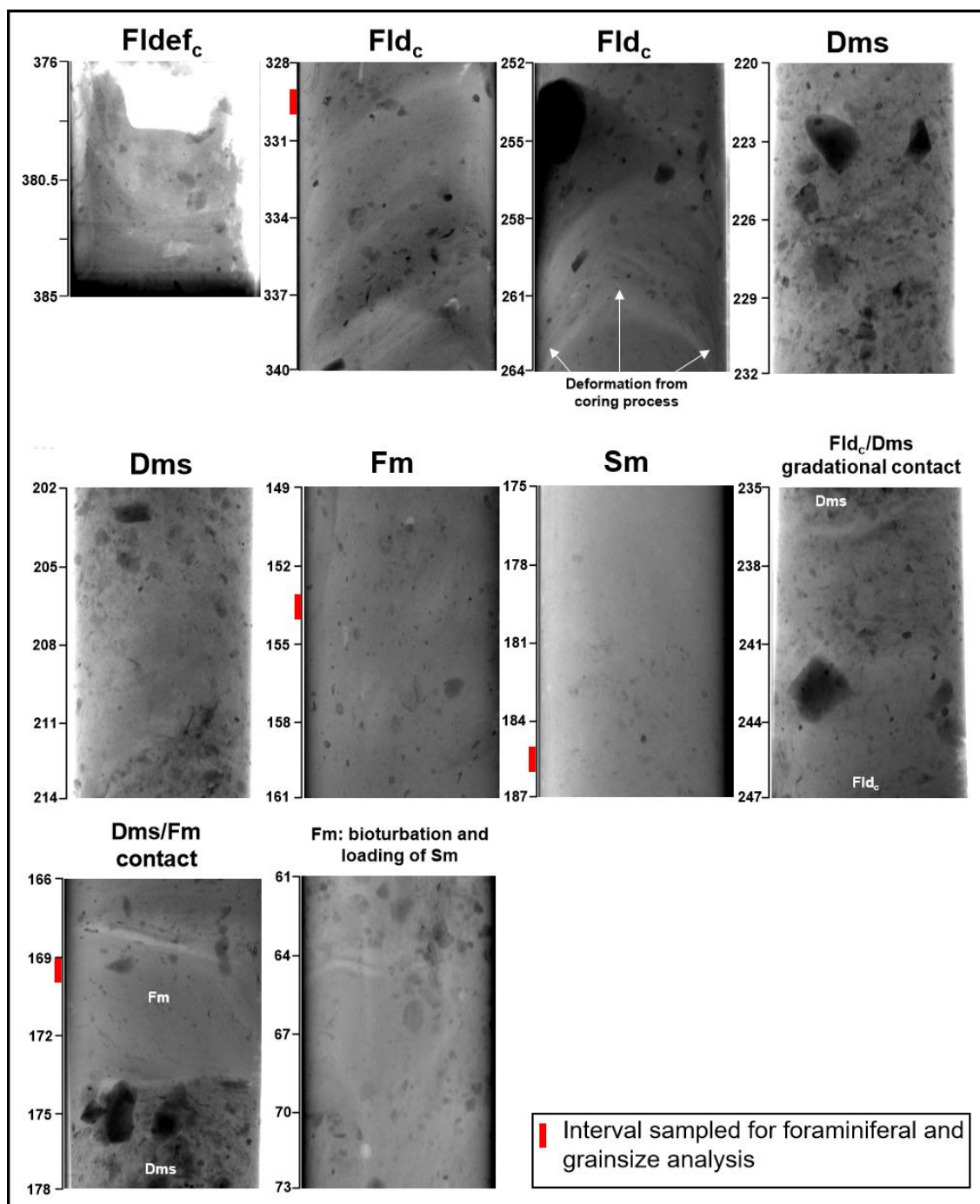


Fig. 5.7: X-radiographs of lithofacies from core 198VC.

Alternatively, these could represent a conformable change in depositional slope and a core crack, respectively (S.L. Callard, pers. comm; Fig. 5.8). While their identification is uncertain, movement along an uneven detachment surface would also explain the series of laminae tilted uniformly from the horizontal in this unit, and as there is no evidence of ductile deformation in facies Fld_c, any failure during overriding may have occurred by brittle fracture. Isolated stringers of lighter-coloured (10YR 6/4) sand occur occasionally in Fld_c and are parallel to lamination.

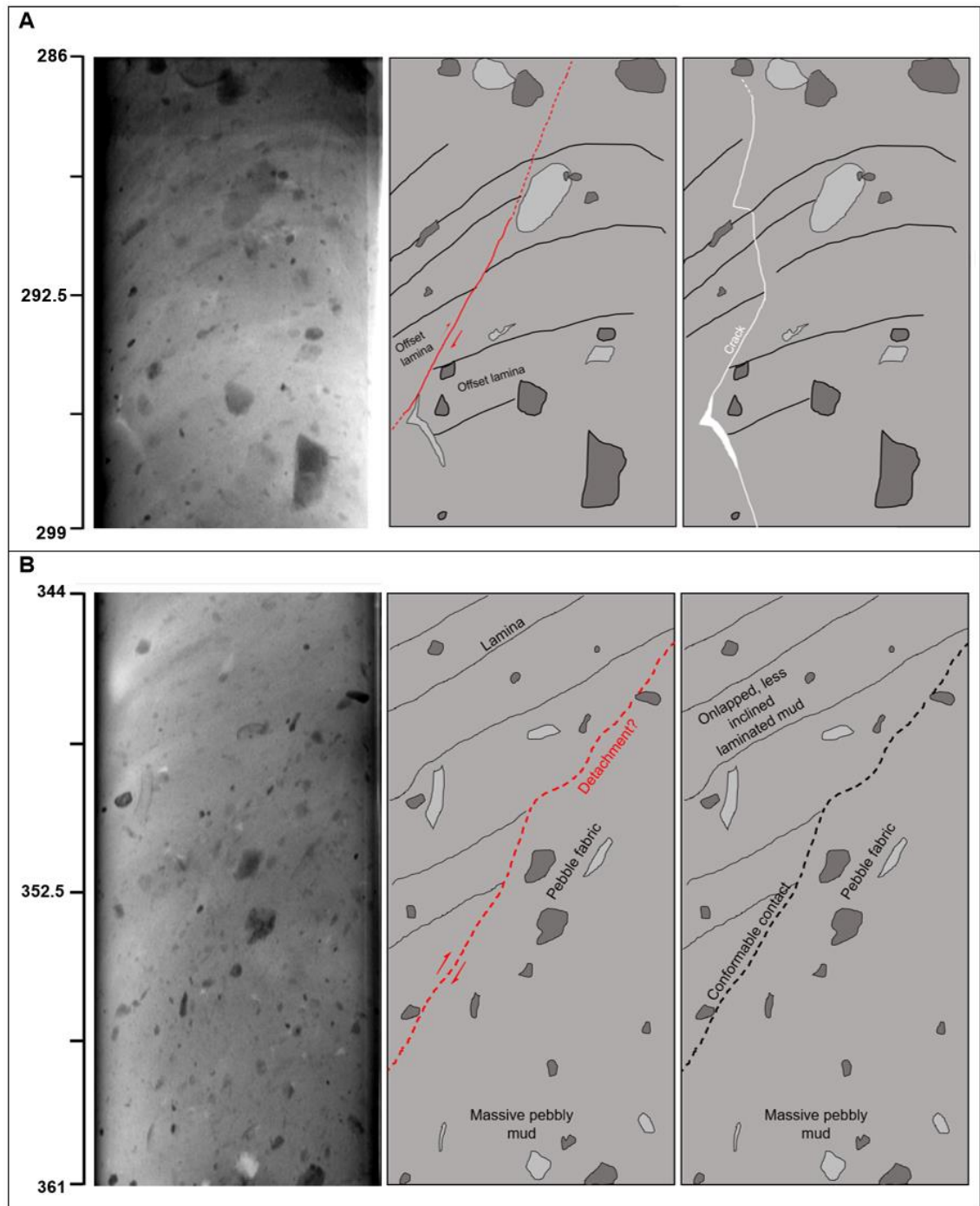


Fig. 5.8: Possible shear planes seen in x-radiographs of facies Fld_c. Scale is core depth in cm. See text for details.

The x-radiographs show that clast long axes generally align with laminae inclination (Fig. 5.8). Lithologies include greenschist, mudstone and a microgranite. In the first 10 cm of the unit, laminae are oriented horizontally, then are inclined at $\sim 40^\circ$ for 70 cm before returning to horizontal in the final 30 cm. Magnetic susceptibility is variable through the unit, ranging from $91.2\text{-}134.4 \times 10^{-5}$ SI except for a sudden spike to a core maximum of 167×10^{-5} SI at 316 cm, where no large or concentrated lithic clasts occur. Gamma-ray density fluctuates through facies Fld_c and is generally highest in this lithofacies ($2.00\text{-}2.23$ g/cm³). This high density is reflected in the resistivity values, also generally higher than in overlying units ($0.79\text{-}1.49$ Ω·m). Water content overall increases upwards through the unit, from 14-20%.

Dms (244-173 cm)

Facies Fld_c is overlain across a gradational contact by a 71 cm-thick stratified diamicton with considerably lower shear strength (6-20 kPa) than in underlying lithofacies. The stratification is imparted by variations in the concentration of sand and coarser material in the silty clay matrix, and is inclined throughout the unit at $\sim 30^\circ$ (Fig. 5.7). The strata have diffuse margins and vary in thickness from $\sim 0.4\text{-}30$ cm, with the finer strata usually thinner. The coarse material is generally angular and is dominantly granule-sized, although clasts up to coarse pebble size (≤ 3 cm) occur. The proportion of shell fragments exceeds that of lithic grains in this coarser material. Lithologies include granite, basalt and sandstone. No clast long-axis alignment is seen in x-radiographs (Fig. 5.7). All samples from this unit were taken from coarser strata, and grain-size analysis shows upward-coarsening through Dms (see Fig. 5.9), with material coarser than fine sand accounting for 30-54%. Due to the unconsolidated structure this textural trend is also seen in the upward decrease in water content (from 23-18%) and increase in resistivity ($0.81\text{-}1.19$ Ω·m). The stratification appears evident in gamma-ray density fluctuations (of ~ 0.09 g/cm³) through facies Dms (Fig. 5.9). Magnetic susceptibility values ($88.5\text{-}117 \times 10^{-5}$ SI) are comparable to those in underlying lithofacies. A radiocarbon age of 25.556 ± 0.237 ka BP was obtained by Ó Cofaigh et al. (submitted) from the basal 2 cm of facies Dms, on a monospecific sample of *Elphidium excavatum*.

Fm (173-55 cm)

Facies Dms is overlain along a sharp contact by 1.18 m of brown massive mud with generally finer and more dispersed coarse material than in Fld_c (see >2 mm IRD graph in Fig. 5.9). The basal 12 cm appears to contain subtle lamination only visible on x-radiographs, some of which is deformed (Fig. 5.7). Shear strength is low overall in facies Fm (8-38 kPa), with highest values in the bottom ~ 40 cm.

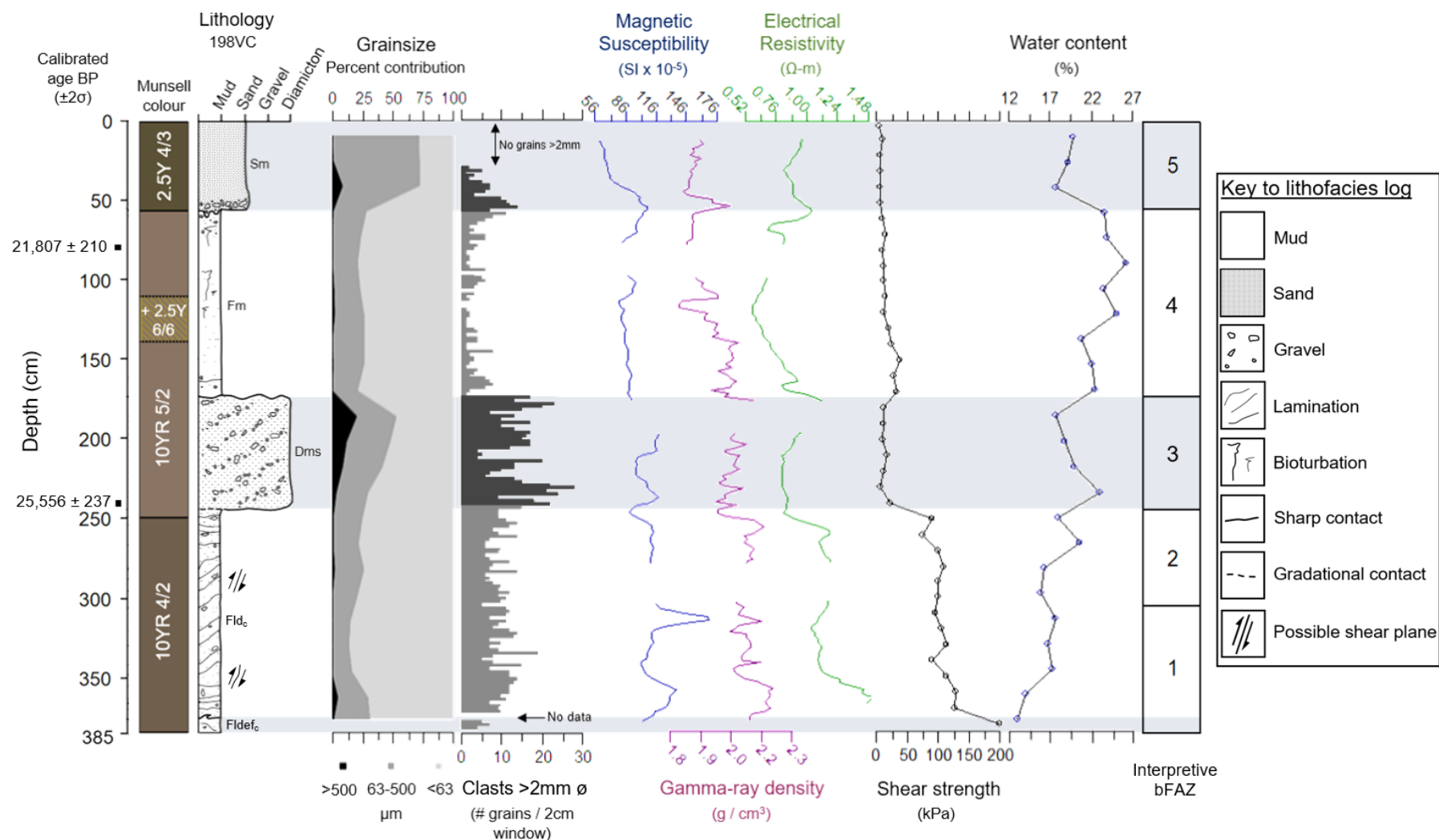


Fig. 5.9: Sedimentologic data for core 198VC. Radiocarbon ages, shear strength, magnetic susceptibility and gamma-ray density data is from Ó Cofaigh et al. (submitted). The depth intervals of lithofacies indicated on the log are extended across the diagram partly as grey shading. Each value on the ‘Clasts >2mm ϕ ’ graph represents 54 cm^3 of sediment. Dark shaded portions of the ‘Clasts >2mm ϕ ’ graph represent intervals where >2mm clasts are not considered to have been deposited at the core site by iceberg-rafting. Lithofacies codes are explained in Table 2.

The content of fine-medium sand (22-27%) is similar to that in the upper half of facies Fld_c. Angular shell material of medium-coarse sand size is dispersed throughout. Bioturbation is visible from 123 cm upwards and is associated with dispersed pockets of yellow fine sand rich in shell material. Magnetic susceptibility and electrical resistivity values decline gradually through facies Fm but show increases coinciding with bioturbation in the upper portion of the unit. Clasts reach medium pebble size (≤ 1 cm) and long axes are generally vertical outside the deformed basal 12 cm and intensely bioturbated intervals. Facies Fm becomes significantly clast-richer in the 10 cm below the contact to Sm, where diffuse pods of shelly, granule-rich sand occur (Fig. 5.7). A date of 21.807 ± 0.210 ka BP was obtained by Ó Cofaigh et al. (submitted) on a monospecific sample of *E. clavatum* from 80-77 cm depth in upper Fm.

Sm (55-0 cm)

Core 198VC is capped across an irregular, loaded contact by an upward-fining shell-rich sand unit. The lower 18 cm of Sm is poorly sorted and contains angular clasts up to coarse pebble size, above 37 cm fining into grey-yellow sand mostly of fine-medium grade. Shell fragments are larger and better-preserved than in underlying units. As in the case of the capping gravel in core 146VC, clast lithologies appear less variable than in the underlying sequence and are dominated by black shale, with schist and granite also present.

Faunal data

5.2.3. Foraminiferal assemblages

85 calcareous and seven agglutinated benthic species were identified in 198VC, along with 14 planktonic species (see Appendix 1). The dominant fauna contrasts strongly with 146VC (cf. Figs. 5.4, 5.10, 5.12). Unlike in 146VC, test preservation is very good throughout 198VC, even in consolidated lithofacies, with large, fragile tests often intact (including features such as pseudospines and Lagenids' necks). Of the 92 benthic species, 66 have maximum abundances representing $< 2\%$ relative abundance throughout, and 29 occur in less than three samples. Four of the 14 planktic species have maximum abundances representing $< 2\%$ relative abundance throughout, with all species occurring in at least four samples. Absolute foraminiferal concentrations throughout 198VC (3757-17790 individuals/g) are 2-3 orders of magnitude greater than in all glaciogenic lithofacies in 146VC. In 198VC, the proportion of planktic foraminifera in non-bioturbated glaciogenic lithofacies (average benthic:planktic ratio = 1.3) is significantly higher

than in 146VC (average benthic:planktic ratio = 35.9). As in 146VC, absolute abundance is highest in the diamictic and capping lithofacies (facies Dms and Sm). The benthic faunal data was divided into 5 interpretive benthic foraminiferal assemblage zones (bFAZs) (Fig. 5.10), and as all but one zone coincide with lithostratigraphic units, faunal data is described below by lithofacies. The debris flow unit (facies Dms) was designated as a separate zone as its unknown provenance and upward-coarsening granulometry prevents analysis of those samples as a meaningful sequence of in-situ assemblages. The unconformably-capping sand unit (facies Sm) was also designated as a separate zone. In contrast to the 5 FAZs delineated for the benthic faunal data, as might be expected, the planktic abundance trends in 198VC showed very limited variation between lithofacies through the glacial sequence and required separation into just two FAZs (pFAZ 1 and 2). As these were driven by abundance trends (Fig. 5.12), the planktic data is described by FAZ. All species relative abundance data presented and quoted represents percentages of the total (agglutinated + calcareous) assemblage (percentage abundances have been calculated separately for the benthic and planktic assemblages). Test concentrations reported below refer to benthic or planktic individuals as appropriate, while fragments are not differentiated into benthic or planktic.

Benthic foraminiferal assemblages

Fldef_c (1 sample)

The assemblage in Fldef_c is dominated by *T. angulosa* (18.5%), *C. lobatulus* (11%) and *Bulimina marginata* (10%), with *Uvigerina peregrina* (9%) and *C. laevigata* (7%) also important. The concentration of tests (2338 individuals/g) and test fragments (466 fragments/g) is very similar to those in overlying facies Fld_c but considerably lower than in Dms and Sm. Values of diversity measures are relatively high compared with averages for overlying lithofacies (40 taxa, $\alpha = 11.8$, dominance low at 0.92).

Fld_c (8 samples)

A significant faunal change occurs within facies Fld_c which warrants the delineation of a new FAZ (bFAZ 2) within this lithofacies (see Fig. 5.10).

bFAZ 1 (continuing from Fldef_c)

The assemblage in the lower half of Fld_c remains similar to that in Fldef_c, dominated by *T. angulosa* (13-22%) and *C. lobatulus* (10-16%), with *U. peregrina* (8-15%), *C. refulgens* (7-12%), *B. marginata* (5-9%) and *C. laevigata* (4-8%) important. This assemblage is consistent until 297 cm core depth.

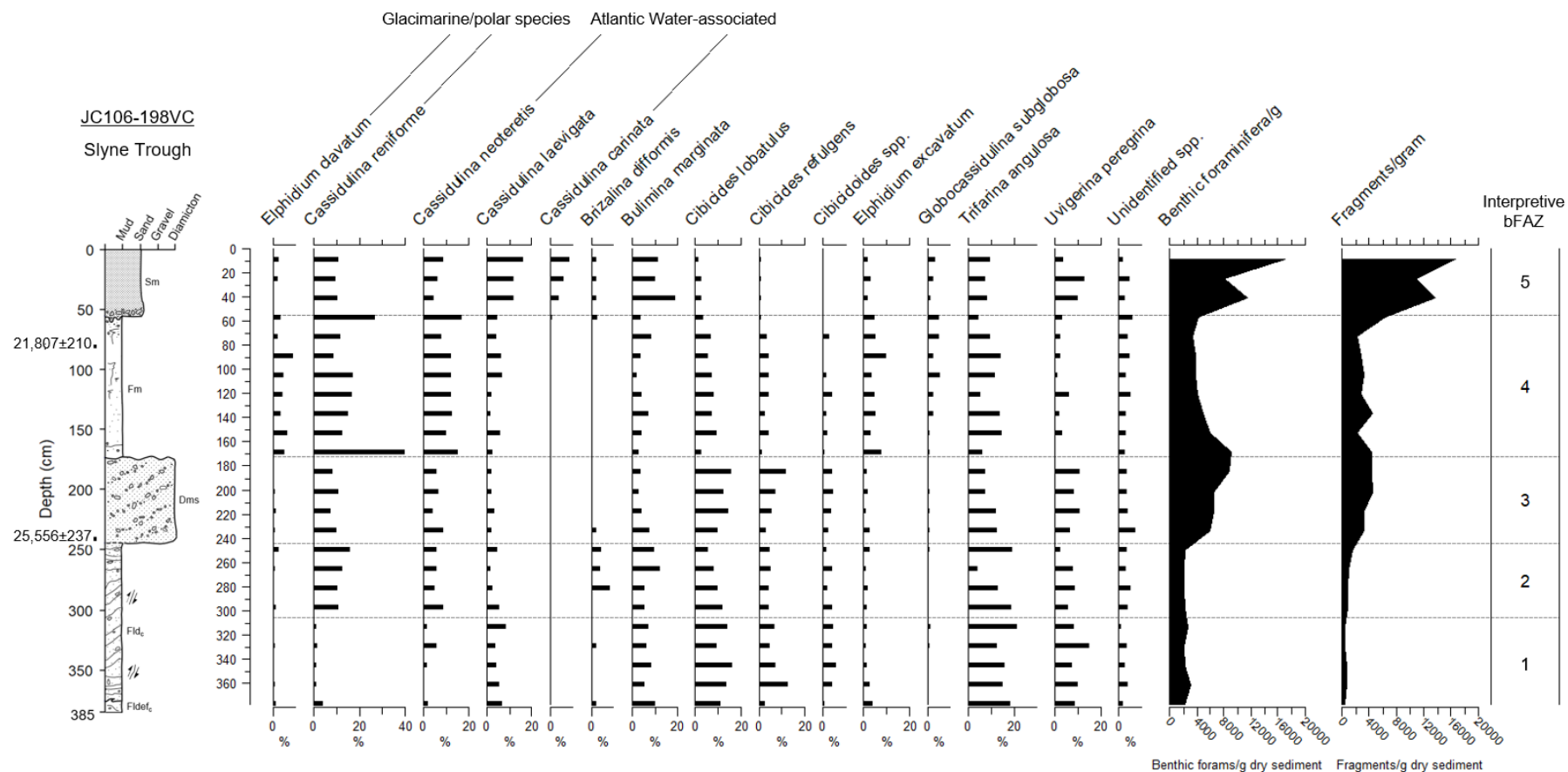


Fig. 5.10: Benthic foraminiferal species abundance for species comprising $\geq 5\%$ of the total (calcareous + agglutinated) benthic assemblage in 198VC. The interpretive bFAZs highlight inferred lithofacies influence on foraminiferal assemblages, except for the zone 1/2 boundary, which delimits a change in faunal composition not associated with any lithologic/stratigraphic change (see Section 4.2.6. for zonation approach).

bFAZ 2

In the sample at 297 cm, *C. reniforme* suddenly becomes an important species (11%) and *C. neoteretis* replaces *C. laevigata* as a more minor component. No lithologic change is seen in this section of facies Fld_c, with the faunal change occurring within inclined laminated pebbly muds rich in shells and shell fragments. Above this depth, assemblages show a gradual increase in *C. reniforme* (to 16%), as decreases are seen in *T. angulosa* (19-4%), *C. lobatulus* (12-6%) and *C. laevigata* (5-2%). *Brizalina difformis* and *Buccella frigida* emerge as minor species. The uppermost sample in Fld_c shows a large increase in *T. angulosa* (to 20%) and an increase in *C. laevigata* (to 5%), but corresponds to the gradational interval between Fld_c and Dms (Fig. 5.9). Concentrations of tests (2054-3142 individuals/g) remain relatively consistent through Fld_c, while test fragments show a gradual increase from 329 cm (473-1514 fragments/g). Species richness and Fisher's α fluctuate in the lower half of the facies before staying reduced for the upper 37 cm (39-29 taxa, α from 11.9 to 7.7), as dominance gradually decreases (Fig. 5.11).

Dms (4 samples)

Samples through Dms remain dominated by *C. lobatulus* (10-16%), *T. angulosa* (7-13%), *C. reniforme* (7-11%), and *U. peregrina* (7-11%). *C. refulgens* (3-12%), *C. neoteretis* (4-9%) and *B. marginata* (3-8%) are still important species, while *Cibicidoides spp.* (2-5%), *B. frigida* (2-4%), *C. laevigata* (2-3%) and *Discanomalina coronata* (1-4%) are minor throughout. Increases in the relative abundances of *C. lobatulus* and *C. refulgens*, and decreases in *T. angulosa* and *B. marginata* coincide with upward-coarsening grain size distributions in these samples. Concentrations of tests (6096-8905 individuals/g) and test fragments (3284-4559 fragments/g) increase through the unit and are higher throughout than in most of the glacial sequence (Fig. 5.10).

Fm (8 samples)

The assemblages in Fm are dominated by *C. reniforme* (9-40%) and *C. neoteretis* (8-17%), with *T. angulosa* fluctuating (5-15%). *E. clavatum* (2-9%) first becomes significant in this lithofacies and represents an important species along with *E. excavatum* (3-10%), *C. lobatulus* (3-9%), *B. marginata* (2-9%) and *C. laevigata* (2-7%). *Globocassidulina subglobosa* first appears as a minor species in Fm, at 1-6%. *U. peregrina*, an important species in all other lithofacies, is minor throughout.

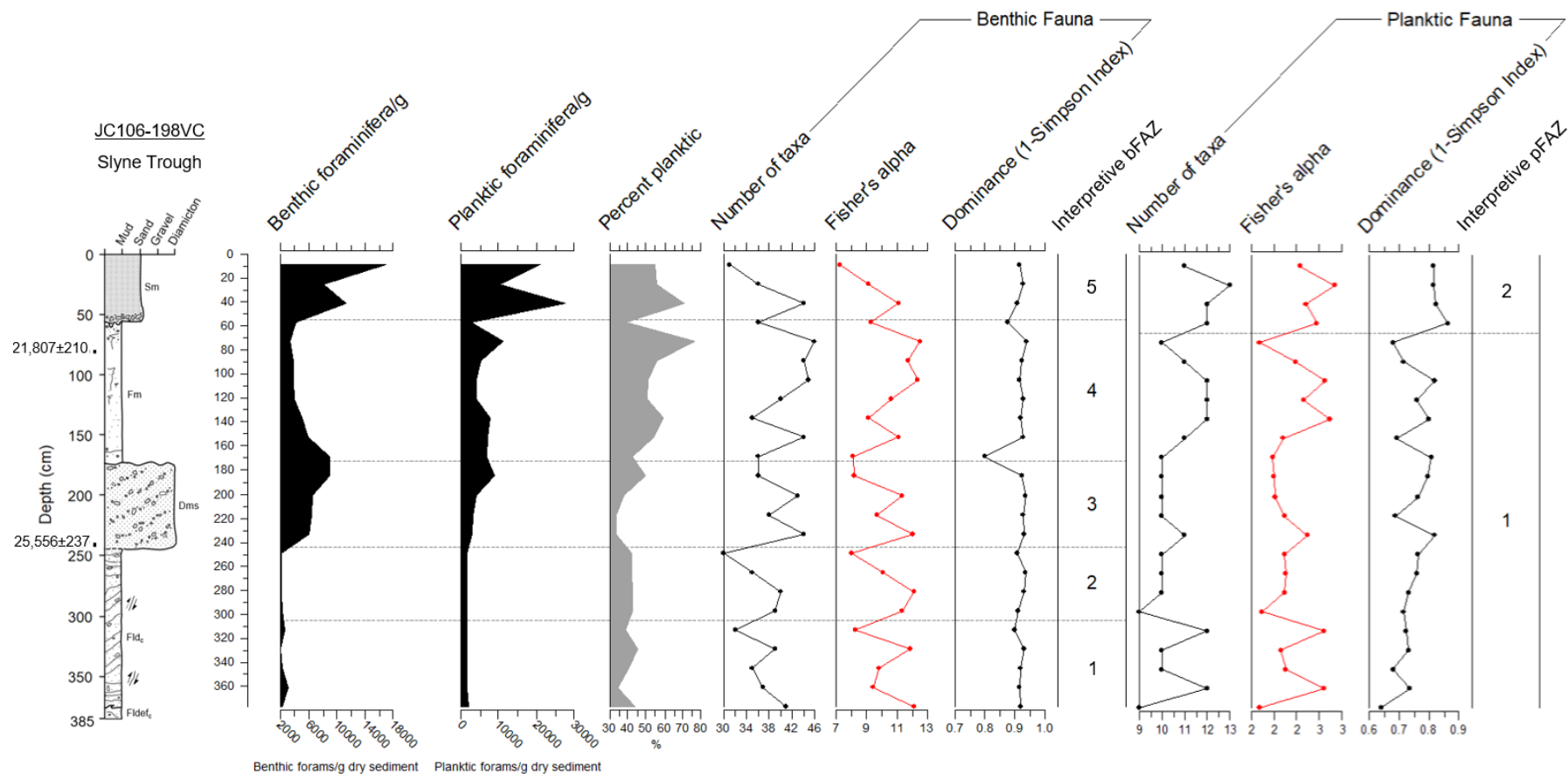


Fig. 5.11: Benthic and planktic foraminiferal concentrations, percentage of planktic individuals and diversity measures for the benthic and planktic assemblages in 198VC. Diversity parameter meanings are explained in Section 4.2.5.

The lowermost sample from the lithofacies (169 cm) is characterised by a reduced diversity assemblage (35 taxa, $\alpha = 7.9$, dominance increased to 0.78) markedly dominated by *C. reniforme* (40%), and is from the weakly laminated, contorted mud seen in the basal 12 cm (Fig. 5.7). The uppermost sample also shows high abundances of *C. reniforme* and *C. neoteretis* and is from a bioturbated interval 2 cm below the loaded contact with Sm. The concentration of tests decreases significantly through all but the uppermost sample in Fm (9054-3442 individuals/g), while the content of test fragments fluctuates at 2244-4628 fragments/g. Species richness and Fisher's α vary initially around lower values before increasing to core maxima in the upper half of the unit (45 taxa, $\alpha = 12.3$) and declining sharply in the uppermost sample (Fig. 5.11).

Sm (3 samples)

Assemblages in the capping sand unit are dominated by *B. marginata* (11-20%) and *C. laevigata* (12-16%). *C. reniforme* (10-11%), *T. angulosa* (7-10%), *U. peregrina* (4-10%) and *C. neoteretis* (5-9%) are also important. *Cassidulina carinata* (4-9%) appears as a significant species following complete absence in underlying lithofacies. Contents of tests (8126-17005 individuals/g) and test fragments (10811-16731 fragments/g) are considerably higher than in most of the glacial sequence (Fig. 5.10).

Planktic foraminiferal assemblages

pFAZ 1 (385-65 cm; 20 samples)

Planktic assemblage composition through the glacial sequence remains relatively consistent through all but the uppermost sample of Fm, which was assigned to the second pFAZ. The assemblages are dominated by *Neogloboquadrina pachyderma* (33-57%) and *Globigerina bulloides* (3-21%), with *Turborotalita quinqueloba* (3-14%) and *Globigerinella siphonifera* (1-17%) generally important but fluctuating throughout. *Neogloboquadrina incompta* remains relatively consistent at 4-13%. Planktic foraminifera represent 33-76.6% of all sampled foraminifera in pFAZ 1, with usually higher proportions in Fm (average 54%) than in consolidated lithofacies (average 40%). The percentage of planktic individuals shows a strong upward increase within the Dms facies (Fig. 5.11), but this may be affected by upward-coarsening in this unit. Planktic foraminiferal diversity measures for pFAZ 1 have lowest values in Fldef_c, and highest values in the lower half of Fld_c and central portion of Fm (Fig. 5.11).

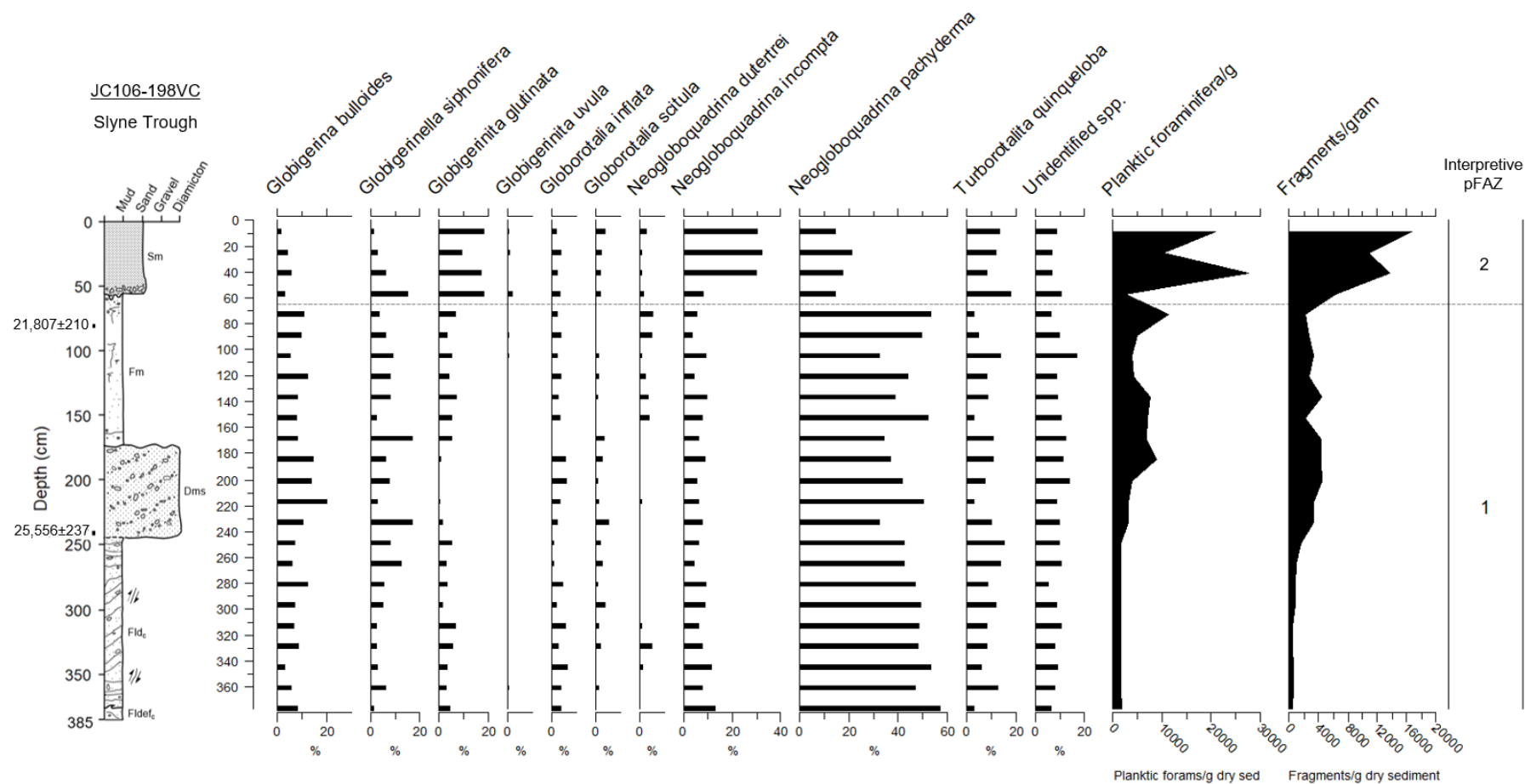


Fig. 5.12: Foraminiferal species abundance for species comprising $\geq 2\%$ of the planktic assemblage in 198VC. Interpretive pFAZs delimit changes in faunal composition as faunal trends in the planktic dataset were not associated with any lithologic/stratigraphic changes (see Section 4.2.6. for zonation approach).

pFAZ 2 (65-0 cm; 4 samples)

pFAZ 2 comprises the uppermost sample of Fm and all of facies Sm. It represents a significant faunal change marked by a considerable increase of *N. incompta* (9→32%) at the expense of *N. pachyderma* (15→22%). This particular change appears transitional in the uppermost sample of Fm at 57 cm where Sm and Fm are mixed by bioturbation and loading. *Globigerinita glutinata* (10-19%) becomes markedly more important as *G. bulloides* is reduced (2-6%) and *G. siphonifera* decreases (15→2%). *T. quinqueloba* remains significant (9-18%). Concentrations of planktic foraminifera reach core maximum values in zone 2 (10258-27738 individuals/g) while their contribution to the total assemblage (40-71%) remains consistent with planktic percentages in upper pFAZ 1 (facies Fm).

CHAPTER 6

INTERPRETATION

This chapter presents palaeoenvironmental interpretations of the sedimentological and faunal data presented in Chapter 5 and integrates them to reconstruct the deglacial oceanographic conditions and sedimentary processes recorded by the core sequences. These reconstructions will be discussed in the context of early deglacial conditions elsewhere along the Atlantic margin of the BIIS and regional palaeoceanographic conditions in the Northeast Atlantic in Chapter 7 (Discussion).

6.1. JC106-146VC

6.1.1. Lithofacies and foraminiferal assemblages

The glacial sequence (excluding facies Gm) in core 146VC is assumed to be essentially continuous on the basis of conformable lithofacies contacts and no sedimentologic evidence for unconformities. However, this cannot be confirmed due to lack of sufficient chronologic data for an age-depth model. The lithofacies interpretations of 146VC following Callard et al. (2018) are extended and partly modified here, and related to oceanographic conditions using the foraminiferal data.

Dmm_c (Basal diamicton) (419-405.2 cm)

The basal unit of core 146VC, facies *Dmm_c*, shows considerably higher shear strength (by ≥ 84 kPa) than all overlying lithofacies, indicating significant consolidation prior to the deposition of succeeding units (Fig. 5.2). In addition, it contains clasts with variable lithologies, has high magnetic susceptibility and includes dispersed, comminuted shell material (see Section 5.1.2.). These characteristics suggest that this diamicton was deposited subglacially and derived from a combination of terrigenous sources and marine deposits (cf. Diekmann et al. 2000; Ó Cofaigh & Evans 2001b; Peters et al. 2016). Following the sub-bottom profiler data interpretation of Callard et al. (2018) however, this basal diamicton does not belong to the acoustic unit which is structurally formed into till sheets, moraine ridges and grounding-zone wedges on the outer shelf. Rather, it appears to correspond to the unit underlying these features, which has a massive structure and a furrowed, corrugated upper reflector (see Fig. 5.1C). This acoustic unit may represent the Barra Formation of Malin-Hebrides region stratigraphic schemes (see Davies et al. 1984; Stoker et al. 1993), which has not been directly dated but has been considered to represent ‘late Devensian’ glacial marine sedimentation (Fyfe et al. 1993; Dove et al. 2015). The foraminiferal

assemblage in Dmm_c is very similar to that in overlying glacimarine deposits (see Fig. 5.4), with no significant content of non-Arctic or glacimarine species. As such, Dmm_c may represent the uppermost Barra Formation reworked and consolidated into a firm diamicton by the ILGM BFIS advance.

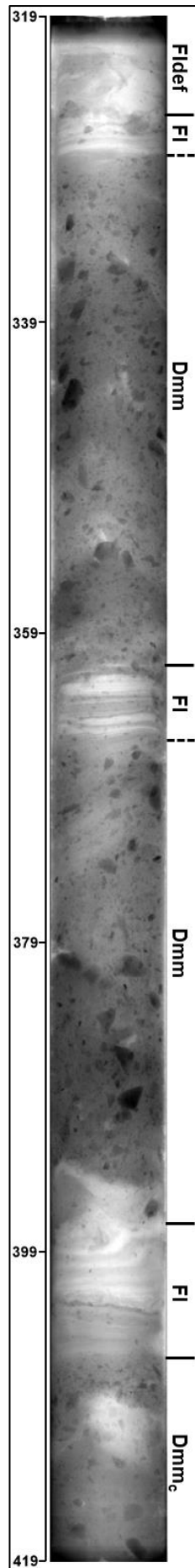
Deposition of consolidated basal tills on the Malin shelf edge is chronologically constrained by a radiocarbon date on a shell fragment from within the till to sometime after 26.7 ka BP, and before 25.9 ka BP by the earliest age obtained on benthic foraminifera from overlying glacimarine deposits (from 369-372 cm in 146VC; Callard et al. 2018; Fig. 5.2). These diamictons therefore represent the ILGM advance of the grounded BFIS to a ~1000 year-duration maximum at the Malin shelf edge.

Sequence of alternating Fl and Dmm units (405.2-328.3 cm)

Facies Dmm_c is overlain by 77 cm of laminated mud beds (3-11 cm thick) alternating with thicker units of massive diamicton (28-33 cm thick) (Figs. 5.2, 6.1). The presence of lamination and considerable drop in shear strength (to ~26 kPa) in these lithofacies suggests they were deposited in a subaqueous setting and were not subsequently overridden by grounded ice (Svendsen et al. 1992; Lowe & Anderson 2002; Ó Cofaigh et al. 2005). These lithofacies are interpreted to represent early deglacial sedimentation, deposited from sometime after 26.7 ka BP until sometime between 24.4 ka BP and 23.8 ka BP, following the retreat of the BFIS from the shelf edge (Callard et al. 2018).

Sequences of alternating laminated mud and massive diamicton are commonly reported from glacimarine environments (see Jennings & Weiner 1996; Ó Cofaigh & Dowdeswell 2001; Matthiessen et al. 2010), where they have been explained as forming through variation in the relative importance of iceberg-rafting over suspension settling due to episodic sea-ice development (Dowdeswell et al. 1994; Dowdeswell et al. 2000). Callard et al. (2018) suggested this mechanism as possibly explaining these sequences on the Malin shelf. Similar sequences can also occur under more temperate conditions, on an annual timescale, where summer meltwater sedimentation overwhelms iceberg-rafting, in the absence of sea-ice (Cowan et al. 1997; Ullrich et al. 2009; Hogan et al. 2016). While improved constraints on sedimentation rates could resolve this, sea-ice development is inferred provisionally, as it is more consistent with the foraminiferal assemblages and low abundance throughout 146VC (see below).

Fig. 6.1 (overleaf): X-radiograph of core 146VC, Section E/5, showing the sequence of facies from the basal diamicton (Dmm_c) to facies Fldef. Scale is core depth in cm.



The higher sand content of the Dmm units relative to FI (doubled, to $\leq 12\%$ by weight) supports predominance of iceberg-rafting during their deposition, and/or higher meltwater fluxes during these sea ice-free periods (cf. Vorren et al. 1984; Cowan et al. 1999; Jennings et al. 2014). While these alternating sequences are generally more ice-distal deposits (Ó Cofaigh & Dowdeswell 2001), the still significant content of >2 mm grains in the thin FI intervals (see Fig. 5.2) might suggest a more ice-proximal *mélange/sikussak* setting where immobilised icebergs were concentrated and releasing coarser debris (see Syvitski et al. 1996; Dowdeswell et al. 1998; Forwick & Vorren 2009). Trapping of icebergs in the area of the 146VC site could have been aided by constriction between the ice margin and GZW1a to the west (see Fig. 3 of Callard et al. 2018).

Foraminiferal assemblages in the alternating Dmm and FI intervals are dominated by *Elphidium clavatum*, *Cassidulina reniforme* and *Elphidium excavatum*, with minor *Cibicides lobatulus* and *Elphidium albiumbilicatum*. The presence of *Nonionellina labradorica* (1-3%) and *Nonion* species (1-4%), although minor, may support the suppressed iceberg-rafting interpretation above as these capitalise on fresh phytodetritus and tolerate dysoxia, so in cold environments are often associated with the enhanced productivity at the sea-ice edge (Rytter et al. 2002; Gooday 2003; Seidenkrantz 2013). *E. clavatum* tolerates fluctuating temperature, salinity, food availability and turbidity, therefore often dominates in ice-proximal settings (Linke & Lutze 1993; Hald & Korsun 1997; Korsun & Hald 1998; Nielsen et al. 2010), but is also common under more stable Arctic conditions (Hald et al. 1994).

In glacially-influenced marine environments, *C. reniforme* is generally most abundant in more ice-distal settings where salinity is more stable and higher productivity generates higher organic matter fluxes (Korsun & Hald 1998; 2000). It is also common, usually with *E. clavatum*, in Arctic shelf environments influenced by polar waters (e.g. Mudie et al. 1984; Hald & Vorren 1987; Jennings et al. 2004). *E. excavatum* (= *E. excavatum selseyensis* of other studies) is not associated with glacialmarine environments and is usually reported from boreal settings in relatively shallow, oligotrophic and oxygenated waters (see Sejrup et al. 2004; Polovodova et al. 2009; Darling et al. 2016). *E. clavatum* was identified

from the presence of a calcite boss in the umbilicus and closing/closed sutural depressions in the umbilical area (e.g. Schweizer et al. 2011), however, sutural form was not always clear, and Feyling-Hanssen (1972) noted that the boss can be absent in *E. clavatum*. Given their high proportion, many individuals assigned to *E. excavatum* here may therefore represent *E. clavatum*, or a large reworked contribution of *E. excavatum*; either would be consistent with an overall interpretation as an ice-proximal glacimarine environment.

The epifaunal species *C. lobatulus* is often present in glacimarine environments, where it lives attached to dropstones or other firm substrates (Korsun & Hald 1998), likely exploiting strong currents/oligotrophic conditions. A notable characteristic of many *E. clavatum*, *C. reniforme* and *C. lobatulus* specimens retrieved from the Dmm-FI alternations was their relatively small size (~0.2-0.3 mm test diameters). High proportions of small individuals are observed in harsh, ecologically-stressful glacimarine environments, where species at tolerance limits show restricted development and higher mortality (often due to reduced food availability and rapid burial) leading to greater accumulation of juvenile and small specimens (Feyling-Hanssen 1982; Korsun et al. 1995). *E. albiumbilicatum* is widely distributed (see Darling et al. 2016; Murray & Alve 2016), but often reported from reduced-salinity settings in cold, shallow Arctic waters (e.g. Kubischta et al. 2010; Korsun et al. 2012; Limoges et al. 2018), and therefore is also consistent with a proximal glacimarine interpretation. The low content (4-6 individuals/sample) of planktic foraminifera (mostly *Globigerina bulloides*) in these lithofacies suggests extreme sea ice conditions limiting off-shelf productivity (Jansen et al. 1983; Hald & Vorren 1987) and/or the advection of planktic individuals from the open ocean onto the shelf, as planktic foraminiferal production is generally limited over continental shelves (Murray 1976; Gibson 1989). This was also inferred from similarly low planktic:benthic ratios on the Hebridean shelf during deglaciation by Austin (1991). Generally low organic matter flux is suggested by the well-preserved lamination in the FI intervals as this is consistent with limited macrofaunal bioturbation (Vorren et al. 1984; Lemmen 1990). Limited macrobenthos influence is characteristic of these alternating mud-diamict deposits in modern Arctic environments (Ó Cofaigh & Dowdeswell 2001).

Fldef (325.7-307.5 cm)

The sequence of alternating Dmm and FI intervals is overlain by a package of clast-poor contorted laminated mud. The low shear strength (20 kPa) and elevated water content (28%) in this unit, combined with convolute laminae, is consistent with remobilisation of laminated sediments which became unstable due to rapid deposition in a subaqueous setting (Scott et al. 1991; Ó Cofaigh et al. 2002; 2004). Such sediment failure is common in basin fills (such as the 146VC sequence), as steeper depositional surfaces at the basin edges can encourage downslope remobilisation (Ó

Cofaigh & Dowdeswell 2001), particularly in glacial marine settings where sedimentation rates can be very high (e.g. Syvitski et al. 1996; Lønne 1997). The foraminiferal assemblage in facies Fldef remains dominated by *E. clavatum*, *C. reniforme* and *E. excavatum*, with minor *C. lobatulus* and *E. albiumbilicatum* as in the underlying lithofacies, implying persistence of cold glacial marine conditions.

Fl (307.5-233.5 cm)

The 74 cm-thick Fl unit (Fig. 6.2) overlying facies Fldef is characterised by considerably finer granulometry (98-99% mud by weight), with significantly reduced content of clasts >2 mm (0-8 grains/2 cm window; see Fig. 5.2). Foraminiferal abundance (including agglutinating species) is also substantially reduced in this unit (to 0-7 individuals/g, see Fig. 5.4), most likely indicating very low surface productivity and organic matter availability (Nørgaard-Pedersen et al. 2003; Ouellet-Bernier et al. 2014; Jennings et al. 2018) and/or high sedimentation rates (Austin 1991) during this period. Two potential explanations for such low productivity in a glacial marine environment include perennial sea-ice cover and the presence of an ice-shelf (e.g. Domack et al. 2001; Cape et al. 2014). Both of these situations have been associated with the formation of clast-poor laminated muds such as Fl (e.g. Vorren et al. 1984; Gilbert et al. 1990; Jennings et al. 2017). Counts of >2 mm clasts in Fl are frequently zero, but never for more than 6 cm at a time (Fig. 5.2), suggesting a relatively constant supply of coarse clasts to the core site, though sedimentation rates are unknown. This is possible under an ice-shelf (Ó Cofaigh & Dowdeswell 2001) but also under perennial sea ice, provided immobilised icebergs were melting out over the core site. Persistence of an ice-shelf terminus configuration during BFIS retreat across the outer shelf is implied by the presence of a second GZW (GZW1b), located ~3 km inshore of the 146VC site (see Fig. 5.1C) (Dowdeswell & Fugelli 2012; Batchelor & Dowdeswell 2015). This requires that the two narrower, sharper-crested ridges between these GZWs are associated with ice-shelf retreat, possibly as crevasse fills, from tidal motion of the grounding-line, or as iceberg-grounding features (e.g. Shipp et al. 2002; Jakobsson et al. 2011; Dowdeswell et al. 2020). However, the iceberg-rafting implied by the underlying facies Dmm intervals (described above) suggests open-water conditions and therefore, that the ice-shelf was not wide enough to induce sub-ice shelf conditions at the core site during the subsequent deposition of the Fl unit. Sub-ice shelf deposition of facies Fl would have required considerable extension of the ice-shelf during stabilisation at GZW1b (see Fig. 6.3 panel 2). On this basis, the Fl unit is interpreted to record perennial sea-ice cover buttressing the BFIS ice-shelf during its stabilisation at GZW1b. Unfortunately, however, identifying a regional signature of the BFIS terminus configuration from other cores west of GZW1b is frustrated by their frequent lack of undisturbed deglacial lithofacies due to bottom-current winnowing (see Callard et al. 2018).

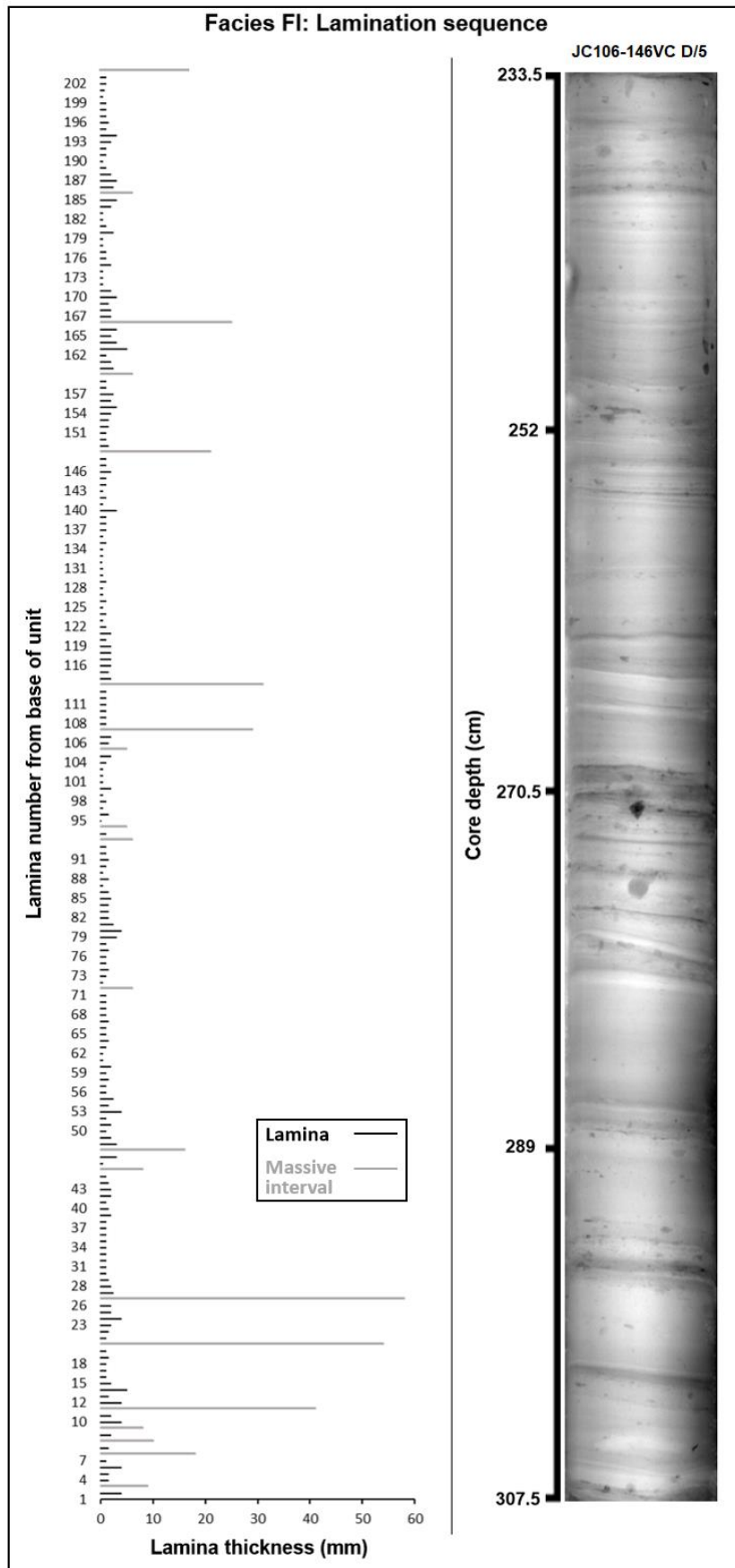


Fig. 6.2: Thickness and sequence of laminae and massive intervals in the facies F1 unit. Note dominantly horizontal clast long axes in the x-radiograph. X-radiograph shows the full unit.

A notable feature of the lamination sequence in facies F1 is the occurrence of apparently massive fine intervals 3-5 cm thick, which interrupt lamination primarily in the lower half of the unit (Fig. 6.2). The irregular lamination interspersed with massive intervals in the lower half of F1 strongly parallels descriptions of tidally-influenced glacial marine muds where freshly-deposited, loosely-consolidated 'fluffy' laminae (comprising silt and flocs of clay; Curran et al. 2004) are reworked by tidal currents to form homogenised intervals (Mackiewicz et al. 1984; Kilfeather et al. 2011). Dense brines intermittently released by sea-ice formation or basal freeze-on to an ice-shelf could also produce such intervals (Powell 1984; Elverhøi et al. 1989; Hemer et al. 2007). Operation of tidal and/or brine currents during F1 deposition may also be suggested by the dominantly horizontal long axes of coarse clasts throughout facies F1 (Domack & Lawson 1985; Fig. 6.2), considering the softness of these sediments (shear strength 13-15 kPa). Thinning of the massive intervals through the upper portion of the unit (Fig. 6.2) may suggest weakening of these currents and/or decreasing sedimentation rates over time (Domack & Harris 1998; Hemer et al. 2007; Smith et al. 2019).

The low numbers of foraminifera retrieved from F1 (≤ 31 individuals/sample) mostly comprised very small specimens of *C. reniforme* and *E. clavatum*. Three specimens of *Neogloboquadrina pachyderma* and one specimen of *G. bulloides* were the only planktic foraminifera found in the unit. If low foraminiferal abundance is attributed to limited food supply due to perennial sea-ice cover at the core site, it is most likely that the planktic foraminifera in F1 were transported from open water, by tidal and/or bottom current activity. Such advection of foraminifera is well-documented, at least for ice-shelf cavities (e.g. Domack & Harris 1998; Hillenbrand et al. 2017; Minzoni et al. 2017). Combined with the limited food availability for benthic communities, such advection probably explains the premature death implied by the generally small size of the foraminiferal specimens in F1. It is possible that this sea-ice covered environment was particularly harsh in the area of the core site, with turbidity and low salinity enhanced by reduced exchange with the open ocean due to the nearby shelf-edge GZW1a.

F1d (233.5-230 and 209-202.5 cm)

F1 is succeeded by a thin interval of facies F1d, which brackets the final Dmm unit in the 146VC sequence. Facies F1d has characteristics intermediate between F1 and Dmm, representing a laminated, clast-rich diamictic mud. Such transitional intervals have been interpreted as representing conditions of partially-suppressed iceberg rafting against a background of fine-grained sedimentation via suspension settling from turbid meltwater plumes (e.g. Jennings & Weiner 1996; Rütther et al. 2012; Marienfeld 1992; Dowdeswell et al. 1994; Fig. 5.3). The bracketing occurrence of facies F1d would therefore suggest that resumption of coarser rain-out

(represented by facies Dmm) following the ice-covered period implied by facies Fl was gradual rather than abrupt. The upper Fld interval would then imply that the subsequent period of intensive rain-out (represented by the overlying facies Dmm and Fmd) was partially suppressed for a brief period.

Dmm (230-209 cm)

The final, 21 cm-thick occurrence of facies Dmm in 146VC is thinner and initially coarser in particle-size (by 8-12% more >500 μm fraction) than its previous occurrences (Fig. 5.2). As in the previous Dmm units, clast lithologies and long-axis orientations are variable, which combined with its initially coarser granulometry and bracketing by undeformed facies Fld suggests predominance of iceberg-rafting during deposition of this final Dmm unit, rather than as a subglacial till (Domack & Lawson 1985; Grobe 1987; Smith & Andrews 2000). The content of test fragments reaches a core maximum (excluding capping facies Gm), suggesting elevated input of reworked detritus in a probably ice-proximal environment (Hald et al. 1990; Licht et al. 1999). Foraminiferal abundance shows an abrupt and large increase into this unit, from a barren sample in uppermost Fl to ≥ 300 tests/sample in lowermost Dmm. This increase in foraminiferal concentration likely reflects elevated productivity associated with disintegration of perennial sea-ice (Principato et al. 2005; Kilfeather et al. 2011; Minzoni et al. 2017). The foraminiferal assemblages and abundance in facies Dmm strongly resemble those in the underlying units (dominated by *E. clavatum*, *E. excavatum* and *C. reniforme*), implying cold and relatively ice-proximal conditions but with moderate fine-grained sedimentation rates. Small specimens of *E. clavatum* occur, but in lower proportions than in underlying lithofacies. The proportion of planktic individuals (benthic:planktic ratio = 44) is as low as in the units preceding facies Fl, suggesting continued low surface productivity in the adjacent open ocean, now probably due to meltwater at the surface rather than sea ice. Deposition of this unit was dated by Callard et al. (2018) to 23.8 ka BP from a sample of mixed benthic foraminifera.

Fmd (202.5-140 cm)

The upper of the bracketing Fld intervals is succeeded by a unit of pebble-rich massive mud. Clasts >2 mm are present at all levels but with fluctuating concentrations (see Fig. 5.2), and generally have vertically-oriented long axes. These characteristics are consistent with persistent iceberg-rafting against a background of suspension settling from turbid meltwater plumes, probably in a more ice-distal environment (Svendsen et al. 1992; Evans et al. 2005). Foraminiferal assemblages remain dominated by *E. clavatum*, *E. excavatum* and *C. reniforme*, implying persistence of cold water conditions. *C. lobatulus* is more important than in underlying units,

possibly due to increased availability of hard substrates through iceberg-rafting. In addition, its slight upward increase in abundance might reflect increasing bottom-current strength (Hald & Korsun 1997; Kubischta et al. 2010), which may be supported by the upward increase in >500 µm sand content in this lithofacies (see Fig. 5.2).

Fm (140-15.5 cm)

Facies Fm comprises 124.5 cm of massive, soft (shear strength 8-15 kPa) mud containing few clasts >2 mm. It succeeds facies Fmd across a gradational boundary and its content of >2 mm clasts decreases upwards. Such massive, clast-poor muds are commonly reported from distal glacimarine settings where they reflect the combined effect of reduced importance of iceberg-rafting and increased bioturbation with distance from the ice margin (Jaeger & Nittrouer 1999; Evans & Pudsey 2002), however, no clear bioturbation structures are visible in the x-radiographs. As such, combined with underlying facies Fmd, facies Fm records increasing distance from the BFIS margin as it retreated across the shelf. This is also suggested by the declining magnetic susceptibility values (Fig. 5.2), which indicate decreasing clast and (terrigenous) heavy mineral contribution over time. Foraminiferal assemblages remain consistent with underlying lithofacies, dominated by *E. clavatum*, *E. excavatum* and *C. reniforme* with minor *C. lobatulus*, until the uppermost Fm. Absolute abundance is generally significantly reduced in Fm relative to Fmd, except for the upper two samples which are probably affected by mixing with overlying facies Gm, in the form of loading and gravelly sand-filled burrows penetrating the uppermost Fm (see Section 5.1.3. and Fig. 5.3). Planktic foraminifera remain at low proportions in Fm (benthic:planktic ratios of 8-53), however, these ratios are uncertain due to low absolute abundance. The benthic assemblage composition in Fm implies that ocean temperatures on the shelf remained cold into increasingly ice-distal conditions. It is notable, however, that the chilled Atlantic Water-associated *Cassidulina neoteretis* (Mackensen & Hald 1988; Cronin et al. 2019; Jennings et al. 2020) appears at 41 cm in the upper Fm (representing 8%) but is not important in the overlying samples (Fig. 5.4). This might indicate a late-stage Atlantic Water influx otherwise obscured by the unconformably-overlying Gm and its loading and bioturbation into uppermost Fm.

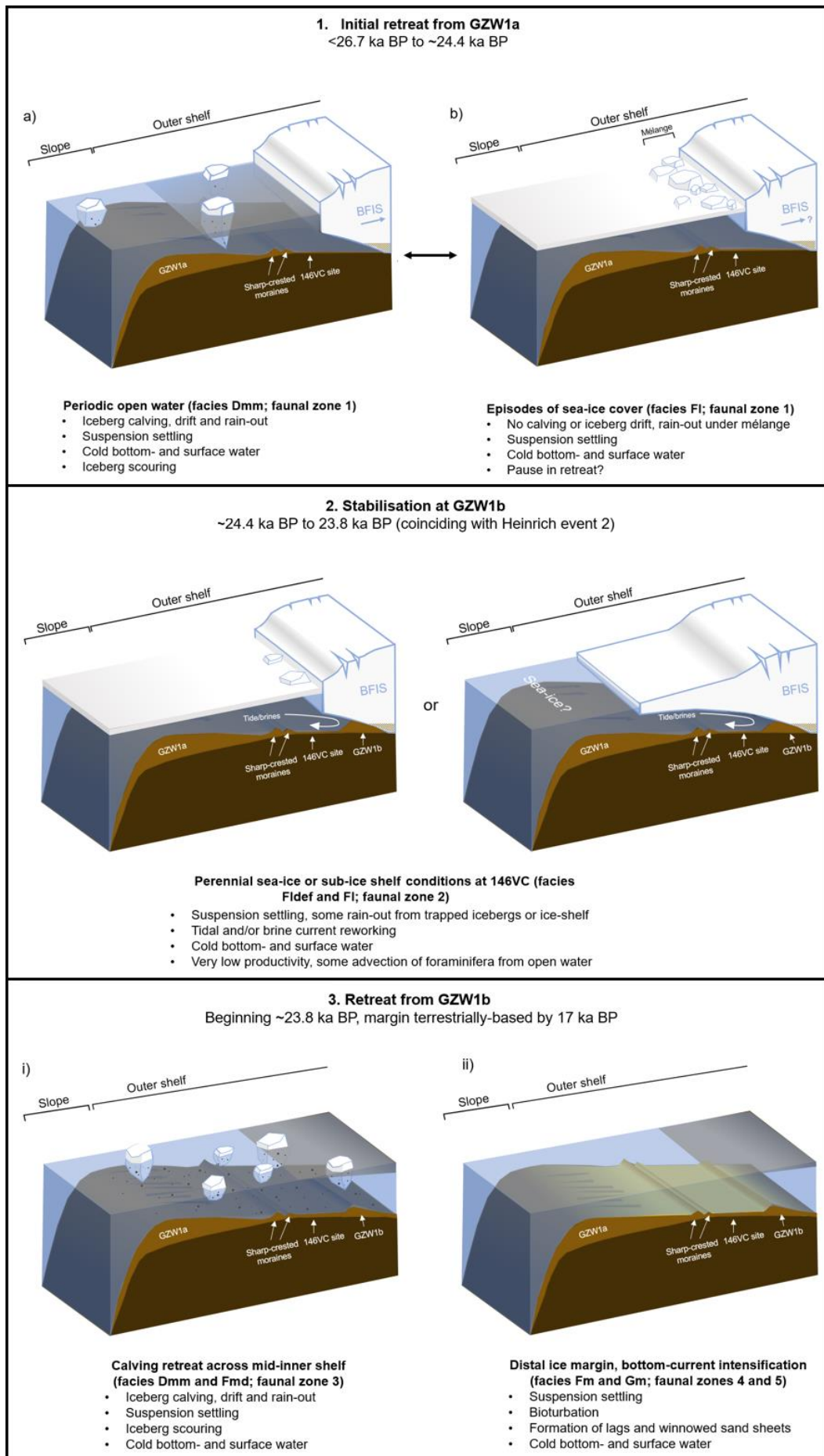
Gm (15.5-0 cm)

The sampled foraminiferal assemblage in facies Gm is markedly different from that persisting through the underlying lithofacies (except for the uppermost two samples affected by bioturbation and loading, see Figs. 5.3, 5.4). It is dominated by *Trifarina angulosa*, with *C. lobatulus*, *Textularia sagittula* and *Cassidulina laevigata* also important. Test and test fragment

concentrations are 2-3 orders of magnitude greater in facies Gm than in all underlying lithofacies, and the planktic proportion is also higher relative to underlying units (benthic:planktic ratio = 6). The lack of fine sediment, overall coarser grain-size, clast-supported structure and high bioclast content of facies Gm are consistent with a lag deposit formed through winnowing of clast-bearing glacimarine/subglacial sediments by bottom currents (Dobson & Haynes 1973; Holtedahl & Bjerkli 1982; Viana et al. 1998; Stoker et al. 2011; Callard et al. 2018). Foraminifera-rich lag gravel and winnowed shelly sand deposits are widespread surface sediments on the Irish and British shelves, where they are often transported and redistributed by tidal currents and waves (e.g. Pingree & Griffiths 1979; King et al. 2019). The benthic foraminiferal assemblage in facies Gm therefore most likely comprises individuals from various time periods and transported from different habitats on the shelf and upper slope (e.g. Murray 1985; 2004). Indeed, the Gm assemblage represents a mixture of strong current-associated species (*Trifarina*, *Textularia* and *Cibicides* species; Edwards 1982; Mackensen et al. 1985; Schönfeld 1997), species generally associated with higher nutrient availability and finer substrates (e.g. *C. laevigata*; Austin & Evans 2000; Milker et al. 2009) and polar/glacimarine conditions (*E. clavatum* and *C. reniforme*). An essentially equivalent assemblage was reported by Murray (1985) from rippled sands on the Hebridean shelf. Attached epifaunal species are frequently abundant in these surface sands, indicating current transport as these require firm substrates and accumulate in these mobile sandy substrates if detached following death (Dobson & Haynes 1973; Murray 2004). The higher proportion of planktic foraminifera in facies Gm probably reflects more productive postglacial conditions in the open ocean and easier advection of tests onto the shelf through postglacial sea-level rise and current intensification.

6.1.2. Summary and relation of interpretations to geomorphological context of core 146VC

Initial retreat of the BFIS across the outer shelf beginning after 26.7 ka BP (Callard et al. 2018) was associated with an ice-shelf margin configuration, in an environment characterised by cold surface and seafloor water temperatures and episodic development of extensive sea-ice (Fig. 6.3). Atlantic Water was not present on the Malin shelf during this time. Narrower ridges inshore of the outermost GZW (GZW1a) on the northern Malin shelf edge (see Fig. 3a of Callard et al. 2018) may represent crevasse-fills, tidal heaving of the grounding-zone, or iceberg grounding, during retreat across the outer shelf. The BFIS grounding-line then stabilised at GZW1b (3 km inshore of 146VC) sometime around 25.9 ka BP, implying persistence of the ice-shelf margin configuration at this position (Fig. 6.3).



←
Fig. 6.3 (previous page): Schematic figure showing deglacial depositional environments interpreted from 146VC lithofacies. In panel 2 the sub-ice shelf scenario is considered less likely (see text).

Laminated, clast- and foraminifera-poor muds deposited at 146VC sometime between 24.4 ka BP and 23.8 ka BP probably record perennial, buttressing sea-ice and tidal and/or brine currents during the occupation of GZW1b. This period coincided with Heinrich event 2 (~24 ka BP; Hemming 2004), and ocean temperatures on the shelf remained cold, with a benthic foraminiferal assemblage common in modern Arctic or distal glacimarine environments.

Retreat of the BFIS from GZW1b, beginning before 23.2 ka BP, occurred over a sustained period of calving rather than through a catastrophic event. Retreat from the outer shelf was not interrupted by subsequent readvances (glacitected sediments and overprinted/corrugated ice-marginal structures are not observed on the mid-inner Malin shelf) and occurred under continuing cold bottom- and surface water conditions. This probably rapid retreat by calving would have been aided by the overdeepened troughs on the mid-shelf, in which there are no ice-marginal structures to indicate temporary stabilisations (Callard et al. 2018). It is also reflected in intensive iceberg-scouring of the outer shelf down to water depths of ~190 m (Dunlop et al. 2010; Sacchetti et al. 2012) and inner shelf (but buried here under thick postglacial deposits; see Fig. 4a of Callard et al. 2018). Low temperatures persisted through ice-distal conditions on the outer shelf, no longer influenced by iceberg-rafting (therefore, possibly as late as 17 ka BP; Tarlati et al. 2020), but it is possible that chilled Atlantic Water began to influence the shelf later in this period. Winnowing of diamictic glacial deposits by strengthened bottom currents (probably from the early Holocene onwards; Armishaw et al. 2000) left gravelly lags and generated foraminifera-rich sands as extensive surface deposits (Fig. 6.3). These presently form sand-waves and -sheets on the Malin shelf (Pendlebury & Dobson 1976; Dunlop et al. 2010).

6.2. JC106-198VC

6.2.1. Lithofacies and foraminiferal assemblages

In contrast to 146VC, several erosive and unconformable contacts occur in the 198VC sequence. Therefore, due to the lack of an age-depth model, it is uncertain how much of the sequence has been lost, and as for 146VC, sedimentation rates are unknown. The foraminiferal assemblages in 198VC are characterised throughout by relatively high diversity (α spans 7.0-12.3), high planktic foraminiferal proportions (benthic:planktic ratios span 0.3-2.0) and high preservation quality, thereby differing significantly from the variably preserved, clearly glacimarine/Arctic

assemblages in 146VC. The lithofacies interpretations of Ó Cofaigh et al. (submitted) are extended here and partly modified with reference to associated oceanographic conditions.

Fldef_c (385-375.5 cm)

The basal 9.5 cm of core 198VC comprises deformed laminated sandy clay characterised by very high shear strength (200 kPa; ≥ 70 kPa than the overlying facies Fld_c). The seismic profile along the ridge from which 198VC was retrieved shows a horizon of infilled iceberg scours underlying the recovery limit of the core (see Fig. 5.6C, noting vertical scale and core recovery of 3.85 m). It is evident from this profile that 198VC does not sample the acoustically-impenetrable core of the ridge, interpreted as highly consolidated subglacial diamicton (Ó Cofaigh et al. submitted). In addition, the presence of laminations in this facies is inconsistent with subglacial till (e.g. Evans et al. 2006). Fldef_c is therefore interpreted as glacial marine sediment originally deposited during the first ILGM retreat from the outer shelf (see Section 5.2.1), with its very high consolidation reflecting readvance during this first period of retreat. Its consolidation may have been further increased during the subsequent final readvance onto Porcupine Bank (see section 5.2.1). Following this interpretation, Fldef_c represents a preceding period of glacial marine deposition to overlying facies Fld_c. However, as its foraminiferal assemblage is identical to that in lower Fld_c (also bFAZ 1 and pFAZ 1), the assemblage in Fldef_c is not interpreted separately.

Fld_c (375.5-244 cm)

Facies Fld_c is a ~1.3 m-thick unit of firm laminated sandy mud with abundant pebbles and shell material (Fig. 6.4). This facies belongs to a consolidated mud lithofacies association retrieved only on the eastern margin of the Slyne Trough by Ó Cofaigh et al. (submitted) (cores 197VC, 198VC and 199VC; see Fig. 5.6). In these cores, the consolidated mud association is characterised by frequent, gradational alternation between massive and laminated facies, and shear strengths of 26-130 kPa. Foraminiferal assemblages in bFAZ 1 (Fldef_c and the lower half of Fld_c) are dominated by *T. angulosa*, *C. lobatulus* and *Uvigerina peregrina*, with *Cibicides refulgens*, *Bulimina marginata* and *C. laevigata* important (Fig. 5.10). Notably, the polar/glacial marine-associated *C. reniforme* and *E. clavatum* account for only 1-4% and 0-1% in bFAZ 1, respectively.

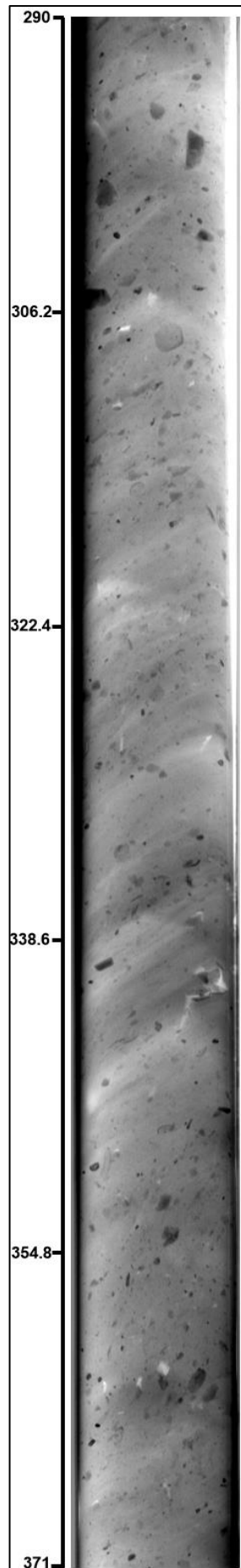
Some of these dominant species in bFAZ 1 are associated with strong current regimes (*T. angulosa*, *C. lobatulus*, *C. refulgens*; Mackensen et al. 1985; Klitgaard-Kristensen et al. 2002; Schönfeld 2002), while the remainder are generally important in calmer conditions with high nutrient fluxes, frequently dysoxic conditions and usually in temperate settings (*U. peregrina*, *B. marginata* and *C. laevigata*; Lutze & Coulbourn 1984; Murray 1991; Fontanier et al. 2002). It is

clear that taxa generally associated with nutrient-rich mid-upper continental slopes (Brizalinids, Buliminids and Uvigerinids; Gooday 2003; Jorissen et al. 2007; Duros et al. 2011) are considerably more important in the 198VC assemblages than shallower-water ‘shelf’ taxa such as Elphidiids (Murray 1991) (see Table A4, Appendix 1). *Elphidium* species become more important in deglacial assemblages across the mid-inner western Irish shelf (see Peters et al. 2020). Almost all taxa in bFAZ 1 are found in modern surface sediment dead assemblages above ~700 m depth in the southern Slyne Trough-northern Porcupine Seabight, particularly in rippled sands and silty substrates with scattered clasts (cf. Table A4, Appendix 1 with Weston 1985; Rüggeberg et al. 2007; Margreth et al. 2009; Fentimen et al. 2020). These winnowed substrates reflect the present hydrography of the area (Smeulders et al. 2014), which is characterised by the ENAW-advecting SEC (see Section 3.2.).

pFAZ 1 (Fig. 5.12) shows moderate proportions of the cold surface water-associated *N. pachyderma* (43-57%), lower proportions of subpolar-temperate species (*Turborotalita quinqueloba* 3-16%, *N. incompta* 5-13% and *G. bulloides* 6-13%), with persistent but low contributions ($\leq 17\%$ total) of temperate-subtropical species including *Globigerinella siphonifera*, *Globigerinita glutinata* and *Globorotalia inflata* (Bé & Tolderlund 1971; Hemleben et al. 1989; Bauch 1994; Kucera et al. 2005; Kucera 2007; Schiebel et al. 2017). This would be consistent with Arctic planktic assemblages in areas influenced by Atlantic Water (e.g. Lloyd et al. 1996; Alonso-Garcia et al. 2011; Husum & Hald 2012). The composition of pFAZ 1 closely resembles planktic assemblages from GS-3 in the northeast Atlantic, which are interpreted to represent subsurface Atlantic Water inflow (see e.g. Dokken & Hald 1996; Rasmussen et al. 1996b; 2002; Rasmussen & Thomsen 2008). However, as no chronological information is available for the planktic foraminifera, these could also largely represent transported reworked tests. If this is the case, their source sediment(s) was strikingly consistent throughout deglaciation, as suggested by the persistence of pFAZ 1 through bFAZs 1-4 (cf. Figs 5.10, 5.12).

Radiocarbon results for the consolidated mud association indicate highly variable ages of the benthic foraminiferal test populations, ranging from 22.6 ka BP to infinite, and not in stratigraphic order up-core (see Ó Cofaigh et al. submitted). The dates imply that reworking particularly affects species other than *E. clavatum*, as all samples of mixed benthic foraminifera or monospecific *Bulimina elongata* dated to ≥ 37.2 ka BP, compared with ≤ 31.9 ka BP for monospecific *E. clavatum* samples, irrespective of stratigraphic level. This suggests that the weakness of the glacimarine/Arctic faunal signal in bFAZ 1 at least partly reflects dilution by reworked tests, rather than temperate, nutrient-rich bottom waters in the deglacial environment.

Fig 6.4 (overleaf): X-radiograph of core 198VC, Section D/4, showing part of facies Fld_c. Scale is core depth in cm. The transition from bFAZ 1 to bFAZ 2 occurs between 313 and 297 cm.



While ages of up to 31.9 ka BP for *E. clavatum* samples in these lithofacies (Ó Cofaigh et al. submitted) indicate some reworked test contribution from the mid-inner shelf by glaciogenic processes (Hald et al. 1994; Rüggeberg et al. 2007; Fentimen et al. 2020), there is no sedimentologic evidence for mass movement in the consolidated mud association, despite its slope setting.

Another possible explanation for the persistent, high contribution of reworked tests with a generally continental slope affinity and/or association with strong currents (benthic test concentrations are 2054–3142 individuals/g in Fld_c) is along-slope winnowing and transport by bottom currents (e.g. Holtedahl & Bjerkli 1982; Viana et al. 1998). This would imply similarity to the present current regime and surface sediment assemblage generation in the area (Section 3.2.; Margreth et al. 2009; Fentimen et al. 2020). Activity of a northward current at least during final retreat from the outer shelf is suggested by the orientations of iceberg scours in the Slyne Trough (see Fig. 3 of Ó Cofaigh et al. submitted), with scour deepening up south-facing slopes (Peters et al. 2015; Thébaudeau et al. 2016, their Fig. 3). Furthermore, muddy, IRD-rich contourites spanning the last glacial period occur extensively along the western slope of the Bank (Øvebrø et al. 2005; 2006; Fig. 6.5) and the eastern Seabight (e.g. Van Rooij 2004). Many sedimentological characteristics of facies Fld_c would also be consistent with such contourites from glaciated margins (e.g. Howe et al. 1994; Stoker 1995; Howe 1996; Armishaw et al. 2000; Lucchi & Rebesco 2007). The composition and duration of pFAZ 1, and the consistently high test concentrations in Fld_c are more easily explained by persistence of a northward current than solely by mass flow and/or iceberg rafting. bFAZ 1 is therefore interpreted to record an early deglacial environment with suspension settling and iceberg-rafting, some glaciogenic mass flow and a persistent northward current likely advecting Atlantic Water and tests winnowed from the slope.

A considerable benthic faunal change occurs midway through facies Fld_c (transition to bFAZ 2; Fig. 5.10), marked by increased importance of species associated with colder settings (*C. reniforme* and *Cassidulina neoteretis*) and decreases in the dominant strong-current associated species (*T. angulosa* and *C. lobatulus*).

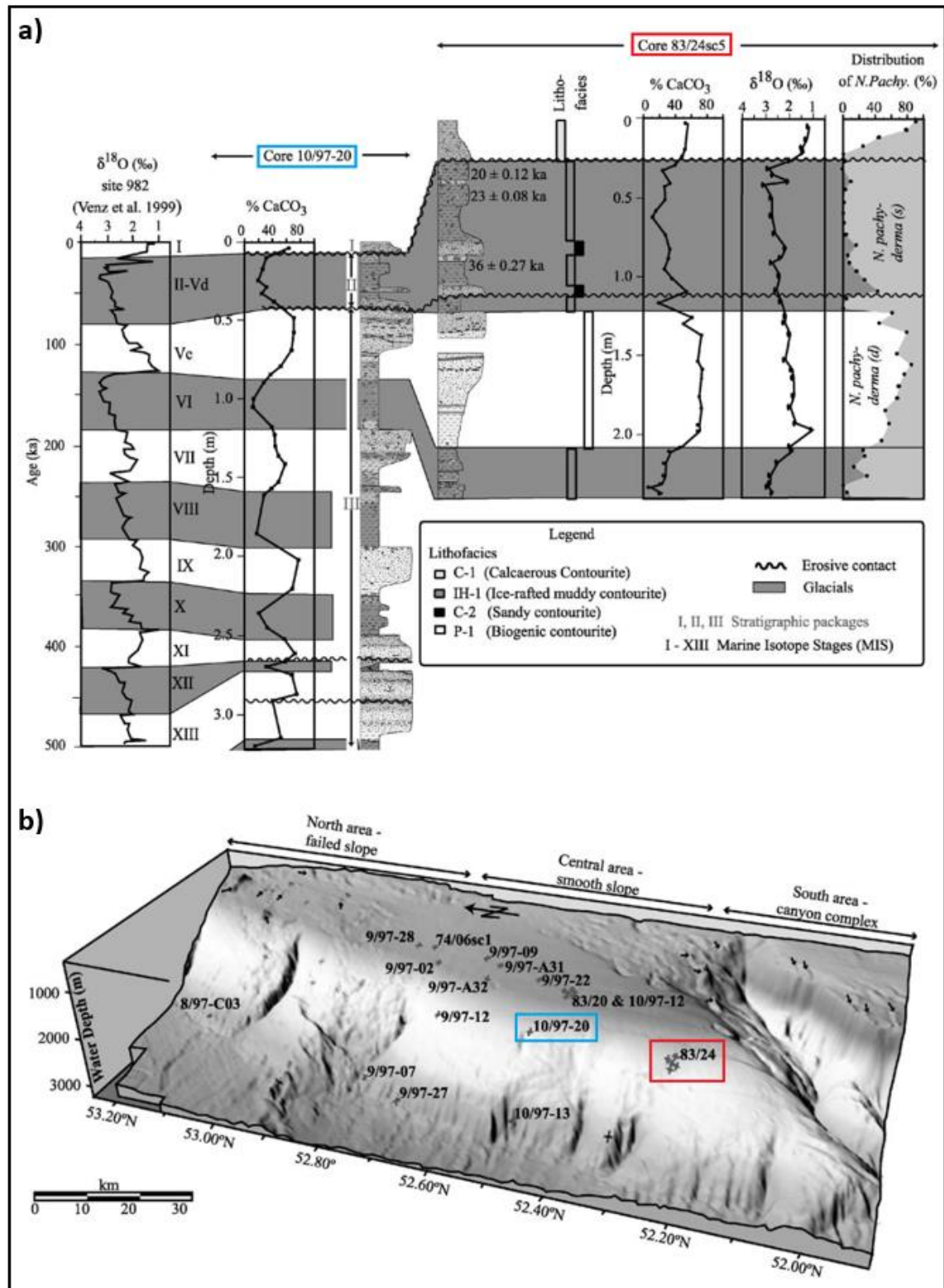


Fig. 6.5: A: Stratigraphic correlation of contourites on the western slope of Porcupine Bank (from Øvebrø et al. 2006). Facies 'IH-1' comprises weakly laminated mud with abundant IRD; its radiocarbon dates spanning the Last Glacial Maximum are shown. *N. pachyderma* relative abundance represents the >150 μm fraction. B: Location map for cores in panel A (boxed). Note that water depths for cores in panel A are 1432-1527 m.

C. reniforme is generally found under relatively productive conditions in polar/glacimarine settings (see Section 6.1.1.), and *C. neoteretis* is usually restricted to environments influenced by chilled/modified Atlantic Water in Arctic settings (Mackensen & Hald 1988; Cronin et al. 2019; Jennings et al. 2020). It is also apparent that *C. neoteretis* increases at the expense of *C. laevigata* in bFAZ 2 (see Fig. 5.10). This is notable as it could suggest a gradual chilling or transformation by cold, less saline water of nutrient-rich Atlantic Water if the latter is represented by bFAZ 1, as suggested above (Jennings & Helgadottir 1994; Steinsund 1994; Taldenkova et al. 2012). An increased influence of meltwater at the core site is also consistent with the reduction in the strong current-associated species and declining benthic foraminiferal diversity through bFAZ 2 (e.g. Seidenkrantz et al. 2013; Jennings et al. 2020) (Fig. 5.11). This could have paralleled the modern hydrographic situation in the northern Slynne Trough, where the northward-flowing ENAW mixes with the cooler, lower-salinity shelf water as it is forced to shoal by the northward-shallowing bathymetry (Kloppmann et al. 2001; Figs. 2.3, 3.5). The shear strength of Fld_c indicates that glacial overriding followed its deposition, consistent with the interpretation of bFAZ 2 as recording increasing meltwater influence as the ice margin readvanced towards the core site.

Dms (244-173 cm)

A 71 cm-thick stratified, matrix-supported diamicton unit succeeds Fld_c above a gradational contact. Shear strength reduces considerably into this facies (from 90 kPa to ~10 kPa), suggesting it was deposited following final grounding-line retreat from the core site. A radiocarbon date of 25.6 ka BP on monospecific *E. clavatum* from the base of this unit therefore constrains the timing of this final BIIS retreat from the outer shelf (Ó Cofaigh et al. submitted). The textural segregation between more and less clast-rich diamicton and the inclined stratification in this unit are consistent with deposition of the unit as subaqueous, cohesive debris flow(s) (Nemec & Steel 1984; Eyles 1987; Benn 1996), as interpreted by Ó Cofaigh et al. (submitted). Similar stratified diamictons are described from the outer Hebridean Shelf (Stoker 1988), where they are interpreted to represent a succession of subaqueous cohesive flows with varying clast contribution at source, varying degrees of matrix-support during flow or upward evolution into turbidity currents (Lowe 1982), deposited in a grounding line-proximal setting. The foraminiferal assemblages in *Dms* (bFAZ 3) are therefore likely to represent a mixture of reworked and autochthonous tests, with flow-related grain segregation affecting species proportions as apparent from gradational abundance trends and the upward increase in absolute abundance and planktic foraminiferal content (see Figs. 5.10, 5.12). The benthic assemblages remain broadly consistent with those of bFAZ 2, which is interpreted as an Atlantic Water-influenced glacimarine environment. This suggests that following overriding of facies Fld_c, Atlantic Water was also present early during the

final retreat from the core site, possibly having persisted in the region through final reoccupation of Porcupine Bank but displaced and/or modified by meltwater (cf. Lloyd et al. 2005; Seidenkrantz et al. 2013; Taldenkova et al. 2012; see Fig. 6.6 panel 2b).

Fm (173-55 cm)

A unit of massive, clast-poor mud overlies facies Dms, and is characterised by gradually declining magnetic susceptibility values and increasing visible bioturbation up-core. This is also seen in the Fm unit in 146VC, which is interpreted to represent increasingly distal glacimarine sedimentation (see Section 6.1.1.). This interpretation is supported by a radiocarbon date of 21.8 ka BP on monospecific *E. clavatum* obtained by Ó Cofaigh et al. (submitted) from ~20 cm below the upper contact, by which time the ice-margin was retreating from the mid- to inner shelf (Roberts et al. 2020; Ó Cofaigh et al. submitted). The lowermost benthic foraminiferal assemblage in the Fm contrasts significantly with that in all other samples in 198VC, dominated by *C. reniforme* (40%) and characterised by considerably reduced diversity and high absolute abundance (Figs 5.10, 5.11). Given the position of this assemblage 4 cm above facies Dms (Fig. 5.7), its unusual composition is interpreted as a recolonisation assemblage following the disturbance of the benthic environment by deposition of the debris flow(s). Recolonisation assemblages are generally characterised by low diversity, high absolute abundance and domination by opportunistic species, as seen here (Korsun et al. 1995; Alve 1999; Hess et al. 2005).

Succeeding samples in Fm are consistently dominated by *C. reniforme*, *C. neoteretis* and *T. angulosa*, with *E. clavatum* (2-9%) and *Globocassidulina subglobosa* (1-6%) becoming important for the first time (bFAZ 4). These assemblages are consistent with a distal glacimarine environment influenced by chilled/modified Atlantic Water and moderately strong currents (Qvale 1986; Jennings & Weiner 1996; Schmiedl et al. 1997). This environment appears to have remained consistent as the ice margin retreated ~100 km to the inner shelf (Callard et al. 2020; Roberts et al. 2020, Fig. 5.10). The proportion of planktic foraminifera in Fm (benthic:planktic ratio spans 0.7-1.3) is higher than in F1def_c and F1d_c (1.3-1.6). This suggests increasing shelf-ocean exchange (partly due to RSL rise) and increasing surface productivity as the ice margin became more distal. RSL rise of ~20 m has been modelled for the Slyne Trough during this period (see Fig. 13E of Ó Cofaigh et al. submitted). The planktic assemblage remains consistent (pFAZ 1), interpreted as either directly recording surface/shallow subsurface Atlantic Water advection or a persistent transport of reworked tests to the core site by bottom currents (probably of Atlantic Water, see above).

Sm (55-0 cm)

Facies Fm is overlain above a loaded contact by an upward-fining gravelly sand unit (Sm). Facies Sm is rich in large, well-preserved shell material and contains the highest concentrations of foraminiferal tests and test fragments of all 198VC lithofacies. The benthic foraminiferal assemblages in Sm (bFAZ 5) contain relatively even proportions of typical Arctic/glacimarine species (*C. reniforme* and *C. neoteretis*) and temperate, high productivity-associated species (*B. marginata*, *C. laevigata*, *U. peregrina*), with reduced proportions of strong current-preferring species (*T. angulosa*, *Cibicides* species). These characteristics and the high foraminiferal concentration are consistent with a postglacial winnowed sand deposit (Ó Cofaigh et al. submitted; see discussion of facies Gm in Section 6.1.1.), containing a mixture of glacial and postglacial-age tests typical of modern dead assemblages from mid-upper slope depths in the Porcupine Seabight (e.g. Weston 1985; Rüggeberg et al. 2007; Fentimen et al. 2020). A distinct change in the planktic assemblage occurs within facies Sm (transition to pFAZ 2), marked by a shift in dominance from *N. pachyderma* (53→18%) to *N. incompta* (6→30%) (Fig. 5.12). The composition of pFAZ 2 resembles modern living planktic foraminiferal populations in the region (e.g. Ottens 1991; Chapman 2010), particularly in the size fraction 150-250 µm (Harbers et al. 2010; Section 3.2.), so it is likely that pFAZ 2 dominantly comprises postglacial-age tests recording warmer surface waters and enhanced nutrient availability, but with species proportions influenced by current activity.

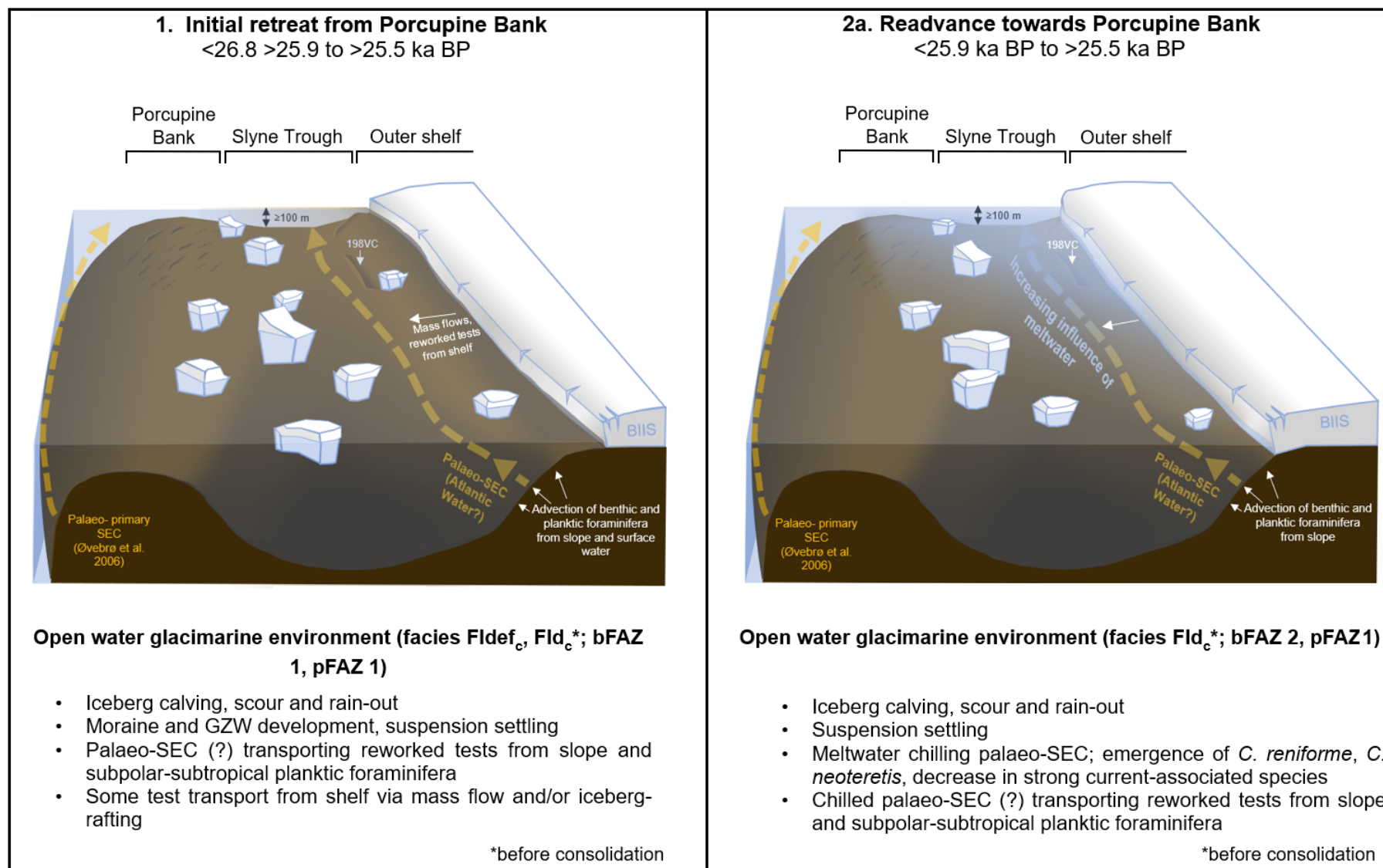
6.2.2. Summary and relation of interpretations to geomorphological context of core 198VC

The earliest deglacial environment(s) recorded in 198VC (occurring by 25.9 ka BP) was/were characterised by suspension settling and iceberg-rafting, and a sustained high input of reworked tests inferred here to reflect bottom current transport with some contribution from the shelf via glacigenic mass flows and/or iceberg-rafting (Fig. 6.6 panel 1). This proposed environment is similar to that interpreted for the western slope of Porcupine Bank between 36 and 20 ka BP by Øvebrø et al. (2005; 2006) and the eastern margin of the Porcupine Seabight by Van Rooij (2004) and Van Rooij et al. (2007a). It is likely that this bottom current was northward and advecting Atlantic Water (see above and Section 2.3.3.), but the high reworked component in the benthic assemblages prevents clear insight into the bottom-water characteristics. As the BIIS readvanced towards the core site (sometime between 25.9 ka BP and ~25.0 ka BP; Ó Cofaigh et al. submitted), the abundance of strong current-associated species decreased, as species indicating glacimarine/Arctic conditions and chilled Atlantic Water emerged. This probably reflects increasing meltwater influence at the core site, which would have been aided by the relatively shallow bathymetry on the Porcupine Saddle/Slyne Ridge (Fig. 6.6 panel 2a).

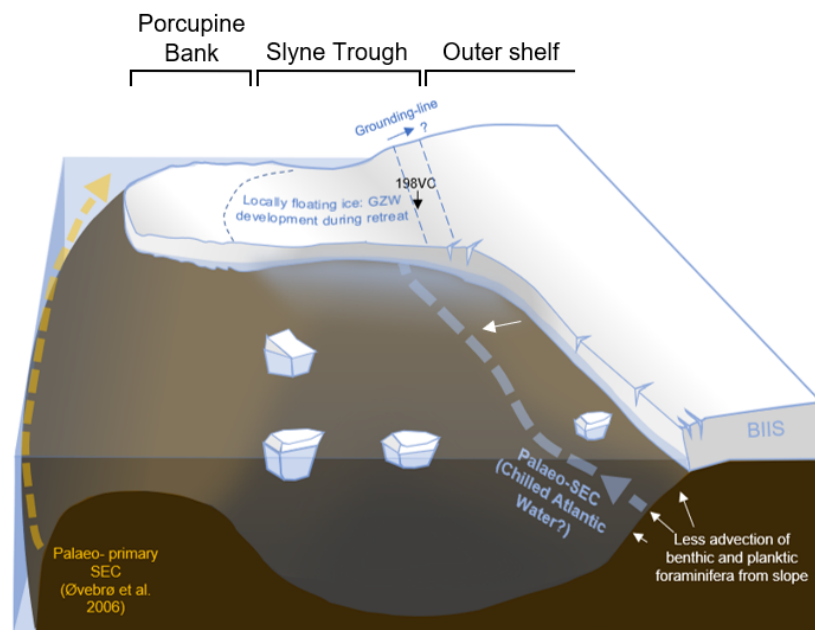
The ice-margin configuration during this readvance to Porcupine Bank is uncertain, however, Ó Cofaigh et al. (submitted) provide evidence for varying accommodation space in front of the grounding-line across the Slyne Trough-Porcupine Bank area. Morphological transitions from GZWs into narrow ridges, implying a reduction in accommodation space, occur across shallowing bathymetry onto the eastern flank of Porcupine Bank (Ó Cofaigh et al. submitted, their Fig. 3). Additionally, deposition of consolidated subglacial diamicton on the Bank (~25.0 ka BP) coincides with or closely follows final grounding-line retreat from the 198VC site (~25.5 ka BP) on the opposite flank of the Trough (see Ó Cofaigh et al. submitted). Furthermore, the sediments overridden during this readvance (Fld_c) show weak homogenisation, suggesting low cumulative strains, and high RSL (≥ 200 m) is modelled for the central Slyne Trough during this period (Ó Cofaigh et al. submitted). These observations seem consistent with grounded ice on the Bank coinciding with at least partially floating ice in the Trough (Fig. 6.6 panel 2b), particularly as sharp-crested ridges are essentially confined to depths < 300 m.

Final grounding-line retreat from the 198VC site on the outer shelf occurred ~25.5 ka BP (Ó Cofaigh et al. submitted), in the presence of chilled/modified Atlantic Water. This was associated with localised cohesive debris flow deposition as the grounding-line retreated (Fig. 6.6 panels 2b-3). Activity of a northward current during and/or following this final retreat from the outer shelf is evidenced by iceberg scour orientations in the Slyne Trough. Chilled Atlantic Water influenced the outer shelf until at least 21.8 ka BP, and was associated with RSL rise and moderate current activity as the BIIS retreated to the mid- and inner shelf (Fig. 6.6 panel 3). This Atlantic Water is inferred to also have accompanied subsequent deglaciation across the main central western Irish shelf (Peters et al. 2020). Postglacial conditions were associated with continued sea-level rise, bottom-current intensification and increased surface water warming and productivity, resulting in pervasive winnowing and sand sheet development (Van Rooij et al. 2007b; Foubert et al. 2011; Fig. 6.6 panel 4).

Fig. 6.6 (overleaf): Depositional environments interpreted from 198VC lithofacies and geomorphological features in the Porcupine Bank-Slyne Trough-Outer shelf area (continued overleaf). Water depths are based on RSL modelling for the Slyne Trough (Ó Cofaigh et al. submitted) and are minimum estimates not accounting for any effects of GIA. ‘SEC’ – Shelf Edge Current; ‘ENAW’ – Eastern North Atlantic Water.



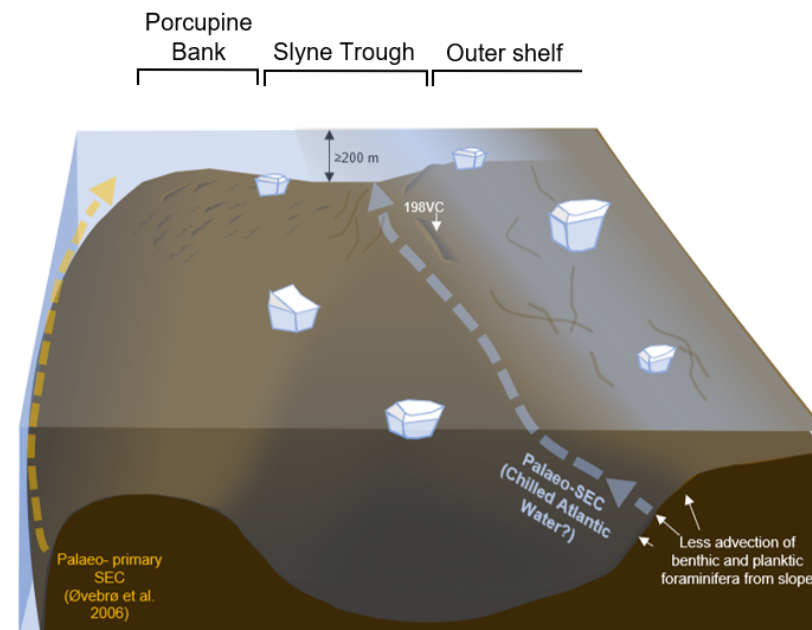
2b. Readvance onto Porcupine Bank ≥25.0 to >24.3 ka BP



Grounded ice on Porcupine Bank, partially floating ice in Slyne Trough (facies Fld_c, Dms; bFAZ 3, pFAZ 1)

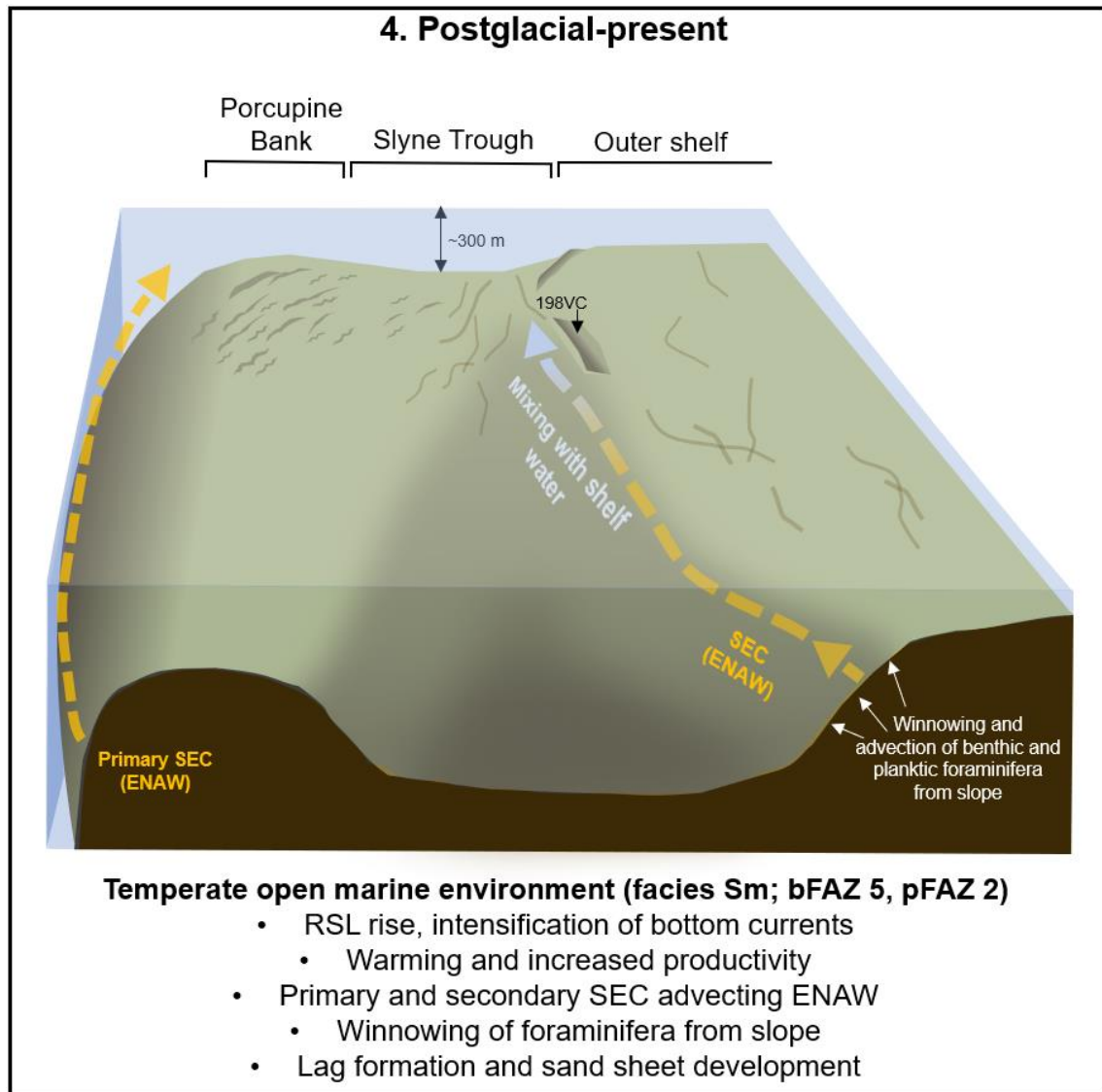
- Variable grounding-line accommodation space in Slyne Trough
- Overriding (consolidation) of Fld_c >25.5 ka BP
- Grounding-line retreat from 198VC site and glacial debris flow deposition ~25.5 ka BP
- Deposition of subglacial diamicton on Porcupine Bank ~25.0 ka BP, in Trough ≤24.3 ka BP

3. Retreat across main western Irish shelf ≤24.3 ka BP to ~17 ka BP



Increasingly distal open glacial marine environment influenced by Atlantic Water (facies Fm; bFAZ 4, pFAZ 1)

- Moraines developed on Porcupine Bank, GZWs developed in Slyne Trough, iceberg scouring of outer shelf
- RSL rise, suspension settling, relatively little iceberg-rafting on main shelf (?)
- Palaeo-SEC (?) chilled by meltwater along margin
- Moderate current strengths with less transport of foraminifera from slope and/or less glacial input of reworked tests



CHAPTER 7

DISCUSSION

7.1. Drivers and modulators of early deglaciation

Recent cross-shelf reconstructions have established that initial retreat along the BIIS's Atlantic margin began during GS-3, and was underway by 25.9-24.8 ka BP (depending on location) (Callard et al. 2018; Ó Cofaigh et al. 2019; Scourse et al. 2019; Ó Cofaigh et al. submitted; Section 2.4.1.). This is consistent with deep-sea IRD records, particularly west of Ireland and Scotland, in which this timing coincides with a rapid increase in the contribution of BIIS IRD, culminating at H2 (e.g. Knutz et al. 2001; Auffret et al. 2002; Van Rooij et al. 2007b; Peck et al. 2007b; Peters et al. 2008; Scourse et al. 2009; Haapaniemi et al. 2010; Hibbert et al. 2010). Following the discussion in Section 2.3.3., the *NEA-GS-3b* warming event (~25.6-24.8 ka BP; Hibbert 2010; Austin et al. 2012) appears to be concurrent with this initial phase of Atlantic BIIS retreat and increase in IRD contribution, so represents a potential external influence on early BIIS deglaciation. However, improved chronological control on the timing of *NEA-GS-3b* is needed (Austin et al. 2012). As clear from Sections 2.2. and 6.1., any role of ocean forcing in initial retreat of the BIIS's Atlantic margin must have been localised, as there is no foraminiferal evidence of Atlantic Water on the Celtic (Scourse et al. 2019), Donegal (Ó Cofaigh et al. 2019) or Malin shelves (this study) during deglaciation.

Additionally, it can be expected that any role for Atlantic Water in initiating and/or driving retreat would have been passive (a background process, the effect of which could be masked by other influences on retreat patterns) and therefore, potentially less easily identified in the deglacial records. This is as the role of atmospheric/oceanic forcing in ice-sheet retreat can be strongly modulated by bathymetry and glaciological conditions (Ó Cofaigh et al. 2008; Stokes et al. 2014; Catania et al. 2018). It is evident from Section 2.2. that local bathymetric factors and oscillatory behaviour were major influences on the pattern of BIIS retreat in all Atlantic sectors (e.g. Callard et al. 2018; Ó Cofaigh et al. 2019; Scourse et al. 2019; Bradwell et al. 2019; Ó Cofaigh et al. submitted). The associated stabilisations and readvances clearly overrode the effect of any Atlantic Water present on the shelf in these regions. Additionally, drainage basin characteristics can strongly control the speed and style of ice-stream response to external forcing (Ó Cofaigh et al. 2008). These observations clearly highlight the importance of careful assessment of the faunal assemblages and degree of reworking in inferring a role of any Atlantic Water in deglaciation.

7.1.1. The Malin shelf

Drivers of deglaciation

The foraminiferal assemblages in core 146VC have been interpreted to record a cold glacimarine environment throughout deglaciation of the Malin shelf, with frequent and extensive sea-ice development and shallow water depths and/or restricted ocean-shelf exchange on account of the very high benthic:planktic ratios (see Sections 5.1.3.; 6.1.1.). Test preservation is usually poorer throughout deglacial lithofacies in 146VC than in 198VC, and is not systematically associated with particular species or relative ice-margin proximity (Section 5.1.3.). In addition, benthic foraminiferal sample ages from deglacial lithofacies in 146VC all postdate maximum ages for basal, advance-stage diamictos (cf. Callard et al. 2018; Ó Cofaigh et al. submitted). While the trends in test and test fragment abundance are very similar, this still suggests that glacial reworking does not explain all poorly-preserved foraminiferal tests in the assemblages. There is no evidence of the organic test linings and importance of agglutinated forms that would be expected from extensive dissolution (e.g. Lloyd 2006a; McCarthy 2011; Sheldon et al. 2016). However, very high benthic:planktic ratios equal to those on the Malin shelf (average 35.9) have been associated with Arctic shelf areas affected by carbonate dissolution (e.g. Hald & Steinsund 1994). Dissolution may also be reflected in the surprisingly low test concentrations in ice-distal lithofacies (absolute abundance in facies Fm drops to ≤ 8 individuals/g), where evidence of bioturbation suggests productive conditions. These may have been conducive to dissolution by increasing CO₂ concentrations in the cold pore- and bottom waters (Aksu 1983; Jennings & Helgadottir 1994).

Even if those ice-proximal samples with poorer preservation contain high reworked contributions, and those in the more ice-distal samples have undergone extensive dissolution, the assemblage composition, including the ice-distal glacimarine sediments, remains consistently dominated by *C. reniforme*, *E. clavatum* and *E. excavatum* (see Section 6.1.2.; Tarlati et al. 2020). Together with the persistent lack of species associated with Atlantic Water or temperate, nutrient-rich settings, the generally low productivity implied by relatively low absolute abundance, the low diversity and the dominance of opportunistic Arctic/glacimarine-associated species, this supports the exclusion of Atlantic Water from the shelf as discussed in Chapter 6. Ocean forcing is therefore ruled out as a trigger or driver of deglaciation in the Malin shelf sector. The cold glacimarine deglacial environment implied by the foraminiferal data supports the proposal of Callard et al. (2018) that BFIS retreat from the Malin shelf edge was in response to GIA-induced RSL rise. This parallels the recent results from the Celtic Sea (Scourse et al. 2019) and Donegal (Ó Cofaigh et al. 2019) shelves, thereby indicating internally-triggered deglaciation along a substantial portion of the BIIS's Atlantic margin.

Modulating factors

Callard et al. (2018) showed the importance of shelf bathymetry in pacing BFIS retreat, with the reverse bed slope of the outer shelf likely encouraging initial deglaciation, and rapid subsequent recession associated with overdeepened troughs on the mid-shelf. Additional factors driving or modulating retreat on the Malin shelf cannot be confidently identified from the data presented in this project. However, it is evident that sedimentological and foraminiferal indications of frequent, severe sea-ice and mélangé development are restricted to the period of slower, more episodic retreat across the outer shelf (Dmm-F1 alternations and facies F1 unit). Extensive, multi-year sea-ice could have been important in buttressing the BFIS during this early stage of retreat, when the ice-shelf terminus spanned the width of the shelf and was unconstrained by topography (Walter et al. 2012; Greene et al. 2018; Gandy et al. 2018). This could have suppressed rapid retreat through calving and potentially allowed sedimentation at the grounding-line to keep pace with the GIA-induced RSL rise (cf. Reeh et al. 2001; Robel 2017; Cowan et al. 2020). These harsh sea-ice conditions coincide approximately with H2, so may at least partly reflect the effect of this event on sea-surface temperatures (e.g. Hoff et al. 2016). Low planktic:benthic ratios and high dominance in deglacial foraminiferal assemblages on the Hebridean shelf imply extensive sea-ice cover and relatively shallow waters during early deglaciation there (Austin 1991). A role for eustatic sea-level rise is unlikely to register in the planktic foraminiferal abundance (which remains low) in the deglacial lithofacies, however, the faster and more sustained retreat from GZW1b across the mid-shelf (Callard et al. 2018; Fig. 6.3 panel 3), beginning ~23.8 ka BP, coincides with the eustatic sea-level rise associated with H2 (2-15 m; Marshall & Koutnik 2006; Siddall et al. 2008). The uninterrupted retreat across the mid-shelf via calving, represented by facies Dmm and Fmd, may therefore reflect significant destabilisation of the BFIS through a combination of overdeepened troughs, eustatic- and GIA-related sea-level rise (Briner et al. 2009; Rydningen et al. 2013; Stokes et al. 2014; Callard et al. 2018).

7.1.2. Porcupine Bank and Slyne Trough

Drivers of deglaciation

The deglacial foraminiferal assemblages in core 198VC contrast markedly with those from the Malin shelf, being characterised by considerably higher diversity, high preservation quality, higher proportions of planktic foraminifera and the importance of species variably associated with temperate, nutrient-rich settings, Atlantic Water and strong bottom currents (see Sections 5.2.3.; 6.2.1.). The earliest portion of the record (bFAZ 1; Fig. 5.10.) is marked by a notable lack of the typical Arctic/glacimarine benthic species *E. clavatum* and *C. reniforme*, which together account for only $\leq 5\%$ in this zone. In bFAZ 2, *C. reniforme* becomes more important ($\leq 16\%$) alongside

the chilled Atlantic Water-associated *C. neoteretis* ($\leq 9\%$), with which it then persists and increases in importance through increasingly ice-distal conditions, where *E. clavatum* reaches 9% (Fig. 5.10; Section 5.2.3.). In Chapter 7, bFAZs 2-4 were therefore interpreted as recording an Atlantic Water-influenced glacial-marine environment. The conditions during earliest deglaciation (represented by bFAZ 1) are more difficult to infer, on account of the frequently high content of reworked tests indicated by radiocarbon results from samples of benthic foraminifera (see radiocarbon dates for LFA2 of Ó Cofaigh et al. submitted). That the *Bulimina*, *Brizalina* and *Uvigerina* species in particular are dominantly reworked, as proposed in Section 6.2.1, is supported by a date of 40.4 ka BP obtained on a monospecific *Bulimina elongata* sample (Ó Cofaigh et al. submitted), and a record of benthic foraminiferal assemblages in the Porcupine Seabight since ~31 ka BP (Rüggeberg et al. 2007; Fig. 7.1).

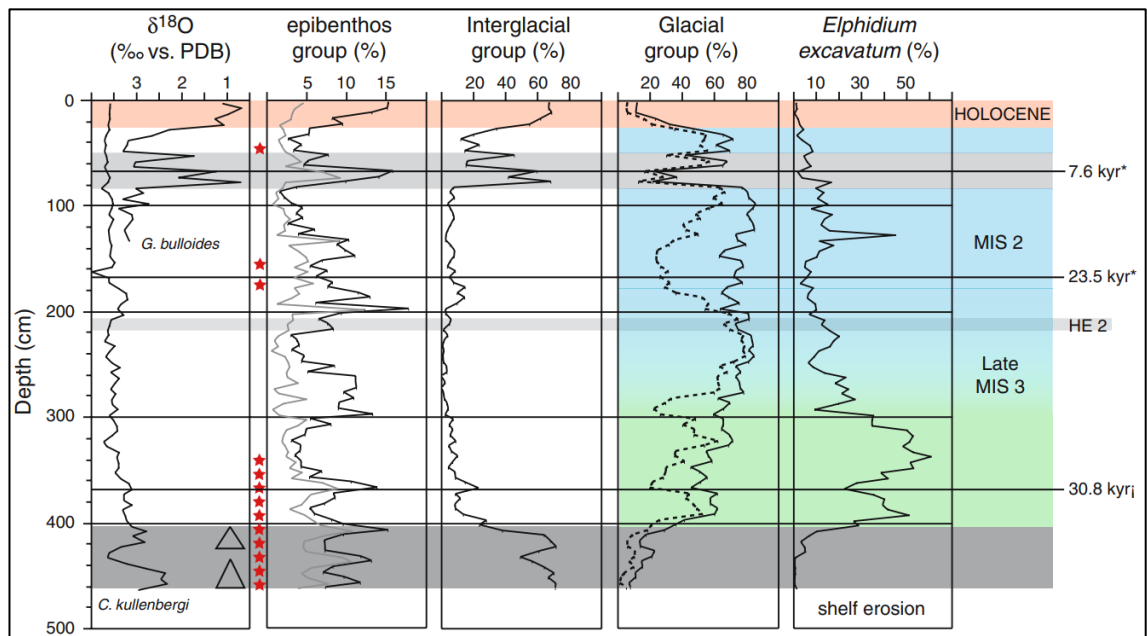


Fig. 7.1: Benthic foraminiferal assemblage record from the Porcupine Seabight. The dotted trend in the ‘glacial group’ plot is the relative abundance of *C. neoteretis*. The ‘interglacial group’ includes *Uvigerina mediterranea*, *U. peregrina*, *T. angulosa*, *C. laevigata*, *B. marginata* and *Bolivina robusta* (cf. *Brizalina spathulata* here?). *E. excavatum* was not included in the relative abundance calculation for *C. neoteretis*, the ‘glacial group’ and ‘interglacial group.’ Grey band at base indicates suspected turbidite deposits, grey band from 45-80 cm indicates heavily bioturbated interval. From Rüggeberg et al. (2007).

In this record, these species are only important before late MIS 3 and in the Holocene, with intervening assemblages instead dominated by *C. neoteretis*, *C. reniforme*, *Cibicidoides kullenbergi* (= *Cibicidoides pachyderma*) and *G. subglobosa* (Fig. 7.1). In Section 6.2.1., it was argued that reworking of the species associated with nutrient-rich temperate settings could have occurred through winnowing and transport along the slope by a northward shelf-edge current, for which there is geomorphic and independent sedimentologic evidence (e.g. Øvebrø et al. 2005;

2006; Van Rooij 2004; Van Rooij et al. 2007a). As such, these species would not necessarily reflect comparable conditions in the deglacial environment (despite resulting from Atlantic Water advection) but nevertheless would dilute the glacimarine/Arctic faunal signal.

It is also possible that the high reworked contribution to the early deglacial assemblages instead reflects a source on the shelf, with delivery via glacial mass flow and/or iceberg-rafting, and does not reflect bottom-current activity during initial retreat. The 198VC site is located on the slope of the main western Irish shelf, which in acoustic profiles shows large-scale depositional architecture consistent with progradation through mass flows from the outer shelf (McCarron et al. 2018; Callard et al. 2020; Fig. 7.2). Furthermore, while *Brizalina*, *Bulimina* and *Uvigerina* species are generally associated with upwelling and eutrophic mid- to upper continental slopes (Gooday 2003; Jorissen et al. 2007), they can also occur on shallower shelf areas if conditions are stratified and sufficiently calm to permit high organic matter fluxes and muddy substrates (e.g. Klitgaard-Kristensen & Sejrup 1996; Mendes et al. 2004; 2012; Plets et al. 2015). In the portion of the record representing ice-distal conditions (facies Fm), there is a reduced relative abundance of *Bulimina marginata* and *Uvigerina peregrina*, which could therefore reflect decreased ice-marginal detrital input of these species (see Fig. 5.10). Glacial contribution of tests from the shelf during early deglaciation is clearly evident in ages of up to 32 ka BP of monospecific *E. clavatum* samples in the consolidated mud association (Ó Cofaigh et al. submitted), as this is an Arctic/glacimarine species generally restricted to shelf settings (Hald et al. 1994; Struck 1997). In addition, the high test preservation quality characterising 198VC does not exclude subglacial reworking (e.g. Austin & McCarroll 1992; Shakesby et al. 2000).

The lack of clear evidence for mass flow in the consolidated mud association could then indicate input of tests by distal turbiditic flows or iceberg-rafting. Combined with the lack of dates for the *C. neoteretis* test populations, the above possibilities expose how the data are insufficient to confidently identify the presence of Atlantic Water in this sector during retreat at present. Provisionally however, Atlantic Water is considered to have been present throughout retreat, including bFAZ 1, primarily as this would be consistent with the planktic foraminiferal assemblage characteristics (see Section 6.2.1), the subsurface temperature record in the Porcupine Seabight (Peck et al. 2008) and bottom-current evidence on the western slope of Porcupine Bank (Øvebrø et al. 2005; 2006) and in the eastern Porcupine Seabight (Van Rooij 2004; Van Rooij et al. 2007a). Atlantic Water is therefore proposed here to have been a driver of retreat in the central western Irish shelf sector, together with GIA-induced RSL rise, from at least ~25.5 ka BP onwards (Bassis et al. 2017; Jennings et al. 2017; Ó Cofaigh et al. submitted).

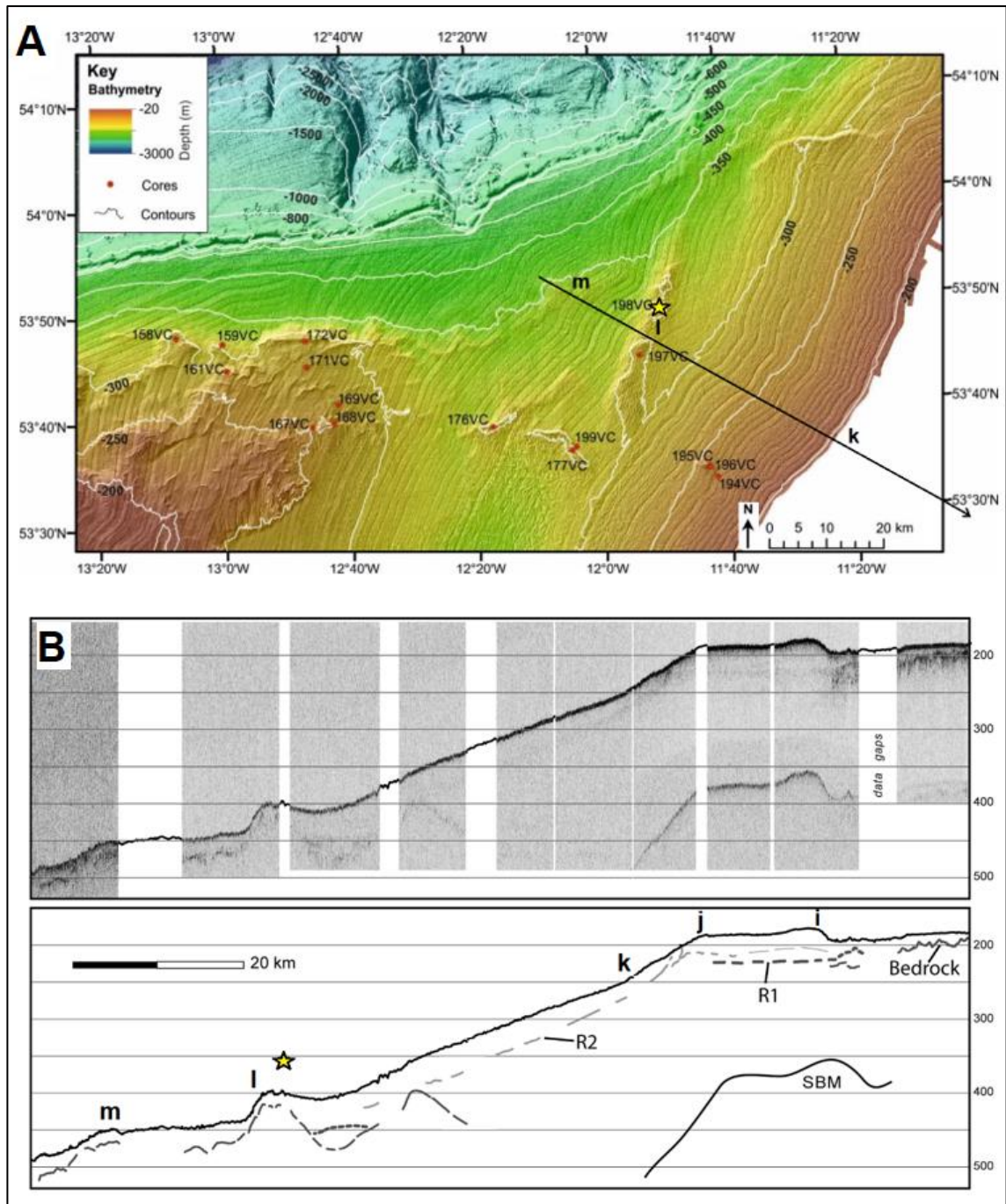


Fig. 7.2: Seismic reflection profile and interpretation of the subsurface depositional structure on the outer central western Irish shelf and slope. Panel A after Ó Cofaigh et al. submitted; B after McCarron et al. 2018). Note that map in A does not show full length of seismic profile in B and that vertical scale in B is two-way travel time in milliseconds. The unit overlying reflector R2 is interpreted to represent downslope-remobilised deglacial sediment (McCarron et al. 2018; Callard et al. 2020) and covers the ridge 'I' where 198VC (star) was recovered. The MSGZC is visible at i-j. 'SBM' denotes a sea-bed multiple.

Further work to establish whether Atlantic Water advection influenced earliest deglaciation should involve additional radiocarbon dating of monospecific samples of temperate- and Atlantic Water-associated benthic and planktic species, in ice-distal and ice-proximal lithofacies. Such

dating could be combined with sortable silt fraction analyses in individual horizons of the consolidated mud association to test its contouritic interpretation proposed in Section 6.2.1. (e.g. Manighetti & McCave 1995; Lekens et al. 2005; McIntyre & Howe 2009). Peters et al. (2020) suggested that nutrient-rich conditions implied by the presence of *C. laevigata*, *Bolivina* (= *Brizalina*) *sp.* and *Uvigerina mediterranea* could instead reflect a terrigenous nutrient supply from the ice margin (cf. Knies & Stein 1998; Stickley et al. 2005). This could be tested by determining Carbon/Nitrogen ratios and $\delta^{13}\text{C}_{\text{org}}$ values to infer the contributions of terrigenous relative to marine organic matter in the deglacial sediments (Meyers 1997; Knies et al. 1999; Ullrich et al. 2009; Hoff et al. 2016).

Modulating factors

A predominantly passive role for Atlantic Water as a deglacial driver is apparent when the faunal assemblages and reconstructed retreat behaviour across the shelf are compared with palaeoceanographic records. If bFAZ 1 represents Atlantic Water advection, the weakness of its Arctic/glacimarine faunal signal could also reflect transport of icebergs and meltwater away from the area, reducing local meltwater influence and thereby sustaining high melt rates at the ice margin during this early phase of retreat (Joughin et al. 2012; Straneo & Cenedese 2015; Alley et al. 2015). Otherwise, if instead bFAZ 2 represents the onset of Atlantic Water advection, the importance of *C. neoteretis* from this zone onwards would suggest that meltwater moderated the Atlantic Water throughout its operation as a driver of retreat (e.g. Lloyd et al. 2005; Taldenkova et al. 2012; Seidenkrantz et al. 2013; Sheldon et al. 2016). Meltwater suppression of the Atlantic Water is implied by the readvance of the BIIS to Porcupine Bank ~25 ka BP in the presence of Atlantic Water and during the *NEA-GS-3b* warming event (see Hibbert 2010; Austin et al. 2012; Sections 2.3.3., 6.2.1.). From the compositions of bFAZs 3 and 4, this influence of meltwater on the Atlantic Water persisted until at least 21.8 ka BP, across the warming pulse immediately following H2 in deeper-located records (e.g. Weinelt et al. 2003; Peck et al. 2008; Austin et al. 2012). During this post-H2 warming, the ice margin was stabilised at the MSGZC (Callard et al. 2020; Ó Cofaigh et al. submitted; Fig. 7.2B). This stillstand implies that bathymetric factors (a pre-existing ice-marginal depocentre), grounding-line sedimentation and meltwater overrode the influence of Atlantic Water and eustatic sea-level rise for as long as ~5 kyr (McCarron et al. 2018; Callard et al. 2020; Ó Cofaigh et al. submitted; cf. Bart et al. 2017).

It is notable that surface and subsurface evidence of iceberg drift (iceberg scours and IRD in deglacial sediments) is limited across the mid- and inner western Irish shelf (see Callard et al. 2020; Roberts et al. 2020), in comparison to the Donegal and Malin shelves (Callard et al. 2018; Ó Cofaigh et al. 2019). This may reflect a comparatively greater role for melting relative to

calving in retreat across the mid- and inner western Irish shelf (cf. Hogan et al. 2016). This would also be consistent with the persistent influence of meltwater on the Atlantic Water during this time implied by bFAZs 3 and 4 (Fig. 5.10), and the occurrence of this stage of retreat during GI-2. Towards the inner shelf, benthic foraminiferal assemblages (Peters et al. 2020) show a progressive decline in the abundance of eutrophic- and Atlantic Water-associated species, possibly reflecting the effect of the bathymetry shallowing by ~100 m on the strength of Atlantic Water influence (cf. Fig. 3a of Peters et al. 2015 with Fig. 7 of Peters et al. 2020). This could have combined with the ‘pinning points’ provided by the Aran Islands to cause extended stillstand and slow retreat rates of the BIIS on the inner shelf (Roberts et al. 2020; Ó Cofaigh et al. submitted).

7.2. The role of bathymetry in ocean forcing along the BIIS’s Atlantic margin

Consideration of these conclusions with recent results from the Celtic and Donegal shelves now allows some perspective on the roles of internal and external drivers in deglaciation along most of the BIIS’s Atlantic margin (four of the five main sectors). In Section 7.1. it was concluded that GIA-induced RSL rise likely triggered and drove deglaciation in both studied sectors, but that Atlantic Water accessed the ice margin in the Porcupine Bank-Slyne Trough region where it was an additional, passive driver of BIIS retreat offshore central western Ireland. This restriction of Atlantic Water influence to the central western Irish shelf seems attributable to the particular bathymetric conditions in the Porcupine Bank-Slyne Trough area and their interaction with Atlantic Water-advecting currents (see Section 6.2.1.: Figs. 2.3, 3.5). The area of the Slyne Trough that records the presence of grounded ice presently has maximum water depths of ~300 m, compared with maximum water depths of ~180-200 m on the Celtic shelf, ~125 m on the Donegal shelf and ~150-200 m on the outer Malin shelf. It is probable that deeper water in the Slyne Trough, combined with GIA and the northward shoaling effect of the Slyne Trough on the Shelf Edge Current (Kloppmann et al. 2001; Figs. 1.1, 2.3) allowed subsurface Atlantic Water to reach the BIIS and influence the outer shelf in this region (Section 6.2.1.) (Fig. 7.3). The Slyne Trough graben would represent an important conduit for Atlantic Water to access the BIIS along its western margin. This is because glacially-overdeepened, cross-shelf troughs often facilitate ocean forcing on higher-latitude margins with longer histories of glaciation (e.g. Christoffersen et al. 2011; Hellmer et al. 2012; Rydningen et al. 2013; Batchelor & Dowdeswell 2014) but are absent or poorly-developed along the BIIS’s Atlantic margin.

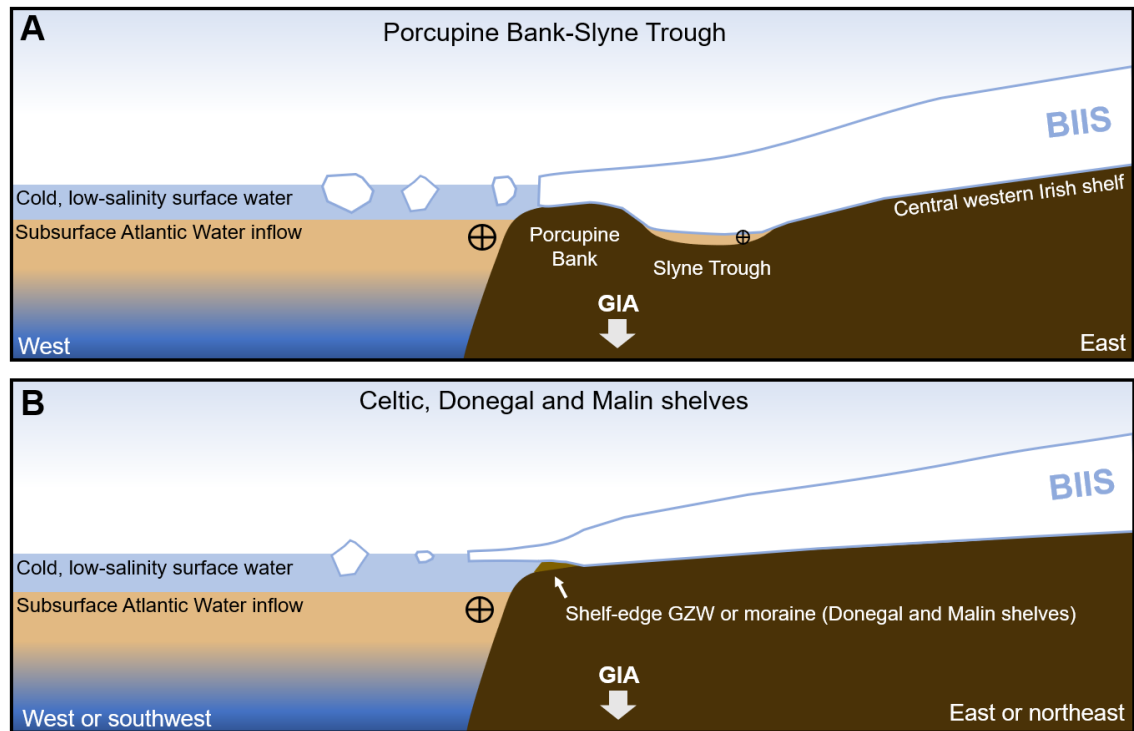


Fig. 7.3: Schematic figure showing the hypothesised role of bathymetry in controlling Atlantic Water access to the BIIS along its Atlantic margin. The figure depicts the situation during initial/early retreat (≥ 25.5 ka BP for Porcupine Bank-Slyne Trough). 'GIA'; Glacioisostatic adjustment. Northward current cores are indicated by the \oplus symbol.

In contrast, shallower water depths on the outer Celtic, Donegal and Malin shelves probably protected ice margins here from the incursion of Atlantic Water, particularly if this was flowing as a subsurface current as palaeoceanographic records suggest (cf. Dyke et al. 2014; 2018; Porter et al. 2018; An et al. 2019). The minimum depth of this subsurface Atlantic Water inflow during stadials has been suggested at ~ 300 m, downstream in the southeast Norwegian Sea (Dokken et al. 2013; Fig. 7.4), approximately the modern depth at the 198VC site (290 m). The development of prominent, wide shelf-edge moraines/GZWs in the Donegal and Malin sectors (see Ó Cofaigh et al. 2012b; 2019; Callard et al. 2018) during maximum glacial extents there could have provided further protection against Atlantic Water advection in these sectors (e.g. Bindenschadler 2006; Eisermann et al. 2020). It is therefore concluded that bathymetry played a critical role in controlling the incursion of Atlantic Water onto the shelf and thus, in causing external forcing of deglaciation where this occurred. GIA-induced RSL rise appears to have dominated where shallower water depths at the shelf edge prevented Atlantic Water access to the BIIS (Fig. 7.3).

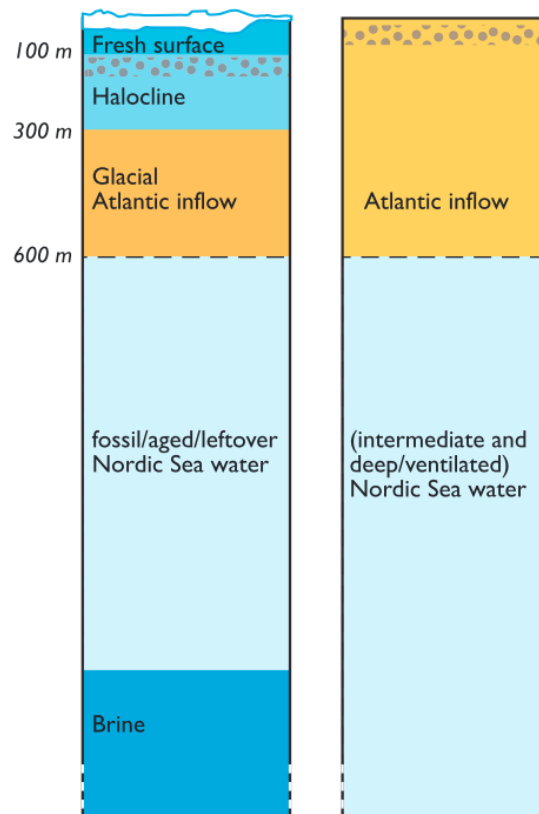


Fig. 7.4: Schematic water-column structure in the southeast Norwegian Sea during stadials (left) and interstadials (from Dokken et al. 2013).

Significance

The conclusion of restricted Atlantic Water influence on the BIIS and its retreat is consistent with an increasing number of modern observations of contrasting water-mass hydrography at the grounding lines of adjacent marine-terminating ice masses (e.g. Porter et al. 2014; Morlighem et al. 2017; Schaffer et al. 2017; 2020). In recent years, these local differences in warm water access to ice margins have been recognised as an important source of spatial and temporal variability in the rates of mass loss from polar ice sheets (e.g. Pritchard et al. 2009; Mouginit et al. 2015; Rignot et al. 2016; Carroll et al. 2018; Porter et al. 2018). This highlights the need to incorporate high-resolution bathymetry and detailed representation of circulation in models informing predictions of sea-level rise (Timmermann et al. 2010; Durand et al. 2011; Sutherland et al. 2013). In this context, the well-constrained deglacial reconstruction for central western Ireland (BRITICE-CHRONO T5 transect, Callard et al. 2020; Roberts et al. 2020; Ó Cofaigh et al. submitted) now potentially has additional value as a detailed record of shelf deglaciation under the influence of warm water on a multi-millennial timescale (Clark et al. 2012; Joughin et al. 2012; The RAISED Consortium et al. 2014; Young & Briner 2015; Stokes et al. 2015).

The results from the Malin shelf are also notable in that they imply largely internally-triggered initial deglaciation along much of the BIIS's Atlantic margin. This is a significant finding given the sensitivity of the BIIS to external forcing on account of its extensive marine margins and its maritime position adjacent to the North Atlantic at the southern limit of marine glaciation in Europe (e.g. Knutz et al. 2001; 2007; Clark et al. 2012). This study suggests that bathymetry played an important role in modulating the role of subsurface Atlantic Water on shelf edge deglaciation of the last BIIS, preventing its influence on the ice margin in most Atlantic sectors but facilitating its localised access to the ice margin in the Porcupine Bank-Slyne Trough region, where it was a driver of retreat offshore central western Ireland (Fig. 7.3).

CHAPTER 8

CONCLUSIONS

In Section 8.1. the conclusions of this study are presented to address the research questions set out in Chapter 1, with recommendations for future research. In Section 8.2., the conclusions as to environmental factors driving and modulating deglaciation in the studied sectors are outlined, along with the role of bathymetry in controlling Atlantic Water access to the BIIS margin.

8.1. Deglacial environments in the Malin shelf and Porcupine Bank-Slyne Trough sectors

Analysis of foraminiferal assemblages and sedimentology in sediment cores JC106-146VC and JC106-198VC successfully allowed testing for the presence of Atlantic Water during deglaciation and for depositional environments during BIIS retreat to be reconstructed in detail for these sectors (objectives 1-3). The reconstructed palaeoenvironmental conditions were compared with palaeoceanographic records from deeper, more ice-distal open-ocean locations along the BIIS's Atlantic margin, providing insight into the influence of northeast Atlantic palaeoceanographic conditions on deglaciation of these BIIS sectors (objective 4).

8.1.1. Research question 1: Do benthic foraminiferal assemblages in early deglacial lithofacies imply the presence of Atlantic Water on the continental shelf during initial BIIS retreat?

The Malin shelf

Benthic foraminiferal assemblages in core JC106-146VC from the outer Malin shelf are dominated by species typical of glacimarine and Arctic environments (*Elphidium clavatum* and *Cassidulina reniforme*) and show relatively low diversity throughout the deglacial lithofacies (Fisher's α average 6.5). Specimens are commonly small in the earliest deglacial sediments, further suggesting a cold glacimarine environment near the tolerance limit for those species, likely due to oligotrophic conditions, high sedimentation rates, fluctuating salinity and low temperatures. Test preservation is variable throughout the deglacial sequence, and may indicate considerable reworking and dissolution in the assemblages. However, a lack of species associated with nutrient-rich conditions and/or Atlantic Water persisting into ice-distal lithofacies supports the interpretation of a cold glacimarine environment of retreat, in which Atlantic Water was not present.

Porcupine Bank and Slyne Trough

Benthic foraminiferal assemblages in core JC106-198VC from the Slyne Trough are characterised by considerably higher diversity (Fisher's α 7.0-12.3), high preservation quality throughout and the importance of species variably associated with temperate, nutrient-rich settings, Atlantic Water and strong bottom currents. Proportions of *E. clavatum* and *C. reniforme* are initially very low (together comprising $\leq 5\%$), before *C. reniforme* emerges alongside the chilled Atlantic Water-associated *Cassidulina neoteretis* prior to BISS readvance over the core site. Following final retreat from the outer shelf, assemblages are dominated by *C. reniforme*, *C. neoteretis* and the strong current-associated *T. angulosa*. While the consistent presence of *C. neoteretis* following an initial lack of Arctic/glacimarine-associated species suggests Atlantic Water presence throughout the deglacial sequence, it is unclear to what degree the temperate, nutrient-rich-associated species present throughout the core represent conditions during deglaciation. This is as previous radiocarbon results imply a high reworked contribution to the early deglacial benthic foraminiferal assemblages. However, the planktic foraminiferal assemblages reported in this project, together with published sedimentologic, geomorphic and palaeoceanographic evidence in the region, suggest northward Atlantic Water advection during deglaciation, and it is considered likely that the high contribution of reworked benthic tests at least partly reflects the activity of this current. Involvement of Atlantic Water in deglaciation in the Slyne Trough and main central western Irish shelf, as inferred here, is consistent with conclusions of previous studies investigating deglacial foraminiferal assemblages in the area (Peters et al. 2015; 2020).

Future work to resolve the implications of the deglacial benthic foraminiferal record offshore central western Ireland should include further radiocarbon dating of monospecific samples of 'temperate' and Atlantic-Water associated benthic foraminifera, combined with sortable silt analyses on suspected contouritic deposits in which they occur. This would elucidate the strength of bottom currents during deglaciation, and whether current strength is related to the contribution of reworked tests. Carbon/Nitrogen and $\delta^{13}\text{C}_{\text{org}}$ ratios should also be determined in the deglacial sediments to evaluate the extent to which productive conditions implied by the assemblages could reflect ice-marginal terrigenous nutrient input (Peters et al. 2020) rather than a marine, Atlantic Water-related nutrient supply.

8.1.2. Research question 2: Do planktic foraminiferal assemblages in early deglacial lithofacies provide information on surface water conditions in the adjacent open ocean during initial BISS retreat?

The Malin shelf

Planktic foraminiferal abundance is very low throughout deglacial lithofacies in core 146VC (0.2-1.3 individuals/g dry sediment; benthic:planktic ratio 7.5-50.5). As planktic foraminiferal production is generally limited over continental shelves, this low abundance suggests that the cold, low-productivity conditions implied by the benthic assemblages extended into the adjacent open ocean (Jansen et al. 1983; Hald & Vorren 1987). Surface ocean conditions adjacent to the shelf were likely characterised by severe sea-ice conditions and/or low surface water salinity. The low planktic proportions in core 146VC could also imply that advection of planktic tests onto the Malin shelf was restricted, possibly due to the extensive sea-ice conditions and/or relatively shallow water depths over the Malin shelf (cf. Austin 1991).

Porcupine Bank-Slyne Trough

The planktic foraminiferal assemblage throughout deglacial lithofacies in core 198VC is characterised by moderate relative abundance of the polar-associated *Neogloboquadrina pachyderma* (33-57%), and of subpolar-subtropical species including *Turborotalita quinqueloba* (3-14%), *Neogloboquadrina incompta* (4-13%) and *Globigerinella siphonifera* (1-17%). This assemblage composition, combined with its persistence through several changes in ice-margin proximity and a BIIS readvance over the core site, suggests that the planktic foraminifera in 198VC were at least partly advected to the core site from south of the Polar Front, most likely in a surface/subsurface Atlantic Water-advecting current. This conclusion is consistent with palaeoceanographic records and northward-oriented iceberg scours in the Slyne Trough (e.g. Peck et al. 2008; Rasmussen et al. 2008; Austin et al. 2012; Peters et al. 2015; Thébaudeau et al. 2016). However, no dating has been carried out on planktic foraminifera from BIIS deglacial sediments on the Atlantic margin, and would be needed to confirm that these assemblages indicate surface/subsurface Atlantic Water presence during deglaciation in the Slyne Trough.

8.1.3. *Research question 3: What depositional environments were associated with early deglaciation, as recorded by sediment core lithofacies and foraminiferal assemblages?*

The Malin shelf

Grounding-zone wedges on the outer Malin shelf and shelf edge imply that the Barra Fan Ice Stream (BFIS) was terminating as an ice-shelf margin during its initial retreat. Narrower ridges between the two prominent grounding-zone wedges on the northern Malin shelf may therefore record interaction of tidal motion with the grounding-line or basal crevasses in the ice-shelf during retreat (cf. Shipp et al. 2002; Dowdeswell et al. 2020). The earliest deglacial lithofacies in core

146VC comprise alternating laminated muds and pebble-rich diamictos, closely resembling sequences from modern Arctic settings where iceberg-rafting is seasonally or episodically suppressed by development of extensive sea-ice. Immobilisation of the icebergs under these conditions allowed suspension settling of fine sediment to predominate as the depositional process, generating the intervals of laminated mud. These conditions occurred on the outer shelf in a proximal glacimarine environment associated with an ice-shelf grounded about 3 km inshore of the 146VC site. Sedimentation rates are likely to have been high as remobilisation occurred during deposition of the core sequence. Iceberg-rafting then appears to have ceased for an extended period, during which a unit of laminated mud, very clast-poor and becoming barren of foraminifera, was deposited most likely under perennial sea-ice cover. There is some evidence that tidal and/or brine currents influenced the seafloor during this time. These conditions were succeeded by resumption of iceberg-rafting across a relatively gradual palaeoenvironmental transition during which sea-ice cover only partially suppressed iceberg drift. Return of open-water conditions was associated with a large increase in productivity and an extended period of iceberg-rafting likely recording final retreat of the BFIS from the outer shelf via calving. In the subsequent increasingly distal glacimarine conditions at the core site, suspension settling dominated deposition, bioturbation intensity increased and iceberg-rafting eventually ceased to supply coarse sediment to the outer shelf.

Porcupine Bank-Slyne Trough

Initial deglaciation in the Porcupine Bank-Slyne Trough region (underway by 25.9 ka BP) was interrupted by readvance episode(s) associated with an oscillating ice margin, as indicated by overridden glacimarine sediments and crenulated GZWs/moraines (Ó Cofaigh et al. submitted). This early deglacial environment was characterised by suspension settling, persistent iceberg-rafting and probably minor mass flow, with no evidence for any extensive development of sea-ice. As explained in Sections 6.2.1. and 7.1.1., it is proposed here that a persistent northward current probably winnowing and transporting foraminiferal tests was active in this environment. A final BIIS readvance to Porcupine Bank is likely to have involved partially floating ice in the Slyne Trough, forming GZWs in the Trough and narrow ridges on the Bank. Final grounding-line retreat from the 198VC site ~25.5 ka BP was accompanied by deposition of cohesive debris flows rich in shell material and foraminiferal tests. Increasingly ice-distal conditions on the outer shelf were characterised by limited iceberg-rafting at the core site, recorded by deposition of massive, clast-poor muds showing an upwards increase in bioturbation and decrease in terrigenous sediment supply. A current in the Slyne Trough was advecting icebergs northward during this period, and is reflected in the 198VC foraminiferal assemblages which imply that moderate current strengths and chilled Atlantic Water influenced the outer shelf until at least 21.8 ka BP.

8.1.4. Research question 4: How do the palaeoenvironmental conditions reconstructed from the foraminiferal assemblages relate to palaeoceanographic changes in the wider Northeast Atlantic during Greenland Stadial 3?

There is now substantial evidence that Atlantic Water advection into the Nordic Seas continued at least episodically, and probably beneath the surface, during stadials of the last glacial period (e.g. Bauch et al. 2001; Rasmussen & Thomsen 2004; 2008; Dokken et al. 2013; Ezat et al. 2014). The western Irish-Scottish margin and Faeroe-Shetland Channel adjacent to the northwestern BIIS were likely to have been an important pathway for this inflow, similarly to the present situation (Lassen et al. 1999; Blindheim & Østerhus 2005; Hoff et al. 2016). A number of % *N. pachyderma* and Mg/Ca records along this pathway, from the Porcupine Seabight to the North Sea slope, register a distinct warming event during GS-3 from ~25.6-24.8 ka BP (the ‘*NEA-GS-3b*’ event; Peck et al. 2008; Rasmussen et al. 2008; Hibbert 2010; Austin et al. 2012). The *NEA-GS-3b* event occurs during the early stages of deglaciation along the BIIS’s Atlantic margin (underway by 25.9-24.8 ka BP depending on location), so represents a potential external influence on early BIIS deglaciation provided the Atlantic Water could access the ice margins on the shelf.

Reconstructed palaeoenvironmental conditions throughout deglaciation of the Malin shelf, as described in Sections 6.1.2. and 7.1.1, show no evidence of Atlantic Water influence and maintain cold bottom- and surface water conditions with frequent severe sea-ice development. This implies that any Atlantic Water advection along the Irish/Scottish margin during this time (~25.9-<23.8 ka BP) could or did not access the Malin shelf, and therefore that deglaciation of this sector was not driven by regional palaeoceanographic events. In contrast, the presence of Atlantic Water species in deglacial sediments from before 25.5 ka BP until at least 21.8 ka BP in Porcupine Bank-Slyne Trough suggest that the *NEA-GS-3b* event and subsequent Atlantic Water advection during GI-2 played a role in deglaciation offshore central western Ireland.

8.2. Forcing and modulation of deglaciation along the BIIS’s Atlantic margin

8.2.1. The Malin shelf

The cold glacimarine deglacial environment and absence of Atlantic Water implied by the foraminiferal assemblages from core 146VC supports the proposal of Callard et al. (2018) that BFIS retreat from the Malin shelf edge was triggered and driven internally by GIA-induced RSL rise. This conclusion is consistent with recent results from the Celtic Sea and Donegal shelf sectors (Ó Cofaigh et al. 2019; Scourse et al. 2019), and therefore implies internally-triggered deglaciation along a substantial portion of the BIIS’s Atlantic margin. Callard et al. (2018)

showed that bathymetry was important in pacing retreat of the BFIS across the Malin shelf, with retreat across the outer shelf aided by reverse bed slope and subsequent deglaciation of the mid-shelf at least partly driven by overdeepened troughs. The early deglacial environment during retreat across the outer Malin shelf was shown in this project to have involved frequent development of extensive, likely perennial sea-ice. The episodic nature of BFIS retreat across the outer shelf, evidenced by successive GZWs and ridges, may therefore partly reflect a buttressing effect by this sea-ice. An episode of particularly severe sea-ice cover preceding final retreat from the outer shelf temporally coincides with H2, potentially reflecting an external influence on BFIS retreat.

8.2.2. *Porcupine Bank-Slyne Trough*

In the Porcupine Bank-Slyne Trough region, early deglacial lithofacies and foraminiferal assemblages, particularly the proportion of planktic foraminifera, indicate that initial retreat occurred in a marine environment, with water depths likely ≥ 100 m. Additionally, it is considered likely here that Atlantic Water was present during early deglaciation, as well as during final retreat from the outer shelf. On this account, it is proposed that deglaciation in this sector was driven by a combination of internal and external factors; high RSL, probably enhanced by GIA, and Atlantic Water advection. The Atlantic Water driver was persistently modulated by meltwater throughout deglaciation on the outer shelf, as implied by the consistent presence of the chilled Atlantic Water-associated benthic foraminifer *C. neoteretis*, and the BIIS appears to have overridden the Atlantic Water influence in a readvance to Porcupine Bank ~ 25.5 - 25.0 ka BP. On the mid-shelf, the presence of a pre-existing ice-marginal depocentre (McCarron et al. 2018; Callard et al. 2020) facilitated an extended stillstand lasting as long as ~ 5 kyr, despite continued RSL rise and Atlantic Water presence on the shelf.

8.2.3. *The role of bathymetry in controlling Atlantic Water access to the BIIS margin*

This study has contributed insights into deglacial forcing from a further two Atlantic BIIS sectors, the Malin shelf and Porcupine Bank-Slyne Trough, allowing some perspective on the roles of internal and external drivers in deglaciation along the BIIS's Atlantic margin (four of its five main sectors). The restriction of Atlantic Water influence to the Porcupine Bank-Slyne Trough region implied by the results of this project are attributed to the presence of the Slyne Trough graben on the Irish margin. It is concluded that the Slyne Trough provided a unique conduit for Atlantic Water advection towards the BIIS, and accounted for greater water depths during initial deglaciation than in the other sectors along the BIIS's Atlantic margin. These greater water depths

in areas occupied by grounded ice (presently ~300 m) appear to have been sufficient to allow Atlantic Water (probably at subsurface depths) to influence the ice margin. In contrast, shallower water depths across the Celtic Sea, Donegal and Malin shelves (presently 125-200 m), combined with the presence of prominent shelf-edge GZWs/moraines, prevented incursion of the Atlantic Water to the ice margin in these sectors.

REFERENCES

- Aksu, A. 1983, 'Holocene and Pleistocene dissolution cycles in deep-sea cores of Baffin Bay and Davis Strait: Palaeoceanographic implications', *Marine Geology*, vol. 53, pp. 331-348.
- Alley, R. et al. 1999, 'Making sense of millennial-scale climate change', in Clark, P. et al. (eds.), *Mechanisms of global change at millennial time scales*, Geophysical Monograph Series vol. 112, American Geophysical Union, Washington, pp. 385-394.
- Alley, R. et al. 2015, 'Oceanic forcing of ice-sheet retreat: West Antarctica and more', *Annual Reviews of Earth and Planetary Science*, vol. 43, pp. 207-231.
- Alonso-Garcia, M. et al. 2011, 'Arctic front shifts in the subpolar North Atlantic during the Mid-Pleistocene (800-400 ka) and their implications for ocean circulation', *Palaeogeography, Palaeoclimatology, Palaeoecology*, vol. 311, pp. 268-280.
- Altenbach, A. et al. 2003, 'Impact of interrelated and interdependent ecological controls on benthic foraminifera: an example from the Gulf of Guinea', *Palaeogeography, Palaeoclimatology, Palaeoecology*, vol. 197, pp. 213-238.
- Alve, E. 1999, 'Colonization of new habitats by benthic foraminifera: a review', *Earth-Science Reviews*, vol. 46, pp. 167-185.
- An, L. et al. 2019, 'Bathymetry of southeast Greenland from Oceans Melting Greenland (OMG) data', *Geophysical Research Letters*, vol. 46, pp. 11197-11205.
- Andersen, K. et al. 2006, 'The Greenland Ice Core Chronology 2005, 15-42 ka. Part 1: constructing the time scale', *Quaternary Science Reviews*, vol. 25, pp. 3246-3257.
- Andrews, J. & Principato, S. 2002, 'Grain-size characteristics and provenance of ice-proximal glacial marine sediments', in Dowdeswell, J. & Ó Cofaigh, C. (eds.), *Glacier-influenced sedimentation on high-latitude continental margins*, Geological Society, London, Special Publication No. 203, London, pp. 305-324.
- Andrews, J. 1998, 'Abrupt changes (Heinrich events) in late Quaternary North Atlantic marine environments: a history and review of data and concepts', *Journal of Quaternary Science*, vol. 13, pp. 3-16.
- Armishaw, J. et al. 2000, 'The Barra Fan: A bottom-current reworked, glacially-fed submarine fan system', *Marine and Petroleum Geology*, vol. 17, pp. 219-238.
- Auffret, G. et al. 2002, 'Terrigenous fluxes at the Celtic margin during the last glacial cycle', *Marine Geology*, vol. 188, pp. 79-108.
- Austin, W. & Evans, J. 2000, 'NE Atlantic benthic foraminifera: modern distribution patterns and palaeoecological significance', *Journal of the Geological Society, London*, vol. 157, pp. 679-691.
- Austin, W. & Kroon, D. 1996, 'Late glacial sedimentology, foraminifera and stable isotope stratigraphy of the Hebridean Continental Shelf, northwest Scotland', in Andrews, J. et al. (eds.), *Late Quaternary Palaeoceanography of the North Atlantic Margins*, Geological Society Special Publication No. 111, Geological Society, London, pp. 187-213.
- Austin, W. & McCarroll, D. 1992, 'Foraminifera from the Irish Sea glacial deposits at Aberdaron, western Llyn, North Wales: palaeoenvironmental implications', *Journal of Quaternary Science*, vol. 7, pp. 311-317.
- Austin, W. 1991, *Late Quaternary benthonic foraminiferal stratigraphy of the western U.K. continental shelf*, PhD Thesis, University of Wales, 206 pp.

- Austin, W. et al. 2012, 'The synchronisation of palaeoclimatic events in the North Atlantic region during Greenland Stadial 3 (ca 27.5 to 23.3 kyr b2k)', *Quaternary Science Reviews*, vol. 36, pp. 154-163.
- Ballantyne, C. & Ó Cofaigh, C. 2007, 'The Last Irish Ice Sheet: Extent and Chronology', in Coxon, P. et al. (eds.), *Advances in Irish Quaternary Studies*, Atlantis Advances in Quaternary Science, vol. 1, Atlantis Press, Paris, pp. 101-149.
- Ballantyne, C. 2010, 'Extent and deglacial chronology of the last British-Irish Ice Sheet: implications of exposure dating using cosmogenic isotopes', *Journal of Quaternary Science*, vol. 25, pp. 515-534.
- Ballantyne, C. et al. 2007, 'The Donegal ice dome, northwest Ireland: dimensions and chronology', *Journal of Quaternary Science*, vol. 22, no. 8, pp. 773-783.
- Barker, R. 1960, *Taxonomic notes on the species figured by H.B. Brady in his report on the foraminifera dredged by the HMS Challenger during the years 1873-1876*, SEPM Special Publication No. 9, 238 pp.
- Bart, P. et al. 2017, 'The paradox of a long grounding during West Antarctic Ice Sheet retreat in the Ross Sea', *Scientific Reports*, vol. 7, pp. 1-8.
- Bassis, J. et al. 2017, 'Heinrich events triggered by ocean forcing and modulated by isostatic adjustment', *Nature*, vol. 542, pp. 332-334.
- Batchelor, C. & Dowdeswell, J. 2014, 'The physiography of high Arctic cross-shelf troughs', *Quaternary Science Reviews*, vol. 92, pp. 68-96.
- Batchelor, C. & Dowdeswell, J. 2015, 'Ice-sheet grounding-zone wedges (GZWs) on high-latitude continental margins', *Marine Geology*, vol. 363, pp. 65-92.
- Bauch, H. 1992, 'Test size variations of planktic foraminifers as response to climatic changes', Abstracts, 4th International Conference on Palaeoceanography, GEOMAR Report vol. 15, p. 56.
- Bauch, H. 1994, 'Significance of variability in *Turborotalita quinqueloba* (Natland) test size and abundance for palaeoceanographic interpretations in the Norwegian-Greenland Sea', *Marine Geology*, vol. 121, pp. 129-141.
- Bauch, H. et al. 2001, 'A multiproxy reconstruction of the evolution of deep and surface waters in the subarctic Nordic seas over the last 30,000 yr', *Quaternary Science Reviews*, vol. 20, pp. 659-678.
- Bé, A. & Tolderlund, D. 1971, 'Distribution and ecology of living planktonic Foraminifera in surface waters of the Atlantic and Indian Oceans', in Funnell, B. & Riedel, W. (eds.), *The Micropalaeontology of Oceans*, University Press, Cambridge, pp. 105-149.
- Becker, L. et al. 2018, 'Ocean-ice sheet interaction along the SE Nordic Seas margin from 35 to 15 ka BP', *Marine Geology*, vol. 402, pp. 99-117.
- Belanger, P. & Streeter, S. 1980, 'Distribution and ecology of benthic foraminifera in the Norwegian-Greenland sea', *Marine Micropaleontology*, vol. 5, pp. 401-428.
- Belyea, L. 2007, 'Revealing the Emperor's new clothes: niche-based palaeoenvironmental reconstruction in the light of recent ecological theory', *The Holocene*, vol. 17, pp. 683-688.
- Benetti, S. et al. 2010, 'Glacial and glacially-related features on the continental margin of northwest Ireland mapped from marine geophysical data', *Journal of Maps*, vol. 6, issue 1, pp. 14-29.

- Benn, D. 1996, 'Subglacial and subaqueous processes near a glacier grounding line: sedimentological evidence from a former ice-dammed lake, Achnasheen Scotland', *Boreas*, vol. 25, pp. 23-36.
- Bergsten, H. 1994, 'Recent benthic foraminifera of a transect from the North Pole to the Yermak Plateau, eastern central Arctic Ocean', *Marine Geology*, vol. 119, pp. 251-267.
- Bernhard, J. 1992, 'Benthic foraminiferal distribution and biomass related to pore-water oxygen content: central California continental slope and rise', *Deep-Sea Research Part A*, vol. 39, pp. 585-605.
- Bindschadler, R. 2006, 'Hitting the ice sheets where it hurts', *Science*, vol. 311, pp. 1720-1721.
- Binns, P. et al. 1974, 'Glacial and post-glacial sedimentation in the Sea of Hebrides', *Nature*, vol. 48, pp. 751-754.
- Birks, H. 1995, 'Quantitative palaeoenvironmental reconstructions', in Maddy, D. & Brew, J. (eds.), *Statistical modelling of Quaternary science data*, Technical Guide 5, Quaternary Research Association, Cambridge, pp. 161-254.
- Birks, H. et al. 2010, 'Strengths and weaknesses of quantitative climate reconstructions based on late-Quaternary biological proxies', *The Open Ecology Journal*, vol. 3, pp. 68-110.
- Blaauw, M. et al. 2010, 'Random walk simulations of fossil proxy data', *The Holocene*, vol. 20, pp. 645-649.
- Blair, T. & McPherson, J. 1999, 'Grain-size and textural classification of coarse sedimentary particles', *Journal of Sedimentary Research*, vol. 69, pp. 6-19.
- Blindheim, J. & Østerhus, S. 2005, 'The Nordic Seas, main oceanographic features', in Drange, H. et al. (eds.), *The Nordic Seas: An integrated perspective*, Geophysical Monograph Series vol. 158, American Geophysical Union, Washington, pp. 11-39.
- Boers, N. et al. 2018, 'Ocean circulation, ice shelf, and sea ice interactions explain Dansgaard-Oeschger cycles', *Proceedings of the National Academy of Sciences of the United States*, vol. 115, 10 pp.
- Bond, G. & Lotti, R. 1995, 'Iceberg discharges into the North Atlantic on millennial time scales during the Last Glaciation', *Science*, vol. 267, pp. 1005-1010.
- Bond, G. et al. 1993, 'Correlations between climate records from North Atlantic sediments and Greenland ice', *Nature*, vol. 365, pp. 143-147.
- Boulton, G. & Hagdorn, M. 2006, 'Glaciology of the British Isles Ice Sheet during the last glacial cycle: form, flow, streams and lobes', *Quaternary Science Reviews*, vol. 25, pp. 3359-3390.
- Bowen, D. 1973, 'The Pleistocene succession of the Irish Sea', *Proceedings of the Geologists' Association*, vol. 84, pp. 249-272.
- Bowen, D. 1985, 'Amino acid geochronology of raised beaches in south west Britain', *Quaternary Science Reviews*, vol. 4, pp. 279-318.
- Bowen, D. et al. 2002, 'New data for the Last Glacial Maximum in Great Britain and Ireland', *Quaternary Science Reviews*, vol. 21, pp. 89-101.
- Boyle, E. & Keigwin, L. 1987, 'North Atlantic thermohaline circulation during the past 20,000 years linked to high-latitude surface temperature', *Nature*, vol. 330, pp. 35-40.
- Bradwell, T. & Stoker, M. 2015, 'Submarine sediment and landform record of a palaeo-ice stream within the British-Irish Ice Sheet', *Boreas*, vol. 44, pp. 255-276.

- Bradwell, T. & Stoker, M. 2016, 'Glacial sediment and landform record offshore NW Scotland: a fjord-shelf-slope transect through a Late Quaternary mid-latitude ice-stream system', in Canals, J. et al. (eds.), *Atlas of Submarine Glacial Landforms: Modern, Quaternary and Ancient*, Geological Society, London, Memoir 46, pp. 421-428.
- Bradwell, T. 2013, 'Identifying palaeo-ice-stream tributaries on hard beds: Mapping glacial bedforms and erosion zones in NW Scotland', *Geomorphology*, vol. 201, pp. 397-414.
- Bradwell, T. et al. 2007, 'Geomorphological signature and flow dynamics of the Minch palaeo-ice stream, northwest Scotland', *Journal of Quaternary Science*, vol. 22, pp. 609-617.
- Bradwell, T. et al. 2008a, 'Megagrooves and streamlined bedrock in NW Scotland: The role of ice streams in landscape evolution', *Geomorphology*, vol. 97, pp. 135-156.
- Bradwell, T. et al. 2008b, 'The northern sector of the last British Ice Sheet: Maximum extent and demise', *Earth-Science Reviews*, vol. 207-226.
- Bradwell, T. et al. 2019, 'Ice-stream demise dynamically conditioned by trough shape and bed strength', *Science Advances*, vol. 5, 14 pp.
- Briner, J. et al. 2009, 'Rapid early Holocene retreat of a Laurentide outlet glacier through an Arctic fjord', *Nature Geoscience*, vol. 2, pp. 496-499.
- Broecker, W. et al. 1992, 'Origin of the northern Atlantic's Heinrich events', *Climate Dynamics*, vol. 6, pp. 265-273.
- Bronk Ramsey, C. 2008, 'Depositional models for chronological records', *Quaternary Science Reviews*, vol. 27, pp. 42-60.
- Burrows, M. & Thorpe, S. 1999, 'Drifter observations of the Hebrides slope current and nearby circulation patterns', *Annales Geophysicae*, vol. 17, pp. 280-302.
- Callard, S. et al. 2018, 'Extent and retreat history of the Barra Fan Ice Stream offshore western Scotland and northern Ireland during the last glaciation', *Quaternary Science Reviews*, vol. 201, pp. 280-302.
- Callard, S. et al. 2020, 'Oscillating retreat of the last British-Irish Ice Sheet on the continental shelf offshore Galway Bay, western Ireland', *Marine Geology*, vol. 420, 17 pp.
- Cape, M. et al. 2014, 'Polynya dynamics drive primary production in the Larsen A and B embayments following ice shelf collapse', *Journal of Geophysical Research: Oceans*, vol. 119, pp. 572-594.
- Carroll, D. et al. 2018, 'Subannual and seasonal variability of Atlantic-origin waters in two adjacent west Greenland fjords', *Journal of Geophysical Research: Oceans*, vol. 123, pp. 6670-6687.
- Carstens, J. & Wefer, G. 1992, 'Recent distribution of planktic foraminifera in the Nansen Basin, Arctic Ocean', *Deep-Sea Research*, vol. 39, Supplement 2, pp. 8507-8524.
- Carstens, J. et al. 1997, 'Distribution of planktic foraminifera at the ice margin in the Arctic (Fram Strait)', *Marine Micropalaeontology*, vol. 29, pp. 257-269.
- Catania, G. et al. 2018, 'Geometric controls on tidewater glacier retreat in central western Greenland', *Journal of Geophysical Research: Earth Surface*, vol. 123, pp. 2024-2038.
- Chapman, M. & Shackleton, N. 1998, 'Millennial-scale fluctuations in North Atlantic heat flux during the last 150,000 years', *Earth and Planetary Science Letters*, vol. 159, pp. 57-70.

- Chapman, M. 2010, 'Seasonal production patterns of planktonic foraminifera in the NE Atlantic Ocean: Implications for paleotemperature and hydrographic reconstructions', *Paleoceanography*, vol. 25, 9 pp.
- Chauhan, T. et al. 2014, 'Glacial history and paleoceanography of the southern Yermak Plateau since 132 ka BP', *Quaternary Science Reviews*, vol. 92, pp. 155-169.
- Chiverell, R. et al. 2013, 'Bayesian modelling the retreat of the Irish Sea Ice Stream', *Journal of Quaternary Science*, vol. 28, pp. 200-209.
- Christoffersen, P. et al. 2011, 'Warming of waters in an East Greenland fjord prior to glacier retreat: mechanisms and connection to large-scale atmospheric conditions', *The Cryosphere*, vol. 5, pp. 701-714.
- Clark, C. et al. 2012, 'Pattern and timing of retreat of the last British-Irish Ice Sheet', *Quaternary Science Reviews*, vol. 44, pp. 112-146.
- Clark, P. et al. 2000, 'Interpreting Iceberg Deposits in the Deep Sea', *Science*, vol. 290, pp. 51-52.
- Clark, P. et al. 2009, 'The Last Glacial Maximum', *Science*, vol. 325, pp. 710-714.
- CLIMAP Project Members 1976, 'The surface of the ice-age Earth', *Science*, vol. 191, pp. 1131-1137.
- CLIMAP Project Members 1981, *Seasonal reconstructions of the Earth's surface at the last glacial maximum*, GSA Map and Chart Series, MC-36, Geological Society of America, Boulder.
- Cook, A. et al. 2019, 'Atmospheric forcing of rapid marine-terminating glacier retreat in the Canadian Arctic Archipelago', *Science Advances*, vol. 5, 10 pp.
- Cortijo, E. et al. 1996, 'Changes in sea surface hydrology associated with Heinrich event 4 in the North Atlantic Ocean between 40° and 60°N', *Earth and Planetary Science Letters*, vol. 146, pp. 29-45.
- Cowan, E. et al. 1997, 'Temperate glacimarine varves: An example from Disenchantment Bay, Alaska', *Journal of Sedimentary Research*, vol. 67, pp. 536-549.
- Cowan, E. et al. 1999, 'Cyclic sedimentation associated produced by fluctuations in meltwater discharge, tides and marine productivity in an Alaskan fjord', *Sedimentology*, vol. 46, pp. 1109-1126.
- Cowan, E. et al. 2020, 'Sediment controls dynamic behaviour of a Cordilleran Ice Stream at the Last Glacial Maximum', *Nature Communications*, vol. 11, pp. 1-9.
- Cronin, T. et al. 2012, 'Deep Arctic Ocean warming during the last glacial cycle', *Nature Geoscience*, vol. 5, pp. 631-634.
- Cronin, T. et al. 2019, 'The benthic Foraminifera *Cassidulina* from the Arctic Ocean: Application to paleoceanography and biostratigraphy', *Micropaleontology*, vol. 65, pp. 105-125.
- Culver, S. & Buzas, M. 2000, 'Global latitudinal species diversity gradient in deep-sea benthic foraminifera', *Deep-Sea Research Part I*, vol. 47, pp. 259-275.
- Curran, K. et al. 2004, 'Fine-grained sediment flocculation below the Hubbard Glacier meltwater plume, Disenchantment Bay, Alaska', *Marine Geology*, vol. 203, pp. 83-94.
- Dahlgren, K. & Vorren, T. 2003, 'Sedimentary environment and glacial history during the last 40 ka of the Vøring continental margin, mid-Norway', *Marine Geology*, vol. 193, pp. 93-127.

- Dahlgren, K. et al. 2002, 'Late Quaternary glacial development of the mid-Norwegian margin-65 to 68°N', *Marine and Petroleum Geology*, vol. 19, pp. 1089-1113.
- Dansgaard, W. et al. 1993, 'Evidence for general instability of past climate from a 250-kyr ice-core record', *Nature*, vol. 364, pp. 218-220.
- Darling, K. et al. 2016, 'The genetic diversity, phylogeography and morphology of Elphidiidae (Foraminifera) in the Northeast Atlantic', *Marine Micropaleontology*, vol. 129, pp. 1-23.
- Davies, H. et al. 1984, 'A revised seismic stratigraphy for Quaternary deposits on the inner continental shelf west of Scotland between 55°30'N and 57°30'N', *Boreas*, vol. 13, pp. 49-66.
- De Mol, B. et al. 2002, 'Large deep-water coral banks in the Porcupine Basin, southwest of Ireland', *Marine Geology*, vol. 188, pp. 193-231.
- de Stigter, H. et al. 1998, 'Bathymetric distribution and microhabitat partitioning of live (Rose Bengal stained) benthic foraminifera along a shelf to bathyal transect in the southern Adriatic Sea', *Journal of Foraminiferal Research*, vol. 28, pp. 40-65.
- de Vernal, A. et al. 2000, 'Reconstruction of sea-surface temperature, salinity, and sea-ice cover in the northern North Atlantic during the last glacial maximum based on dinocyst assemblages', *Canadian Journal of Earth Sciences*, vol. 37, pp. 725-750.
- Delhez, E. 1998, 'Macroscale ecohydrodynamic modeling on the Northwest European Continental Shelf', *Journal of Marine Systems*, vol. 16, pp. 171-190.
- den Dulk, M. et al. 2000, 'Benthic foraminifera as proxies for organic matter flux and bottom water oxygenation? A case history from the northern Arabian Sea', *Palaeogeography, Palaeoclimatology, Palaeoecology*, vol. 161, pp. 337-359.
- Dennison, J. & Hay, W. 1967, 'Estimating the needed sampling area for subaquatic ecologic studies', *Journal of Paleontology*, vol. 41, pp. 706-708.
- Diekmann, B. et al. 2000, 'Terrigenous sediment supply in the Scotia Sea (Southern Ocean): response to Late Quaternary ice dynamics in Patagonia and on the Antarctic Peninsula', *Paleogeography, Paleoclimatology, Paleoecology*, vol. 162, pp. 357-387.
- Diz, P. & Francés, G. 2009, 'Postmortem processes affecting benthic foraminiferal assemblages in the Ría de Vigo, Spain: Implications for paleoenvironmental studies', *Journal of Foraminiferal Research*, vol. 39, pp. 166-179.
- Dobson, M. & Haynes, J. 1973, 'Association of Foraminifera with hydroids on the deep shelf', *Micropaleontology*, vol. 19, pp. 78-90.
- Dokken, T. & Hald, M. 1996, 'Rapid shifts during isotope stages 2-4 in the Polar North Atlantic', *Geology*, vol. 24, pp. 599-602.
- Dokken, T. & Jansen, E. 1999, 'Rapid changes in the mechanism of ocean convection during the last glacial period', *Nature*, vol. 401, pp. 458-461.
- Dokken, T. et al. 2013, 'Dansgaard-Oeschger cycles: Interactions between ocean and sea ice intrinsic to the Nordic Seas', *Paleoceanography*, vol. 28, 13 pp.
- Domack, E. & Harris, P. 1998, 'A new depositional model for ice shelves, based upon sediment cores from the Ross Sea and the Mac. Robertson shelf, Antarctica', *Annals of Glaciology*, vol. 27, pp. 281-284.

- Domack, E. & Ishman, S. 1993, 'Oceanographic and physiographic controls on modern sedimentation within Antarctic fjords', *Geological Society of America Bulletin*, vol. 105, pp. 1175-1189.
- Domack, E. & Lawson, D. 1985, 'Pebble fabric in an ice-rafted diamicton', *The Journal of Geology*, vol. 93, pp. 577-591.
- Domack, E. et al. 1999, 'Late Pleistocene-Holocene retreat of the West Antarctic Ice Sheet system on the Ross Sea: Part 2 – Sedimentologic and stratigraphic signature', *GSA Bulletin*, vol. 111, pp. 1517-1536.
- Domack, E. et al. 2001, 'Cruise reveals history of Holocene Larsen Ice Shelf', *Eos*, vol. 82, pp. 13-24.
- Dove, D. et al. 2015, 'Submarine glacial landforms record late Pleistocene ice-sheet dynamics, Inner Hebrides, Scotland', *Quaternary Science Reviews*, vol. 123, pp. 76-90.
- Dowdeswell, J. & Fugelli, E. 2012, 'The seismic architecture and geometry of grounding-zone wedges formed at the marine margins of past ice sheets', *Geological Society of America Bulletin*, vol. 124, pp. 1750-1761.
- Dowdeswell, J. et al. 1994, 'The origin of massive diamicton facies by iceberg-rafting and scouring, Scoresby Sund, East Greenland', *Sedimentology*, vol., 41, pp. 21-35.
- Dowdeswell, J. et al. 1998, 'Glacimarine sedimentary processes and facies on the Polar North Atlantic margins', *Quaternary Science Reviews*, vol. 17, pp. 243-272.
- Dowdeswell, J. et al. 2000, 'An origin for laminated glacimarine sediments through sea-ice build-up and suppressed iceberg rafting', *Sedimentology*, vol. 47, pp. 557-576.
- Dowdeswell, J. et al. 2020, 'Delicate seafloor landforms reveal past Antarctic grounding-line retreat of kilometres per year', *Science*, vol. 368, pp. 1020-1024.
- Dunlop, P. et al. 2010, 'Marine geophysical evidence for ice sheet extension and recession on the Malin Shelf: New evidence for the western limits of the British Irish Ice Sheet', *Marine Geology*, vol. 276, pp. 86-99.
- Dunlop, P. et al. 2011, 'Mapping Ireland's glaciated continental margin using marine geophysical data', *Developments in Earth Surface Processes*, vol. 15, pp. 339-357.
- Duplessy, J-C. et al. 1991, 'Surface salinity reconstruction of the North Atlantic Ocean during the last glacial maximum', *Oceanologica Acta*, vol. 14, pp. 311-324.
- Durand, G. et al. 2011, 'Impact of bedrock description on modelling ice sheet dynamics', *Geophysical Research Letters*, vol. 38, 6 pp.
- Duros, P. et al. 2011, 'Live (stained) benthic foraminifera in the Whittard Canyon, Celtic margin (NE Atlantic)', *Deep-Sea Research I*, vol. 58, pp. 128-146.
- Duros, P. et al. 2014, 'Benthic foraminiferal thanatocoenoses from the Cap-Ferret Canyon area (NE Atlantic): A complex interplay between hydro-sedimentary and biological processes', *Deep Sea Research Part II: Topical Studies in Oceanography*, vol. 104, pp. 145-163.
- Dyke, L. et al. 2014, 'Evidence for the asynchronous retreat of large outlet glaciers in southeast Greenland at the end of the last glaciation', *Quaternary Science Reviews*, vol. 99, pp. 244-259.
- Dyke, L. et al. 2018, 'The deglaciation of coastal areas of southeast Greenland', *The Holocene*, vol. 28, pp. 1535-1544.

- Edwards, P. 1982, 'Ecology and distribution of selected foraminiferal species in the North Minch Channel, northwestern Scotland', in Banner, F. & Lord, A. (eds.), *Aspects of Micropalaeontology*, Springer, Dordrecht, pp. 111-141.
- Eisermann, H. et al. 2020, 'Bathymetry beneath ice shelves of western Dronning Maud Land, East Antarctica, and implications on ice shelf stability', *Geophysical Research Letters*, vol. 47, 10 pp.
- Ellet, D. 1979, 'Some oceanographic features of Hebridean water', *Proceedings of the Royal Society of Edinburgh*, vol. 77B, pp. 61-74.
- Ellet, D. et al. 1986, 'The hydrography of the Rockall Channel – an overview', *Proceedings of the Royal Society of Edinburgh*, vol. 88B, pp. 61-81.
- Elliot, A. et al. 1991, 'Monthly distributions of surface and bottom temperatures in the northwest European shelf seas', *Continental Shelf Research*, vol. 11, pp. 453-466.
- Elverhøi, A. et al. 1980, 'Glacial erosion, sedimentation and microfauna in the inner part of Kongsfjorden, Spitsbergen', *Norsk Polarinstitutt Skrifter*, No. 172, pp. 33-62.
- Elverhøi, A. et al. 1989, 'Glaciomarine sedimentation in the epicontinental seas exemplified by the northern Barents sea', *Marine Geology*, vol. 85, pp. 225-250.
- Evans, D. & Benn, D. 2004, 'Facies description and the logging of sedimentary exposures', in Evans, D. & Benn, D. (eds.), *A practical guide to the study of glacial sediments*, Arnold, London, pp. 11-51.
- Evans, D. et al. 2006, 'Subglacial till: Formation, sedimentary characteristics and classification', *Earth-Science Reviews*, vol. 78, pp. 115-176.
- Evans, D. Ó Cofaigh, C. 2003, 'Depositional evidence for marginal oscillations of the Irish Sea ice stream in southeast Ireland during the last glaciation', *Boreas*, vol. 32, pp. 76-101.
- Evans, J. & Pudsey, C. 2002, 'Sedimentation associated with Antarctic Peninsula ice shelves: implications for palaeoenvironmental reconstructions of glaciomarine sediments', *Journal of the Geological Society, London*, vol. 159, pp. 233-237.
- Evans, J. et al. 2005, 'Late Quaternary glacial history, flow dynamics and sedimentation along the eastern margin of the Antarctic Peninsula Ice Sheet', *Quaternary Science Reviews*, vol. 24, pp. 741-774.
- Evans, W. et al. 2015, 'Bedforms on the northwest Irish shelf: indication of modern active sediment transport and overprinting of paleo-glacial sedimentary deposits', *Journal of Maps*, vol. 11, pp. 561-574.
- Everest, J. et al. 2013, 'New age constraints for the maximum extent of the last British-Irish Ice Sheet (NW Sector)', *Journal of Quaternary Science*, vol. 28, pp. 2-7.
- Eyles, N. 1987, 'Late Pleistocene debris-flow deposits in large glacial lakes in British Columbia and Alaska', *Sedimentary Geology*, vol. 53, pp. 33-71.
- Eyles, N. & McCabe, A. 1989, 'The late Devensian (<22,000 BP) Irish Sea Basin: The sedimentary record of a collapsed ice sheet margin', *Quaternary Science Reviews*, vol. 8, pp. 307-351.
- Eynaud, F. et al. 2002, 'Norwegian sea-surface palaeoenvironments of marine oxygen-isotope stage 3: the paradoxical response of dinoflagellate cysts', *Journal of Quaternary Science*, vol. 17, pp. 349-359.
- Ezat, M. et al. 2014, 'Persistent intermediate water warming during cold stadials in the southeastern Nordic Seas during the past 65 k.y.', *Geology*, vol. 42, pp. 663-666.

- Fannin, N. 1989, *Offshore investigations 1966-87*, British Geological Survey Technical Report WB/89/2, British Geological Survey, Keyworth, 36 pp.
- Fatela, F. & Taborda, R. 2002, 'Confidence limits of species proportions in microfossil assemblages', *Marine Micropalaeontology*, vol. 45, pp. 169-174.
- Fentimen, R. et al. 2018, 'Benthic foraminifera in a deep-sea high-energy environment: the Moira Mounds (Porcupine Seabight, SW of Ireland)', *Swiss Journal of Geosciences*, vol. 111, pp. 561-572.
- Fentimen, R. et al. 2020, 'Impact of bottom waters on benthic foraminiferal assemblages in a cold-water coral environment: The Moira Mounds (NE Atlantic)', *Marine Micropaleontology*, vol. 154, 14 pp.
- Feyling-Hanssen, R. 1972, 'The foraminifer *Elphidium excavatum* (Terquem) and its variant forms', *Micropalaeontology*, vol. 18, pp. 337-354.
- Feyling-Hanssen, R. 1982, 'Foraminiferal zonation of a boring in Quaternary deposits of the northern North Sea', *Bulletin of the Geological Society of Denmark*, vol. 31, pp. 29-47.
- Fisher, R. et al. 1943, 'The relation between the number of species and the number of individuals in a random sample of an animal population', *The Journal of Animal Ecology*, vol. 12, pp. 42-58.
- Fontanier, C. et al. 2002, 'Live benthic foraminiferal faunas from the Bay of Biscay: faunal density, composition, and microhabitats', *Deep-Sea Research Part I*, vol. 49, pp. 751-785.
- Forwick, M & Vorren, T. 2009, 'Late Weichselian and Holocene sedimentary environments and ice rafting in Isfjorden, Spitsbergen', *Palaeogeography, Palaeoclimatology, Palaeoecology*, vol. 280, pp. 258-274.
- Foubert, A. et al. 2005, 'New view of the Belgica Mounds, Porcupine Seabight, NE Atlantic: preliminary results from the *Polarstern* ARK-XIX/3a ROV cruise', in Freiwald, A. & Roberts, J. (eds.), *Deep-water corals and ecosystems*, Springer, Heidelberg, pp. 403-415.
- Foubert, A. et al. 2011, 'The Moira Mounds, small cold-water coral mounds in the Porcupine Seabight, NE Atlantic: Part B-Evaluating the impact of sediment dynamics through high-resolution ROV-borne bathymetric mapping', *Marine Geology*, vol. 282, pp. 65-78.
- Frank, N. et al. 2004, 'Eastern North Atlantic deep-sea corals: tracing upper intermediate water $\Delta^{14}\text{C}$ during the Holocene', *Earth and Planetary Science Letters*, vol. 219, pp. 297-309.
- Fronval, T. et al. 1995, 'Oceanic evidence for coherent fluctuations in Fennoscandian and Laurentide ice sheets on millennial timescales', *Nature*, vol. 374, pp. 443-446.
- Furze, M. et al. 2018, 'Deglaciation and ice shelf development at the northeast margin of the Laurentide Ice Sheet during the Younger Dryas chronozone', *Boreas*, vol. 47, pp. 271-296.
- Fyfe, J. et al. 1993, *The geology of the Malin-Hebrides sea area*, HMSO for the British Geological Survey, London, 108 pp.
- Gandy, N. et al. 2018, 'Marine ice sheet instability and ice shelf buttressing of the Minch Ice Stream, northwest Scotland', *The Cryosphere*, vol. 12, pp. 3635-3651.
- Ganopolski, A. & Rahmstorf, S. 2001, 'Rapid changes of glacial climate simulated in a coupled climate model', *Nature*, vol. 409, pp. 153-158.

- Garcia, X. et al. 2014, 'Constraints on a shallow offshore gas environment determined by a multidisciplinary geophysical approach: The Malin Sea, NW Ireland', *Geochemistry, Geophysics, Geosystems*, vol. 15, pp. 867-885.
- Gibson, T. 1989, 'Planktonic Benthonic Foraminiferal Ratios: Modern Patterns and Tertiary Applicability', *Marine Micropaleontology*, vol. 15, pp. 29-52.
- Gilbert, R. et al. 1990, 'Holocene sedimentary environment of Cambridge Fiord, Baffin Island, Northwest Territories', *Canadian Journal of Earth Sciences*, vol. 27, pp. 271-280.
- Gooday, A. & Jorissen, F. 2012, 'Benthic foraminiferal biogeography: Controls on global distribution patterns in deep-water settings', *Annual Reviews of Marine Science*, vol. 2, pp. 237-262.
- Gooday, A. 2003, 'Benthic foraminifera (Protista) as tools in deep-water palaeoceanography: Environmental influences on faunal characteristics', in Southward, A. et al. (eds.), *Advances in marine biology*, Academic Press, Amsterdam, pp. 1-90.
- Gordon, A. et al. 2002, 'Bay of Bengal nutrient-rich benthic layer', *Deep-Sea Research Part II*, vol. 49, pp. 1411-1421.
- Görlich, K. et al. 1987, 'Suspension settling effect on macrobenthos biomass distribution in Hornsund fjord, Spitsbergen', *Polar Research*, vol. 5, pp. 175-192.
- Gowen, R. et al. 1998, 'Plankton distributions in relation to physical oceanographic features on the southern Malin Shelf, August 1996', *ICES Journal of Marine Science*, vol. 55, pp. 1095-1111.
- Graham, D. et al. 1990, 'The biostratigraphy and chronostratigraphy of BGS Borehole 78/4, North Minch', *Scottish Journal of Geology*, vol. 26, pp. 65-75.
- Greene, C. et al. 2018, 'Seasonal dynamics of Totten Ice Shelf controlled by sea ice buttressing', *The Cryosphere*, vol. 12, pp. 2869-2882.
- Greenwood, S. & Clark, C. 2009, 'Reconstructing the last Irish Ice Sheet 2: a geomorphologically-driven model of ice sheet growth, retreat and dynamics', *Quaternary Science Reviews*, vol. 28, pp. 3101-3123.
- Grimm, E. 1987, 'CONISS: A Fortran 77 program for stratigraphically constrained cluster analysis by the method of incremental sum of squares', *Computers and Geosciences*, vol. 13, pp. 13-35.
- Grimm, E. n.d., 'TiliaIT'. Retrieved 10/05/2020 from <https://www.tiliait.com/>
- Grobe, H. 1987, 'A simple method for the determination of ice-rafted debris in sediment cores', *Polarforschung*, vol. 57, pp. 123-126.
- Grousset, F. et al. 1993, 'Patterns of ice-rafted detritus in the glacial North Atlantic (40-55°N)', *Paleoceanography*, vol. 8, pp. 175-192.
- Haapaniemi, A. et al. 2010, 'Source, timing, frequency and flux of ice-rafted detritus to the Northeast Atlantic margin, 30-12 ka: testing the Heinrich precursor hypothesis', *Boreas*, vol. 39, pp. 576-591.
- Haflidason, H. et al. 1997, 'Marine geological/geophysical cruise report on the western Irish margin: Donegal Bay, Clew Bay, Galway Bay, Irish Shelf and Rockall Trough', University of Bergen, Bergen.
- Hagen, S. & Hald, M. 2002, 'Variation in surface and deep water circulation in the Denmark Strait, North Atlantic, during marine isotope stages 3 and 2', *Paleoceanography*, vol. 17, 16 pp.

- Hald, M. & Korsun, S. 1997, 'Distribution of modern benthic foraminifera from fjords of Svalbard, European Arctic', *Journal of Foraminiferal Research*, vol. 27, pp. 101-122.
- Hald, M. & Vorren, T. 1987, 'Foraminiferal stratigraphy and environment of late Weichselian deposits on the continental shelf off Troms, Northern Norway', *Marine Micropaleontology*, vol. 12, pp. 129-160.
- Hald, M. et al. 1990, 'Middle and late Weichselian stratigraphy in shallow drillings from the southwestern Barents Sea: foraminiferal, amino acid and radiocarbon evidence', *Norsk Geologisk Tidsskrift*, vol. 70, pp. 241-257.
- Hald, M. et al. 1994, 'Recent and late Quaternary distribution of *Elphidium excavatum* f. *clavata* in Arctic seas', *Cushman Foundation Special Publication No. 32*, pp. 141-153.
- Hald, M. et al. 2001, 'Abrupt climatic change during the last interglacial-glacial cycle in the polar North Atlantic', *Marine Geology*, vol. 176, pp. 121-137.
- Hald, M. et al. 2007, 'Variations in temperature and extent of Atlantic Water in the northern North Atlantic during the Holocene', *Quaternary Science Reviews*, vol. 26, pp. 3423-3440.
- Hammer, Ø. 2020, *PAST PAleontological Statistics version 4.02 Reference Manual* (280 pp.). Retrieved 09/05/2020 from <https://folk.uio.no/ohammer/past/past4manual.pdf>
- Hansen, A. & Knudsen, K. 1995, 'Recent foraminiferal distribution in Freemansundet and Early Holocene stratigraphy on Edgeøya, Svalbard', *Polar Research*, vol. 14, pp. 215-238.
- Hansen, B. & Østerhus, J. 2000, 'North Atlantic-Nordic Seas exchanges', *Progress in Oceanography*, vol. 45, pp. 109-208.
- Harbers, A. et al. 2010, 'Short term dynamics of planktonic foraminiferal sedimentation in the Porcupine Seabight', *Micropaleontology*, vol. 56, pp. 259-274.
- Hebbeln, D. et al. 1994, 'Moisture supply for northern ice-sheet growth during the last glacial maximum', *Nature*, vol. 370, pp. 357-360.
- Hebbeln, D. et al. 1998, 'Paleoceanography of the last interglacial/glacial cycle in the polar north Atlantic', *Quaternary Science Reviews*, vol. 17, pp. 125-153.
- Hebbeln, D. et al. 2016, 'Good neighbours shaped by vigorous currents: Cold-water coral mounds and contourites in the North Atlantic', *Marine Geology*, vol. 378, pp. 171-185.
- Hellmer, H. et al. 2012, 'Twenty-first-century warming of a large Antarctic ice-shelf cavity by a redirected coastal current', *Nature*, vol. 485, pp. 225-228.
- Hemer, M. et al. 2007, 'Sedimentological signatures of the sub-Amery Ice Shelf circulation', *Antarctic Science*, vol. 4, pp. 497-506.
- Hemleben, C. et al. 1989, *Modern planktonic foraminifera*, Springer, New York, 362 pp.
- Hesemann, M. 2015, 'The foraminifera.eu database: concept and status', *Palaeontologia Electronica*, vol. 18, pp. 1-14.
- Hess, S. et al. 2005, 'Benthic foraminiferal recovery after recent turbidite deposition in Cap Breton canyon, Bay of Biscay', *Journal of Foraminiferal Research*, vol. 35, pp. 114-129.
- Hibbert, F. 2010, *Dynamics of the British Ice Sheet and Prevailing Hydrographic Conditions for the last 175,000 years: An investigation of marine sediment core MD04-2822 from the Rockall Trough*, PhD thesis, University of St. Andrews, 248 pp.

- Hibbert, F. et al. 2010, 'British Ice Sheet dynamics inferred from north Atlantic ice-rafted debris records spanning the last 175 000 years', *Journal of Quaternary Science*, vol. 25, no. 4, pp. 461-482.
- Hiemstra, J. et al. 2006, 'New evidence for a grounded Irish Sea glaciation of the Isles of Scilly, UK', *Quaternary Science Reviews*, vol. 25, pp. 299-309.
- Hill, A. 1995, 'Leakage of barotropic slope currents onto the continental shelf', *Journal of Physical Oceanography*, vol. 25, pp. 1617-1621.
- Hill, A. 1998, 'The Malin cascade in winter 1996', *Journal of Marine Research*, vol. 56, pp. 87-106.
- Hillenbrand, C-D. et al. 2017, 'West Antarctic Ice Sheet retreat driven by Holocene warm water incursions', *Nature*, vol. 547, pp. 43-48.
- Hillgruber, N. & Kloppmann, M. 1999, 'Distribution and feeding of blue whiting *Micromesistius poutassou* larvae in relation to different water masses in the Porcupine Bank area, west of Ireland', *Marine Ecology Progress Series*, vol. 187, pp. 213-225.
- Hogan, K. et al. 2016, 'Deglaciation of a major palaeo-ice stream in Disko Trough, West Greenland', *Quaternary Science Reviews*, vol. 147, pp. 5-26.
- Holliday, N. 2003, 'Air-sea interaction and circulation changes in the northeast Atlantic', *Journal of Geophysical Research*, vol. 108, 11 pp.
- Holtedahl, H. & Bjerkli, K. 1982, 'Late Quaternary sediments and stratigraphy on the continental shelf off Møre-Trøndelag, W. Norway', *Marine Geology*, vol. 45, pp. 179-226.
- Hopkins, T. 1991, 'The GIN Sea – A synthesis of its physical oceanography and literature review 1972-1985', *Earth-Science Reviews*, vol. 30, pp. 175-318.
- Howe, J. 1996, 'Turbidite and contourite sediment waves in the northern Rockall Trough, North Atlantic Ocean', *Sedimentology*, vol. 43, pp. 219-234.
- Howe, J. et al. 1994, 'Late Cenozoic sediment drift complex, northeast Rockall Trough, North Atlantic', *Paleoceanography*, vol. 9, pp. 989-999.
- Howe, J. et al. 2012, 'Submarine geomorphology and glacial history of the Sea of Hebrides, UK', *Marine Geology*, vol. 315-318, pp. 64-76.
- Huang, W. et al. 1991, 'A satellite and field view of the Irish Shelf front', *Continental Shelf Research*, vol. 11, pp. 543-562.
- Husum, K. & Hald, M. 2012, 'Arctic planktic foraminiferal assemblages: Implications for subsurface temperature reconstructions', *Marine Micropaleontology*, vol. 96-97, pp. 38-47.
- Husum, K. et al. 2015, 'Recent benthic foraminifera in the Arctic Ocean and Kara Sea continental margin', *Arktos*, vol. 1:5, 17 pp.
- Huthnance, J. et al. 2001, 'Physical structures, advection and mixing in the region of Goban Spur', *Deep-Sea Research II*, vol. 48, pp. 2979-3021.
- Huthnance, J. et al. 2009, 'Deep ocean exchange with west-European shelf seas', *Ocean Science*, vol. 5, pp. 621-634.
- Huybers, P. & Wunsch, C. 2009, 'Paleophysical Oceanography with an Emphasis on Transport Rates', *Annual Review of Marine Science*, vol. 2, pp. 1-34.

- Hydes, D. et al. 2004, 'External and internal control of winter concentrations of nutrients (N, P and Si) in north-west European shelf seas', *Estuarine, Coastal and Shelf Science*, vol. 59, pp. 151-161.
- Ireland, H. 1967, 'Preparatory techniques for microfossils and inorganic insoluble residues', *Journal of Paleontology*, vol. 41, p. 523.
- Jackson, S. et al. 2009, 'Ecology and the ratchet of events: Climate variability, niche dimensions, and species distributions', *Proceedings of the National Academy of Sciences of the USA*, vol. 106, pp. 19685-19692.
- Jacobs, S. et al. 2011, 'Stronger ocean circulation and increased melting under Pine Island Glacier ice shelf', *Nature Geoscience*, vol. 4, pp. 519-523.
- Jaeger, J. & Nittrouer, C. 1999, 'Sediment deposition in an Alaskan fjord: Controls on the formation and preservation of sedimentary structures in Icy Bay', *Journal of Sedimentary Research*, vol. 69, pp. 1011-1026.
- Jakobsson, M. et al. 2011, 'Geological record of ice shelf break-up and grounding-line retreat, Pine Island Bay, West Antarctica', *Geology*, vol. 39, pp. 691-694.
- Jansen, E. et al. 1983, 'Late Weichselian paleoceanography of the southeastern Norwegian Sea', *Norsk Geologisk Tidsskrift*, vol. 63, pp. 117-146.
- Jennings, A. & Helgadottir, G. 1994, 'Foraminiferal assemblages from the fjords and shelf of eastern Greenland', *Journal of Foraminiferal Research*, vol. 24, pp. 123-144.
- Jennings, A. & Weiner, N. 1996, 'Environmental change in eastern Greenland during the last 1300 years: evidence from foraminifera and lithofacies in Nansen Fjord, 68°N', *The Holocene*, vol. 6, pp. 179-191.
- Jennings, A. et al. 2004, 'Modern foraminiferal faunas of the southwestern to northern Iceland shelf: Oceanographic and environmental controls', *Journal of Foraminiferal Research*, vol. 34, pp. 180-207.
- Jennings, A. et al. 2014, 'Paleoenvironments during Younger Dryas-Early Holocene retreat of the Greenland Ice Sheet from outer Disko Trough, central west Greenland', *Journal of Quaternary Science*, vol. 29, pp. 27-40.
- Jennings, A. et al. 2017, 'Ocean forcing of Ice Sheet retreat in central west Greenland from LGM to the early Holocene', *Earth and Planetary Science Letters*, vol. 472, pp. 1-13.
- Jennings, A. et al. 2018, 'Baffin Bay paleoenvironments in the LGM and HS1: Resolving the ice-shelf question', *Marine Geology*, vol. 402, pp. 5-16.
- Jennings, A. et al. 2020, 'Modern foraminiferal assemblages in northern Nares Strait; Petermann Fjord, and beneath Petermann ice tongue, NW Greenland', *Arctic, Antarctic and Alpine Research*, vol. 52, pp. 491-511.
- Jernas, P. et al. 2018, 'Annual changes in Arctic fjord environment and modern benthic foraminiferal fauna: Evidence from Kongsfjorden, Svalbard', *Global and Planetary Change*, vol. 163, pp. 119-140.
- Johnsen, S. et al. 1992, 'Irregular glacial interstadials recorded in a new Greenland ice core', *Nature*, vol. 359, pp. 311-313.
- Johnstone, G. & Mykura, W. 1989, *British Regional Geology: The Northern Highlands of Scotland (4th Edition)*, HMSO, London, 219 pp.
- Joint, I. et al. 1986, 'Seasonal production of photosynthetic picoplankton and nanoplankton in the Celtic Sea', *Marine Ecology Progress Series*, vol. 28, pp. 251-258.

- Jonkers, L. et al. 2010, 'A reconstruction of sea surface warming in the northern North Atlantic during MIS 3 ice-rafting events', *Quaternary Science Reviews*, vol. 29, pp. 1791-1800.
- Jorissen, F. et al. 1992, 'Vertical distribution of benthic foraminifera in the northern Adriatic Sea: The relation with the organic flux', *Marine Micropaleontology*, vol. 19, pp. 131-146.
- Jorissen, F. et al. 1995, 'A conceptual model explaining benthic foraminiferal microhabitats', *Marine Micropaleontology*, vol. 26, pp. 3-15.
- Jorissen, F. et al. 2007, 'Paleoceanographical proxies based on deep-sea benthic foraminiferal assemblage characteristics', in Hillaire-Marcel, C. & de Vernal, A. (eds.), *Proxies in Late Cenozoic Paleoceanography: Part 2: Biological tracers and biomarkers*, Elsevier, Amsterdam, pp. 263-326.
- Juggins, S. & Birks, H. 2012, 'Quantitative Environmental Reconstructions from Biological Data', in Birks, H. et al. (eds.), *Tracking environmental change using lake sediments: Data handling and numerical techniques* (Developments in Paleoenvironmental Research vol. 5), Springer, Dordrecht, pp. 431-494.
- Juggins, S. 2016, 'C2 Version 1.7.7', Newcastle University. Retrieved 10/05/2020 from <https://www.staff.ncl.ac.uk/stephen.juggins/software/C2Home.htm>
- Kandiano, E. & Bauch, H. 2002, 'Implications of planktic foraminiferal size fractions for the glacial-interglacial paleoceanography of the polar North Atlantic', *Journal of Foraminiferal Research*, vol. 32, pp. 245-251.
- Kandiano, E. et al. 2004, 'Sea surface temperature variability in the North Atlantic during the last two glacial-interglacial cycles: comparison of faunal, oxygen isotopic, and Mg/Ca-derived records', *Palaeogeography, Palaeoclimatology, Palaeoecology*, vol. 204, pp. 145-164.
- Kaspi, Y. et al. 2004, 'A "triple sea-ice state" mechanism for the abrupt warming and synchronous ice sheet collapses during Heinrich events', *Paleoceanography*, vol. 19, 12 pp.
- Kellogg, T. 1980, 'Paleoclimatology and paleo-oceanography of the Norwegian and Greenland seas: glacial-interglacial contrasts', *Boreas*, vol. 9, pp. 115-137.
- Kenyon, N. et al. 1998, 'The current swept continental slope and giant carbonate mounds to the west of Ireland', in De Mol, B. (ed.), *Geosphere-Biosphere Coupling: Carbonate mud mounds and cold water reefs*, IOC Workshop Report 143, p. 24.
- Kidwell, S. & Flessa, K. 1995, 'The quality of the fossil record: Populations, species, and communities', *Annual Review of Ecology and Systematics*, vol. 26, pp. 269-299.
- Kilfeather, A. et al. 2011, 'Ice-stream retreat and ice-shelf history in Marguerite Trough, Antarctic Peninsula: Sedimentologic and foraminiferal signatures', *Geological Society of America Bulletin*, vol. 123, pp. 997-1015.
- King, E. et al. 1998, 'End moraines on the northwest Irish continental shelf', Abstract from the 3rd ENAM II workshop, Scotland.
- King, E. et al. 2019, 'The impact of waves and tides on residual sand transport on a sediment-poor, energetic and macrotidal continental shelf', *Journal of Geophysical Research: Oceans*, vol. 124, pp. 4974-5002.
- Kleman, J. & Hättestrand, C. 1999, 'Frozen-bed Fennoscandian and Laurentide ice sheets during the Last Glacial Maximum', *Nature*, vol. 402, pp. 63-66.
- Klitgaard-Kristensen, D. & Sejrup, H.-P. 1996, 'Modern benthic foraminiferal biofacies across the northern North Sea', *Sarsia*, vol. 81, pp. 97-106.

- Klitgaard-Kristensen, D. et al. 2002, 'Distribution of recent calcareous benthic foraminifera in the northern North Sea and relation to the environment', *Polar Research*, vol. 21, pp. 275-282.
- Kloppmann, M. et al. 2001, 'The distribution of blue whiting eggs and larvae on Porcupine Bank in relation to hydrography and currents', *Fisheries Research*, vol. 50, pp. 89-109.
- Knies, J. et al. 1999, 'Late Quaternary growth and decay of the Svalbard/Barents Sea ice sheet and paleoceanographic evolution in the adjacent Arctic Ocean', *Geo-Marine Letters*, vol. 18, pp. 195-202.
- Knies, J. & Stein, R. 1998, 'New aspects of organic carbon deposition and its paleoceanographic implications along the northern Barents Sea margin during the last 30,000 years', *Paleoceanography*, vol. 13, pp. 384-394.
- Knutz, P. 2000, *Late Pleistocene glacial fluctuations and palaeoceanography on the continental margin of northwest Britain*, PhD thesis, University of Wales.
- Knutz, P. et al. 2001, 'Millennial-scale depositional cycles related to British Ice Sheet variability and North Atlantic paleocirculation since 45 kyr B.P., Barra Fan, U.K. margin', *Paleoceanography*, vol. 16, no. 1, pp. 53-64.
- Knutz, P. et al. 2002, 'Glacimarine slope sedimentation, contourite drifts and bottom current pathways on the Barra Fan, UK North Atlantic Margin', *Marine Geology*, vol. 188, pp. 129-146.
- Knutz, P. et al. 2007, 'Centennial-scale variability of the British Ice Sheet: Implications for climate forcing and Atlantic meridional overturning circulation during the last deglaciation', *Paleoceanography*, vol. 22, 14 pp.
- Korsun, S. & Hald, M. 1998, 'Modern benthic foraminifera off Novaya Zemlya tidewater glaciers, Russian Arctic', *Arctic and Alpine Research*, vol. 30, pp. 61-77.
- Korsun, S. & Hald, M. 2000, 'Seasonal dynamics of benthic foraminifera in a glacially-fed fjord of Svalbard, European Arctic', *Journal of Foraminiferal Research*, vol. 30, pp. 251-271.
- Korsun, S. et al. 1995, 'Recent foraminifera in glaciomarine sediments from three arctic fjords of Novaya Zemlja and Svalbard', *Polar Research*, vol. 14, pp. 15-32.
- Korsun, S. et al. 2012, 'Freshwater discharge and the distribution of intertidal foraminifera, outer Chupa Inlet, Western White Sea', *Труды Зоологического института РАН Приложение*, No. 2, pp. 235-243.
- Kubischta, F. et al. 2010, 'Late Quaternary foraminiferal record in Murchisonfjorden, Nordaustlandet, Svalbard', *Polar Research*, vol. 29, pp. 283-297.
- Kucera, M. 2007, 'Planktonic foraminifera as tracers of past oceanic environments', *Developments in Marine Geology*, vol. 1, Elsevier, Amsterdam, pp. 213-262
- Kucera, M. et al. 2005, 'Reconstruction of sea-surface temperatures from assemblages of planktonic foraminifera: multi-technique approach based on geographically constrained calibration data sets and its application to glacial Atlantic and Pacific Oceans', *Quaternary Science Reviews*, vol. 24, pp. 951-998.
- Labeyrie, L. & Duplessy, J-C. 1985, 'Changes in the oceanic $^{13}\text{C}/^{12}\text{C}$ ratio during the last 140 000 years: High-latitude surface water records', *Palaeogeography, Palaeoclimatology, Palaeoecology*, vol. 50, pp. 217-240.
- Labeyrie, L. et al. 1992, 'Changes in the vertical structure of the North Atlantic Ocean between glacial and modern times', *Quaternary Science Reviews*, vol. 11, pp. 401-413.

- Lambeck, K. et al. 2014, 'Sea level and global ice volumes from the last glacial maximum to the Holocene', *Proceedings of the National Academy of Sciences of the USA*, vol. 111, pp. 15296-15303.
- Lassen, S. et al. 1999, 'Northeast Atlantic sea surface circulation during the past 30-10 ¹⁴C kyr B.P.', *Paleoceanography*, vol. 14, pp. 616-625.
- Lee, A. & Ramster, J. 1981, *Atlas of the seas around the British Isles*, Ministry of Agriculture, Fisheries and Food, HMSO, Lowestoft, 75 pp.
- Lekens, W. et al. 2005, 'Laminated sediments preceding Heinrich event 1 in the Northern North Sea and Southern Norwegian Sea: Origin, processes and regional linkage', *Marine Geology*, vol. 216, pp. 27-50.
- Lemmen, D. 1990, 'Glaciomarine sedimentation in Disraeli Fiord, High Arctic Canada', *Marine Geology*, vol. 94, pp. 9-22.
- Licht, K. et al. 1999, 'Distinguishing subglacial till and glacial marine diamictos in the western Ross Sea, Antarctica: Implications for a last glacial maximum grounding line', *GSA Bulletin*, vol. 111, pp. 91-103.
- Limoges, A. et al. 2018, 'Linking the modern distribution of biogenic proxies in high Arctic Greenland shelf sediments to sea ice, primary productivity and Arctic-Atlantic inflow', *Journal of Geophysical Research: Biogeosciences*, vol. 123, pp. 760-786.
- Linke, P. & Lutze, G. 1993, 'Microhabitat preferences of benthic foraminifera-a static concept or a dynamic adaptation to optimize food acquisition?', *Marine Micropaleontology*, vol. 20, pp. 215-234.
- Linke, P. 1992, 'Metabolic adaptations of deep-sea benthic foraminifera to seasonally varying food input', *Marine Ecology Progress Series*, vol. 81, pp. 51-63.
- Livingstone, S. et al. 2012, 'Antarctic palaeo-ice streams', *Earth-Science Reviews*, vol. 111, pp. 90-128.
- Lloyd, J. 2006a, 'Modern distribution of benthic foraminifera from Disko Bugt, west Greenland', *Journal of Foraminiferal Research*, vol. 36, pp. 315-331.
- Lloyd, J. 2006b, 'Late Holocene environmental change in Disko Bugt, west Greenland: interaction between climate, ocean circulation and Jakobshavn Isbrae', *Boreas*, vol. 35, pp. 35-49.
- Lloyd, J. et al. 1996, 'Deglaciation history and palaeoceanography of the western Spitsbergen margin since the last glacial maximum', in Austin, J. et al. (eds.), *Late Quaternary Palaeoceanography of the North Atlantic Margins*, Geological Society London Special Publication No. 111, Geological Society, London, pp. 289-301.
- Lloyd, J. et al. 2005, 'Early Holocene palaeoceanography and deglacial chronology of Disko Bugt, West Greenland', *Quaternary Science Reviews*, vol. 24, pp. 1741-1755.
- Lloyd, J. et al. 2011, 'A 100-year record of ocean temperature control on the stability of Jakobshavn Isbrae, West Greenland', *Geological Society of America Bulletin*, vol. 39, pp. 867-870.
- Lo Giudice Capelli, E. & Austin, W. 2019, 'Size matters: Analyses of benthic foraminiferal assemblages across differing size fractions', *Frontiers in Marine Science*, vol. 6, 8 pp.
- Lønne, I. 1997, 'Facies characteristics of a proglacial turbiditic sand-lobe at Svalbard', *Sedimentary Geology*, vol. 109, pp. 13-35.

- Loubere, P. 1991, 'Deep-sea benthic foraminiferal assemblage response to a surface ocean productivity gradient', *Paleoceanography*, vol. 6, pp. 193-204.
- Lowe, A. & Anderson, J. 2002, 'Reconstruction of the West Antarctic ice sheet in Pine Island Bay during the Last Glacial Maximum and its subsequent retreat history', *Quaternary Science Reviews*, vol. 21, pp. 1879-1897.
- Lowe, D. 1982, 'Sediment gravity flows: II: Depositional models with special reference to the deposits of high-density turbidity currents', *Journal of Sedimentary Petrology*, vol. 52, pp. 279-297.
- Lucchi, R. & Rebesco, M. 2007, 'Glacial contourites on the Antarctic Peninsula margin: insight for paleoenvironmental and paleoclimatic conditions', in Viana, A. & Rebesco, M. (eds.), *Economic and Palaeoceanographic Significance of Contourite Deposits*, Geological Society, London, Special Publication No. 276, pp. 111-127.
- Lutze, G. & Coulbourn, W. 1984, 'Recent benthic foraminifera from the continental margin of northwest Africa: Community structure and distribution', *Marine Micropaleontology*, vol. 8, pp. 361-401.
- Mackensen, A. & Douglas, R. 1989, 'Down-core distribution of live and dead deep-water benthic foraminifera in box cores from the Weddell Sea and the California continental border land', *Deep Sea Research Part A*, vol. 36, pp. 879-900.
- Mackensen, A. & Hald, M. 1988, '*Cassidulina teretis* Tappan and *C. laevigata* D'Orbigny: Their modern and late Quaternary distribution in northern seas', *Journal of Foraminiferal Research*, vol. 18, pp. 16-24.
- Mackensen, A. 1997, '„Zur Paläoozeanographie hoher Breiten: Stellvertreterdaten aus Foraminiferen"', *Berichte Polarforschung*, vol. 243, pp. 1-146. (In German).
- Mackensen, A. et al. 1985, 'The distribution of living benthic foraminifera on the continental slope and rise off southwest Norway', *Marine Micropaleontology*, vol. 9, pp. 275-306.
- Mackensen, A. et al. 1993, 'Benthic foraminiferal assemblages from the eastern South Atlantic Polar Front region between 35° and 57°S: Distribution, ecology and fossilization potential', *Marine Micropaleontology*, vol. 22, pp. 33-69.
- Mackiewicz, N. et al. 1984, 'Interlaminated ice-proximal glacial marine sediments in Muir Inlet, Alaska', *Marine Geology*, vol. 57, pp. 113-147.
- Manighetti, B. & McCave, I. 1995, 'Late glacial and Holocene palaeocurrents around Rockall Bank, NE Atlantic Ocean', *Paleoceanography*, vol. 10, pp. 611-626.
- Marcott, S. et al. 2011, 'Ice-shelf collapse from subsurface warming as a trigger for Heinrich events', *Proceedings of the National Academy of Sciences of the United States*, vol. 108, pp. 13415-13419.
- Marienfeld, P. 1992, 'Postglacial sedimentary history of Scoresby Sund, East Greenland', *Polarforschung*, vol. 60, pp. 181-195.
- Marshall, S. & Koutnik, M. 2006, 'Ice sheet action versus reaction: Distinguishing between Heinrich events and Dansgaard-Oeschger cycles in the North Atlantic', *Paleoceanography*, vol. 21, 13 pp.
- Maslin, M. et al. 1995, 'Surface water temperature, salinity, and density changes in the northeast Atlantic during the last 45,000 years: Heinrich events, deep water formation, and climatic rebounds', *Paleoceanography*, vol. 10, pp. 527-544.

- Masson, D. et al. 1989, 'Geology of Porcupine Bank and Goban Spur, northeastern Atlantic – preliminary results of the Cyaporc submersible cruise', *Marine Geology*, vol. 87, pp. 105-119.
- Matthiessen, J. et al. 2010, 'Pleistocene Glacial Marine Sedimentary Environments at the Eastern Mendeleev Ridge, Arctic Ocean', *Polarforschung*, vol. 79, pp. 123-137.
- McCabe, A. et al. 1986, 'Late-Pleistocene tidewater glaciers and glaciomarine sequences from north County Mayo, Republic of Ireland', *Journal of Quaternary Science*, vol. 1, pp. 73-84.
- McCabe, A. et al. 1993, 'Glaciomarine facies from the western sector of the last British Ice Sheet, Malin Beg, County Donegal, Ireland', *Quaternary Science Reviews*, vol. 12, pp. 35-45.
- McCabe, A. et al. 2007a, 'Radiocarbon constraints on readvances of the British-Irish Ice Sheet in the northern Irish Sea Basin during the last deglaciation', *Quaternary Science Reviews*, vol. 26, pp. 1204-1211.
- McCabe, A. et al. 2007b, 'Radiocarbon constraints on the history of the western Irish ice sheet prior to the Last Glacial Maximum', *Geology*, vol. 35, no. 2, pp. 147-150.
- McCarroll, D. 2001, 'Deglaciation of the Irish Sea Basin: a critique of the glaciomarine hypothesis', *Journal of Quaternary Science*, vol. 16, pp. 393-404.
- McCarron, S. et al. 2018, 'A Plio-Pleistocene sediment wedge on the continental shelf west of central Ireland', *Marine Geology*, vol. 399, pp. 97-114.
- McCarthy, D. 2011, *Late Quaternary ice-ocean interactions in central West Greenland*, unpublished PhD thesis, University of Durham, 292 pp.
- McCartney, M. & Talley, L. 1982, 'The subpolar mode water of the North Atlantic Ocean', *Journal of Physical Oceanography*, vol. 12, pp. 1169-1188.
- McCune, B. & Grace, J. 2002, *Analysis of ecological communities*, MJM Software Publishing, Glenenden Beach, Oregon, 300 pp.
- McGonigle, C. et al. 2009, 'Evaluation of image-based multibeam sonar backscatter classification for benthic habitat discrimination and mapping at Stanton Banks, UK', *Estuarine, Coastal and Shelf Science*, vol. 81, pp. 423-437.
- McIntyre, K. & Howe, J. 2009, 'Bottom-current variability during the last glacial-deglacial transition, Northern Rockall Trough and Faroe Bank Channel, NE Atlantic', *Scottish Journal of Geology*, vol. 45, pp. 43-57.
- McMahon, T. et al. 1995, 'Some oceanographic features of northeastern Atlantic waters west of Ireland', *ICES Journal of Marine Science*, vol. 52, pp. 221-232.
- McManus, J. et al. 1999, 'A 0.5-Million-Year record of millennial-scale climate variability in the North Atlantic', *Science*, vol. 283, pp. 971-975.
- Meincke, J. 1986, 'Convection in the oceanic waters west of Britain', *Proceedings of the Royal Society of Edinburgh*, vol. 88B, pp. 127-139.
- Meland, M. et al. 2008, 'Water mass properties and exchange between the Nordic seas and the northern North Atlantic during the period 23-6 ka: Benthic oxygen isotope evidence', *Paleoceanography*, vol. 23, 19 pp.
- Mendes, I. et al. 2004, 'Factors influencing recent benthic foraminifera distribution on the Guadiana shelf (Southwestern Iberia)', *Marine Micropaleontology*, vol. 51, pp. 171-192.

- Mendes, I. et al. 2012, 'Distribution of living benthic foraminifera on the northern Gulf of Cadiz continental shelf', *Journal of Foraminiferal Research*, vol. 42, pp. 18-38.
- Meyers, P. 1997, 'Organic geochemical proxies of paleoceanographic, paleolimnologic, and paleoclimatic processes', *Organic Geochemistry*, vol. 27, pp. 213-250.
- Mignot, J. et al. 2007, 'Atlantic subsurface temperatures: response to a shutdown of the overturning circulation and consequences for its recovery', *Journal of Climate*, vol. 20, pp. 4884-4898.
- Milker, Y. & Schmiedl, G. 2012, 'A taxonomic guide to the benthic shelf foraminifera of the western Mediterranean Sea', *Palaeontologia Electronica*, vol. 15, 134 pp.
- Milker, Y. et al. 2009, 'Distribution of recent benthic foraminifera in shelf carbonate environments of the Western Mediterranean Sea', *Marine Micropaleontology*, vol. 73, pp. 207-225.
- Minzoni, R. et al. 2017, 'Oceanographic influences on the stability of the Cosgrove Ice Shelf, Antarctica', *The Holocene*, vol. 27, pp. 1645-1658.
- Mohn, C. & Beckmann, A. 2002, 'Numerical studies on flow amplification at an isolated shelfbreak bank, with application to Porcupine Bank', *Continental Shelf Research*, vol. 22, pp. 1325-1338.
- Mohn, C. & White, M. 2007, 'Remote sensing and modelling of bio-physical distribution patterns at Porcupine and Rockall Bank, Northeast Atlantic', *Continental Shelf Research*, vol. 27, pp. 1875-1892.
- Mohn, C. et al. 2002, 'Observations of the mass and flow field at Porcupine Bank', *ICES Journal of Marine Science*, vol. 59, pp. 380-392.
- Mojtahid, M. et al. 2005, 'Palaeoclimatology and palaeohydrography of the glacial stages on Celtic and Armorican margins over the last 360 000 yrs', *Marine Geology*, vol. 224, pp. 57-82.
- Mojtahid, M. et al. 2017, 'Changes in northeast Atlantic hydrology during Termination 1: Insights from Celtic margin's benthic foraminifera', *Quaternary Science Reviews*, vol. 175, pp. 45-59.
- Moodley, L. et al. 1997, 'Differential response of benthic meiofauna to anoxia with special reference to Foraminifera (Protista: Sarcodina)', *Marine Ecology Progress Series*, vol. 15B, pp. 151-163.
- Moodley, L. et al. 2005, 'Similar response to phytodetritus deposition in shallow and deep-sea sediments', *Journal of Marine Research*, vol. 63, pp. 457-469.
- Morlighem, M. et al. 2017, 'BedMachine v3: Complete bed topography and ocean bathymetry mapping of Greenland from multibeam echo sounding combined with mass conservation', *Geophysical Research Letters*, vol. 44, pp. 11051-11061.
- Moros, M. et al. 2002, 'Were glacial iceberg surges in the North Atlantic triggered by climate warming?', *Marine Geology*, vol. 192, pp. 393-417.
- Mouginot, J. et al. 2015, 'Fast retreat of Zachariæ Isstrøm, northeast Greenland', *Science*, vol. 350, pp. 1357-1361.
- Mudie, P. et al. 1984, 'Multivariate analysis and quantitative paleoecology of benthic foraminifera in surface and late Quaternary shelf sediments, northern Canada', *Marine Micropaleontology*, vol. 8, pp. 283-313.

- Müller, J. & Stein, R. 2014, 'High-resolution record of late glacial and deglacial sea ice changes in Fram Strait corroborates ice-ocean interactions during abrupt climate shifts', *Earth and Planetary Science Letters*, vol. 403, pp. 446-455.
- Murgese, D. & De Deckker, P. 2005, 'The distribution of deep-sea benthic foraminifera in core tops from the eastern Indian Ocean', *Marine Micropaleontology*, vol. 56, pp. 25-49.
- Murray, J. & Alve, E. 1999, 'Taphonomic experiments on marginal marine foraminiferal assemblages: how much information is preserved?', *Palaeogeography, Palaeoclimatology, Palaeoecology*, vol. 149, pp. 183-197.
- Murray, J. & Alve, E. 2016, 'Benthic foraminiferal biogeography in NW European fjords: A baseline for assessing future change', *Estuarine, Coastal and Shelf Science*, vol. 181, pp. 218-230.
- Murray, J. & Pudsey, C. 2004, 'Living (stained) and dead foraminifera from the newly ice-free Larsen Ice Shelf, Weddell Sea, Antarctica: ecology and taphonomy', *Marine Micropaleontology*, vol. 53, pp. 67-81.
- Murray, J. 1976, 'A method of determining proximity of marginal seas to an ocean', *Marine Geology*, vol. 22, pp. 103-119.
- Murray, J. 1979, *British nearshore foraminiferids: keys and notes for the identification of the species*, Academic Press, London, 69 pp.
- Murray, J. 1982, 'Benthic foraminifera: The validity of living, dead or total assemblages for the interpretation of palaeoecology', *Journal of Micropaleontology*, vol. 1, pp. 137-140.
- Murray, J. 1985, 'Recent Foraminifera from the North Sea (Forties and Ekofisk areas) and the continental shelf west of Scotland', *Journal of Micropaleontology*, vol. 4, pp. 117-125.
- Murray, J. 1985, 'Recent foraminifera from the North Sea (Forties and Ekofisk areas) and the continental shelf west of Scotland', *Journal of Micropaleontology*, vol. 4, pp. 117-125.
- Murray, J. 1991, *Ecology and Palaeoecology of Benthic Foraminifera*, Longman, Harlow, 397 pp.
- Murray, J. 2001, 'The niche of benthic foraminifera, critical thresholds and proxies', *Marine Micropaleontology*, vol. 41, pp. 1-7.
- Murray, J. 2003a, 'An illustrated guide to the benthic foraminifera of the Hebridean Shelf, West of Scotland, with notes on their mode of life', *Palaeontology Electronica*, vol. 5, 31 pp.
- Murray, J. 2003b, 'Foraminiferal assemblage formation in depositional sinks on the continental shelf west of Scotland', *Journal of Foraminiferal Research*, vol. 33, pp. 101-121.
- Murray, J. 2004, 'The Holocene palaeoceanographic history of Muck Deep, Hebridean shelf, Scotland: has there been a change in wave climate in the past 12 000 years?', *Journal of Micropaleontology*, vol. 23, pp. 153-161.
- Murray, J. 2006, *Ecology and Applications of Benthic Foraminifera*, Cambridge University Press, Cambridge, 426 pp.
- Murray, J. et al. 1982, 'Suspended load transport of foraminiferal tests in a tide- and wave-swept sea', *Journal of Foraminiferal Research*, vol. 12, pp. 51-65.
- Nemec, W. & Steel, R. 1984, 'Alluvial and coastal conglomerates: their significant features and some comments on gravelly mass-flow deposits', in Koster, E. & Steel, R. (eds.), *Sedimentology of gravels and conglomerates*, Canadian Society of Petroleum Geologists Memoir 10, pp. 1-31.

- New, A. & Smythe-Wright, D. 2001, 'Aspects of circulation in the Rockall Trough', *Continental Shelf Research*, vol. 21, pp. 777-810.
- Nielsen, M. et al. 2010, 'Water masses in Kangerlussuaq, a large fjord in West Greenland: the processes of formation and the associated foraminiferal fauna', *Polar Research*, vol. 29, pp. 159-175.
- Nigam, R. et al. 1992, 'Can benthic foraminiferal morpho-groups be used as indicators of paleomonsoonal precipitation?', *Estuarine, Coastal and Shelf Science*, vol. 34, pp. 533-542.
- Nørgaard-Pedersen, N. et al. 2003, 'Arctic Ocean during the Last Glacial Maximum: Atlantic and polar domains of surface water mass distribution and ice cover', *Paleoceanography*, vol. 18, 19 pp.
- Ó Cofaigh, C. & Dowdeswell, J. 2001, 'Laminated sediments in glacial marine environments: diagnostic criteria for their interpretation', *Quaternary Science Reviews*, vol. 20, pp. 1411-1436.
- Ó Cofaigh, C. & Evans, D. 2001a, 'Deforming bed conditions associated with a major ice stream of the last British ice sheet', *Geology*, vol. 29, pp. 795-798.
- Ó Cofaigh, C. & Evans, D. 2001b, 'Sedimentary evidence for deforming bed conditions associated with a grounded Irish Sea glacier, southern Ireland', *Journal of Quaternary Science*, vol. 16, pp. 435-454.
- Ó Cofaigh, C. & Evans, D. 2007, 'Radiocarbon constraints on the age of the maximum advance of the British-Irish Ice Sheet in the Celtic Sea', *Quaternary Science Reviews*, vol. 26, pp. 1197-1203.
- Ó Cofaigh, C. et al. (submitted 2020 to *Journal of Quaternary Science*), 'Timing and pace of ice-sheet withdrawal across the marine-terrestrial transition west of Ireland during the last glaciation'.
- Ó Cofaigh, C. et al. 2002, 'Sediment reworking on high-latitude continental margins and its implications for palaeoceanographic studies: insights from the Norwegian-Greenland Sea', in Dowdeswell, J. & Ó Cofaigh, C. (eds.), *Glacier-Influenced Sedimentation on High-Latitude Continental Margins*, Geological Society, London, Special Publication No. 203, London, pp. 325-348.
- Ó Cofaigh, C. et al. 2004, 'Timing and significance of glacially-influenced mass-wasting in the submarine channels of the Greenland Basin', *Marine Geology*, vol. 207, pp. 39-54.
- Ó Cofaigh, C. et al. 2005, 'Flow dynamics and till genesis associated with a marine-based Antarctic palaeo-ice stream', *Quaternary Science Reviews*, vol. 24, pp. 709-740.
- Ó Cofaigh, C. et al. 2008, 'Geological constraints on Antarctic palaeo-ice-stream retreat', *Earth Surface Processes and Landforms*, vol. 33, pp. 513-525.
- Ó Cofaigh, C. et al. 2012a, 'Late Pleistocene chronostratigraphy and ice-sheet limits, southern Ireland', *Quaternary Science Reviews*, vol. 44, pp. 160-179.
- Ó Cofaigh, C. et al. 2012b, 'Marine geophysical evidence for late Pleistocene ice sheet extent and recession off northwest Ireland', *Quaternary Science Reviews*, vol. 44, pp. 147-159.
- Ó Cofaigh, C. et al. 2015, 'Reconstructing the last British-Irish Ice Sheet from continental shelf records: initial results from BRITICE-CHRONO', *Geophysical Research Abstracts*, vol. 17, EGU2015-3567.

- Ó Cofaigh, C. et al. 2019, 'Early deglaciation of the British-Irish Ice Sheet on the Atlantic shelf northwest of Ireland driven by glacioisostatic depression and high relative sea level', *Quaternary Science Reviews*, vol. 208, pp. 76-96.
- Oppo, D. & Lehman, S. 1993, 'Mid-depth circulation of the subpolar North Atlantic during the last glacial maximum', *Science*, vol. 259, pp. 1148-1152.
- Orvik, K. & Niiler, P. 2002, 'Major pathways of Atlantic water in the northern North Atlantic and Nordic Seas toward Arctic', *Geophysical Research Letters*, vol. 29, 4 pp.
- Ottens, J. 1991, 'Planktic foraminifera as North Atlantic water mass indicators', *Oceanologica Acta*, vol. 14, pp. 123-140.
- Ouellet-Bernier, M-M. et al. 2014, 'Paleoceanographic changes in the Disko Bugt area, West Greenland, during the Holocene', *The Holocene*, vol. 24, pp. 1573-1583.
- Øvebrø, L. et al. 2005, 'Temporal and spatial variations in Late Quaternary slope sedimentation along the undersupplied margins of the Rockall Trough, offshore western Ireland', *Norwegian Journal of Geology*, vol. 85, pp. 279-294.
- Øvebrø, L. et al. 2006, 'A record of fluctuating bottom currents on the slopes west of the Porcupine Bank, offshore Ireland – implications for Late Quaternary climate forcing', *Marine Geology*, vol. 225, pp. 279-309.
- Overpeck, J. et al. 2006, 'Paleoclimatic evidence for future ice-sheet instability and rapid sea-level rise', *Science*, vol. 311, pp. 1747-1750.
- Ovsepyan, Y. & Taldenkova, E. 2019, 'Distribution patterns and morphology of *Islandiella norcrossi* (Cushman) in the Upper Quaternary deposits of the Laptev Sea', *Palaeontological Journal*, vol. 53, pp. 15-23.
- Paillard, D. & Labeyrie, L. 1994, 'Role of thermohaline circulation in the abrupt warming after Heinrich events', *Nature*, vol. 372, pp. 162-164.
- Palmer, M. 1993, 'Putting things in even better order: The advantages of canonical correspondence analysis', *Ecology*, vol. 74, pp. 2215-2230.
- Patton, H. et al. 2017, 'Rapid marine deglaciation: asynchronous retreat dynamics between the Irish Sea Ice Stream and terrestrial outlet glaciers', *Earth Surface Dynamics*, vol. 1, pp. 53-65.
- Peck, V. et al. 2006, 'High resolution evidence for linkages between NW European ice sheet instability and Atlantic Meridional Overturning Circulation', *Earth and Planetary Science Letters*, vol. 243, pp. 476-488.
- Peck, V. et al. 2007a, 'Progressive reduction in NE Atlantic intermediate water ventilation prior to Heinrich events: Response to NW European ice sheet instabilities?', *Geochemistry Geophysics Geosystems*, vol. 8, 11 pp.
- Peck, V. et al. 2007b, 'The relationship of Heinrich events and their European precursors over the past 60 ka BP: a multi-proxy ice-rafted debris provenance study in the North East Atlantic', *Quaternary Science Reviews*, vol. 26, pp. 862-875.
- Peck, V. et al. 2008, 'Millennial-scale surface and subsurface paleothermometry from the northeast Atlantic, 55-8 ka BP', *Paleoceanography*, vol. 23, 11 pp.
- Pendlebury, D. & Dobson, M. 1976, 'Sediment and macrofaunal distributions in the eastern Malin Sea, as determined by side-scan sonar and sampling', *Scottish Journal of Geology*, vol. 11, pp. 315-332.

- Perner, K. et al. 2012, 'Holocene palaeoceanographic evolution off West Greenland', *The Holocene*, vol. 23, pp. 374-387.
- Perner, K. et al. 2015, 'Mid to late Holocene strengthening of the East Greenland Current linked to warm subsurface Atlantic water', *Quaternary Science Reviews*, vol. 129, pp. 296-307.
- Peters, C. et al. 2008, 'Magnetic signature of European margin sediments: Provenance of ice-rafted debris and the climatic response of the British ice sheet during Marine Isotope Stages 2 and 3', *Journal of Geophysical Research*, vol. 113, 16 pp.
- Peters, J. et al. 2015, 'Maximum extent and dynamic behaviour of the last British-Irish Ice Sheet west of Ireland', *Quaternary Science Reviews*, vol. 128, pp. 48-68.
- Peters, J. et al. 2016, 'Sedimentology and chronology of the advance and retreat of the last British-Irish Ice Sheet on the continental shelf west of Ireland', *Quaternary Science Reviews*, vol. 140, pp. 101-124.
- Peters, J. et al. 2020, 'Sedimentary and foraminiferal records of Late Quaternary environmental change west of Ireland and implications for the last British-Irish Ice Sheet', *Journal of Quaternary Science*, vol. 35, pp. 609-624.
- Pflaumann, U. et al. 2003, 'Glacial North Atlantic: Sea-surface conditions reconstructed by GLAMAP 2000', *Paleoceanography*, vol. 18, 38 pp.
- Phleger, F. 1964, 'Foraminiferal ecology and marine geology', *Marine Geology*, vol. 1, pp. 16-43.
- Pingree, R. & Griffiths, D. 1979, 'Sand transport paths around the British Isles resulting from M₂ and M₄ tidal interactions', *Journal of the Marine Biological Association of the United Kingdom*, vol. 59, pp. 497-513.
- Pingree, R. & Le Cann, B. 1989, 'Celtic and Armorican slope and shelf residual currents', *Progress in Oceanography*, vol. 23, pp. 303-338.
- Pingree, R. et al. 1978, 'The effects of vertical stability on phytoplankton distributions in the summer on the northwest European shelf', *Deep-Sea Research*, vol. 25, pp. 1011-1028.
- Plets, R. et al. 2015, 'Late Quaternary evolution and sea-level history of a glaciated marine embayment, Bantry Bay, SW Ireland', *Marine Geology*, vol. 369, pp. 251-272.
- Pollard, R. et al. 1996, 'Vivaldi 1991 - A study of the formation, circulation and ventilation of Eastern North Atlantic Central Water'.
- Polovodova, I. et al. 2009, 'Recent benthic foraminifera in the Flensburg Fjord (Western Baltic Sea)', *Journal of Micropalaeontology*, vol. 28, pp. 131-142.
- Pomeroy, L. et al. 1991, 'Bacterial responses to temperature and substrate concentration during the Newfoundland spring bloom', *Marine Ecology Progress Series*, vol. 75, pp. 143-159.
- Porter, D. et al. 2014, 'Bathymetric control of tidewater glacier mass loss in northwest Greenland', *Earth and Planetary Science Letters*, vol. 401, pp. 40-46.
- Porter, D. et al. 2018, 'Identifying spatial variability in Greenland's outlet glacier response to ocean heat', *Frontiers in Earth Science*, vol. 6.
- Powell, R. 1984, 'Glacimarine processes and inductive lithofacies modelling of ice shelf and tidewater glacier sediments based on Quaternary examples', *Marine Geology*, vol. 57, pp. 1-52.

- Powell, R. et al. 1996, 'Observations of the grounding-line area at a floating glacier terminus', *Annals of Glaciology*, vol. 22, pp. 217-223.
- Praeg, D. et al. 2015, 'Ice sheet extension to the Celtic Sea shelf edge at the Last Glacial Maximum', *Quaternary Science Reviews*, vol. 111, pp. 107-112.
- Preston, J. 2009, 'Automated acoustic seabed classification of multibeam images of Stanton Banks', *Applied Acoustics*, vol. 70, pp. 1277-1287.
- Principato, S. 2004, 'X-ray radiographs of sediment cores: a guide to analyzing diamicton', in Francis, P. (ed.), *Image analysis, sediments and paleoenvironments*, Kluwer Academic Publishers, Dordrecht, pp. 165-185.
- Principato, S. et al. 2005, 'Glacial-marine or subglacial origin of diamicton units from the Southwest and North Iceland shelf: Implications for the glacial history of Iceland', *Journal of Sedimentary Research*, vol. 75, pp. 968-983.
- Pritchard, H. et al. 2009, 'Extensive dynamic thinning on the margins of the Greenland and Antarctic ice sheets', *Nature*, vol. 461, pp. 971-975.
- Pritchard, H. et al. 2012, 'Antarctic ice-sheet loss driven by basal melting of ice shelves', *Nature*, vol. 484, pp. 502-505.
- Qvale, G. 1986, 'Distribution of benthic foraminifers in surface sediments along the Norwegian continental shelf between 62° and 72°N', *Norsk Geologisk Tidsskrift*, vol. 66, pp. 209-221.
- Rahmstorf, S. 2003, 'Timing of abrupt climate change: A precise clock', *Geophysical Research Letters*, vol. 30, 4 pp.
- Rasmussen, T. & Thomsen, E. 2004, 'The role of the North Atlantic Drift in the millennial timescale glacial climate fluctuations', *Palaeogeography, Palaeoclimatology, Palaeoecology*, vol. 210, pp. 101-116.
- Rasmussen, T. & Thomsen, E. 2008, 'Warm Atlantic surface water inflow to the Nordic seas 34-10 calibrated ka B.P.', *Paleoceanography*, vol. 23, 13 pp.
- Rasmussen, T. & Thomsen, E. 2015, 'Palaeoceanographic development in Storfjorden, Svalbard, during the deglaciation and Holocene: evidence from benthic foraminiferal records', *Boreas*, vol. 44, pp. 24-44.
- Rasmussen, T. et al. 1996a, 'Circulation changes in the Faeroe-Shetland Channel correlating with cold events during the last glacial period (58-10 ka)', *Geology*, vol. 24, pp. 937-940.
- Rasmussen, T. et al. 1996b, 'Rapid changes in surface and deep water conditions at the Faeroe Margin during the last 58,000 years', *Paleoceanography*, vol. 11, pp. 757-771.
- Rasmussen, T. et al. 1999, 'Climate records and changes in deep outflow from the Norwegian Sea ~ 150-55 ka', *Terra Nova*, vol. 11, pp. 61-66.
- Rasmussen, T. et al. 2002, 'Millennial-scale glacial variability versus Holocene stability: changes in planktic and benthic foraminifera faunas and ocean circulation in the North Atlantic during the last 60 000 years', *Marine Micropaleontology*, vol. 47, pp. 143-176.
- Rasmussen, T. et al. 2003, 'Deep sea records from the southeast Labrador Sea: Ocean circulation changes and ice-rafting events during the last 160,000 years', *Paleoceanography*, vol. 18, 15 pp.
- Rasmussen, T. et al. 2012, 'Reconstruction of inflow of Atlantic Water to Isfjorden, Svalbard during the Holocene: Correlation to climate and seasonality', *Marine Micropaleontology*, vol. 94-95, pp. 80-90.

- Rasmussen, T. et al. 2014, 'Water mass exchange between the Nordic seas and the Arctic Ocean on millennial timescale during MIS 4-MIS 2', *Geochemistry Geophysics Geosystems*, vol. 15, pp. 530-540.
- Rasmussen, T. et al. 2016, 'North Atlantic warming during Dansgaard-Oeschger events synchronous with Antarctic warming and out-of-phase with Greenland climate', *Scientific Reports*, vol. 6, 11 pp.
- Read, H. et al. 1926, *The Geology of Strath Oykeil and Lower Loch Shin*, Memoir of the Geological Survey of Scotland, HMSO, London, 224 pp.
- Reeh, N. et al. 2001, 'Sea ice and the stability of north and northeast Greenland floating glaciers', *Annals of Glaciology*, vol. 33, pp. 474-480.
- Rignot, E. et al. 2012, 'Spreading of warm ocean waters around Greenland as a possible cause for glacier acceleration', *Annals of Glaciology*, vol. 53, pp. 257-266.
- Rignot, E. et al. 2016, 'Bathymetry data reveal glaciers vulnerable to ice-ocean interaction in Uummannaq and Vaigat glacial fjords, west Greenland', *Geophysical Research Letters*, vol. 43, pp. 2667-2674.
- Rijsdijk, K. et al. 2010, 'The glacial sequence at Killiney, SE Ireland: terrestrial deglaciation and polyphase glacitectonic deformation', *Quaternary Science Reviews*, vol. 29, pp. 696-719.
- Robel, A. 2017, 'Thinning sea ice weakens buttressing force of iceberg mélange and promotes calving', *Nature Communications*, vol. 8, pp. 1-7.
- Roberts, D. et al. 2020, 'The deglaciation of the western sector of the Irish Ice Sheet from the inner continental shelf to its terrestrial margin', *Boreas*, pp. 438-460.
- Roberts, J. et al. (2005), 'Monitoring environmental variability around cold-water coral reefs: the use of a benthic photolander and the potential of seafloor observatories', in Freiwald, A. & Roberts, J. (eds.), *Cold-water corals and ecosystems*, Springer, Heidelberg, pp. 483-502.
- Rüggeberg, A. et al. 2007, 'Environmental changes and growth history of a cold-water carbonate mound (Propeller Mound, Porcupine Seabight)', *International Journal of Earth Sciences*, vol. 96, pp. 57-72.
- Rüther, D. et al. 2012, 'Pattern and timing of the northwestern Barents Sea Ice Sheet deglaciation and indications of episodic Holocene deposition', *Boreas*, vol. 41, pp. 494-512.
- Rydningen, T. et al. 2013, 'The marine-based NW Fennoscandian ice sheet: glacial and deglacial dynamics as reconstructed from submarine landforms', *Quaternary Science Reviews*, vol. 68, pp. 126-141.
- Rytter, F. et al. 2002, 'Modern distribution of benthic foraminifera on the north Icelandic shelf and slope', *Journal of Foraminiferal Research*, vol. 32, pp. 217-244.
- Sacchetti, F. et al. 2012, 'Deep-water geomorphology of the glaciated Irish margin from high-resolution marine geophysical data', *Marine Geology*, vol. 291-294, pp. 113-131.
- Sadatzki, H. et al. 2019, 'Sea ice variability in the southern Norwegian Sea during glacial Dansgaard-Oeschger climate cycles', *Science Advances*, vol. 5, 10 pp.
- Sarnthein, M. et al. 1994, 'Changes in east Atlantic deepwater circulation over the last 30,000 years: Eight time slice reconstructions', *Paleoceanography*, vol. 9, pp. 209-267.
- Sarnthein, M. et al. 1995, 'Variations in Atlantic surface ocean paleoceanography, 50°-80°N: A time-slice record of the last 30,000 years', *Paleoceanography*, vol. 10, pp. 1063-1094.

- Sarnthein, M. et al. 2000, 'Fundamental modes and abrupt changes in North Atlantic circulation and climate over the last 60 ky – concepts, reconstruction and numerical modelling', in Schäfer, P. et al. (eds.), *The Northern North Atlantic: A Changing Environment*, Springer, Berlin, pp. 365-410.
- Schafer, C. & Cole, F. 1986, 'Reconnaissance Survey of Benthic Foraminifera from Baffin Island Fiord Environments', *Arctic*, vol. 39, pp. 232-239.
- Schaffer, J. et al. 2017, 'Warm water pathways toward Nioghalvfjærdsfjorden Glacier, Northeast Greenland', *Journal of Geophysical Research: Oceans*, vol. 122, pp. 4004-4020.
- Schaffer, J. et al. 2020, 'Bathymetry constrains ocean heat supply to Greenland's largest glacier tongue', *Nature Geoscience*, vol. 13, pp. 227-231.
- Schiebel, R. & Hemleben, C. 2000, 'Interannual variability of planktonic foraminiferal populations and test flux in the eastern North Atlantic Ocean (JGOFS)', *Deep-Sea Research Part II*, vol. 47, pp. 1809-1852.
- Schiebel, R. et al. 2017, 'Modern planktic foraminifers in the high-latitude ocean', *Marine Micropaleontology*, vol. 136, pp. 1-13.
- Schmiedl, G. et al. 1997, 'Recent benthic foraminifera from the eastern South Atlantic Ocean: Dependence on food supply and water masses', *Marine Micropaleontology*, vol. 32, pp. 249-287.
- Schmuker, B. 2000, 'The influence of shelf vicinity on the distribution of planktic foraminifera south of Puerto Rico', *Marine Geology*, vol. 166, pp. 125-143.
- Schnitker, D. 1979, 'The deep waters of the western north Atlantic during the past 24,000 years, and the re-initiation of the western boundary undercurrent', *Marine Micropalaeontology*, vol. 4, pp. 265-280.
- Schönfeld, J. 1997, 'The impact of Mediterranean Outflow Water (MOW) on benthic foraminiferal assemblages and surface sediments at the southern Portuguese continental margin', *Marine Micropaleontology*, vol. 29, pp. 211-236.
- Schönfeld, J. 1997, 'The impact of the Mediterranean Outflow Water (MOW) on benthic foraminiferal assemblages and surface sediments at the southern Portuguese continental margin', *Marine Micropaleontology*, vol. 29, pp. 211-236.
- Schönfeld, J. 2002, 'Recent benthic foraminiferal assemblages in deep high-energy environments from the Gulf of Cadiz (Spain)', *Marine Micropaleontology*, vol. 44, pp. 141-162.
- Schönfeld, J. et al. 2011, 'Recent benthic foraminiferal assemblages from cold-water coral mounds in the Porcupine Seabight', *Facies*, vol. 57, pp. 187-213.
- Schröder, C. et al. 1987, 'Can smaller benthic foraminifera be ignored in paleoenvironmental analyses?', *Journal of Foraminiferal Research*, vol. 17, pp. 101-105.
- Schröder-Adams, C. et al. 1990, 'Recent Arctic shelf foraminifera: Seasonally ice-covered vs. perennially ice-covered areas', *Journal of Foraminiferal Research*, vol. 20, pp. 8-36.
- Schulz, M. 2002, 'On the 1470-year pacing of Dansgaard-Oeschger warm events', *Paleoceanography*, vol. 17, 9 pp.
- Schweizer, M. et al. 2011, 'Molecular identification of *Ammonia* and *Elphidium* species (Foraminifera, Rotaliida) from the Kiel Fjord (SW Baltic Sea) with rDNA sequences', *Helgoland Marine Research*, vol. 65, pp. 1-10.
- Scoffin, T. & Bowes, G. 1988, 'The facies distribution of carbonate sediments on Porcupine Bank, northeast Atlantic', *Sedimentary Geology*, vol. 60, pp. 125-134.

- Scott, D. & Medioli, F. 1980, 'Living vs. Total Foraminiferal Populations: Their Relative Usefulness in Paleoecology', *Journal of Paleontology*, vol. 54, pp. 814-831.
- Scott, S. et al. 1991, 'Quaternary marine deposits of the Springdale – Hall's Bay area, Newfoundland', *Atlantic Geology*, vol. 27, pp. 181-191.
- Scourse, J. et al. 1990, 'Sedimentology and micropalaeontology of glacial marine sediments from the Central and Southwestern Celtic Sea', in Dowdeswell, J. & Scourse, J. (eds.), *Glacial Marine Environments: Processes and sediments*, Geological Society Special Publication No 53, pp. 329-347.
- Scourse, J. et al. 2009, 'Growth, dynamics and deglaciation of the last British-Irish ice sheet: the deep-sea ice-rafted detritus record', *Quaternary Science Reviews*, vol. 28, pp. 3066-3084.
- Scourse, J. et al. 2019, 'Advance and retreat of the marine-terminating Irish Sea Ice Stream into the Celtic Sea during the Last Glacial: Timing and maximum extent', *Marine Geology*, vol. 412, pp. 53-68.
- Seale, A. et al. 2011, 'Ocean forcing of the Greenland Ice Sheet: Calving fronts and patterns of retreat identified by automatic satellite monitoring of eastern outlet glaciers', *Journal of Geophysical Research*, vol. 116, 16 pp.
- Seidenkrantz, M. 1995, '*Cassidulina teretis* Tappan and *Cassidulina neoteretis* new species (Foraminifera): stratigraphic markers for deep sea and outer shelf areas', *Journal of Micropalaeontology*, vol. 14, pp. 145-157.
- Seidenkrantz, M.-S. 2013, 'Benthic foraminifera as palaeo sea-ice indicators in the subarctic realm – examples from the Labrador Sea-Baffin Bay region', *Quaternary Science Reviews*, vol. 79, pp. 135-144.
- Seidenkrantz, M.-S. et al. 2013, 'Early Holocene large-scale meltwater discharge from Greenland documented by foraminifera and sediment parameters', *Palaeogeography, Palaeoclimatology, Palaeoecology*, vol. 391, pp. 71-81.
- Sejrup, H-P. et al. 2004, 'Benthonic foraminiferal distributions and quantitative transfer functions for the northwest European continental margin', *Marine Micropaleontology*, vol. 53, pp. 197-226.
- Selby, I. 1989, *The Quaternary geology of the Hebridean continental margin*, unpublished PhD thesis, The University of Nottingham.
- Sen Gupta, B. & Machain-Castillo, M. 1993, 'Benthic foraminifera in oxygen-poor habitats', *Marine Micropaleontology*, vol. 20, pp. 183-201.
- Shaffer, G. et al. 2004, 'Ocean subsurface warming as a mechanism for coupling Dansgaard-Oeschger climate cycles and ice-rafting events', *Geophysical Research Letters*, vol. 31, 4 pp.
- Shakesby, R. et al. 2000, 'Foraminifera from the glacial deposits at Broughton Bay, South Wales: a further test of the glaciomarine model of deglaciation of the Irish Sea', *Proceedings of the Geologists' Association*, vol. 111, pp. 147-152.
- Sheldon, C. et al. 2016, 'Ice stream retreat following the LGM and onset of the west Greenland current in Uummannaq Trough, west Greenland', *Quaternary Science Reviews*, vol. 147, pp. 27-46.
- Shipp, S. et al. 2002, 'Retreat signature of a polar ice stream: sub-glacial geomorphic features and sediments from the Ross Sea', in Dowdeswell, J. & Ó Cofaigh, C. (eds.), *Glacier-*

- Influenced Sedimentation on High-Latitude Continental Margins*, Geological Society, London, Special Publication No. 203, pp. 277-304.
- Siddall, M. et al. 2008, 'Marine isotope stage 3 sea level fluctuations: Data synthesis and new model outlook', *Reviews of Geophysics*, vol. 46, 29 pp.
- Simpson, E. 1949, 'Measurement of diversity', *Nature*, vol. 163, p. 688.
- Simpson, J. & Pingree, D. 1978, 'Shallow sea fronts produced by tidal stirring', in Bowman, M. & Esaias, W. (eds), *Oceanic fronts in coastal processes*, Springer, Berlin, pp. 29-42.
- Skei, J. 1983, 'Why sedimentologists are interested in fjords', *Sedimentary Geology*, vol. 36, pp. 75-80.
- Small, D. et al. 2018, 'Trough geometry was a greater influence than climate-ocean forcing in regulating retreat of the marine-based Irish Sea Ice Stream', *GSA Bulletin*, vol. 130, pp. 1981-1999.
- Smeulders, G. et al. 2014, 'Cold-water coral habitats of Rockall and Porcupine Bank, NE Atlantic Ocean: Sedimentary facies and benthic foraminiferal assemblages', *Deep-Sea Research* 2, vol. 99, pp. 270-285.
- Smith, J. et al. 2019, 'The marine geological imprint of Antarctic ice shelves', *Nature Communications*, vol. 10, pp. 1-16.
- Smith, L. & Andrews, J. 2000, 'Sedimentary characteristics in iceberg-dominated fjords, Kangerlussuaq region, East Greenland', *Sedimentary Geology*, vol. 130, pp. 11-25.
- Stanton, B. 1984, 'Return wave heights off south Uist estimated from seven years of data', Institute of Oceanographic Sciences, Report No. 164, pp. 1-56.
- Stashchuk, N. et al. 2017, 'Tidally induced residual current over the Malin Sea continental slope', *Continental Shelf Research*, vol. 139, pp. 21-34.
- Stefánsson, U. & Ólafsson, J. 1991, 'Nutrients and fertility of Icelandic waters', *Journal of the Marine Institute, Reykjavik*, vol 12, no. 3, pp. 1-56.
- Steinsund, P. & Hald, M. 1994, 'Recent calcium carbonate dissolution in the Barents Sea: Paleoceanographic applications', *Marine Geology*, vol. 117, pp. 303-316.
- Steinsund, P. 1994, *Benthic foraminifera in surface sediments of the Barents and Kara Seas: modern and late Quaternary applications*, PhD thesis, University of Tromsø, 111 pp.
- Stickley, C. et al. 2005, 'Deglacial ocean and climate seasonality in laminated diatom sediments, Mac.Robertson Shelf, Antarctica', *Palaeogeography, Palaeoclimatology, Palaeoecology*, vol. 227, pp. 290-310.
- Stoker, M. & Bradwell, T. 2005, 'The Minch palaeo-ice stream, NW sector of the British-Irish Ice Sheet', *Journal of the Geological Society, London*, vol. 163, pp. 425-428.
- Stoker, M. 1988, 'Pleistocene ice-proximal glaciomarine sediments in boreholes from the Hebrides Shelf and Wyville-Thomson Ridge, NW UK Continental Shelf', *Scottish Journal of Geology*, vol. 24, pp. 249-262.
- Stoker, M. 1995, 'The influence of glacial sedimentation on slope-apron development on the continental margin off northwest Britain', in Scrutton, R. et al. (eds.), *The tectonics, sedimentation and palaeoceanography of the North Atlantic region*, Geological Society, London, Special Publication No. 90, pp. 159-177.
- Stoker, M. et al. 1993, *The geology of the Hebrides and West Shetland shelves, and adjacent deep-water areas*, HMSO for the British Geological Survey, London, 149 pp.

- Stoker, M. et al. 2011, 'An overview of the lithostratigraphical framework for the Quaternary deposits on the United Kingdom continental shelf', *British Geological Survey Research Report RR/11/03*, British Geological Survey, Keyworth, 48 pp.
- Stokes, C. & Tarasov, L. 2010, 'Ice streaming in the Laurentide Ice Sheet: A first comparison between data-calibrated numerical model output and geological evidence', *Geophysical Research Letters*, vol. 37, 5 pp.
- Stokes, C. et al. 2014, 'Asynchronous response of marine-terminating outlet glaciers during deglaciation of the Fennoscandian Ice Sheet', *Geology*, vol. 42, pp. 455-458.
- Stokes, C. et al. 2015, 'On the reconstruction of palaeo-ice sheets: Recent advances and future challenges', *Quaternary Science Reviews*, vol. 125, pp. 15-49.
- Straneo, F. & Cenedese, C. 2015, 'The dynamics of Greenland's glacial fjords and their role in climate', *Annual Reviews of Marine Science*, vol. 7, pp. 89-112.
- Straneo, F. et al. 2011, 'Impact of fjord dynamics and glacial runoff on the circulation near Helheim glacier', *Nature Geoscience*, vol. 4, pp. 322-327.
- Struck, U. 1997, 'Paleoecology of benthic foraminifera in the Norwegian-Greenland Sea during the past 500 ka', in Hass, H. & Kaminski, M. (eds.), *Contributions to the Micropaleontology and Paleoceanography of the Northern North Atlantic*, Grzybowski Foundation Special Publication No. 5, pp. 51-82.
- Sutherland, D. & Walker, M. 1984, 'A late Devensian ice-free area and possible interglacial site on the Isle of Lewis, Scotland', *Nature*, vol. 309, pp. 701-703.
- Sutherland, D. et al. 2013, 'Atlantic water variability on the SE Greenland continental shelf and its relationship to SST and bathymetry', *Journal of Geophysical Research: Oceans*, vol. 118, pp. 847-855.
- Svendsen, H. et al. 2002, 'The physical environment of Kongsfjorden-Krossfjorden, an Arctic fjord system in Svalbard', *Polar Research*, vol. 21, pp. 133-166.
- Svendsen, J. et al. 1992, 'The late Weichselian glacial maximum on western Spitsbergen inferred from offshore sediment cores', *Marine Geology*, vol. 104, pp. 1-17.
- Synge, F. 1964, 'The Glacial Succession in West Caernarvonshire', *Proceedings of the Geologists' Association*, vol. 75, pp. 431-444.
- Syvitski, J. & Skei, J. 1983 (eds.), Sedimentology of fjords, *Sedimentary Geology*, vol. 36, pp. 75-342.
- Syvitski, J. et al. 1996, 'Sediment deposition in an iceberg-dominated glacial marine environment, East Greenland: basin fill implications', *Global and Planetary Change*, vol. 12, pp. 251-270.
- Szarek, R. et al. 2009, 'Distribution of recent benthic foraminifera along continental slope of the Sunda Shelf (South China Sea)', *Marine Micropaleontology*, vol. 71, pp. 41-59.
- Taldenkova, E. et al. 2012, 'Benthic and planktic community changes at the North Siberian margin in response to Atlantic water mass variability since last deglacial times', *Marine Micropaleontology*, vol. 96-97, pp. 13-28.
- Tarlatti, S. et al. 2020, 'Final deglaciation of the Malin Sea through meltwater release and calving events', *Scottish Journal of Geology*, vol. 56, pp. 117-133.
- Tate, M. & Dobson, M. 1988, 'Late Permian to early Mesozoic rifting and sedimentation offshore NW Ireland', *Marine and Petroleum Geology*, vol. 6, pp. 49-59.

- Tate, M. 1992, 'Structural framework and tectono-stratigraphic evolution of the Porcupine Seabight Basin, offshore western Ireland', *Marine and Petroleum Geology*, vol. 10, pp. 95-123.
- Ter Braak, C. 1986, 'Canonical correspondence analysis: A new eigenvector technique for multivariate direct gradient analysis', *Ecology*, vol. 67, pp. 1167-1179.
- The RAISED Consortium et al. 2014, 'A community-based geological reconstruction of Antarctic Ice Sheet deglaciation since the Last Glacial Maximum', *Quaternary Science Reviews*, vol. 100, pp. 1-9.
- Thébaudeau, B. et al. 2016, 'Seabed geomorphology of the Porcupine Bank, West of Ireland', *Journal of Maps*, vol. 12, pp. 947-958.
- Thornalley, D. et al. 2015, 'A warm and poorly ventilated deep Arctic Mediterranean during the last glacial period', *Science*, vol. 349, pp. 706-710.
- Tikhonova, A. et al. 2019, 'Image dataset of common benthic foraminiferal taxa in the North Atlantic seafloor surface sediments (59.5°N transect) between the Labrador sea and the Faeroe-Shetland sill', *Data in Brief*, vol. 26, 38 pp.
- Timmermann, R. et al. 2010, 'A consistent data set of Antarctic ice sheet topography, cavity geometry, and global bathymetry', *Earth System Science Data*, vol. 2, pp. 261-273.
- Ullrich, A. et al. 2009, 'Intra-annual variability in benthic foraminiferal abundance in sediments of Disenchantment Bay, an Alaskan glacial fjord', *Arctic, Antarctic and Alpine Research*, vol. 41, pp. 257-271.
- van Aken, H. 2000, 'The hydrography of the mid-latitude northeast Atlantic Ocean: I: The deep water masses', *Deep-Sea Research Part 1*, vol. 47, pp. 757-788.
- Van der Zwaan, G. et al. 1986, '*Uvigerina* from the Atlantic, Paratethys and Mediterranean', *Utrecht Micropaleontological Bulletins*, vol. 35, pp. 7-20.
- Van der Zwaan, G. et al. 1990, 'The depth dependency of planktonic/benthic foraminiferal ratios: Constraints and applications', *Marine Geology*, vol. 95, pp. 1-16.
- Van der Zwaan, G. et al. 1999, 'Benthic foraminifers: proxies or problems?: A review of paleocological concepts', *Earth-Science Reviews*, vol. 46, pp. 213-236.
- van Kreveld, S. et al. 2000, 'Potential links between surging ice sheets, circulation changes, and the Dansgaard-Oeschger cycles in the Irminger Sea, 60-18 kyr', *Paleoceanography*, vol. 15, pp. 425-442.
- van Landeghem, K. et al. 2009, 'Seafloor evidence for palaeo-ice streaming and calving of the grounded Irish Sea Ice Stream: Implications for the interpretation of its final deglaciation phase', *Boreas*, vol. 38, pp. 119-131.
- Van Rooij, D. 2004, *An integrated study of Quaternary sedimentary processes on the eastern slope of the Porcupine Seabight, SW of Ireland*, PhD thesis, University of Ghent, 330 pp.
- Van Rooij, D. et al. 2003, 'Seismic evidence of current-controlled sedimentation in the Belgica Mound province, upper Porcupine Slope, southwest of Ireland', *Marine Geology*, vol. 195, pp. 31-53.
- Van Rooij, D. et al. 2007a, 'Small mounded contourite drifts associated with deep-water coral banks, Porcupine Seabight, NE Atlantic Ocean', in Viana, A. & Rebesco, M. (eds.), *Economic and Palaeoceanographic Significance of Contourite Deposits*, Geological Society, London, Special Publication No. 276, pp. 225-244.

- Van Rooij, D. et al. 2007b, 'Quaternary sediment dynamics in the Belgica mound province, Porcupine Seabight: ice-rafting events and contour current processes', *International Journal of Earth Sciences*, vol. 96, pp. 121-140.
- van Weering, T. & Qvale, G. 1983, 'Recent sediments and foraminiferal distribution in the Skagerrak, northeastern North Sea', *Marine Geology*, vol. 52, pp. 75-99.
- Verma, K. et al. 2018, 'Late Glacial-Holocene record of benthic foraminiferal morphogroups from the eastern Arabian Sea OMZ: Paleoenvironmental implications', *Journal of Earth System Science*, vol. 127, pp.
- Veum, T. et al. 1992, 'Water mass exchange between the North Atlantic and the Norwegian Sea during the past 28,000 years', *Nature*, vol. 356, pp. 783-785.
- Viana, A. et al. 1998, 'Bottom-current-controlled sand deposits – review of modern shallow- to deep-water environments', *Sedimentary Geology*, vol. 115, pp. 53-80.
- Vidal, L. et al. 1998, 'Benthic $\delta^{18}\text{O}$ records in the North Atlantic over the last glacial period (60-10 kyr): Evidence for brine formation', *Paleoceanography*, vol. 13, pp. 245-251.
- Vogt, C. et al. 2001, 'Detailed mineralogical evidence for two nearly identical glacial/deglacial cycles and Atlantic water advection to the Arctic Ocean during the last 90,000 years', *Global and Planetary Change*, vol. 31, pp. 23-44.
- von Weymarn, J. 1979, 'A new concept of glaciation in Lewis and Harris, Outer Hebrides', *Proceedings of the Royal Society of Edinburgh*, vol. 77B, pp. 97-105.
- Voronkov, A. et al. 2013, 'Diversity of hard-bottom fauna relative to environmental gradients in Kongsfjorden, Svalbard', *Polar Research*, vol. 32, 27 pp.
- Vorren, T. et al. 1984, 'Quaternary sediments and environments on the continental shelf off northern Norway', *Marine Geology*, vol. 57, pp. 229-257.
- Walsh, J. et al. 1989, 'Carbon and nitrogen cycling within the Bering/Chukchi Seas: Source regions for organic matter effecting AOU demands of the Arctic Ocean', *Progress in Oceanography*, vol. 22, pp. 277-359.
- Walter, J. et al. 2012, 'Oceanic mechanical forcing of a marine-terminating Greenland glacier', *Annals of Glaciology*, vol. 53, pp. 181-192.
- Wary, M. et al. 2016, 'Norwegian Sea warm pulses during Dansgaard-Oeschger stadials: Zooming in on these anomalies over the 35-41 ka cal BP interval and their impacts on proximal European ice sheet dynamics', *Quaternary Science Reviews*, vol. 151, pp. 255-272.
- Wary, M. et al. 2017a, 'Regional seesaw between the North Atlantic and Nordic Seas during the last glacial abrupt climate events', *Climate of the Past*, vol. 13, pp. 729-739.
- Wary, M. et al. 2017b, 'The southern Norwegian Sea during the last 45 ka: hydrographical reorganizations under changing ice-sheet dynamics', *Journal of Quaternary Science*, vol. 32, pp. 908-922.
- Weinelt, M. et al. 2003, 'Variability of North Atlantic heat transfer during MIS 2', *Paleoceanography*, vol. 18, 16 pp.
- Weston, J. 1985, 'Comparison between Recent benthic foraminiferal faunas of the Porcupine Seabight and Western Approaches Continental Slope', *Journal of Micropalaeontology*, vol. 4, pp. 165-183.

- Wheeler, A. et al. 2000, 'Very high resolution side-scan mapping of deep-water coral mounds: surface morphology and processes affecting growth', *EOS Transactions*, American Geophysical Union, vol. 81, p. 48.
- White, M. & Bowyer, P. 1997, 'The shelf-edge current north-west of Ireland', *Annales Geophysicae*, vol. 15, pp. 1076-1083.
- White, M. 2007, 'Benthic dynamics at the carbonate mound regions of the Porcupine Seabight continental margin', *International Journal of Earth Sciences*, vol. 96, pp. 1-9.
- White, M. et al. 1998, 'Nutrient distributions across the Porcupine Bank', *ICES Journal of Marine Science*, vol. 55, pp. 1082-1094.
- White, M. et al. 2005, 'Deep-water coral development as a function of hydrodynamics and surface productivity around the submarine banks of the Rockall Trough, NE Atlantic', in Freiwald, A. & Roberts, J. (eds.), *Cold-water corals and ecosystems*, Springer, Heidelberg, pp. 503-514.
- Wilson, J. 1977, 'Chapter 7: The role of Manned Submersibles in Sedimentological and Faunal Investigations on the United Kingdom Continental Shelf', in Geyer, A. (ed.), *Submersibles and their use in oceanography and ocean engineering*, Elsevier, Amsterdam, pp. 151-167.
- Wilson, L. & Austin, W. 2002, 'Millennial and sub-millennial-scale variability in sediment colour from the Barra Fan, NW Scotland: implications for British ice sheet dynamics', in Dowdeswell, J. & Ó Cofaigh, C. (eds.), *Glacier-influenced sedimentation on high-latitude continental margins*, Geological Society, London Special Publication No. 203, London, pp. 349-365.
- Wilson, L. et al. 2002, 'The last British Ice Sheet: growth, maximum extent and deglaciation', *Polar Research*, vol. 21, no. 2, pp. 243-250.
- Wilson, P. et al. 2019, 'Deglaciation chronology of the Donegal Ice Centre, north-west Ireland', *Journal of Quaternary Science*, vol. 34, pp. 16-28.
- Wollenburg, J. & Kuhnt, W. 2000, 'The response of benthic foraminifers to carbon flux and primary production in the Arctic Ocean', *Marine Micropaleontology*, vol. 40, pp. 189-231.
- Wollenburg, J. & Mackensen, A. 1998, 'Living benthic foraminifers from the central Arctic Ocean: faunal composition, standing stock and diversity', *Marine Micropaleontology*, vol. 34, pp. 153-185.
- Wunsch, C. 2006, 'Abrupt climate change: An alternative view', *Quaternary Research*, vol. 65, pp. 191-203.
- Wunsch, C. 2010, 'Towards understanding the Paleoocean', *Quaternary Science Reviews*, vol. 29, pp. 1960-1967.
- Xing, J. & Davies, A. 2001, 'The influence of shelf edge flows and wind upon the circulation on the Malin Shelf and in the Irish Sea', *Continental Shelf Research*, vol. 21, pp. 21-45.
- Yordanova, E. & Hohenegger, J. 2007, 'Studies on settling, traction and entrainment of larger benthic foraminiferal tests: implications for accumulation in shallow marine sediments', *Sedimentology*, vol. 54, pp. 1273-1306.
- Young, N. & Briner, J. 2015, 'Holocene evolution of the western Greenland Ice Sheet: Assessing geophysical ice-sheet models with geological reconstructions of ice-margin change', *Quaternary Science Reviews*, vol. 114, pp. 10-17.

- Zaragosi, S. et al. 2001, 'Initiation of the European deglaciation as recorded in the northwestern Bay of Biscay slope environments (Meriadzek Terrace and Trevelyan Escarpment): a multi-proxy approach', *Earth and Planetary Science Letters*, vol. 188, pp. 493-507.

APPENDICES

Appendix 1: Foraminiferal count data

Table A1: 146VC benthic foraminiferal count data (continued to page 166)

| Core: JC106-146VC | Sample depth (cm) | | | | | | | | |
|---------------------------------|-------------------|-----|-----|-----|-----|-----|-----|-----|-----|
| | 412.5 | 402 | 382 | 362 | 345 | 328 | 311 | 293 | 276 |
| <i>Ammonia beccarii</i> | - | - | 1 | 2 | 3 | 5 | - | - | - |
| <i>Amphicoryna scalaris</i> | - | - | 1 | - | - | - | - | - | - |
| <i>Astacolus</i> spp. | - | - | - | - | - | 4 | - | - | - |
| <i>Asteriginata mamilla</i> | - | - | - | - | - | - | - | - | - |
| <i>Astrononion gallowayi</i> | - | 1 | - | - | - | - | 3 | 1 | - |
| <i>Astrononion</i> sp. | - | 2 | 6 | 6 | 3 | - | - | - | - |
| <i>Brizalina</i> spp. | - | - | 1 | 1 | 1 | 1 | - | - | - |
| <i>Brizalina pseudopunctata</i> | - | - | - | - | - | - | - | - | - |
| <i>Brizalina variabilis</i> | 2 | - | 2 | 1 | - | - | - | - | 1 |
| <i>Buccella</i> sp. | 5 | 5 | 11 | 4 | - | 2 | 2 | 1 | - |
| <i>Buccella frigida</i> | - | - | - | 2 | 2 | 1 | 1 | - | - |
| <i>Bulimina aculeata</i> | - | - | - | - | - | - | - | - | - |
| <i>Bulimina elongata</i> | - | 1 | - | - | - | - | - | - | - |
| <i>Bulimina marginata</i> | - | - | - | - | - | 3 | - | 1 | - |
| <i>Bulimina</i> spp. | - | - | 2 | 1 | - | - | 1 | - | - |
| <i>Cancris</i> sp. | - | 1 | - | - | 3 | 1 | - | - | - |
| <i>Cassidulina laevigata</i> | - | - | - | - | - | - | - | - | - |
| <i>Cassidulina neoteretis</i> | - | 3 | - | 1 | 3 | - | - | - | - |
| <i>Cassidulina reniforme</i> | 38 | 36 | 54 | 40 | 64 | 59 | 25 | 21 | 7 |
| <i>Cibicides lobatulus</i> | 14 | 11 | 19 | 13 | 20 | 21 | 5 | 1 | - |
| <i>Cibicides refulgens</i> | 16 | 2 | 6 | 1 | 5 | 5 | 1 | - | - |
| <i>Dentalina</i> sp. | - | - | - | - | 1 | - | - | - | - |
| <i>Discorbis</i> sp. | - | - | - | - | - | - | - | - | - |
| <i>Elphidium advenum</i> | - | - | - | - | - | - | - | - | - |
| <i>Elphidium albumbilicatum</i> | 11 | 7 | 16 | 15 | 6 | 5 | 6 | - | - |
| <i>Elphidium excavatum</i> | 26 | 29 | 49 | 26 | 55 | 92 | 26 | 1 | 2 |
| <i>Elphidium clavatum</i> | 51 | 30 | 62 | 30 | 85 | 69 | 20 | 1 | 3 |
| <i>Elphidium crispum</i> | 3 | - | - | 2 | - | - | - | - | - |
| <i>Elphidium</i> spp. | - | - | 5 | 2 | 4 | 3 | 1 | - | - |
| <i>Fronicularia</i> sp. | - | - | - | - | 1 | 3 | - | - | - |
| <i>Fursenkoina</i> sp. | - | - | - | - | - | - | - | - | - |
| <i>Gavelinopsis praegeri</i> | - | - | 2 | - | - | - | - | - | - |
| <i>Glabratella wrightii</i> | - | - | - | - | - | - | - | - | - |
| <i>Globobulimina</i> sp. | - | - | 1 | - | - | - | - | - | - |
| <i>Globocassidulina</i> sp. | 5 | - | - | - | - | - | - | - | - |
| <i>Haynesina orbiculare</i> | 3 | - | 3 | 3 | 2 | 3 | - | - | - |
| <i>Hyalinea baltica</i> | 1 | - | - | - | 1 | - | - | - | - |
| <i>Lagena</i> sp. | - | - | - | - | - | - | - | - | - |
| <i>Lagena semistriata</i> | - | - | - | - | - | - | - | - | - |
| <i>Lagena striata</i> | - | - | - | - | - | - | - | - | - |
| <i>Lenticulina</i> sp. | 3 | 1 | 12 | 2 | 18 | 10 | 2 | - | 2 |
| <i>Massilina</i> sp. | 1 | - | - | - | - | - | - | - | - |
| <i>Melonis barleeaanum</i> | - | - | - | - | - | - | - | - | - |
| <i>Miliolinella subrotunda</i> | - | - | 4 | - | 3 | - | - | - | 3 |
| <i>Miliolinella</i> sp. | - | - | - | - | - | - | - | - | - |
| <i>Neoconorbina</i> sp. | - | - | - | - | - | - | 1 | - | - |
| <i>Nodosaria</i> spp. | - | - | 1 | - | 3 | 3 | 1 | - | - |
| <i>Nonionellina labradorica</i> | 1 | 1 | 6 | 5 | 5 | 4 | 1 | - | - |
| <i>Nonion</i> spp. | 2 | 5 | 8 | 1 | 1 | 3 | 3 | - | - |
| <i>Nonionella turgida</i> | - | 1 | - | - | - | - | - | - | - |
| <i>Oolina borealis</i> | - | - | - | - | - | 2 | - | - | - |
| <i>Oolina lineata</i> | - | - | - | - | - | - | - | - | - |
| <i>Oolina</i> sp. | - | - | - | - | - | - | 1 | - | - |
| <i>Parafissurina</i> spp. | 2 | - | - | - | - | - | - | - | - |
| <i>Patellina corrugata</i> | - | - | - | 1 | - | - | - | - | - |
| <i>Pyrgo murrhina</i> | - | - | - | - | - | - | - | - | - |
| <i>Pyrgo simplex</i> | - | - | - | - | - | - | - | - | - |
| <i>Pyrgo williamsoni</i> | 1 | - | - | - | - | - | - | - | - |
| <i>Pyrgo</i> spp. | - | - | - | - | - | - | - | - | - |
| <i>Quinqueloculina seminula</i> | - | - | - | 1 | - | - | - | - | - |
| <i>Quinqueloculina</i> spp. | 9 | 4 | 5 | 1 | 5 | - | 2 | - | - |

Appendix 1: Foraminiferal count data

| | | | | | | | | | |
|--------------------------------|---|---|----|----|----|---|----|---|---|
| <i>Rosalina</i> spp. | - | - | 4 | 1 | 2 | 2 | - | - | - |
| <i>Spirillina</i> spp. | - | - | - | - | - | - | 2 | - | - |
| <i>Spiroloculina excavata</i> | - | - | 1 | 2 | 4 | - | - | - | - |
| <i>Spiroloculina</i> spp. | - | - | - | - | - | - | - | - | - |
| <i>Stainforthia concava</i> | - | - | 1 | - | 1 | - | - | - | - |
| <i>Stainforthia fusiformis</i> | - | - | 1 | - | - | - | - | - | - |
| <i>Textularia sagittula</i> | - | - | - | - | - | - | - | - | - |
| <i>Textularia truncata</i> | - | - | - | - | - | - | - | - | - |
| <i>Textularia</i> sp. | - | - | - | - | - | - | 1 | - | - |
| <i>Trifarina angulosa</i> | - | - | 1 | - | - | - | - | - | - |
| <i>Trifarina</i> sp. | - | - | - | - | - | - | - | - | - |
| <i>Uvigerina</i> sp. | - | - | - | 1 | - | 1 | - | - | - |
| Unidentified spp. | 8 | 2 | 21 | 13 | 10 | 6 | 10 | 1 | 2 |

| Core: JC106-146VC | Sample depth (cm) | | | | | | | | |
|----------------------------------|-------------------|-----|-----|-----|-----|-----|-----|-----|-----|
| | 259 | 242 | 228 | 211 | 194 | 177 | 160 | 143 | 126 |
| Benthic species | | | | | | | | | |
| <i>Ammonia beccarii</i> | - | - | 3 | 1 | 4 | 1 | 3 | - | 1 |
| <i>Amphicoryna scalaris</i> | - | - | - | - | - | - | - | - | - |
| <i>Astacolus</i> spp. | - | - | - | - | - | - | - | - | - |
| <i>Asteriginata mamilla</i> | - | - | - | - | - | - | - | - | 1 |
| <i>Astrononion gallowayi</i> | - | - | - | - | - | - | - | - | - |
| <i>Astrononion</i> sp. | - | - | 2 | 1 | 6 | - | 1 | - | 2 |
| <i>Brizalina</i> spp. | - | - | - | 11 | 2 | - | - | - | - |
| <i>Brizalina pseudopunctata</i> | - | - | - | - | - | - | 1 | - | - |
| <i>Brizalina variabilis</i> | - | - | 2 | - | - | 1 | 2 | - | 1 |
| <i>Buccella</i> sp. | - | - | 1 | 8 | - | 5 | 5 | - | 3 |
| <i>Buccella frigida</i> | - | - | 1 | - | 8 | - | - | - | - |
| <i>Bulimina aculeata</i> | - | - | - | - | - | - | - | 1 | - |
| <i>Bulimina elongata</i> | - | - | - | - | - | - | - | - | - |
| <i>Bulimina marginata</i> | - | - | 2 | 1 | 2 | - | 2 | 1 | 1 |
| <i>Bulimina</i> spp. | - | - | - | - | 3 | - | - | - | - |
| <i>Cancris</i> sp. | - | - | - | - | - | - | - | - | - |
| <i>Cassidulina laevigata</i> | - | - | - | - | 1 | - | - | - | - |
| <i>Cassidulina neoteretis</i> | - | - | 1 | - | 2 | 1 | 1 | - | 2 |
| <i>Cassidulina reniforme</i> | 2 | - | 52 | 40 | 55 | 33 | 32 | 17 | 30 |
| <i>Cibicides lobatulus</i> | - | - | 20 | 23 | 28 | 19 | 11 | 7 | 11 |
| <i>Cibicides refulgens</i> | - | - | 1 | 1 | - | 2 | 1 | - | - |
| <i>Dentalina</i> sp. | - | - | - | 1 | - | - | - | - | - |
| <i>Discorbis</i> sp. | - | - | - | - | 1 | - | - | - | - |
| <i>Elphidium advenum</i> | - | - | - | - | - | - | - | - | - |
| <i>Elphidium albiumbilicatum</i> | - | - | 2 | - | 4 | 1 | 2 | 1 | - |
| <i>Elphidium excavatum</i> | - | - | 68 | 70 | 64 | 27 | 16 | 8 | 18 |
| <i>Elphidium clavatum</i> | - | - | 81 | 46 | 65 | 59 | 35 | 10 | 24 |
| <i>Elphidium crispum</i> | - | - | 2 | - | - | - | - | 1 | - |
| <i>Elphidium</i> spp. | - | - | 1 | 1 | - | 2 | 1 | - | - |
| <i>Fronicularia</i> sp. | - | - | 4 | 3 | 2 | 1 | 1 | - | - |
| <i>Fursenkoina</i> sp. | - | - | - | - | - | - | - | - | - |
| <i>Gavelinopsis praegeri</i> | - | - | - | - | - | - | - | - | - |
| <i>Glabratella wrightii</i> | - | - | 1 | - | - | - | - | - | - |
| <i>Globobulimina</i> sp. | - | - | - | - | - | - | - | - | - |
| <i>Globocassidulina</i> sp. | - | - | 2 | - | - | 1 | - | - | - |
| <i>Haynesina orbiculare</i> | - | - | 1 | 3 | 2 | - | - | 1 | - |
| <i>Hyalinea baltica</i> | - | - | - | - | - | - | - | - | - |
| <i>Lagena</i> sp. | - | - | 1 | - | - | - | - | - | - |
| <i>Lagena semistriata</i> | - | - | - | - | - | - | - | - | - |
| <i>Lagena striata</i> | - | - | - | - | - | - | - | - | - |
| <i>Lenticulina</i> sp. | - | - | - | 11 | 6 | 1 | 1 | - | 1 |
| <i>Massilina</i> sp. | - | - | - | - | - | - | - | - | - |
| <i>Melonis barleeaanum</i> | - | - | - | - | - | - | - | - | - |
| <i>Miliolinella subrotunda</i> | - | - | 3 | - | 1 | - | - | - | - |
| <i>Miliolinella</i> sp. | - | - | - | - | 2 | - | - | - | - |
| <i>Neoconorbina</i> sp. | - | - | - | - | 1 | - | - | - | - |
| <i>Nodosaria</i> spp. | - | - | 3 | 1 | - | - | 1 | - | - |
| <i>Nonionella labradorica</i> | - | - | 3 | 4 | 1 | 3 | - | - | 2 |
| <i>Nonion</i> spp. | - | - | - | - | - | - | 1 | - | 1 |
| <i>Nonionella turgida</i> | - | - | - | - | - | - | - | - | - |
| <i>Oolina borealis</i> | - | - | - | - | - | - | - | - | - |
| <i>Oolina lineata</i> | - | - | - | - | - | - | - | - | - |
| <i>Oolina</i> sp. | - | - | 1 | - | - | - | - | - | - |
| <i>Parafissurina</i> spp. | - | - | 1 | 1 | 1 | - | - | - | - |

Appendix 1: Foraminiferal count data

| | | | | | | | | | |
|---------------------------------|---|---|----|----|----|---|----|---|---|
| <i>Patellina corrugata</i> | - | - | - | - | 1 | - | - | 1 | - |
| <i>Pyrgo murrhina</i> | - | - | - | - | 1 | - | - | - | - |
| <i>Pyrgo simplex</i> | - | - | - | - | - | - | - | - | - |
| <i>Pyrgo williamsoni</i> | - | - | 1 | - | 1 | - | 2 | 1 | - |
| <i>Pyrgo spp.</i> | - | - | - | 1 | - | 3 | - | - | - |
| <i>Quinqueloculina seminula</i> | - | - | - | - | - | - | - | - | - |
| <i>Quinqueloculina spp.</i> | - | - | 10 | 13 | 6 | 5 | 3 | - | - |
| <i>Rosalina spp.</i> | - | - | 3 | 2 | 2 | 2 | 2 | 1 | 1 |
| <i>Spirillina spp.</i> | - | - | 5 | 3 | 1 | - | - | - | 1 |
| <i>Spiroloculina excavata</i> | - | - | - | - | - | - | - | - | - |
| <i>Spiroloculina spp.</i> | - | - | - | 1 | - | 3 | - | - | - |
| <i>Stainforthia concava</i> | - | - | 1 | - | - | - | - | - | 1 |
| <i>Stainforthia fusiformis</i> | - | - | - | 2 | - | 1 | - | - | - |
| <i>Textularia sagittula</i> | - | - | - | - | - | - | - | - | - |
| <i>Textularia truncata</i> | - | - | 1 | - | - | - | - | - | - |
| <i>Textularia sp.</i> | - | - | 2 | 1 | - | 1 | - | - | - |
| <i>Trifarina angulosa</i> | - | - | 1 | - | 1 | - | 2 | - | - |
| <i>Trifarina sp.</i> | - | - | - | - | - | - | - | - | - |
| <i>Uvigerina sp.</i> | - | - | 1 | - | - | 2 | - | - | - |
| Unidentified spp. | - | - | 10 | 15 | 24 | 7 | 10 | 1 | 5 |

| Core: JC106-146VC | Sample depth (cm) | | | | | | |
|----------------------------------|-------------------|----|----|----|----|----|----|
| | 109 | 92 | 75 | 58 | 41 | 24 | 7 |
| <i>Ammonia beccarii</i> | - | 1 | 1 | - | - | 1 | 1 |
| <i>Amphicoryna scalaris</i> | - | - | - | - | - | 1 | 1 |
| <i>Astacolus spp.</i> | - | - | - | - | - | - | - |
| <i>Asteriginata mamilla</i> | - | - | - | - | - | - | - |
| <i>Astrononion gallowayi</i> | - | - | - | - | - | - | - |
| <i>Astrononion sp.</i> | - | - | - | - | 1 | - | - |
| <i>Brizalina spp.</i> | - | - | - | - | 2 | - | - |
| <i>Brizalina pseudopunctata</i> | - | - | - | - | - | - | - |
| <i>Brizalina variabilis</i> | 1 | - | - | - | - | 3 | - |
| <i>Buccella sp.</i> | - | 1 | 1 | - | - | - | - |
| <i>Buccella frigida</i> | - | - | - | - | - | - | - |
| <i>Bulimina aculeata</i> | - | - | - | - | - | - | - |
| <i>Bulimina elongata</i> | - | - | - | - | - | - | - |
| <i>Bulimina marginata</i> | - | 1 | - | - | - | 8 | 3 |
| <i>Bulimina spp.</i> | - | - | - | - | - | - | - |
| <i>Cancris sp.</i> | - | - | - | - | - | - | - |
| <i>Cassidulina laevigata</i> | - | 1 | - | - | 7 | 58 | 43 |
| <i>Cassidulina neoteretis</i> | - | - | - | - | 7 | 1 | 5 |
| <i>Cassidulina reniforme</i> | 5 | 11 | 6 | 6 | 14 | 9 | 15 |
| <i>Cibicides lobatulus</i> | 3 | 1 | 2 | 2 | 11 | 46 | 53 |
| <i>Cibicides refulgens</i> | - | - | - | - | 2 | 11 | 8 |
| <i>Dentalina sp.</i> | - | - | - | - | - | - | - |
| <i>Discorbis sp.</i> | - | - | - | - | - | - | - |
| <i>Elphidium advenum</i> | - | - | - | - | - | 1 | - |
| <i>Elphidium albiumbilicatum</i> | 1 | 1 | - | - | 1 | - | - |
| <i>Elphidium excavatum</i> | 3 | 6 | 4 | 5 | 2 | 1 | - |
| <i>Elphidium clavatum</i> | 4 | 3 | 9 | 6 | 7 | - | - |
| <i>Elphidium crispum</i> | - | - | - | - | - | - | - |
| <i>Elphidium spp.</i> | - | - | - | - | - | - | 2 |
| <i>Fronducularia sp.</i> | - | - | 1 | - | - | - | - |
| <i>Fursenkoina sp.</i> | - | - | - | - | 1 | - | - |
| <i>Gavelinopsis praegeri</i> | - | - | - | - | 2 | - | - |
| <i>Glabratella wrightii</i> | - | - | - | - | - | - | - |
| <i>Globobulimina sp.</i> | - | - | - | - | - | - | - |
| <i>Globocassidulina sp.</i> | - | - | - | - | - | - | - |
| <i>Haynesina orbiculare</i> | - | - | - | - | 1 | - | - |
| <i>Hyalinea baltica</i> | - | - | - | - | - | 2 | 2 |
| <i>Lagena sp.</i> | - | - | - | - | - | - | - |
| <i>Lagena semistriata</i> | - | - | - | - | - | 1 | - |
| <i>Lagena striata</i> | - | - | - | - | - | 2 | - |
| <i>Lenticulina sp.</i> | - | 1 | 1 | - | - | 2 | - |
| <i>Massilina sp.</i> | - | - | - | - | - | - | - |
| <i>Melonis barleeenum</i> | - | - | - | - | 1 | - | - |
| <i>Miliolinella subrotunda</i> | - | - | 1 | - | 1 | - | 1 |
| <i>Miliolinella sp.</i> | - | - | - | - | - | - | - |
| <i>Neoconorbina sp.</i> | - | - | - | - | - | - | - |

| | | | | | | | | |
|---------------------------------|---|---|---|---|----|----|----|----|
| <i>Nodosaria</i> spp. | - | - | - | - | - | - | - | 1 |
| <i>Nonionellina labradorica</i> | 1 | 1 | - | 1 | - | - | - | - |
| <i>Nonion</i> spp. | - | - | - | - | 1 | 1 | - | - |
| <i>Nonionella turgida</i> | - | - | - | - | - | - | - | - |
| <i>Oolina borealis</i> | - | - | - | - | - | - | - | - |
| <i>Oolina lineata</i> | - | - | - | - | - | - | - | 4 |
| <i>Oolina</i> sp. | - | - | - | - | - | - | - | - |
| <i>Parafissurina</i> spp. | - | - | - | - | - | - | - | - |
| <i>Patellina corrugata</i> | - | - | - | - | - | - | - | - |
| <i>Pyrgo murrhina</i> | - | - | - | - | - | - | - | - |
| <i>Pyrgo simplex</i> | - | - | - | - | - | - | - | 1 |
| <i>Pyrgo williamsoni</i> | - | - | - | - | - | 1 | - | 1 |
| <i>Pyrgo</i> spp. | - | 1 | - | - | - | - | - | - |
| <i>Quinqueloculina seminula</i> | 2 | - | - | - | - | 6 | - | 2 |
| <i>Quinqueloculina</i> spp. | 1 | 1 | - | - | - | 2 | - | - |
| <i>Rosalina</i> spp. | - | - | - | - | 1 | 6 | - | - |
| <i>Spirillina</i> spp. | - | - | - | - | - | - | - | - |
| <i>Spiroloculina excavata</i> | - | - | - | - | - | - | - | 2 |
| <i>Spiroloculina</i> spp. | - | - | - | - | - | - | - | - |
| <i>Stainforthia concava</i> | - | - | - | 1 | - | - | - | - |
| <i>Stainforthia fusiformis</i> | - | - | - | - | - | 2 | - | - |
| <i>Textularia sagittula</i> | 1 | - | 1 | - | 13 | 45 | 52 | - |
| <i>Textularia truncata</i> | - | - | - | - | 2 | 17 | 14 | - |
| <i>Textularia</i> sp. | - | - | - | - | 2 | 21 | 11 | - |
| <i>Trifarina angulosa</i> | - | - | 1 | - | 9 | 62 | 74 | - |
| <i>Trifarina</i> sp. | - | - | - | - | - | 4 | 4 | - |
| <i>Uvigerina</i> sp. | - | - | - | - | - | - | - | - |
| Unidentified spp. | 2 | 3 | 2 | - | 1 | 2 | - | 18 |

Table A2: 146VC planktic foraminiferal count data

| Core: JC106-146VC | Sample depth (cm) | | | | | | | | |
|--------------------------------------|-------------------|-----|-----|-----|-----|-----|-----|-----|-----|
| Planktic species | 412.5 | 402 | 382 | 362 | 345 | 328 | 311 | 293 | 276 |
| <i>Globigerina bulloides</i> | 4 | 4 | 5 | 2 | 4 | 1 | - | 1 | - |
| <i>Globorotalia truncatulinoides</i> | - | - | - | - | - | - | - | - | - |
| <i>Neogloboquadrina pachyderma</i> | - | - | - | 4 | 1 | 4 | - | 2 | 1 |
| <i>Neogloboquadrina</i> sp. | - | - | - | - | - | - | - | - | - |
| <i>Orbulina universa</i> | - | - | - | - | - | - | - | - | - |
| Unidentified spp. | - | - | 1 | - | - | - | - | - | - |

| Core: JC106-146VC | Sample depth (cm) | | | | | | | | |
|--------------------------------------|-------------------|-----|-----|-----|-----|-----|-----|-----|-----|
| Planktic species | 259 | 242 | 228 | 211 | 194 | 177 | 160 | 143 | 126 |
| <i>Globigerina bulloides</i> | - | - | 1 | 1 | - | - | 2 | - | - |
| <i>Globorotalia truncatulinoides</i> | - | - | - | - | - | - | - | - | - |
| <i>Neogloboquadrina pachyderma</i> | - | - | 5 | - | 2 | - | - | - | - |
| <i>Neogloboquadrina</i> sp. | - | - | - | 5 | - | 2 | - | - | 1 |
| <i>Orbulina universa</i> | - | - | - | - | - | - | - | - | - |
| Unidentified spp. | - | - | - | - | 3 | 1 | - | - | 1 |

| Core: JC106-146VC | Sample depth (cm) | | | | | | |
|--------------------------------------|-------------------|----|----|----|----|----|----|
| Planktic species | 109 | 92 | 75 | 58 | 41 | 24 | 7 |
| <i>Globigerina bulloides</i> | - | - | 1 | - | 14 | 35 | 14 |
| <i>Globorotalia truncatulinoides</i> | - | - | - | - | 1 | - | - |
| <i>Neogloboquadrina pachyderma</i> | - | - | - | - | 18 | 49 | 22 |
| <i>Neogloboquadrina sp.</i> | - | - | - | - | - | - | - |
| <i>Orbulina universa</i> | - | - | - | - | - | 1 | 6 |
| Unidentified spp. | - | - | 3 | - | - | 35 | 14 |

Table A3: 146VC foraminiferal sample statistics

| Core: JC106-146VC | Sample depth (cm) | | | | | | | | |
|--|-------------------|------|------|------|------|------|------|------|------|
| | 412.5 | 402 | 382 | 362 | 345 | 328 | 311 | 293 | 276 |
| Total benthic | 202 | 142 | 306 | 178 | 311 | 308 | 115 | 28 | 20 |
| Total planktic | 4 | 4 | 6 | 6 | 5 | 5 | 0 | 3 | 1 |
| Absolute abundance | 206 | 146 | 312 | 184 | 316 | 313 | 115 | 31 | 21 |
| Estimated tests · gram ⁻¹ | 37.7 | 31.5 | 60.1 | 38.7 | - | - | 24.7 | 7.5 | 5.2 |
| Fragment count | 96 | 56 | 72 | 84 | 52 | 75 | 30 | 2 | 4 |
| Fragmentation index | 0.32 | 0.28 | 0.19 | 0.31 | 0.14 | 0.19 | 0.21 | 0.06 | 0.16 |
| Estimated fragments · gram ⁻¹ | 17.6 | 12.1 | 13.9 | 17.7 | - | - | 6.4 | 0.5 | 1.0 |
| Residue weight (g) | 1.41 | 0.46 | 1.14 | 0.41 | 1.23 | 1.07 | 0.23 | 0.04 | 0.03 |
| Dry bulk sample weight (g) | 5.46 | 4.63 | 5.19 | 4.75 | 5.75 | 5.60 | 4.66 | 4.15 | 4.03 |
| Entire residue picked? | Y | Y | Y | Y | N | N | Y | Y | Y |
| Sample facies | Dmm _c | Fl | Dmm | Fl | Dmm | Dmm | Fldf | Fl | Fl |

| Core: JC106-146VC | Sample depth (cm) | | | | | | | | |
|--|-------------------|------|------|------|------|------|------|------|------|
| | 259 | 242 | 228 | 211 | 194 | 177 | 160 | 143 | 126 |
| Total benthic | 2 | 0 | 294 | 265 | 298 | 181 | 136 | 51 | 106 |
| Total planktic | 0 | 0 | 6 | 6 | 5 | 3 | 2 | 0 | 2 |
| Absolute abundance | 2 | 0 | 300 | 271 | 303 | 184 | 138 | 51 | 108 |
| Estimated tests · gram ⁻¹ | 0.5 | 0 | - | 55.9 | - | 40.1 | 27.3 | 11.8 | 24.4 |
| Fragment count | 1 | 2 | 98 | 144 | 42 | 29 | 17 | 3 | 9 |
| Fragmentation index | 0.33 | 1.00 | 0.25 | 0.35 | 0.12 | 0.14 | 0.11 | 0.06 | 0.08 |
| Estimated fragments · gram ⁻¹ | 0.3 | 0.5 | - | 29.7 | - | 6.3 | 3.4 | 0.7 | 2.0 |
| Residue weight (g) | 0.02 | 0.01 | 0.71 | 0.45 | 0.61 | 0.33 | 0.25 | 0.17 | 0.24 |
| Dry bulk sample weight (g) | 3.89 | 4.05 | 5.53 | 4.85 | 5.03 | 4.59 | 5.05 | 4.31 | 4.43 |
| Entire residue picked? | Y | Y | N | Y | N | Y | Y | Y | Y |
| Sample facies | Fl | Fl | Dmm | Dmm | Fldf | Fldf | Fldf | Fm | Fm |

| Core: JC106-146VC | Sample depth (cm) | | | | | | |
|--|-------------------|------|------|------|------|--------|--------|
| | 109 | 92 | 75 | 58 | 41 | 24 | 7 |
| Total benthic | 24 | 33 | 30 | 21 | 89 | 316 | 319 |
| Total planktic | 0 | 0 | 4 | 0 | 33 | 120 | 56 |
| Absolute abundance | 24 | 33 | 34 | 21 | 122 | 436 | 375 |
| Estimated tests · gram ⁻¹ | 5.7 | 8.0 | 8.1 | 5.2 | 29.9 | 5891.9 | 5067.6 |
| Fragment count | 6 | 2 | 2 | 1 | 15 | 56 | 77 |
| Fragmentation index | 0.20 | 0.06 | 0.06 | 0.05 | 0.11 | 0.11 | 0.17 |
| Estimated fragments · gram ⁻¹ | 1.4 | 0.5 | 0.5 | 0.2 | 3.7 | 756.8 | 1040.5 |
| Residue weight (g) | 0.08 | 0.07 | 0.07 | 0.12 | 0.1 | 0.41 | 1.52 |
| Dry bulk sample weight (g) | 4.22 | 4.12 | 4.22 | 4.07 | 4.08 | 4.17 | 5.45 |
| Entire residue picked? | Y | Y | Y | Y | Y | N | N |
| Sample facies | Fm | Fm | Fm | Fm | Fm | Fm | Gm |

Note:

Estimated quantities per gram represent the dry weight of the bulk sediment sample, except for the samples from 24 and 7 cm, where they are based on an estimate of processed residue (see Section 4.2.5.). Missing values are due to failure to quantify subsampled residue. The fragmentation index F was calculated as $F = A/(A + B)$ where A is the fragment count and B is absolute abundance.

Table A4: 198VC benthic foraminiferal count data (continued to page 172)

| Core: JC106-198VC | Sample depth (cm) | | | | | | | | |
|---------------------------------|-------------------|-----|-----|-----|-----|-----|-----|-----|-----|
| | 377 | 361 | 345 | 329 | 313 | 297 | 281 | 265 | 249 |
| Benthic species | | | | | | | | | |
| <i>Ammonia beccarii</i> | - | - | - | - | - | - | - | 1 | - |
| <i>Amphicoryna scalaris</i> | 1 | - | - | - | - | - | - | - | - |
| <i>Amphistegina lessonii</i> | 1 | 2 | 1 | - | - | - | - | - | - |
| <i>Astrononion gallowayi</i> | 2 | - | - | 1 | - | - | 1 | - | - |
| <i>Bolivinita quadrilatera</i> | - | - | - | 1 | - | - | - | - | - |
| <i>Brizalina</i> spp. | - | - | - | - | 1 | 2 | 3 | 4 | 4 |
| <i>Brizalina difformis</i> | 8 | 1 | - | 6 | - | 2 | 26 | 12 | 15 |
| <i>Brizalina pseudopunctata</i> | 1 | - | - | 2 | 1 | - | - | 3 | - |
| <i>Brizalina spathulata</i> | 4 | 8 | 6 | 5 | 3 | 6 | 3 | 5 | 8 |
| <i>Brizalina subaenariensis</i> | - | - | - | - | - | - | - | - | 1 |
| <i>Brizalina subspinescens</i> | - | - | - | 1 | - | - | - | - | - |
| <i>Brizalina variabilis</i> | 3 | - | - | - | - | - | - | - | - |
| <i>Buccella frigida</i> | 1 | - | - | 6 | - | 4 | 12 | 8 | 14 |
| <i>Bulimina aculeata</i> | 8 | 14 | 15 | 5 | 5 | 2 | - | - | - |
| <i>Bulimina elongata</i> | 6 | 1 | 2 | 3 | 3 | 2 | 2 | 5 | 1 |
| <i>Bulimina gibba</i> | 12 | 11 | 14 | 5 | 16 | 1 | 7 | 10 | 5 |
| <i>Bulimina marginata</i> | 35 | 25 | 29 | 19 | 27 | 18 | 17 | 39 | 32 |
| <i>Bulimina mexicana</i> | - | - | - | - | - | - | - | - | - |
| <i>Bulimina</i> spp. | - | - | - | - | - | - | - | - | - |
| <i>Bulimina striata</i> | - | 1 | 1 | - | - | - | - | - | - |
| <i>Carpenteria balaniformis</i> | - | - | - | - | - | - | - | - | - |
| <i>Cassidulina carinata</i> | - | - | - | - | - | - | - | - | - |
| <i>Cassidulina laevigata</i> | 24 | 24 | 14 | 11 | 33 | 18 | 9 | 6 | 16 |
| <i>Cassidulina neoteretis</i> | 7 | 1 | 5 | 18 | 6 | 31 | 16 | 19 | 19 |
| <i>Cassidulina reniforme</i> | 15 | 5 | 3 | 5 | 5 | 37 | 34 | 41 | 51 |
| <i>Cassidulinoides bradyi</i> | - | - | - | - | - | - | - | - | - |
| <i>Cibicides lobatulus</i> | 38 | 64 | 54 | 29 | 56 | 42 | 32 | 27 | 19 |
| <i>Cibicides refulgens</i> | 9 | 58 | 24 | 15 | 27 | 14 | 14 | 17 | 16 |
| <i>Cibicidoides pachyderma</i> | 2 | 18 | 3 | 4 | 7 | 2 | 3 | 7 | 1 |
| <i>Cibicidoides</i> spp. | 4 | 19 | 19 | 13 | 19 | 15 | 6 | 14 | 5 |
| <i>Cornuspira</i> sp. | - | - | - | - | - | - | - | - | - |
| <i>Discanomalina coronata</i> | - | 5 | 4 | 4 | 5 | 1 | 4 | 2 | - |
| <i>Eggerella bradyi</i> | - | - | - | - | - | - | - | - | - |
| <i>Elphidium advenum</i> | - | - | - | - | - | - | - | - | - |
| <i>Elphidium albumbilicatum</i> | - | - | - | - | - | - | - | - | - |

Appendix 1: Foraminiferal count data

| | | | | | | | | | |
|------------------------------------|----|----|----|----|----|----|----|----|----|
| <i>Elphidium excavatum</i> | 14 | 12 | 6 | 3 | 7 | 5 | 6 | 4 | 8 |
| <i>Elphidium clavatum</i> | 5 | 4 | - | 3 | 3 | 6 | 1 | 4 | 8 |
| <i>Elphidium crispum</i> | 1 | - | - | - | - | - | - | - | - |
| <i>Elphidium gerthi</i> | - | - | - | - | - | - | - | - | - |
| <i>Elphidium incertum</i> | - | - | - | - | - | - | - | - | - |
| <i>Elphidium spp.</i> | - | - | - | - | - | - | - | - | - |
| <i>Elphidium williamsoni</i> | - | - | - | - | - | - | - | - | - |
| <i>Fissurina orbignyana</i> | - | - | - | - | - | - | - | - | - |
| <i>Fissurina spp.</i> | - | - | - | - | - | - | - | - | - |
| <i>Fursenkoina sp.</i> | - | - | - | - | - | - | - | - | 1 |
| <i>Globocassidulina subglobosa</i> | 2 | - | 1 | 3 | 7 | 1 | 1 | 2 | 4 |
| <i>Guttulina communis</i> | - | - | 1 | 2 | - | 1 | - | - | - |
| <i>Gyroidina sp.</i> | - | - | - | - | - | - | - | - | - |
| <i>Hansenisca soldanii</i> | 4 | 4 | 2 | 6 | - | 2 | 1 | 3 | - |
| <i>Hyalinea baltica</i> | 2 | - | - | - | - | - | - | - | - |
| <i>Karreriella bradyi</i> | - | - | - | - | - | - | - | 1 | - |
| <i>Lagena sp.</i> | - | - | - | - | - | 1 | - | - | - |
| <i>Lagena striata</i> | - | - | - | - | - | - | - | - | - |
| <i>Lenticulina orbicularis</i> | - | 1 | - | - | - | - | - | - | - |
| <i>Lenticulina spp.</i> | 3 | 4 | - | - | 3 | 2 | 2 | 1 | 1 |
| <i>Lenticulina torrida</i> | - | - | - | - | - | - | - | - | - |
| <i>Melonis barleeaanum</i> | 6 | 16 | 8 | 9 | 10 | 4 | 6 | 8 | 6 |
| <i>Miliammina fusca</i> | 7 | 7 | 2 | 2 | - | - | 1 | 3 | - |
| <i>Miliolinella subrotunda</i> | - | - | - | - | - | 2 | - | - | - |
| <i>Miliolinella sp.</i> | - | - | - | - | - | - | - | - | - |
| <i>Nodosaria spp.</i> | - | - | - | - | - | - | - | - | - |
| <i>Nonionellina labradorica</i> | - | - | - | - | - | - | - | - | - |
| <i>Nonion spp.</i> | - | 1 | 1 | 3 | - | 2 | 1 | - | - |
| <i>Nonionella turgida</i> | - | - | - | - | - | - | - | - | - |
| <i>Oolina borealis</i> | - | 1 | - | - | - | - | - | - | - |
| <i>Oolina lineata</i> | - | - | - | - | - | - | - | - | - |
| <i>Oolina sp.</i> | - | - | - | - | - | - | 1 | - | - |
| <i>Parafissurina spp.</i> | - | - | 1 | - | 1 | 1 | - | - | - |
| <i>Planulina ariminensis</i> | - | - | 1 | 2 | 1 | 2 | 1 | 1 | 2 |
| <i>Pullenia bulloides</i> | 1 | 3 | 1 | 1 | - | 1 | 1 | - | - |
| <i>Pullenia quinqueloba</i> | - | 1 | 3 | - | - | - | 2 | - | - |
| <i>Pyrgo simplex</i> | - | - | - | - | - | - | 1 | - | - |
| <i>Pyrgo williamsoni</i> | 1 | 1 | - | - | - | 1 | - | 1 | - |
| <i>Quinqueloculina lata</i> | - | - | - | - | - | - | - | - | - |
| <i>Quinqueloculina seminula</i> | - | 3 | 7 | 2 | 8 | 2 | 3 | 4 | 1 |
| <i>Quinqueloculina spp.</i> | 3 | - | 2 | 2 | 2 | 4 | 2 | - | - |
| <i>Quinqueloculina stalkerii</i> | - | - | - | - | - | - | - | - | - |
| <i>Rosalina spp.</i> | - | - | - | 2 | - | - | 1 | - | 1 |
| <i>Sigmoilopsis schlumbergeri</i> | 2 | 2 | - | - | - | - | - | - | - |
| <i>Sphaeroidina bulloides</i> | 1 | - | - | - | 1 | - | 1 | - | - |
| <i>Stainforthia fusiformis</i> | - | - | - | - | - | - | 1 | 1 | - |
| <i>Textularia sagittula</i> | 2 | 5 | 6 | 4 | 3 | 1 | 2 | - | 1 |
| <i>Textularia truncata</i> | 1 | - | 1 | - | 1 | - | - | 1 | - |
| <i>Textularia spp.</i> | 3 | 4 | 5 | 5 | 5 | 3 | 3 | 4 | 2 |
| <i>Trifarina angulosa</i> | 64 | 71 | 53 | 39 | 84 | 65 | 41 | 13 | 64 |
| <i>Trifarina sp.</i> | 1 | - | - | 1 | - | 1 | - | - | - |
| <i>Triloculina angusteoralis</i> | - | - | - | - | - | - | - | - | - |
| <i>Triloculina sp.</i> | - | 1 | - | - | - | - | - | - | - |
| <i>Triloculina trigonula</i> | - | - | - | - | - | - | - | - | - |
| <i>Uvigerina mediterranea</i> | 3 | 1 | 9 | 4 | 2 | 3 | 4 | 12 | 2 |
| <i>Uvigerina peregrina</i> | 31 | 47 | 24 | 46 | 32 | 20 | 28 | 25 | 8 |
| <i>Uvigerina sp.</i> | - | - | - | - | - | - | - | - | - |
| Unidentified spp. | 8 | 19 | 8 | 12 | 5 | 15 | 16 | 10 | 12 |

Appendix 1: Foraminiferal count data

| Core: JC106-198VC | Sample depth (cm) | | | | | | | | |
|------------------------------------|-------------------|-----|-----|-----|-----|-----|-----|-----|-----|
| | 233 | 217 | 201 | 185 | 169 | 153 | 137 | 121 | 105 |
| Benthic species | | | | | | | | | |
| <i>Ammonia beccarii</i> | 2 | - | - | - | 1 | - | - | 1 | - |
| <i>Amphicoryna scalaris</i> | - | - | - | - | - | - | - | - | - |
| <i>Amphistegina lessonii</i> | - | - | 1 | - | - | - | - | - | - |
| <i>Astrononion gallowayi</i> | - | - | - | - | 1 | 1 | - | 2 | 7 |
| <i>Bolivinita quadrilatera</i> | - | - | - | - | - | 1 | - | - | - |
| <i>Brizalina</i> spp. | 3 | 5 | - | 1 | 4 | - | 1 | 1 | 1 |
| <i>Brizalina difformis</i> | 9 | 3 | 1 | - | 1 | 1 | - | 1 | 1 |
| <i>Brizalina pseudopunctata</i> | 1 | 1 | - | - | - | - | - | - | - |
| <i>Brizalina spathulata</i> | 6 | 7 | 4 | 8 | 6 | 7 | 16 | 8 | 13 |
| <i>Brizalina subaenariensis</i> | - | - | - | - | 2 | - | - | - | - |
| <i>Brizalina subspinescens</i> | 2 | 1 | 3 | 4 | 2 | 2 | 1 | 2 | - |
| <i>Brizalina variabilis</i> | 1 | 1 | - | - | 1 | - | - | 1 | 2 |
| <i>Buccella frigida</i> | 17 | 14 | 19 | 15 | 11 | 4 | 11 | 9 | 7 |
| <i>Bulimina aculeata</i> | 1 | - | - | - | - | 15 | 6 | 2 | 5 |
| <i>Bulimina elongata</i> | 1 | 1 | 2 | 5 | 1 | - | 1 | - | 1 |
| <i>Bulimina gibba</i> | 2 | 6 | 2 | 6 | 4 | 5 | 7 | 5 | 7 |
| <i>Bulimina marginata</i> | 34 | 22 | 14 | 25 | 19 | 24 | 29 | 19 | 9 |
| <i>Bulimina mexicana</i> | - | - | - | - | - | - | - | - | - |
| <i>Bulimina</i> spp. | - | - | - | - | - | - | - | - | - |
| <i>Bulimina striata</i> | - | - | - | - | - | - | 1 | 1 | 1 |
| <i>Carpenteria balaniformis</i> | - | - | - | - | - | - | - | - | - |
| <i>Cassidulina carinata</i> | - | - | - | - | - | - | - | - | - |
| <i>Cassidulina laevigata</i> | 9 | 16 | 10 | 16 | 18 | 34 | 7 | 10 | 33 |
| <i>Cassidulina neoteretis</i> | 40 | 21 | 34 | 39 | 103 | 57 | 52 | 54 | 56 |
| <i>Cassidulina reniforme</i> | 45 | 35 | 55 | 54 | 268 | 71 | 63 | 75 | 79 |
| <i>Cassidulinoides bradyi</i> | - | - | - | - | - | - | - | - | 1 |
| <i>Cibicides lobatulus</i> | 46 | 71 | 62 | 104 | 19 | 53 | 30 | 38 | 33 |
| <i>Cibicides refulgens</i> | 15 | 27 | 36 | 80 | 10 | 25 | 10 | 19 | 19 |
| <i>Cibicidoides pachyderma</i> | 2 | 5 | 6 | 15 | - | 7 | 1 | 2 | - |
| <i>Cibicidoides</i> spp. | 11 | 17 | 23 | 27 | 7 | 13 | 6 | 19 | 7 |
| <i>Cornuspira</i> sp. | - | - | - | - | - | - | - | - | - |
| <i>Discanomalina coronata</i> | 6 | 15 | 17 | 26 | - | 1 | 3 | 7 | 1 |
| <i>Edgella bradyi</i> | - | - | 1 | - | - | - | - | 1 | 1 |
| <i>Elphidium advenum</i> | - | - | 1 | - | - | - | - | - | - |
| <i>Elphidium albiumbilicatum</i> | 1 | - | - | - | - | - | - | - | 1 |
| <i>Elphidium excavatum</i> | 12 | 5 | 10 | 10 | 53 | 17 | 21 | 22 | 16 |
| <i>Elphidium clavatum</i> | 4 | 8 | 5 | 5 | 37 | 35 | 16 | 20 | 22 |
| <i>Elphidium crispum</i> | - | - | - | - | - | - | - | - | - |
| <i>Elphidium gerthi</i> | - | - | - | 2 | - | - | - | - | - |
| <i>Elphidium incertum</i> | - | - | - | 1 | - | - | - | - | - |
| <i>Elphidium</i> spp. | - | - | - | - | - | 4 | - | - | 1 |
| <i>Elphidium williamsoni</i> | - | - | - | 1 | - | - | - | - | - |
| <i>Fissurina orbignyana</i> | - | - | - | - | - | - | - | - | - |
| <i>Fissurina</i> spp. | - | 2 | 3 | - | 3 | 2 | 2 | 1 | 1 |
| <i>Fursenkoina</i> sp. | 1 | 1 | - | - | - | - | - | - | - |
| <i>Globocassidulina subglobosa</i> | 5 | 5 | 5 | 2 | 7 | 6 | 10 | 13 | 26 |
| <i>Guttulina communis</i> | - | - | 2 | - | - | - | - | - | - |
| <i>Gyroidina</i> sp. | - | - | - | - | - | - | - | - | - |
| <i>Hansenisca soldanii</i> | 3 | 2 | 1 | 2 | - | 5 | 2 | 2 | 2 |
| <i>Hyalinea baltica</i> | - | - | - | - | 2 | 6 | - | - | 1 |
| <i>Karrerella bradyi</i> | - | - | 1 | - | - | 1 | - | - | - |
| <i>Lagena</i> sp. | - | - | - | - | - | - | - | - | - |
| <i>Lagena striata</i> | 1 | - | - | - | - | - | - | - | - |
| <i>Lenticulina orbicularis</i> | - | - | - | - | - | - | - | - | - |
| <i>Lenticulina</i> spp. | 1 | - | 1 | - | - | 1 | 1 | 2 | 1 |
| <i>Lenticulina torrida</i> | - | - | - | - | - | 1 | - | - | - |
| <i>Melonis barleeaanum</i> | 10 | 5 | 6 | 9 | 7 | 13 | 7 | 7 | 5 |
| <i>Miliammina fusca</i> | 2 | 4 | 12 | 4 | - | 4 | 3 | 2 | 1 |
| <i>Miliolinella subrotunda</i> | 3 | - | - | - | - | - | - | 1 | - |
| <i>Miliolinella</i> sp. | - | - | - | - | 1 | - | - | - | - |
| <i>Nodosaria</i> spp. | - | - | - | - | - | - | - | - | - |
| <i>Nonionellina labradorica</i> | - | - | - | - | 4 | 6 | - | - | 3 |
| <i>Nonion</i> spp. | 3 | 1 | - | 1 | 1 | 1 | - | - | 1 |
| <i>Nonionella turgida</i> | - | - | - | - | - | - | - | - | - |
| <i>Oolina borealis</i> | - | - | - | - | - | - | - | - | - |

Appendix 1: Foraminiferal count data

| | | | | | | | | | |
|-----------------------------------|----|----|----|----|----|----|----|----|----|
| <i>Oolina lineata</i> | - | - | - | - | - | - | 1 | - | - |
| <i>Oolina sp.</i> | - | - | - | - | - | 1 | - | - | - |
| <i>Parafissurina spp.</i> | - | - | - | - | - | - | - | - | - |
| <i>Planulina ariminensis</i> | 3 | 4 | 2 | 3 | - | 3 | 1 | - | 1 |
| <i>Pullenia bulloides</i> | 1 | - | 2 | 1 | - | 3 | 2 | - | - |
| <i>Pullenia quinqueloba</i> | 2 | - | - | 3 | 8 | 3 | 1 | - | - |
| <i>Pyrgo simplex</i> | - | - | - | - | - | - | - | - | - |
| <i>Pyrgo williamsoni</i> | - | - | - | - | - | - | - | - | - |
| <i>Quinqueloculina lata</i> | - | - | - | - | - | - | - | 1 | - |
| <i>Quinqueloculina seminula</i> | 3 | 10 | 7 | 12 | 2 | 2 | - | 1 | 1 |
| <i>Quinqueloculina spp.</i> | 2 | - | 1 | - | 2 | - | - | - | 1 |
| <i>Quinqueloculina stalkerii</i> | - | - | - | - | - | - | - | 2 | - |
| <i>Rosalina spp.</i> | - | 1 | 1 | - | 1 | - | - | - | 1 |
| <i>Sigmoilopsis schlumbergeri</i> | 1 | 2 | 2 | 2 | 1 | - | 1 | 1 | - |
| <i>Sphaeroidina bulloides</i> | - | - | 1 | - | - | - | - | 1 | 1 |
| <i>Stainforthia fusiformis</i> | - | - | - | - | - | - | - | - | - |
| <i>Textularia sagittula</i> | 3 | 9 | 7 | 8 | - | 1 | - | - | - |
| <i>Textularia truncata</i> | - | 3 | 1 | - | 2 | 1 | - | - | - |
| <i>Textularia spp.</i> | 8 | - | 8 | 9 | - | 2 | 4 | 5 | 4 |
| <i>Trifarina angulosa</i> | 57 | 58 | 35 | 48 | 43 | 85 | 55 | 23 | 54 |
| <i>Trifarina sp.</i> | - | - | - | - | - | - | - | - | - |
| <i>Triloculina angusteoralis</i> | - | 1 | - | - | - | - | - | - | - |
| <i>Triloculina sp.</i> | - | - | 1 | - | - | - | - | - | - |
| <i>Triloculina trigonula</i> | - | - | - | - | - | 1 | - | - | - |
| <i>Uvigerina mediterranea</i> | 8 | 16 | 24 | 14 | - | 13 | 16 | 18 | 7 |
| <i>Uvigerina peregrina</i> | 30 | 53 | 42 | 74 | 1 | 17 | 9 | 28 | 5 |
| <i>Uvigerina sp.</i> | - | - | - | - | - | - | - | - | 1 |
| Unidentified spp. | 34 | 21 | 18 | 23 | 17 | 19 | 12 | 23 | 15 |

| Core: JC106-198VC | Sample depth (cm) | | | | | |
|----------------------------------|-------------------|-----------|-----------|-----------|-----------|----------|
| | 89 | 73 | 57 | 41 | 25 | 9 |
| Benthic species | 89 | 73 | 57 | 41 | 25 | 9 |
| <i>Ammonia beccarii</i> | - | 2 | - | - | 1 | - |
| <i>Amphicoryna scalaris</i> | - | - | - | 1 | 1 | 2 |
| <i>Amphistegina lessonii</i> | - | - | - | - | - | - |
| <i>Astrononion gallowayi</i> | 1 | 2 | 1 | - | 3 | - |
| <i>Bolivinita quadrilatera</i> | - | - | - | - | - | - |
| <i>Brizalina spp.</i> | - | - | 1 | 1 | 2 | - |
| <i>Brizalina difformis</i> | 1 | - | 12 | 14 | 9 | 13 |
| <i>Brizalina pseudopunctata</i> | - | - | - | 1 | - | - |
| <i>Brizalina spathulata</i> | 10 | 3 | 4 | 8 | 14 | 17 |
| <i>Brizalina subaenariensis</i> | - | 1 | - | 1 | - | - |
| <i>Brizalina subspinescens</i> | 1 | - | - | 1 | - | 1 |
| <i>Brizalina variabilis</i> | 1 | 1 | 1 | - | - | - |
| <i>Buccella frigida</i> | 6 | 9 | 11 | 2 | 3 | 11 |
| <i>Bulimina aculeata</i> | 3 | 6 | - | 1 | 3 | 1 |
| <i>Bulimina elongata</i> | 3 | 5 | - | 1 | - | - |
| <i>Bulimina gibba</i> | 4 | 16 | - | 3 | 2 | - |
| <i>Bulimina marginata</i> | 18 | 43 | 16 | 113 | 48 | 60 |
| <i>Bulimina mexicana</i> | 1 | - | - | - | - | 1 |
| <i>Bulimina spp.</i> | - | - | 1 | 1 | - | - |
| <i>Bulimina striata</i> | - | - | - | 1 | 1 | - |
| <i>Carpenteria balaniformis</i> | - | 1 | - | - | - | - |
| <i>Cassidulina carinata</i> | - | - | 3 | 24 | 28 | 46 |
| <i>Cassidulina laevigata</i> | 31 | 22 | 22 | 68 | 55 | 84 |
| <i>Cassidulina neoteretis</i> | 60 | 39 | 74 | 28 | 29 | 48 |
| <i>Cassidulina reniforme</i> | 44 | 55 | 118 | 60 | 44 | 57 |
| <i>Cassidulinoides bradyi</i> | - | - | 1 | 1 | - | 1 |
| <i>Cibicides lobatulus</i> | 28 | 34 | 17 | 16 | 12 | 8 |
| <i>Cibicides refulgens</i> | 21 | 17 | 4 | 5 | 4 | 6 |
| <i>Cibicidoides pachyderma</i> | 2 | 3 | 1 | - | - | - |
| <i>Cibicidoides spp.</i> | 3 | 15 | 1 | 2 | 2 | - |
| <i>Cornuspira sp.</i> | - | 1 | - | - | - | - |
| <i>Discanomalina coronata</i> | 4 | 1 | 1 | - | 1 | - |
| <i>Eggerella bradyi</i> | - | - | - | - | - | - |
| <i>Elphidium advenum</i> | - | - | - | - | - | - |
| <i>Elphidium albiumbilicatum</i> | 1 | - | - | 1 | - | - |
| <i>Elphidium excavatum</i> | 50 | 26 | 20 | 11 | 15 | 10 |

Appendix 1: Foraminiferal count data

| | | | | | | |
|------------------------------------|----|----|----|----|----|----|
| <i>Elphidium clavatum</i> | 45 | 11 | 16 | 4 | 9 | 15 |
| <i>Elphidium crispum</i> | - | - | - | - | - | - |
| <i>Elphidium gerthi</i> | - | - | - | - | - | - |
| <i>Elphidium incertum</i> | - | - | - | - | - | - |
| <i>Elphidium spp.</i> | 1 | 1 | - | - | - | - |
| <i>Elphidium williamsoni</i> | - | - | - | - | - | - |
| <i>Fissurina orbignyana</i> | - | - | 1 | - | - | - |
| <i>Fissurina spp.</i> | 3 | 2 | 1 | 2 | - | 4 |
| <i>Fursenkoina sp.</i> | - | 1 | - | - | - | - |
| <i>Globocassidulina subglobosa</i> | 12 | 25 | 23 | 9 | 13 | 18 |
| <i>Guttulina communis</i> | - | - | - | - | - | - |
| <i>Gyroidina sp.</i> | - | - | - | 1 | - | - |
| <i>Hansenisca soldanii</i> | 2 | 2 | 2 | 1 | 2 | - |
| <i>Hyalinea baltica</i> | 3 | - | 5 | 16 | 13 | 16 |
| <i>Karrerella bradyi</i> | - | - | - | - | - | - |
| <i>Lagena sp.</i> | - | - | - | - | - | - |
| <i>Lagena striata</i> | - | - | - | - | - | - |
| <i>Lenticulina orbicularis</i> | - | - | - | - | - | - |
| <i>Lenticulina spp.</i> | 1 | 2 | - | - | - | - |
| <i>Lenticulina torrida</i> | - | - | - | - | - | - |
| <i>Melonis barleeenum</i> | 3 | 7 | 2 | 5 | 2 | 5 |
| <i>Miliammina fusca</i> | 1 | 3 | - | - | - | - |
| <i>Miliolinella subrotunda</i> | 1 | 1 | 1 | - | - | - |
| <i>Miliolinella sp.</i> | - | 1 | - | - | - | - |
| <i>Nodosaria spp.</i> | - | - | - | 1 | - | - |
| <i>Nonionellina labradorica</i> | 1 | 1 | - | - | - | - |
| <i>Nonion spp.</i> | 2 | - | 1 | 1 | - | 1 |
| <i>Nonionella turgida</i> | - | - | - | 1 | 1 | 1 |
| <i>Oolina borealis</i> | - | - | - | - | - | - |
| <i>Oolina lineata</i> | - | 1 | - | - | - | - |
| <i>Oolina sp.</i> | - | - | - | - | - | - |
| <i>Parafissurina spp.</i> | - | - | - | - | - | - |
| <i>Planulina ariminensis</i> | 1 | 2 | - | - | - | - |
| <i>Pullenia bulloides</i> | 3 | 9 | - | 2 | 2 | 2 |
| <i>Pullenia quinqueloba</i> | 1 | 1 | 3 | 1 | 1 | 3 |
| <i>Pyrgo simplex</i> | - | - | - | - | - | - |
| <i>Pyrgo williamsoni</i> | 1 | - | - | - | - | - |
| <i>Quinqueloculina lata</i> | - | - | - | - | - | - |
| <i>Quinqueloculina seminula</i> | 1 | 3 | - | - | - | - |
| <i>Quinqueloculina spp.</i> | - | 1 | - | - | - | - |
| <i>Quinqueloculina stalkerii</i> | - | - | - | - | 2 | - |
| <i>Rosalina spp.</i> | - | - | - | - | 2 | - |
| <i>Sigmoilopsis schlumbergeri</i> | 1 | - | 1 | - | - | - |
| <i>Sphaeroidina bulloides</i> | - | - | 1 | 1 | - | - |
| <i>Stainforthia fusiformis</i> | - | - | - | - | - | - |
| <i>Textularia sagittula</i> | - | 1 | - | - | - | - |
| <i>Textularia truncata</i> | - | 2 | - | 6 | 4 | 4 |
| <i>Textularia spp.</i> | 2 | 5 | 2 | 22 | 7 | 3 |
| <i>Trifarina angulosa</i> | 70 | 47 | 21 | 49 | 34 | 51 |
| <i>Trifarina sp.</i> | - | - | - | - | - | - |
| <i>Triloculina angusteoralis</i> | - | - | - | - | - | - |
| <i>Triloculina sp.</i> | - | - | - | - | - | - |
| <i>Triloculina trigonula</i> | - | - | - | - | - | - |
| <i>Uvigerina mediterranea</i> | 6 | 19 | 6 | 18 | 7 | 7 |
| <i>Uvigerina peregrina</i> | 13 | 13 | 14 | 58 | 60 | 19 |
| <i>Uvigerina sp.</i> | - | - | - | 1 | - | - |
| Unidentified spp. | 23 | 21 | 27 | 15 | 21 | 11 |

Table A5: 198VC planktic foraminiferal count data

| Core: JC106-198VC | Sample depth (cm) | | | | | | | | |
|--------------------------------------|-------------------|-----|-----|-----|-----|-----|-----|-----|-----|
| Planktic species | 377 | 361 | 345 | 329 | 313 | 297 | 281 | 265 | 249 |
| <i>Globigerina bulloides</i> | 23 | 14 | 7 | 22 | 17 | 19 | 30 | 15 | 18 |
| <i>Globigerinella siphonifera</i> | 4 | 16 | 7 | 6 | 7 | 13 | 14 | 29 | 20 |
| <i>Globigerinita glutinata</i> | 13 | 8 | 8 | 14 | 17 | 4 | 8 | 7 | 12 |
| <i>Globigerinita uvula</i> | - | 1 | - | - | - | - | - | - | - |
| <i>Globorotalia hirsuta</i> | - | 1 | - | - | - | - | - | - | - |
| <i>Globorotalia inflata</i> | 11 | 11 | 16 | 8 | 14 | 5 | 11 | 3 | 3 |
| <i>Globorotalia truncatulinoides</i> | - | 1 | - | - | 1 | - | - | - | 1 |
| <i>Globorotalia scitula</i> | 2 | 4 | 1 | 5 | 4 | 11 | 3 | 7 | 5 |
| <i>Neogloboquadrina dutertrei</i> | - | - | 4 | 13 | 2 | - | - | 1 | - |
| <i>Neogloboquadrina incompta</i> | 36 | 20 | 27 | 20 | 15 | 23 | 22 | 11 | 15 |
| <i>Neogloboquadrina pachyderma</i> | 155 | 116 | 121 | 122 | 119 | 125 | 110 | 98 | 101 |
| <i>Orbulina universa</i> | - | - | - | - | - | - | - | - | - |
| <i>Trilobatus trilobus</i> | - | - | - | - | 1 | - | 1 | - | - |
| <i>Turborotalita quinqueloba</i> | 9 | 33 | 14 | 21 | 20 | 31 | 21 | 33 | 38 |
| Unidentified spp. | 18 | 21 | 21 | 21 | 27 | 22 | 13 | 26 | 24 |

| Core: JC106-198VC | Sample depth (cm) | | | | | | | | |
|--------------------------------------|-------------------|-----|-----|-----|-----|-----|-----|-----|-----|
| Planktic species | 233 | 217 | 201 | 185 | 169 | 153 | 137 | 121 | 105 |
| <i>Globigerina bulloides</i> | 24 | 49 | 42 | 46 | 26 | 30 | 19 | 46 | 13 |
| <i>Globigerinella siphonifera</i> | 39 | 8 | 23 | 19 | 54 | 11 | 19 | 31 | 23 |
| <i>Globigerinita glutinata</i> | 4 | 1 | - | 3 | 17 | 21 | 16 | 16 | 12 |
| <i>Globigerinita uvula</i> | - | - | - | - | - | - | - | - | 1 |
| <i>Globorotalia hirsuta</i> | - | - | - | - | - | 1 | 1 | 1 | - |
| <i>Globorotalia inflata</i> | 6 | 9 | 19 | 18 | 2 | 14 | 7 | 16 | 6 |
| <i>Globorotalia truncatulinoides</i> | 1 | - | - | 1 | - | - | - | - | - |
| <i>Globorotalia scitula</i> | 13 | 4 | 3 | 9 | 11 | 3 | 2 | 5 | 4 |
| <i>Neogloboquadrina dutertrei</i> | - | 3 | 1 | - | - | 17 | 8 | 9 | 3 |
| <i>Neogloboquadrina incompta</i> | 18 | 15 | 17 | 28 | 20 | 30 | 22 | 18 | 23 |
| <i>Neogloboquadrina pachyderma</i> | 73 | 119 | 124 | 115 | 109 | 202 | 86 | 163 | 78 |
| <i>Orbulina universa</i> | - | - | 1 | - | - | - | - | - | - |
| <i>Trilobatus trilobus</i> | 1 | - | - | - | 1 | - | 1 | 1 | 1 |
| <i>Turborotalita quinqueloba</i> | 23 | 7 | 24 | 34 | 35 | 12 | 20 | 31 | 34 |
| Unidentified spp. | 22 | 21 | 42 | 36 | 39 | 43 | 21 | 33 | 42 |

| Core: JC106-198VC | Sample depth (cm) | | | | | |
|--------------------------------------|-------------------|-----|----|-----|----|----|
| Planktic species | 89 | 73 | 57 | 41 | 25 | 9 |
| <i>Globigerina bulloides</i> | 30 | 51 | 9 | 21 | 13 | 4 |
| <i>Globigerinella siphonifera</i> | 18 | 16 | 43 | 22 | 9 | 4 |
| <i>Globigerinita glutinata</i> | 11 | 32 | 52 | 61 | 28 | 48 |
| <i>Globigerinita uvula</i> | 1 | - | 6 | - | 3 | 1 |
| <i>Globorotalia hirsuta</i> | - | - | - | - | - | - |
| <i>Globorotalia inflata</i> | 13 | 13 | 10 | 10 | 13 | 6 |
| <i>Globorotalia truncatulinoides</i> | - | 1 | - | 1 | 1 | - |
| <i>Globorotalia scitula</i> | 2 | - | 6 | 7 | 7 | 11 |
| <i>Neogloboquadrina dutertrei</i> | 16 | 28 | 6 | 4 | 3 | 8 |
| <i>Neogloboquadrina incompta</i> | 11 | 27 | 24 | 107 | 95 | 81 |
| <i>Neogloboquadrina pachyderma</i> | 146 | 251 | 41 | 62 | 63 | 38 |
| <i>Orbulina universa</i> | - | - | 1 | 1 | 2 | - |
| <i>Trilobatus trilobus</i> | - | - | - | - | - | - |
| <i>Turborotalita quinqueloba</i> | 15 | 15 | 51 | 30 | 35 | 36 |
| Unidentified spp. | 30 | 33 | 31 | 25 | 21 | 23 |

Table A6: 198VC foraminiferal sample statistics

| Core: JC106-198VC | Sample depth (cm) | | | | | | | | |
|--|-------------------|------------------|------------------|------------------|------------------|------------------|------------------|------------------|------------------|
| | 377 | 361 | 345 | 329 | 313 | 297 | 281 | 265 | 249 |
| Total benthic | 346 | 465 | 336 | 304 | 389 | 342 | 316 | 318 | 328 |
| Total planktic | 271 | 246 | 226 | 252 | 244 | 253 | 233 | 230 | 237 |
| Absolute abundance | 617 | 711 | 562 | 556 | 633 | 595 | 549 | 548 | 565 |
| Estimated tests · gram ⁻¹ | 4168.9 | 4804.1 | 3797.3 | 3756.8 | 4277.0 | 4020.3 | 3709.5 | 3702.7 | 3817.6 |
| Fragment count | 69 | 99 | 92 | 70 | 90 | 119 | 137 | 146 | 224 |
| Fragmentation index | 0.10 | 0.12 | 0.14 | 0.11 | 0.12 | 0.27 | 0.20 | 0.21 | 0.38 |
| Estimated fragments · gram ⁻¹ | 466.2 | 668.9 | 621.6 | 473.0 | 608.1 | 804.1 | 925.7 | 986.5 | 1513.5 |
| Residue weight (g) | 0.92 | 0.75 | 0.49 | 0.43 | 0.44 | 0.62 | 0.73 | 0.58 | 0.69 |
| Dry bulk sample weight (g) | 3.04 | 2.99 | 2.94 | 3.08 | 2.97 | 2.96 | 3.02 | 2.85 | 2.88 |
| Entire residue picked? | N | N | N | N | N | N | N | N | N |
| Sample facies | Fld _c | Fld _c | Fld _c | Fld _c | Fld _c | Fld _c | Fld _c | Fld _c | Fld _c |

| Core: JC106-198VC | Sample depth (cm) | | | | | | | | |
|--|-------------------|--------|---------|---------|---------|---------|---------|--------|--------|
| | 233 | 217 | 201 | 185 | 169 | 153 | 137 | 121 | 105 |
| Total benthic | 451 | 479 | 489 | 659 | 670 | 574 | 409 | 450 | 456 |
| Total planktic | 224 | 236 | 296 | 309 | 314 | 384 | 222 | 370 | 240 |
| Absolute abundance | 675 | 715 | 785 | 968 | 984 | 958 | 631 | 820 | 696 |
| Estimated tests · gram ⁻¹ | 9121.6 | 9662.2 | 10608.1 | 17789.8 | 15789.4 | 13075.2 | 12524.6 | 8220.7 | 7905.4 |
| Fragment count | 248 | 243 | 253 | 138 | 167 | 124 | 137 | 122 | 195 |
| Fragmentation index | 0.27 | 0.25 | 0.24 | 0.12 | 0.15 | 0.11 | 0.18 | 0.13 | 0.22 |
| Estimated fragments · gram ⁻¹ | 3351.4 | 3283.8 | 4558.6 | 4336.9 | 4339.9 | 2295.5 | 4628.4 | 2747.8 | 3293.9 |
| Residue weight (g) | 1.21 | 1.59 | 1.78 | 1.67 | 0.60 | 0.75 | 0.76 | 0.69 | 0.62 |
| Dry bulk sample weight (g) | 4.62 | 4.91 | 4.94 | 5.05 | 2.86 | 2.96 | 2.91 | 2.86 | 2.82 |
| Entire residue picked? | N | N | N | N | N | N | N | N | N |
| Sample facies | Dms | Dms | Dms | Dms | Fm | Fm | Fm | Fm | Fm |

| Core: JC106-198VC | Sample depth (cm) | | | | | |
|--|-------------------|---------|--------|---------|---------|---------|
| | 89 | 73 | 57 | 41 | 25 | 9 |
| Total benthic | 490 | 484 | 436 | 579 | 457 | 526 |
| Total planktic | 293 | 467 | 280 | 351 | 293 | 260 |
| Absolute abundance | 783 | 951 | 716 | 930 | 750 | 786 |
| Estimated tests · gram ⁻¹ | 8844.4 | 14711.7 | 6911.2 | 39177.3 | 18383.6 | 37918.8 |
| Fragment count | 164 | 93 | 138 | 174 | 128 | 208 |
| Fragmentation index | 0.17 | 0.09 | 0.16 | 0.16 | 0.15 | 0.21 |
| Estimated fragments · gram ⁻¹ | 2770.3 | 2244.2 | 6343.1 | 13750.6 | 10810.8 | 16731.0 |
| Residue weight (g) | 0.57 | 0.67 | 0.75 | 1.89 | 2.15 | 2.08 |
| Dry bulk sample weight (g) | 2.80 | 2.86 | 2.74 | 3.00 | 3.01 | 2.93 |
| Entire residue picked? | N | N | N | N | N | N |
| Sample facies | Fm | Fm | Fm | Sm | Sm | Sm |

Note:

Estimated quantities per gram are computed based on an estimate of the weight of residue processed, maintaining full counting tray quantities of residue at ~0.074 g (see Section 4.2.5.). The fragmentation index F was calculated as $F = A/(A + B)$ where A is the fragment count and B is absolute test abundance.

Appendix 2: Faunal data plots including species accounting for $\geq 2\%$ relative abundance

Core 146VC

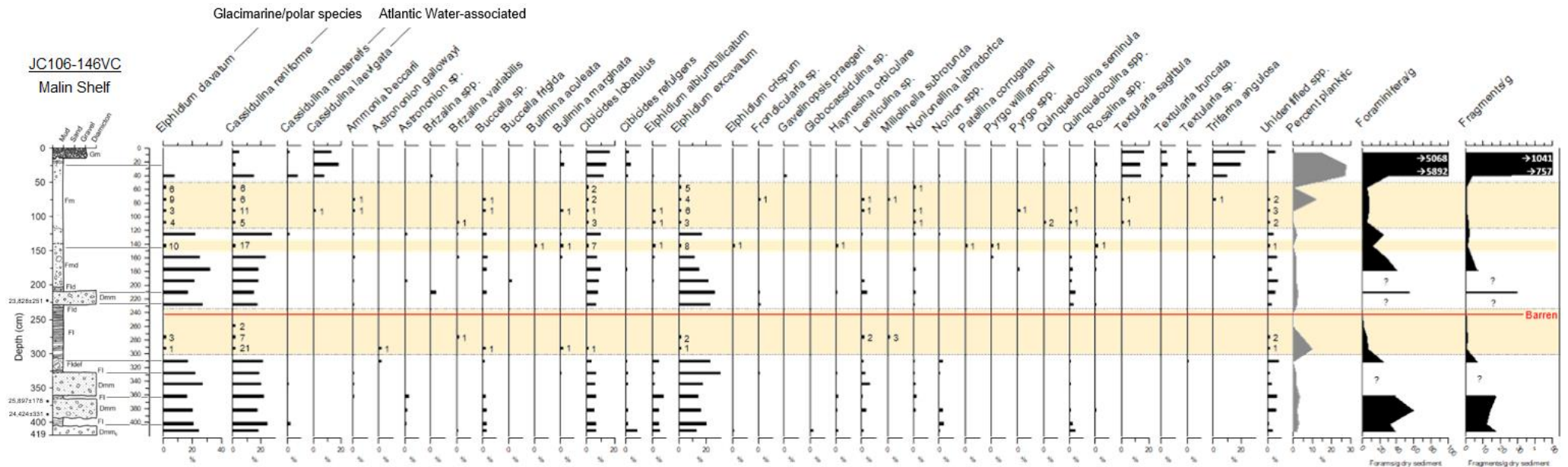


Fig. A1.: Benthic foraminiferal species abundance for species comprising $\geq 2\%$ of the total (calcareous + agglutinated) benthic assemblage in 146VC. Abundance is presented as absolute counts for samples with low abundance (2-51 individuals). Low-abundance intervals are highlighted in yellow. The red line marks a barren sample at 242 cm. Numbers in white give the quantity of tests and test fragments per gram for the uppermost two samples (note 10^2 -fold increase in these values). Question marks represent samples lacking this data (345, 328, 228 and 194 cm). Solid grey lines extending to the log clarify the sampled facies.

Appendix 3: Foraminiferal species lists

Core 146VC

 Calcareous benthic taxa

Ammonia beccarii Linnaeus, 1758
Amphicoryna scalaris Batsch, 1791
Astacolus spp.
Asteriginata mamilla Williamson, 1848
Astrononion gallowayi Loeblich & Tappan, 1953
Astrononion sp.
Brizalina spp.
Brizalina pseudopunctata Höglund, 1947
Brizalina variabilis Williamson, 1858
Buccella sp.
Buccella frigida Cushman, 1921
Bulimina aculeata d'Orbigny, 1826
Bulimina elongata d'Orbigny, 1846
Bulimina marginata d'Orbigny, 1826
Bulimina spp.
Cancris sp.
Cassidulina laevigata d'Orbigny, 1826
Cassidulina neoteretis Seidenkrantz, 1995
Cassidulina reniforme Nørvang, 1945
Cibicides lobatulus Walker & Jacob, 1798
Cibicides refulgens de Montfort, 1808
Dentalina sp.
Discorbis sp.
Elphidium advenum Cushman, 1922
Elphidium albiumbilicatum Weiss, 1954
Elphidium excavatum Terquem, 1875
Elphidium clavatum Cushman, 1930
Elphidium crispum Linnaeus, 1758
Elphidium spp.
Fronicularia sp.
Fursenkoina sp.
Gavelinopsis praegeri Heron-Allen & Earland, 1913
Glabratella wrightii Brady, 1881
Globobulimina sp.
Globocassidulina sp.
Haynesina orbiculare Brady, 1881
Hyalinea baltica Schröter, 1783
Lagena sp.

Lagena semistriata Williamson, 1848
Lagena striata d'Orbigny, 1839
Lenticulina spp.
Massilina sp.
Melonis barleeianum Williamson, 1858
Miliolinella subrotunda Montagu, 1803
Miliolinella sp.
Neoconorbina sp.
Nodosaria spp.
Nonionellina labradorica Dawson, 1860
Nonion spp.
Nonionella turgida Williamson, 1858
Oolina borealis Loeblich & Tappan, 1954
Oolina lineata Williamson, 1848
Oolina sp.
Parafissurina spp.
Patellina corrugata Williamson, 1858
Pyrgo murrhina Schwager, 1866
Pyrgo simplex d'Orbigny, 1846
Pyrgo williamsoni Silvestri, 1923
Pyrgo spp.
Quinqueloculina seminula Linnaeus, 1758
Quinqueloculina spp.
Rosalina spp.
Spirillina spp.
Spiroloculina excavata d'Orbigny, 1846
Spiroloculina spp.
Stainforthia concava Höglund, 1947
Stainforthia fusiformis Williamson, 1858
Trifarina angulosa Williamson, 1858
Trifarina sp.
Uvigerina sp.

Agglutinated (benthic) taxa

Textularia sagittula DeFrance, 1824 (morphological group of Murray 1971)
Textularia truncata Höglund, 1947
Textularia sp.

Planktic taxa

Globigerina bulloides d'Orbigny, 1826
Globigerina spp.
Globorotalia truncatulinoides d'Orbigny, 1839
Neogloboquadrina pachyderma Ehrenberg, 1861
Neogloboquadrina sp.
Orbulina universa d'Orbigny, 1839

Table A7: List of foraminiferal species identified in core 146VC. See Section 4.2.3. for taxonomic references used.

Core 198VC

Calcareous benthic taxa

Ammonia beccarii Linnaeus, 1758
Amphicoryna scalaris Batsch, 1791
Amphistegina lessonii d'Orbigny, 1843
Astrononion stelligerum d'Orbigny, 1839
Astrononion sp.
Bolivinita quadrilatera Schwager, 1866
Brizalina spp.
Brizalina difformis Williamson, 1858
Brizalina pseudopunctata Höglund, 1947
Brizalina spathulata Williamson, 1858
Brizalina subaenariensis Cushman, 1922
Brizalina subspinescens Cushman, 1922
Brizalina variabilis Williamson, 1858
Buccella frigida Cushman, 1921
Bulimina aculeata d'Orbigny, 1826
Bulimina elongata d'Orbigny, 1846
Bulimina gibba Fornasini, 1902
Bulimina marginata d'Orbigny, 1826
Bulimina mexicana Cushman, 1922
Bulimina spp.
Bulimina striata d'Orbigny, 1843
Carpenteria balaniformis Gray, 1858
Cassidulina carinata Silvestri, 1896
Cassidulina laevigata d'Orbigny, 1826
Cassidulina neoteretis Seidenkrantz, 1995
Cassidulina reniforme Nørvang, 1945
Cassidulinoides bradyi Norman, 1881
Cibicides lobatulus Walker & Jacob, 1798
Cibicides refulgens de Montfort, 1808
Cibicidoides pachyderma Rzehak, 1886
Cibicidoides spp.
Cornuspira sp.
Discanomalina coronata Parker & Jones, 1857
Elphidium advenum Cushman, 1922
Elphidium albiumbilicatum Weiss, 1954
Elphidium excavatum Terquem, 1875
Elphidium clavatum Cushman, 1930
Elphidium crispum Linnaeus, 1758
Elphidium gerthi van Voorthuysen, 1957
Elphidium incertum Williamson, 1858
Elphidium spp.

Elphidium williamsoni Haynes, 1973
Fissurina orbignyana Seguenza, 1862
Fissurina spp.
Fursenkoina sp.
Globocassidulina subglobosa Brady, 1881
Guttulina communis d'Orbigny, 1826
Gyroidina sp.
Hansenisca soldanii d'Orbigny, 1826
Hyalinea baltica Schröter, 1783
Lagena sp.
Lagena striata d'Orbigny, 1839
Lenticulina orbicularis d'Orbigny, 1826
Lenticulina sp.
Lenticulina torrida Cushman, 1923
Melonis barleeianum Williamson, 1858
Miliolinella subrotunda Montagu, 1803
Miliolinella sp.
Nodosaria spp.
Nonionellina labradorica Dawson, 1860
Nonion spp.
Nonionella turgida Williamson, 1858
Oolina borealis Loeblich & Tappan, 1954
Oolina lineata Williamson, 1848
Oolina sp.
Parafissurina spp.
Planulina ariminensis d'Orbigny, 1826
Pullenia bulloides d'Orbigny, 1846
Pullenia quinqueloba Reuss, 1851
Pyrgo simplex d'Orbigny, 1846
Pyrgo williamsoni Silvestri, 1923
Quinqueloculina lata Terquem, 1876
Quinqueloculina seminula Linnaeus, 1758
Quinqueloculina spp.
Quinqueloculina stalker Loeblich & Tappan, 1953
Rosalina spp.
Sphaeroidina bulloides d'Orbigny, 1826
Stainforthia fusiformis Williamson, 1858
Trifarina angulosa Williamson, 1858
Trifarina sp.
Triloculina angusteoralis Wiesner, 1923
Triloculina sp.
Triloculina trigonula Lamarck, 1804
Uvigerina mediterranea Brady, 1884
Uvigerina peregrina Cushman, 1923
Uvigerina sp.

Agglutinated (benthic) taxa

Eggerella bradyi Cushman, 1911
Karrerella bradyi Cushman, 1911
Miliammina fusca Brady, 1870
Sigmoilopsis schlumbergeri Silvestri, 1904
Textularia sagittula Defrance, 1804 (morphological group of Murray 1971)
Textularia truncata Höglund, 1947
Textularia spp.

Planktic taxa

Globigerina bulloides d'Orbigny, 1826
Globigerinella siphonifera d'Orbigny, 1839
Globigerinita glutinata Egger, 1893
Globigerinita uvula Ehrenberg, 1861
Globorotalia hirsuta d'Orbigny, 1839
Globorotalia inflata d'Orbigny, 1839
Globorotalia truncatulinoides d'Orbigny, 1839
Globorotalia scitula Brady, 1882
Neogloboquadrina dutertrei d'Orbigny, 1839
Neogloboquadrina pachyderma Ehrenberg, 1861
Neogloboquadrina incompta Cifelli, 1961
Orbulina universa d'Orbigny, 1839
Trilobatus trilobus Reuss, 1850
Turborotalita quinqueloba Natland, 1938

Table A8: List of foraminiferal species identified in 198VC. See Section 4.2.3. for taxonomic references used.

Appendix 4: Foraminiferal diversity statistics

Table A9: Benthic foraminiferal diversity statistics for core 146VC

| Core: JC106-146VC | Sample depth (cm) | | | | | | | | |
|------------------------|-------------------|------|------|------|------|------|-------|------|------|
| | 412.5 | 402 | 382 | 362 | 345 | 328 | 311 | 293 | 276 |
| Number of species | 19 | 17 | 28 | 26 | 26 | 23 | 20 | 7 | 6 |
| Fisher's α | 5.2 | 5.1 | 7.7 | 8.7 | 6.8 | 5.8 | 7.3 | 3.1 | 3.2 |
| Dominance (1-D) | 0.85 | 0.83 | 0.87 | 0.86 | 0.83 | 0.81 | 0.84 | 0.39 | 0.77 |
| Benthic:Planktic ratio | 50.5 | 35.5 | 51.0 | 29.7 | 62.2 | 61.6 | 115.0 | 9.3 | 20.0 |

| Core: JC106-146VC | Sample depth (cm) | | | | | | | | |
|------------------------|-------------------|-----|------|------|------|------|------|------|------|
| | 259 | 242 | 228 | 211 | 194 | 177 | 160 | 143 | 126 |
| Number of species | 1 | - | 34 | 25 | 29 | 22 | 22 | 12 | 17 |
| Fisher's α | - | - | 10.1 | 6.9 | 8.2 | 6.7 | 7.7 | 5.0 | 5.9 |
| Dominance (1-D) | - | - | 0.82 | 0.85 | 0.84 | 0.81 | 0.83 | 0.80 | 0.81 |
| Benthic:Planktic ratio | 2.0 | - | 49.0 | 44.2 | 59.6 | 60.3 | 68.0 | 51.0 | 53.0 |

| Core: JC106-146VC | Sample depth (cm) | | | | | | |
|------------------------|-------------------|------|------|------|------|------|------|
| | 109 | 92 | 75 | 58 | 41 | 24 | 7 |
| Number of species | 10 | 13 | 11 | 6 | 21 | 26 | 23 |
| Fisher's α | 7.1 | 8.7 | 6.7 | 2.8 | 8.7 | 6.7 | 5.8 |
| Dominance (1-D) | 0.86 | 0.80 | 0.82 | 0.77 | 0.90 | 0.87 | 0.85 |
| Benthic:Planktic ratio | 24.0 | 33.0 | 7.5 | 21.0 | 2.7 | 2.6 | 5.7 |

Note: Number of species, Fisher's α and dominance all refer to the benthic assemblages only (see Section 4.2.5.). Missing Fisher's α and dominance values are due to barren samples. Missing Benthic:Planktic ratio value at 242 cm is due to barren sample. Samples at 311, 259, 143, 109, 92 and 58 cm are barren of planktic foraminifera.

Table A10: Benthic foraminiferal diversity statistics for core 198VC

| Core: JC106-198VC | Sample depth (cm) | | | | | | | | |
|------------------------|-------------------|------|------|------|------|------|------|------|------|
| | 377 | 361 | 345 | 329 | 313 | 297 | 281 | 265 | 249 |
| Number of species | 40 | 36 | 34 | 38 | 31 | 38 | 39 | 34 | 29 |
| Fisher's α | 11.8 | 9.2 | 9.5 | 11.7 | 8.0 | 11.1 | 12.0 | 9.8 | 7.8 |
| Dominance (1-D) | 0.92 | 0.91 | 0.92 | 0.93 | 0.90 | 0.91 | 0.93 | 0.93 | 0.90 |
| Benthic:Planktic ratio | 1.3 | 1.9 | 1.5 | 1.2 | 1.6 | 1.4 | 1.4 | 1.4 | 1.4 |

| Core: JC106-198VC | Sample depth (cm) | | | | | | | | |
|------------------------|-------------------|------|------|------|------|------|------|------|------|
| | 233 | 217 | 201 | 185 | 169 | 153 | 137 | 121 | 105 |
| Number of species | 43 | 37 | 42 | 35 | 35 | 43 | 34 | 39 | 44 |
| Fisher's α | 12.0 | 9.5 | 11.2 | 8.0 | 7.9 | 10.9 | 8.9 | 10.4 | 12.2 |
| Dominance (1-D) | 0.93 | 0.92 | 0.93 | 0.92 | 0.79 | 0.92 | 0.92 | 0.92 | 0.91 |
| Benthic:Planktic ratio | 2.0 | 2.0 | 1.7 | 1.0 | 1.3 | 0.8 | 0.7 | 1.0 | 1.0 |

| Core: JC106-198VC | Sample depth (cm) | | | | | |
|------------------------|-------------------|------|------|------|------|------|
| | 89 | 73 | 57 | 41 | 25 | 9 |
| Number of species | 43 | 45 | 35 | 43 | 35 | 30 |
| Fisher's α | 11.6 | 12.3 | 9.2 | 10.8 | 9.0 | 6.9 |
| Dominance (1-D) | 0.92 | 0.94 | 0.86 | 0.91 | 0.92 | 0.91 |
| Benthic:Planktic ratio | 0.8 | 0.3 | 1.6 | 0.4 | 0.8 | 0.8 |

Table A11: Planktic foraminiferal diversity statistics for core 198VC

| Core: JC106-198VC | Sample depth (cm) | | | | | | | | |
|------------------------|-------------------|------|------|------|------|------|------|------|------|
| | 377 | 361 | 345 | 329 | 313 | 297 | 281 | 265 | 249 |
| Number of species | 8 | 11 | 9 | 9 | 11 | 8 | 9 | 9 | 9 |
| Fisher's α | 1.6 | 2.4 | 1.9 | 1.9 | 2.4 | 1.6 | 1.9 | 1.9 | 1.9 |
| Dominance (1-D) | 0.59 | 0.69 | 0.62 | 0.69 | 0.67 | 0.67 | 0.70 | 0.71 | 0.72 |
| Benthic:Planktic ratio | 1.3 | 1.9 | 1.5 | 1.2 | 1.6 | 1.4 | 1.4 | 1.4 | 1.4 |

| Core: JC106-198VC | Sample depth (cm) | | | | | | | | |
|------------------------|-------------------|------|------|------|------|------|------|------|------|
| | 233 | 217 | 201 | 185 | 169 | 153 | 137 | 121 | 105 |
| Number of species | 10 | 9 | 9 | 9 | 9 | 10 | 11 | 11 | 11 |
| Fisher's α | 2.2 | 1.9 | 1.8 | 1.8 | 1.8 | 1.9 | 2.5 | 2.2 | 2.5 |
| Dominance (1-D) | 0.79 | 0.63 | 0.71 | 0.76 | 0.77 | 0.62 | 0.77 | 0.72 | 0.78 |
| Benthic:Planktic ratio | 2.0 | 2.0 | 1.7 | 1.0 | 1.3 | 0.8 | 0.7 | 1.0 | 1.0 |

| Core: JC106-198VC | Sample depth (cm) | | | | | |
|------------------------|-------------------|------|------|------|------|------|
| | 89 | 73 | 57 | 41 | 25 | 9 |
| Number of species | 10 | 9 | 11 | 11 | 12 | 10 |
| Fisher's α | 2.1 | 1.6 | 2.4 | 2.2 | 2.6 | 2.1 |
| Dominance (1-D) | 0.66 | 0.63 | 0.84 | 0.80 | 0.79 | 0.79 |
| Benthic:Planktic ratio | 0.8 | 0.3 | 1.6 | 0.4 | 0.8 | 0.8 |

Appendix 5: Grain-size and water content data**Table A12:** Grain-size and water content measurements for core 146VC

| Core: JC106-146VC | | | | |
|--------------------------|---|--|--|------------------------|
| Sample depth (cm) | >500 μm | 500-63 μm | <63 μm | % Water content |
| 7 | 55.05 | 27.89 | 17.06 | 17.67 |
| 24 | 9.35 | 9.83 | 80.82 | 34.12 |
| 41 | 0.25 | 2.45 | 97.30 | 36.84 |
| 58 | 0.25 | 2.95 | 96.81 | 37.19 |
| 75 | 0.24 | 1.66 | 98.10 | 35.08 |
| 92 | 0.24 | 1.70 | 98.06 | 36.62 |
| 109 | 1.19 | 1.90 | 96.92 | 37.20 |
| 126 | 0.90 | 5.42 | 93.68 | 32.16 |
| 143 | 1.39 | 3.94 | 94.66 | 33.28 |
| 160 | 25.15 | 4.95 | 69.90 | 25.63 |
| 177 | 3.92 | 7.19 | 88.89 | 29.71 |
| 194 | 4.57 | 12.13 | 83.30 | 24.13 |
| 211 | 2.27 | 9.28 | 88.45 | 28.68 |
| 228 | 19.71 | 12.84 | 67.45 | 17.83 |
| 242 | 0.00 | 0.25 | 99.75 | 37.60 |
| 259 | 0.26 | 0.51 | 99.23 | 38.84 |
| 276 | 0.00 | 0.74 | 99.26 | 38.66 |
| 293 | 0.24 | 0.96 | 98.80 | 33.60 |
| 311 | 0.86 | 4.94 | 94.21 | 27.86 |
| 328 | 5.18 | 19.11 | 75.71 | 19.31 |
| 345 | 8.00 | 21.39 | 70.61 | 18.09 |
| 362 | 6.32 | 8.63 | 85.05 | 21.49 |
| 382 | 12.33 | 21.97 | 65.70 | 16.43 |
| 402 | 3.02 | 9.94 | 87.04 | 20.58 |
| 412.5 | 7.14 | 25.82 | 67.03 | 13.33 |

Table A13: Grain-size and water content measurements for core 198VC

| Core: JC106-198VC | | | | |
|--------------------------|---|--|--|------------------------|
| Sample depth (cm) | >500 μm | 500-63 μm | <63 μm | % Water content |
| 9 | 0.68 | 70.99 | 28.33 | 19.73 |
| 25 | 1.33 | 71.43 | 27.24 | 19.09 |
| 41 | 9.33 | 63.00 | 27.67 | 17.81 |
| 57 | 1.46 | 27.37 | 71.17 | 23.46 |
| 73 | 1.05 | 23.43 | 75.52 | 23.73 |
| 89 | 1.07 | 20.36 | 78.57 | 25.93 |
| 105 | 1.77 | 21.99 | 76.24 | 23.16 |
| 121 | 2.45 | 24.13 | 73.43 | 24.74 |
| 137 | 1.03 | 26.12 | 72.85 | 20.71 |
| 153 | 1.35 | 25.34 | 73.31 | 21.90 |
| 169 | 0.70 | 20.98 | 78.32 | 22.28 |
| 185 | 20.79 | 33.07 | 46.14 | 17.75 |
| 201 | 12.35 | 36.03 | 51.62 | 18.62 |
| 217 | 9.37 | 32.38 | 58.25 | 19.90 |
| 233 | 3.90 | 26.19 | 69.91 | 22.87 |
| 249 | 1.39 | 23.96 | 74.65 | 17.95 |
| 265 | 1.75 | 20.35 | 77.89 | 20.39 |
| 281 | 2.65 | 24.17 | 73.18 | 16.34 |
| 297 | 0.68 | 20.95 | 78.38 | 15.91 |
| 313 | 1.01 | 14.81 | 84.18 | 17.73 |
| 329 | 0.65 | 13.96 | 85.39 | 16.76 |
| 345 | 0.34 | 16.67 | 82.99 | 17.42 |
| 361 | 5.35 | 25.08 | 69.57 | 14.08 |
| 377 | 1.64 | 30.26 | 68.09 | 13.14 |

Note: All grain-size fraction values are percentages of the dry bulk sediment sample weights. Water content is given as a percentage of the weight of the wet bulk sediment sample.

Appendix 6: >2 mm clast counts from x-radiographs

Table A14: >2 mm clast counts from x-radiographs for core 146VC

| Core: JC106-146VC | | | | | | | | | | | | | | | |
|-------------------|-------------|------------|-------------|------------|-------------|------------|-------------|------------|-------------|------------|-------------|------------|-------------|------------|-------------|
| Depth (cm) | Grain count | Depth (cm) | Grain count | Depth (cm) | Grain count | Depth (cm) | Grain count | Depth (cm) | Grain count | Depth (cm) | Grain count | Depth (cm) | Grain count | Depth (cm) | Grain count |
| 0 | - | 56 | 0 | 112 | 2 | 168 | 5 | 224 | 9 | 280 | 0 | 336 | 13 | 392 | 28 |
| 2 | - | 58 | 0 | 114 | 1 | 170 | 5 | 226 | 11 | 282 | 0 | 338 | 12 | 394 | 11 |
| 4 | - | 60 | 0 | 116 | 3 | 172 | 6 | 228 | 11 | 284 | 0 | 340 | 19 | 396 | 3 |
| 6 | - | 62 | 1 | 118 | 7 | 174 | 15 | 230 | 16 | 286 | 1 | 342 | 9 | 398 | 3 |
| 8 | - | 64 | 0 | 120 | 8 | 176 | 9 | 232 | 11 | 288 | 2 | 344 | 11 | 400 | 2 |
| 10 | - | 66 | 0 | 122 | 6 | 178 | 17 | 234 | 8 | 290 | 0 | 346 | 12 | 402 | 3 |
| 12 | - | 68 | 1 | 124 | 0 | 180 | 6 | 236 | 1 | 292 | 2 | 348 | 22 | 404 | 3 |
| 14 | - | 70 | 0 | 126 | 4 | 182 | 4 | 238 | 3 | 294 | 3 | 350 | 15 | 406 | 9 |
| 16 | - | 72 | 0 | 128 | 2 | 184 | 6 | 240 | 4 | 296 | 1 | 352 | 17 | 408 | 13 |
| 18 | - | 74 | 0 | 130 | 2 | 186 | 7 | 242 | 2 | 298 | 0 | 354 | 16 | 410 | 18 |
| 20 | 10 | 76 | 1 | 132 | 2 | 188 | 10 | 244 | 1 | 300 | 2 | 356 | 16 | 412 | 11 |
| 22 | 13 | 78 | 0 | 134 | 4 | 190 | 12 | 246 | 1 | 302 | 0 | 358 | 12 | 414 | 14 |
| 24 | 10 | 80 | 1 | 136 | 3 | 192 | 12 | 248 | 3 | 304 | 2 | 360 | 23 | 416 | 7 |
| 26 | 3 | 82 | 1 | 138 | 1 | 194 | 6 | 250 | 4 | 306 | 3 | 362 | 11 | 418 | 12 |
| 28 | 11 | 84 | 0 | 140 | 3 | 196 | 11 | 252 | 3 | 308 | 5 | 364 | 7 | 392 | 28 |
| 30 | 17 | 86 | 0 | 142 | 7 | 198 | 8 | 254 | 1 | 310 | 0 | 366 | 8 | 394 | 11 |
| 32 | 5 | 88 | 2 | 144 | 14 | 200 | 5 | 256 | 0 | 312 | 2 | 368 | 12 | 396 | 3 |
| 34 | 5 | 90 | 1 | 146 | 9 | 202 | 3 | 258 | 0 | 314 | 0 | 370 | 12 | 398 | 3 |
| 36 | 5 | 92 | 1 | 148 | 5 | 204 | 8 | 260 | 5 | 316 | 4 | 372 | 9 | 400 | 2 |
| 38 | 1 | 94 | 2 | 150 | 6 | 206 | 8 | 262 | 4 | 318 | 2 | 374 | 12 | 402 | 3 |
| 40 | 4 | 96 | 0 | 152 | 9 | 208 | 7 | 264 | 1 | 320 | 2 | 376 | 21 | 404 | 3 |
| 42 | 1 | 98 | 0 | 154 | 10 | 210 | 5 | 266 | 0 | 322 | 0 | 378 | 15 | 406 | 9 |
| 44 | 4 | 100 | 1 | 156 | 10 | 212 | 10 | 268 | 0 | 324 | 1 | 380 | 12 | 408 | 13 |
| 46 | 5 | 102 | 1 | 158 | 9 | 214 | 6 | 270 | 3 | 326 | 5 | 382 | 8 | 410 | 18 |
| 48 | 0 | 104 | 4 | 160 | 7 | 216 | 8 | 272 | 1 | 328 | 4 | 384 | 12 | 412 | 11 |
| 50 | 2 | 106 | 8 | 162 | 6 | 218 | 4 | 274 | 1 | 330 | 9 | 386 | 18 | 414 | 14 |
| 52 | 0 | 108 | 4 | 164 | 8 | 220 | 5 | 276 | 4 | 332 | 9 | 388 | 23 | 416 | 7 |
| 54 | 0 | 110 | 2 | 166 | 7 | 222 | 9 | 278 | 4 | 334 | 10 | 390 | 14 | 418 | 12 |

Note: Depth values represent the core depth of the centre of the 2 cm window used to count the >2 mm grains. Missing values are from gravel lithofacies (facies Gm) where individual >2 mm grains could not be differentiated on the x-radiographs.

Table A15: >2 mm clast counts from x-radiographs for core 198VC

| Core: JC106-198VC | | | | | | | | | | | | | |
|-------------------|-------------|------------|-------------|------------|-------------|------------|-------------|------------|-------------|------------|-------------|------------|-------------|
| Depth (cm) | Grain count | Depth (cm) | Grain count | Depth (cm) | Grain count | Depth (cm) | Grain count | Depth (cm) | Grain count | Depth (cm) | Grain count | Depth (cm) | Grain count |
| 1 | 0 | 57 | 11 | 112 | 2 | 168 | 6 | 224 | 6 | 280 | 8 | 336 | 19 |
| 3 | 0 | 59 | 8 | 114 | 0 | 170 | 2 | 226 | 13 | 282 | 7 | 338 | 8 |
| 5 | 0 | 61 | 6 | 116 | 0 | 172 | 1 | 228 | 15 | 284 | 14 | 340 | 5 |
| 7 | 0 | 63 | 4 | 118 | 1 | 174 | 17 | 230 | 22 | 286 | 6 | 342 | 8 |
| 9 | 0 | 65 | 2 | 120 | 2 | 176 | 13 | 232 | 28 | 288 | 7 | 344 | 15 |
| 11 | 0 | 67 | 3 | 122 | 2 | 178 | 23 | 234 | 21 | 290 | 6 | 346 | 7 |
| 13 | 0 | 69 | 2 | 124 | 1 | 180 | 20 | 236 | 24 | 292 | 8 | 348 | 12 |
| 15 | 0 | 71 | 6 | 126 | 1 | 182 | 15 | 238 | 9 | 294 | 10 | 350 | 12 |
| 17 | 0 | 73 | 6 | 128 | 1 | 184 | 7 | 240 | 18 | 296 | 9 | 352 | 14 |
| 19 | 0 | 75 | 2 | 130 | 3 | 186 | 13 | 242 | 22 | 298 | 12 | 354 | 14 |
| 21 | 0 | 77 | 4 | 132 | 4 | 188 | 10 | 244 | 15 | 300 | 9 | 356 | 13 |
| 23 | 0 | 79 | 3 | 134 | 1 | 190 | 17 | 246 | 9 | 302 | 11 | 358 | 12 |
| 25 | 0 | 81 | 1 | 136 | 4 | 192 | 10 | 248 | 9 | 304 | 10 | 360 | 12 |
| 27 | 2 | 83 | 1 | 138 | 4 | 194 | 13 | 250 | 9 | 306 | 5 | 362 | 12 |
| 29 | 5 | 84 | 2 | 140 | 1 | 196 | 17 | 252 | 11 | 308 | 11 | 364 | 10 |
| 31 | 1 | 86 | 2 | 142 | 1 | 198 | 16 | 254 | 14 | 310 | 12 | 366 | 11 |
| 33 | 3 | 88 | 1 | 144 | 8 | 200 | 15 | 256 | 12 | 312 | 11 | 368 | 7 |
| 35 | 2 | 90 | 2 | 146 | 2 | 202 | 17 | 258 | 8 | 314 | 7 | 370 | 10 |
| 37 | 5 | 92 | 6 | 148 | 3 | 204 | 17 | 260 | 9 | 316 | 11 | 372 | 9 |
| 39 | 7 | 94 | 0 | 150 | 3 | 206 | 12 | 262 | 14 | 318 | 9 | 374 | 10 |
| 41 | 7 | 96 | 3 | 152 | 2 | 208 | 4 | 264 | 7 | 320 | 8 | 376 | - |
| 43 | 6 | 98 | 5 | 154 | 1 | 210 | 5 | 266 | 6 | 322 | 12 | 378 | - |
| 45 | 3 | 100 | 6 | 156 | 4 | 212 | 4 | 268 | 6 | 324 | 14 | 380 | 5 |
| 47 | 10 | 102 | 4 | 158 | 3 | 214 | 20 | 270 | 10 | 326 | 13 | 382 | 7 |
| 49 | 11 | 104 | 3 | 160 | 2 | 216 | 13 | 272 | 9 | 328 | 7 | 384 | 4 |
| 51 | 12 | 106 | 0 | 162 | 6 | 218 | 13 | 274 | 6 | 330 | 10 | | |
| 53 | 14 | 108 | 3 | 164 | 7 | 220 | 10 | 276 | 7 | 332 | 7 | | |
| 55 | 7 | 110 | 1 | 166 | 8 | 222 | 7 | 278 | 12 | 334 | 9 | | |

Note: Depth values represent the core depth of the centre of the 2 cm window used to count the >2 mm grains. Missing values for 375-379 cm are from an interval previously sampled for radiocarbon dating, where insufficient core material remained.